Republic of Iraq
Ministry of Higher Education
and Scientific Research
University of Babylon
College of Engineering
Civil Engineering Department

Flexural and Shear Behavior of Prestressed Concrete Beams Strengthened With Precast SIFCON Laminates Under Repeated Loads

A Thesis
Submitted to the College of Engineering of the University of Babylon in Partial Fulfillment of the Requirements for the Degree of Doctor of Philosophy in the Engineering /Civil Engineering /Structure

By
Hawra Mohamed Ali Mohamed Taher Jamal
(B.Sc. Civil Engineering, 2002)
(M.Sc. Structural Engineering, 2016)

Supervised by
Prof. Dr. Mustafa B. Dawood

February **2022**

بِسْمِ اللَّهِ الرَّحْمَـٰنِ الرَّحِيمِ

(قَالُواْ سُبْحَانَكَ لاَ عِلْمَ لَنَا إِلاَّ مَا عَلَّمْتَنَا

إِنَّكَ أَنتَ الْعَلِيمُ الْحَكِيمُ)

صدق الله العلي العظيم

سورة البقرة (٣٢)

Certificate

I certify that the preparation of this dissertation titled " **Flexural and Shear Behavior of Prestressed Concrete Beams Strengthened with Precast SIFCON Laminates Under Repeated Loads**", was prepared by "**Hawra Mohamed Ali Mohamed Taher Jamal**", under our supervision at University of Babylon as a fulfillment of the partial requirements for the degree of Doctor of Philosophy in Civil Engineering (Structural Engineering).

Signature: M.B. Dawood

Name: **Prof. Dr. Mustafa B. Dawood**

Date: / /

Certificate of the Examining Committee

We certify that as an examining committee that we have read this dissertation entitled " **Flexural and Shear Behavior of Prestressed Concrete Beams Strengthened with Precast SIFCON Laminates Under Repeated Loads** ", and examined the student " **Hawra Mohamed Ali Mohamed Taher Jamal** ", in its content and what related to it, and found it meets the standard of dissertation for the degree of Doctor of Philosophy in the Civil Engineering /Structure Engineering.

Signature: H. Al-Hassani
Name: **Prof. Dr. Hisham M.Al-Hassani**
(Chairman)
Date: / /

Signature:
Name: **Prof. Dr. Haitham H. Muteb**
(Member)
Date: / /

Signature:
Name: **Prof. Dr. Adel A. Al-Azzawi**
(Member)
Date: / /

Signature:
Name: **Prof. Dr.Qasim M. Shakir**
(Member)
Date: / /

Signature: R.F. Hassan
Name: **Asst. Prof. Dr. Rafea F. Hassan**
(Member)
Date: / /

Signature: M.B. Dawood
Name: **Prof. Dr. Mustafa B. Dawood**
(Member and Supervisor)
Date: / /

Approved of the Civil Engineering Department

Signature:
Name: **Prof. Dr. Thair J. Mizhir**
Head of the Civil Engineering Department
Date: / /

Approved of the College of Engineering

Signature:
Name: **Prof. Dr. Hatem H. Obeid**
Date: / /
Dean of the College of Engineering

Dedication

To the Memory of My Mother and Father

To My Inspirational Professor

To my lovely sons Ali, Mohmmed and Ameer

With eternal love and respect

Hawra

Acknowledgments

First of all, I would like to express my deepest gratitude to the Almighty God for giving me the power to carry out this research.

I wish to express my deepest gratitude and appreciation to my supervisor ***Prof.Dr.Mustafa B. Dawood*** for his supervision, precious advices, technical guidance, continuous encouragements, and remarkable patience in reviewing my dissertation, I am really indebted to him.

I want to thank the Civil Engineering Department at Babylon University, the teaching staff of PhD courses since they gave me many good things through my study.

I want to extend my deepest appreciation to all the staff in the laboratories of the faculty of engineering at the University of Technology and Karbala Precast company for their kind support and help on the technical and administrative aspects of the experimental work.

ABSTRACT

The loading on bridges, harbors, multi-story parking garages, airport facilities, and many other structures are often repeated that are usually built with precast prestressed concrete beams. These beams can be deficient because of local damages and develop cracks as a result of improper transportation and handling. Therefore, it is very important to develop an efficient strengthening technique in order to restore the lost capacity or even outperform it. A reliable and less expensive solution is proposed herein to retrofit the beams at the construction site rather than returning them to the manufacturing plant.

This study presents an experimental and numerical investigation of the flexural and shear behavior of indeterminate prestressed concrete beams strengthening with precast SIFCON laminates under monotonic static and repeated loading of limited cycles. The experimental program has been conducted on twenty unbonded post-tensioned prestressed high strength concrete (HSC) beams specimens with a (200×300) mm rectangular cross-section with length (4300 mm) tested as continuously supported subjected under two concentrated point loading in mid of each span and using for the strengthening these beams sixty-six precast SIFCON laminates. They were divided into two identical categories, each consisting of ten specimens. The first category was studied flexural behavior; the second category was studied shear behavior. Each category consisted of two groups as follows: the first group consisted of beams tested under monotonic static loading, the second group consisted of beams tested under repeated loading ranging between 0.4 to 0.6 of the ultimate loads produced from the static test.

Various parameters were investigated in the experimental program, including the length of laminates in the sagging and hogging region, three different bonding methods two of which are innovative, the full and partial wrapping, and different patterns of shear strengthening. Measurements were made for, midspan deflections, failure mode, toughness, moments distribution, crack widths, and strains in concrete.

The experimental results indicate the flexural strengthening of the prestressed concrete beams led to positively affected by delaying the first crack appearance time, the first cracking load of the tested beams increased between (56.2%-102.2%) and increased the ultimate flexural load capacity of the test beams (36.9%-57%). The new innovative end anchorage systems proved to be efficient to prevent the end-debonding failure of precast SIFCON laminates also had a significant contribution in improving behavior as a whole.

When the beams tested under repeated loads are a little reduced the ultimate flexural load capacity of the test beams (0.86%-5.87%) is compared with the strength of the same beams under monotonic static loading. The strengthened beams with static loading conditions show significant growth in moment redistribution (9.1-10.6) % at the central support and (5.5-6.4) % at mid-span, respectively. The ratio for moment redistribution for the negative moments of beams tested under repeated load increased by about (5%-9.03%) compared with similar beams under static loading conditions.

The results also refer that using precast SIFCON laminates as shear external strengthening of prestressed concrete beams is an effective technique in increasing the beam shear capacity it led to delaying the first crack appearance time , the first cracking load of the tested beams reached (23.7% -105.7%), Increased the ultimate shear load capacity of the tested beams (10.3%-46.5%), as well as beams that are tested under repeated loads, is a little reduced in ultimate shear capacity (2.2%-3.8%), comparing with the strength of the same beams under monotonic static loading.

The current study also showed the possibility of transforming a brittle failure mode to relatively ductile failure eventually failed after warning signs such as snapping sounds and peeling of the SIFCON with ample warnings before failure.

In numerical part of this study using the ABAQUS software program was carried out for all the tested specimens. The results were compared with those of

experimental work; a good agreement was obtained between the analytical and experimental results, then was studied new parameters.

The main conclusions which can draw are: that these investigations gave a good indication about using precast SIFCON laminates in improving the flexural and shear strength of continuous prestressed HSC beams; the innovative binding methods in this study were very effective, and the effect of repeated loading limited cycles on the tested specimens was minimal.

List of Contents

List of Figures

List of Tables

List of Notation and Symbols

Sign	Mean
AA	Aluminum alloy
ABAQUS	Software Package
ACI	American Concrete Institute
ASTM	American Society for Testing and Materials
CFRP	Carbon fiber reinforced polymer
EBR	Externally bonded reinforcement
Exp.	Experimental
FA	Fly ash
FEM	Finite element model
FRCM	Fabric Reinforced Cementitious Matrix
FRC	Fiber reinforced concrete
FRP	Fiber reinforced polymer
GFRC	Glass fiber reinforced concrete
GPa	Gega Pascal (GN/m2)
HRWR	High Range Water Reducing Agent
HSC	High Strength Concrete
LVDT	Linear Variable Displacement Transducer
MBC	Mineral-based composite
MPC	Magnesium phosphate cement
MPa	Mega Pascal (ѳN/m2)
NSM	Near-Surface Mounted
OPC	ordinary portland cement
RC	Reinforced concrete
SF	Silica fume
SIFCON	Slurry Infiltrated Fibrous Concrete
SP	Superplasticizer

TRC	Textile-reinforced concrete
TRM	Textile-reinforced mortar
PSC	Prestressed concrete
Pu	Ultimate load
P_{cr}	Cracking load

CHAPTER ONE

INTRODUCTION

CHAPTER ONE

INTRODUCTION

1.1 General

Various communities worldwide devote a significant portion of their budget to the construction and maintenance of civil infrastructure. Harbors, bridges, water structures, buildings, schools, parking garages, and airport facilities are examples of long-term investments. A lot of such structures are constructed with precast pre-stressed concrete elements.

Prestressed concrete (PSC) structures are generally durable and created for effectively supporting loads throughout the anticipated service life related to structural members; yet, they deteriorate over time due to many faults in design inadequate design or construction. The unanticipated increase in the levels of load along with changes in structure use, bad quality of the used materials, seismic damages, or changes in the environmental reasons and natural conditions, damages because of corrosion, loss of prestressing, collision, and the continuously-growing applied loads.

Local damage and cracks generated owing to improper storage in manufacturing plants, as well as incorrect handling and transportation, are other girder defect sources. Also, the developed local damage and cracks in girder throughout handling and transportation at construction sites cause replacing girders by contractors, increasing the costs. Repairing structural elements is critical, not just for the weakened elements, yet to strengthen novel structural concrete elements; as a result, strengthened structural elements can support (safely) the design load under a variety of harsh environmental conditions without sustaining extreme damage.

It is not often viable to replace and demolish structures which have become structurally inadequate. Because of financial limitations, retrofitting and strengthening such structures may be the best option. Instead of returning the girders to the manufacturing factory, a more dependable and cost-effective option is presented for fixing them at the building site. Various strengthening procedures are provided and utilized for retrofitting or strengthening certain reinforced concrete structures in order to properly restore its strength and serviceability[1].

In structural concrete, the introduction of adequate prestressing procedures has undoubtedly been a significant advancement. It allowed concrete to effectively compete in areas where steel construction had traditionally dominated, such as high-rise buildings, long-span bridges, offshore structures and pressure vessels.

Prestressing and post-tensioning are well understood, providing a beautiful, effective, and inexpensive wide range of application-specific solutions. When dealing with prestressed concrete beams, the allowable permissible tension stresses are fully and partially prestressed. Completely prestressing is when all tensile stresses in members are eliminated under full-service load, while partially prestressing permits larger tension stresses in the concrete, which causes cracking when the structure is overloaded[2].

Slurry infiltrated fibrous concrete (SIFCON) can be defined as one of the significant materials with outstanding characteristics. It's a new type of high-performance fiber reinforced concrete created with a specially developed cement-based slurry as well as a penetrating steel fiber bed. SIFCON has been shown in studies to be a creative building material with a wide range of ductility and high strength. SIFCON was used as a strengthening layer for traditional concrete members in earlier studies; consequently, it is going to be used for strengthening prestressed concrete beams in the presented work[3].

A brief explanation of PSC, statically indeterminate members, prestressed concrete beams under repeated loading, high strength concrete (HSC), and (SIFCON) is introduced in this chapter as well as the layout of the dissertation and the main objectives of the present work.

1.2 Prestressed Concrete (PSC)

Prestressing is a technique used to overcome the natural tension fragility of concrete. prestressing is the process of applying an initial compressive load to a structure in order to eliminate or lessen the internal tensile forces and, as a result, control or eliminate cracking[4].As a result, the benefits of prestressed concrete members include increased span length, slender more aesthetically pleasing sections and better protection against corrosion[5]. Figure (1-1) shows an example of prestressed construction.

(a) (b)

Figure (1-1) The Roseville City Hall Annex: (a) view of the completed building; and (b) a view of the erection of the exterior frame. Post-tensioning strand extensions can be seen at the leftmost column [6]

1.2.1 Prestressing Methods

A- Post-tensioning: After the concrete has been cast and cemented, the steel tendons are tensioned. Tensioning is done by two major techniques: stretching the steel wires by hydraulic jacks that are set to apply tension, and then replacing the jacks with permanent anchorages. A tendon is typically constructed from fine wires, filaments, or bars. Bars are usually tensioned one at a time, whereas wires and strands can be grouped together. The steel tendons are first put in the formwork and then covered with waterproof paper or a metal duct (sheath). Bonded tendons are tendons that are bonded to the concrete. Unbonded tendons have no bond from the beginning to the end of the tendon because of the lack of grout on the tendon.

B- Pre-tensioning: Before the concrete is cast, the steel tendons are tensioned. When the concrete has been laid and set, the tendons are fastened to some abutments and then cut or freed. Bond transfers the prestressing force to the concrete via the tendon. Pretensioning occurs before casting in permanent beds used in the construction industry, which are prefabricated with pretensioned precast concrete pieces.

C- External prestressing: Uses external tendons or flat jacks to apply the prestressing force between the permanent rigid abutments and concrete member ends differently from the previous techniques; the member doesn't have internal prestressing tendons[7].

Based on the structural member's design, the tendons might have a curved (bent), straight, or circular profile. In addition, straight tendons are utilized in solid as well as hollow-cored slabs, while bent tendons are utilized in beams and the majority of structural elements. In circular structures like silos, tanks, and pipes, circular tendons are applied[8]. The prestressing methods are shown in Figure (1-2).

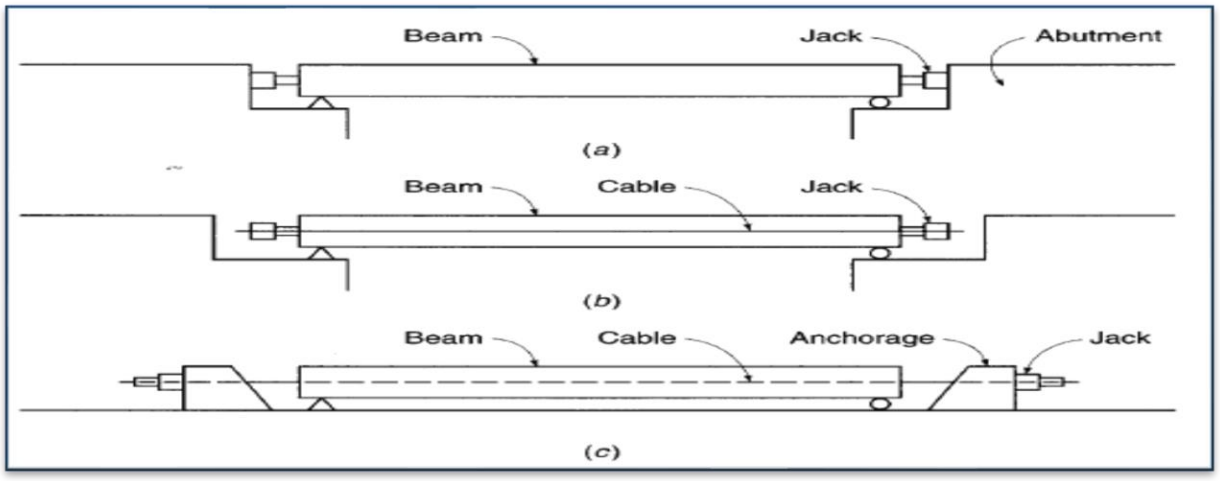

Figure (1-2) Prestressing methods:(a) post-tensioning by jacking against abutment, (b) post-tensioning with jacks reacting against beam, (c) pretensioning with tendon stressed between fixed external anchorage [9]

1.2.2 Types of Prestressing

Prestressing of reinforced concrete members may be recognized as one of two types, namely full and partial.

Full pre-stressing is that kind of pre-stressing in which tensile stress at service load is completely eliminated. This was the goal of prestressing early in the development of prestressed concrete. In heavily prestressed members, some disadvantages can be observed; (i) large upward deflection may occur, (ii) heavily prestressed members may have a tendency for severe shortening in the longitudinal direction, (iii) furthermore, failure may have sudden and brittle mode when the members are overloaded, so warning is little before the collapse[9].

Partial prestressing is a kind of prestressing. At full-service load, tensile stress and, as a result, some limited cracking is allowable; also, non-prestressed and prestressed steel are provided as main reinforcement for flexure. Here the excessive upward deflection and problem of shortening along member longitudinal axis are considered to be avoided. Also, there is a reduction in prestressing steel amount. When prestress suitable degree is chosen as the nature

of loading, many factors must be considered: live to dead load ratio, frequency of full-service load occurrence, and corrosive environment presence[9].

In the present work, partial prestressing using the unbonded post-tensioning technique is adopted to perform concrete prestressing in required prestressed specimens.

1.3 High Strength Concrete (HSC)

High strength concrete (HSC) is defined by ACI committee 363R as "concrete with a certain average compressive strength of (41MPa) or greater at 28 days." It's a term which is determined by a variety of factors, including construction methods and the quality regarding locally accessible concrete materials[10].HSC production methods and technologies do not differ significantly from those required for regular grade concrete; in any case, the accentuation on quality control might be larger with HSC. One of its important uses in the production of the prestressed concrete structure[11].

1.4 Statically Indeterminate Members

Members that are statically indeterminate or continuous, in statics, the number of unknown reactions is greater than the number of equilibrium equations. When assessing continuous members, material characteristics, structure geometry, geometric compatibility, equilibrium, and arrangement must all be taken into account [12].

The presence of an infinite number of different reactions and internal actions satisfying equilibrium for any set of loads applied to a statically indeterminate structure leads to the discovery of a new class of stress-strain relationships that are geometric compatible with the structure's constituent materials, but only one set of reactions and internal actions that satisfies both equilibrium and geometric compatibility. For the internal actions to be properly determined, imposed loads

and imposed deformations must be implemented for structural design. Bending moments are less, and deflections are reduced for a given span and load, provided the cross-sectional area remains constant. Indeterminate members can be made smaller in cross-section, providing additional flexibility in sizing members for aesthetic reasons [4] Figure (1-3) shows a statically indeterminate bridge.

Figure (1-3) Statically indeterminate bridge [12]

1.5 Prestressed Concrete Beams Under Repeated Loading

The structural members should be designed for serviceability requirements in addition to strength. A better understanding of the cracking and deformation of concrete beams subjected to different types of loading will improve the serviceability design. Research on the serviceability of concrete has become more important in the last few years. Loading on offshore structures, highways, multistory car parking, and many other structures are often repeated in nature. Extensive theoretical and experimental studies of both reinforced and prestressed concrete beams for a long time have resulted in extremely significant approaches for serviceability design under static loads. However, the effects of repeated load on the cracking and deflection of prestressed concrete beams are still rare and not quite understood. Concrete structures exposed to repeated loading experience higher deflection compared with static loading. These deflections include considerable permanent sets. With the increase in the number of load cycles, the

permanent deflections are also increased. This phenomenon has been noticed by many researchers; however, relevant experimental information is still few[13].

1.6 Slurry Infiltrated Fibrous Concrete (SIFCON)

The kind of fiber reinforced cement composite known as SIFCON can be regarded as a specialized slurry infiltrated form of fiber reinforced cement composite. The fiber volume proportion in these composites varies between 5% and 30%. In this technology, fibers are inserted within the moulds before being created. Once the fine aggregate and cement-rich flowable slurry have been added, a cementing slurry is poured or pumped into the fibers[14].The SIFCON materials exhibit amazing mechanical capabilities, with exceptional tensile, compressive, shear, and flexural strengths, as well as remarkable durability values[15]. It is important to pay attention to four major design considerations while creating a SIFCON product. These four characteristics, all referred to as slurry strength, fiber volume, fiber position, and fiber type, are all factors to consider. The following qualities will be present in slurry toughened composites: The hardened slurry's modulus of elasticity, tensile strength, and compressive strength influence the SIFCON composite's behavior [16]. Figure (1-4) illustrates the use of SIFCON in a bridge.

Figure (1-4) SIFCON was used for construction of the deck overlay of a bridge over the River Sava at Globoko, Slovenia [17]

1.7 Research Significance

Numerous studies have been conducted on simply supported, prestressed beams which are additionally reinforced with different composites but very limited for continuous prestressed concrete beams. This PhD study intends to find out if precast SIFCON laminates are effective when it comes to reinforcing continuous beams. It is the first time to use precast SIFCON laminate to strengthening these high-strength prestressed concrete beams. Two additional measurements (i.e., the ultimate load and moment enhancement ratios) are used to evaluate the strengthened beams' capacity augmentation. For simply supported beams, these two values will always be the same, but for continuous beams, it will be discovered that they are different.

1.8 The Goal of The Research

In this research, the key aims might be stated as follows:

1- Exploring behavior and investigating the feasibility of flexure and shear strengthening of prestressed concrete continuous beams with precast SIFCON Laminates precast SIFCON Laminates under monotonic static and repeated loads.

2- To investigate the extent the suitability of different bonding methods between the prestressed beams and precast SIFCON laminates:

(a) Gluing with epoxy only.

(b) Gluing with epoxy and addition end anchored steel plate.

(c) Gluing with epoxy and addition U shape end anchored steel plate.

3- To verify the effect of different variables of the precast SIFCON laminates, including length, shape, the bonding method, and zones of the strengthening.

4- Studying the possibility and the extent of the moment redistribution in prestressed concrete indeterminate beams strengthening with precast SIFCON laminates.

5- Following the validation of the numerical model simulated by this application with the results obtained experimentally, a parametric study is carried out using the ABAQUS software in order to cover some parameters affecting the behavior that was not taken into consideration during the experimental work.

1.9 Structure of the Dissertation

This study is carried out to achieve the above-mentioned goals in six chapters as presented below:

Chapter one: is a general introductory chapter about prestressed concrete, high strength concrete, slurry infiltrated fibrous concrete, indeterminate structure, and serviceability of prestressed concrete under repeated loading.

Chapter two: reviews the previous studies and researches related to the subject of the present study.

Chapter three: includes the characteristics regarding the utilized materials as well as the experimental work details.

Chapter four: deals with the discussion, presentation, and evaluation regarding the experimental results.

Chapter five: presented the numerical simulation of the specimens under monotonic static loading and repeated loading using the ABAQUS finite element software program.

Chapter six: provides the conclusions obtained from this work, suggestions and recommendations for future studies.

CHAPTER TWO

LITERATURE REVIEW

CHAPTER TWO

LITERATURE REVIEW

2.1 General

This chapter summarizes previous research on flexural and shear strengthening of prestressed concrete structures using various materials and methods, slurry infiltrated fibrous concrete (SIFCON) preparation and strengthening the reinforced concrete members using the SIFCON laminates.

2.2 Strengthening of Prestressed Concrete Beams

The researchers used various materials for strengthening prestressed concrete beams in shear and flexural. This section covers the approaches for strengthening prestressed concrete beams and the behavior related to strengthened prestressed concrete beams in flexure and shear.

2.2.1 Using Fiber Reinforced polymers (FRP) Laminates

As a result of their high tensile strength, ease of installation, durability, lightweight, corrosion resistance, fiber reinforced polymers outperform conventional strengthening approaches[18].

Peterman & Reed (2004) [19] studied the strengthened of double-tee section prestressed concrete bridge girders in the shear and flexure by using sheets of carbon fiber reinforced polymer (CFRP) as shown in Figure (2-1). They used three specimens analyzed from an overloaded bridge one girder uses a reference, two specimens are strengthened and repaired. All three were subjected to a series of failure tests to determine their flexural and shear capacities.

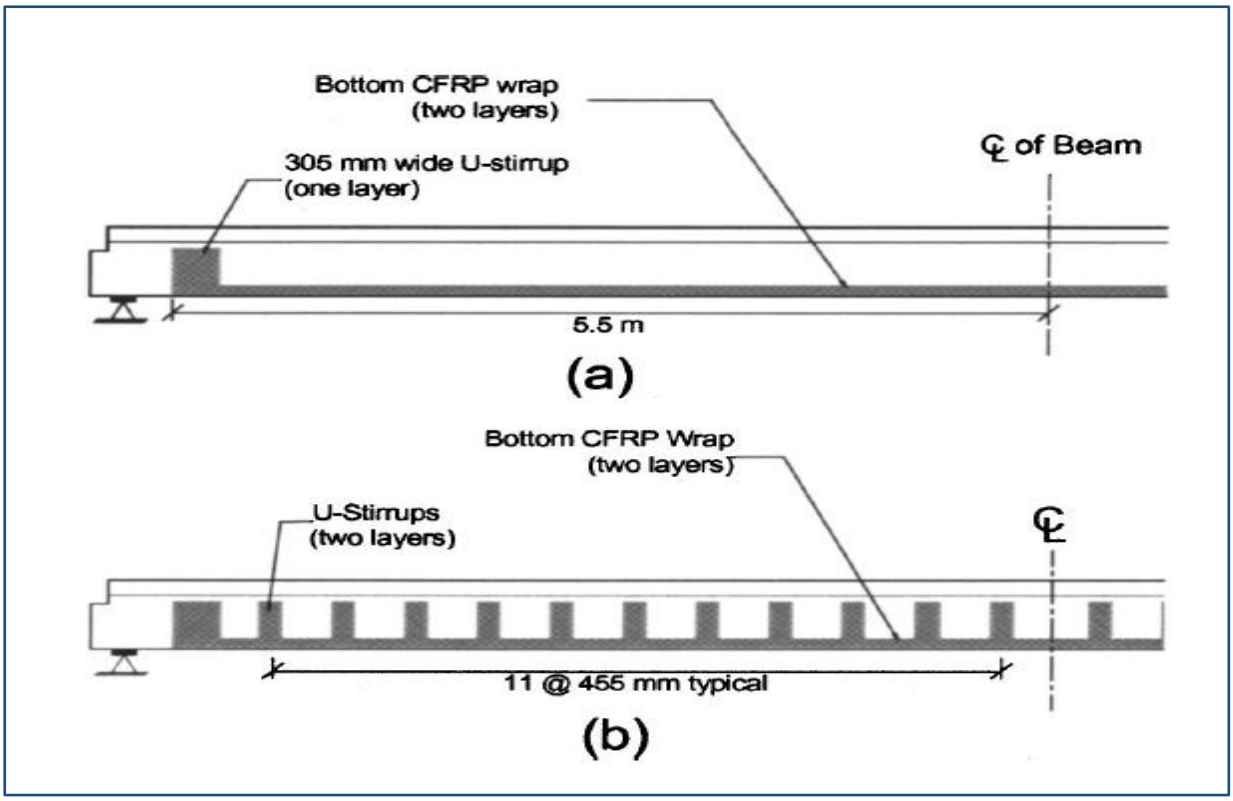

Figure (2-1) The specimen dimension and strengthening shape [19]

Transverse CFRP sheets caused an increase in the specimens' shear capacity examined by up to 28%, yet didn't prevent bond failures. With the use of two longitudinal carbon fiber reinforcement layers, this has resulted in an increase in flexural capacity of the specimens by more than 25% of the base strength and more than 50% of the strength of the original design.

Larson et al. (2005) [20] investigated five samples of pretensioned prestressed concrete tee beams section under live-load conditions for the specified range of the prestressing strand stress as shown in Figure (2-2). The experimental test consists of beam pre-cracking, strengthening those beams with the CFRP, and loading them mechanically to investigate the impact of the increase of live load on the strand fatigue. Beams have been either monotonically loaded to their ultimate capacity or fatigued cyclically and after that loaded monotonically to failure. This work showed that high strengthening levels of 70% and 113% can be achieved while regulating stress range fatigue requirements.

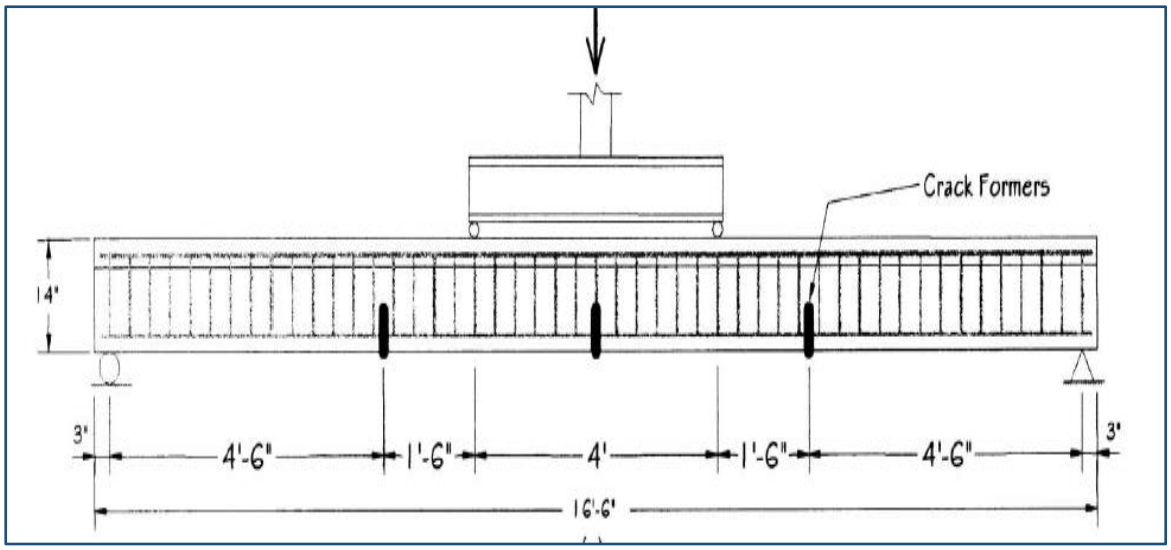

Figure (2-2) Beams dimensions [20]

Ary & Kang (2012) [21] tested two prestressed concrete I beams that have (U) shape strips of the CFRP, as well as a companion prestressed concrete I beam with no shear strengthened as shown in Figure (2-3).

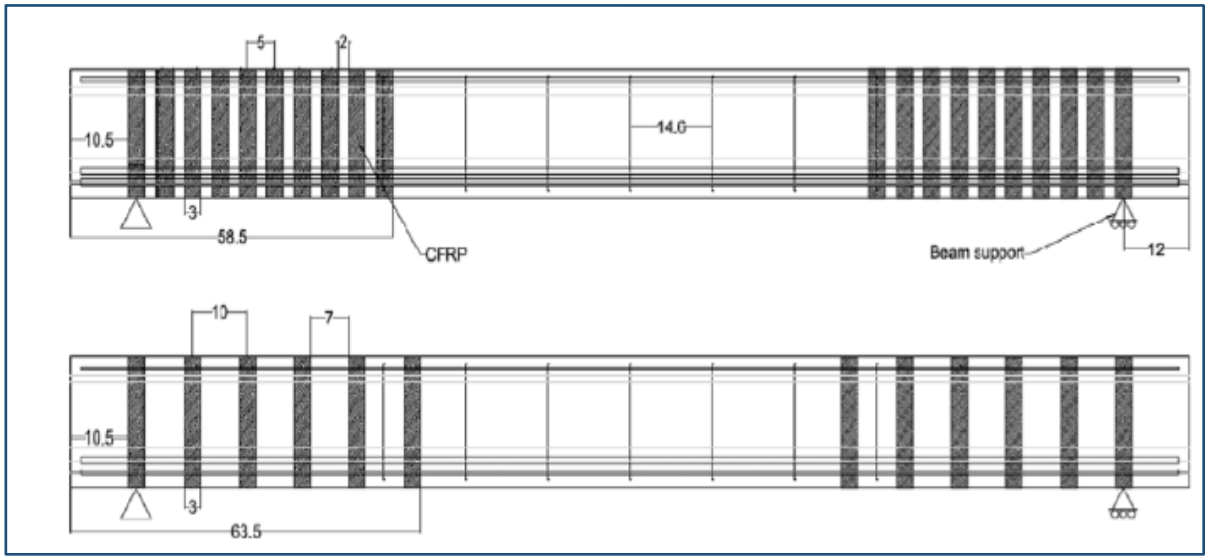

Figure (2-3) Beams dimensions and applied CFRP configurations[21]

The use of CFRP strips spaced not more than half the effective depth has demonstrated encouraging outcomes. In addition, in rapprochement to the reference beam's shear capacity, the spacing enhanced the strengthened beam's ductility by 28% while increasing its shear capacity as well by 38%. As a result, strips' spacing utilized for reinforcing the test specimen must be considered

carefully, as spacing greater than half effective depth had no effect on the strengthened beam's shear behavior.

Afefy et al. (2016) [1] Studied the retrofitting of three pre-cracked actual size double-tee pre-tensioned concrete girders with a depth of (810) mm and width of (3,200) mm, (16,900) mm length, and used pre-tensioned strands. Flexure strengthened by CFRP Sheets the Girder's configuration of the CFRP sheets for Girder are depicted in Figure (2-4). The strengthening approach used was adequate in terms of both failure load and ductility. Furthermore, according to the results of the experiments, the flexural and shear resistances of the retrofitted girders are at least 60% larger than those predicted using equations accessible in design codes. Indicating that the retrofitted girders outperform the calculations by a wide margin. The suggested configurations of the CFRP strengthening increased the ultimate load-carrying capacity by about 118% from the control girder.

Figure (2-4) Dimension and configuration of the CFRP sheets for Girders [1]

Truong et al.(2018) [22] tested nine unbonded prestressed concrete tee-beams in large sizes, the dimensions of the test beams are (200) mm in flange width, the depth (360) mm, and (6000) mm in length as illustrated in Figure (2-5). One unstrengthened control beam and the other beams have been externally strengthened with varying numbers of CFRP sheets. CFRP sheets considerably boosted the flexural capacity as much as 37%, lowered deflection in the state of serviceability, enhanced ductility, and decreased crack width as much as 48% of tested beams. Furthermore, the CFRP sheets and transverse U-strip anchorage system had a substantial impact on strain in the tendons of strengthened beams.

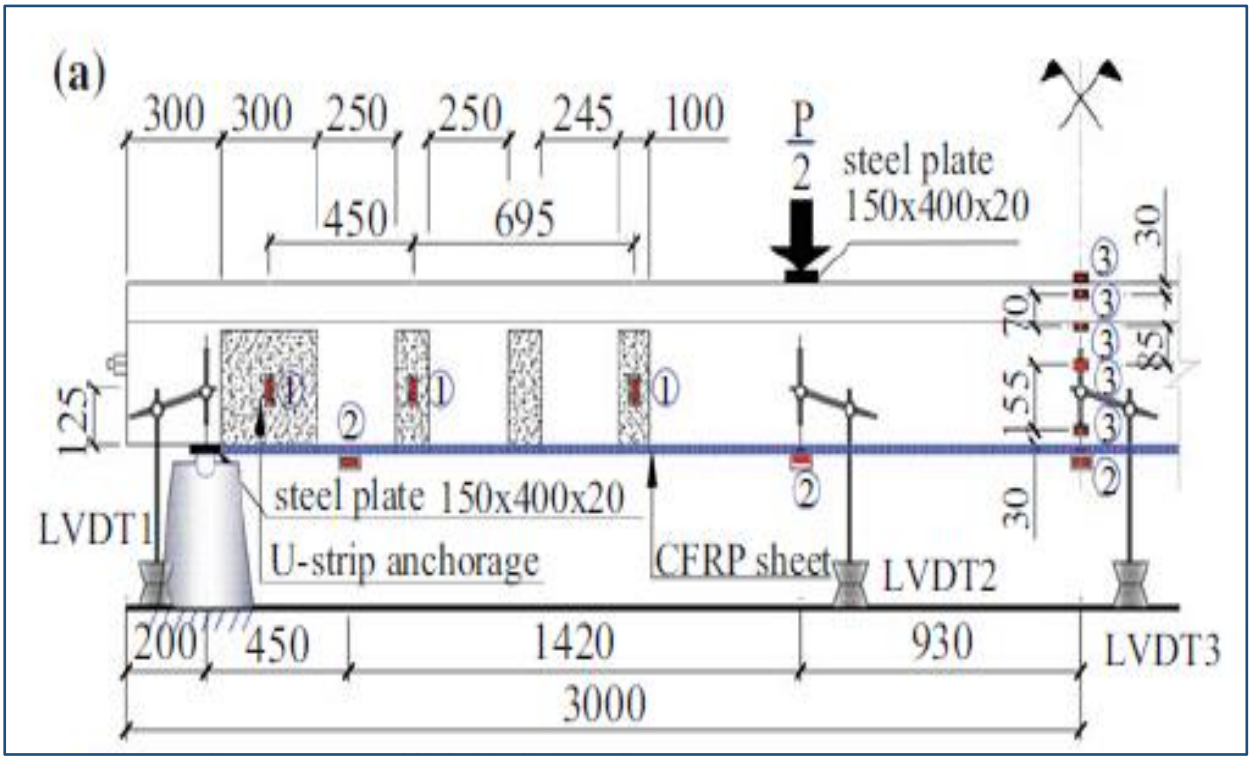

Figure (2-5) CFRP strengthening layout [22]

2.2.2 Using Near-Surface Mounted (NSM)

NSM can be defined as a strengthening approach that uses epoxy resins as adhesive in the applications of the FRP and has caught the attention of the world's engineers. It works by bonding pre-cut grooves in concrete cover with FRP bars

or laminates. Grooves could be used for the flexure strengthening in the tensile surfaces that are related to reinforced concrete members or the shear strengthening in the beam sides, with 50% of groove-filled by the adhesive and the composites of FRP that have been embedded in such grooves, and adhesive filled in the groove and levelled after that.[23]

Ghasemi et al. (2016) [24] investigated experimentally the flexural behavior of continuous (2-span) unbonded post-tensioned beams strengthened with CFRP. A total of seven beams with dimensions (250 x150x6000) mm long was tested. One beam unstrengthened used as a control beam the other beams were strengthened in positive and negative zones through externally bonded reinforcement (EBR) and internally NSM approaches, in addition, to avoid end-debonding failure in specimens that have been strengthened using the EBR process as shown in Figure (2-6).

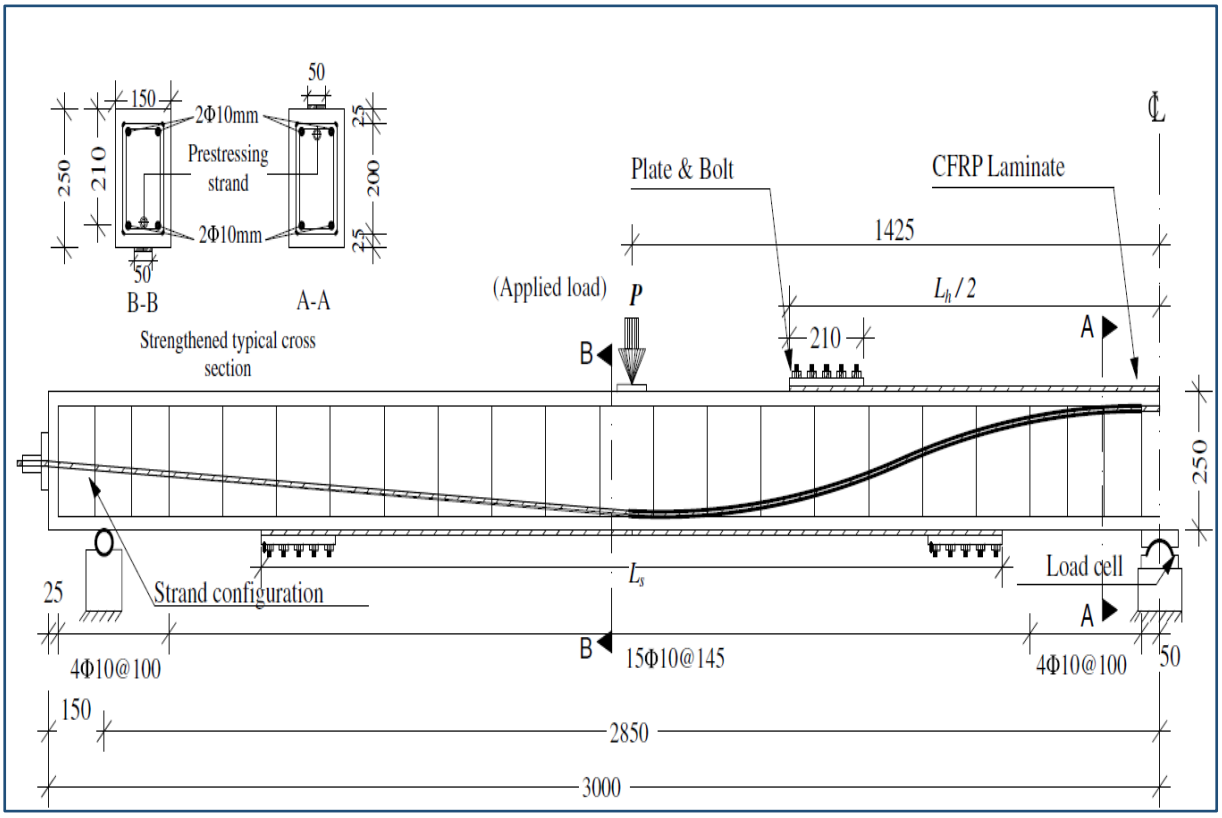

Figure (2-6) Tested beams[24]

The results revealed that CFRP strengthening significantly enhanced both the service as well as ultimate states regarding continuous unbonded post-tension concrete beams and that the NSM approach is more efficient compared to EBR, notably in expressions of ultimate load and crack spread. The load was increased slightly higher for beams strengthened using the NSM approach compared to the beams strengthened using the EBR approach. The CFRP laminate considerably decreased and changed the moment redistribution ratio between (22.89 and 4.75)% at midspan and between (38.15 and 7.91) % at central support.

Kuntal et al. (2017) [25] investigated the effectiveness of CFRP shear strengthening near the surface of high-strength prestressed concrete beams. Also, the effectiveness of different NSM FRP strengthening configurations was investigated through testing twelve pretensioned concrete beams which have been cast without and with stirrups. Six of those beams did not have vertical stirrups, whereas the others did. All of the beams have a (150) mm x (300) mm rectangular cross-section. In addition, the beams have been (1800) mm long, with a (1650) mm distance between the support beams when tested under shear. As indicated in the Figure (2-7), all beams have been tested under two-point loading with a 2.50 shear span to depth ratio for simulating dominant shear behavior. Figure (2-8) shows the complete technique for NSM CFRP shear strengthening.

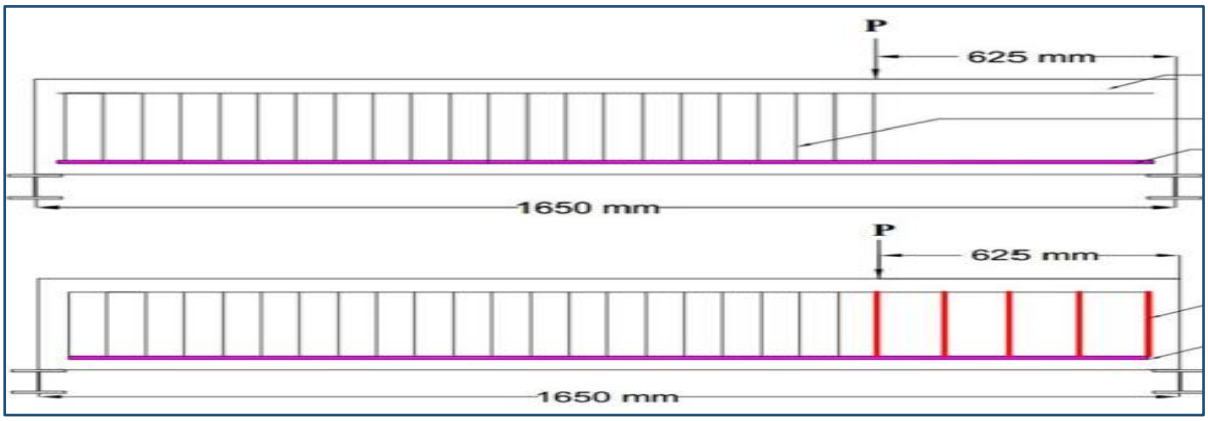

a-beams with stirrups and without stirrups

Figure (2-7) Prestressed beams strengthening using CFRP [25]

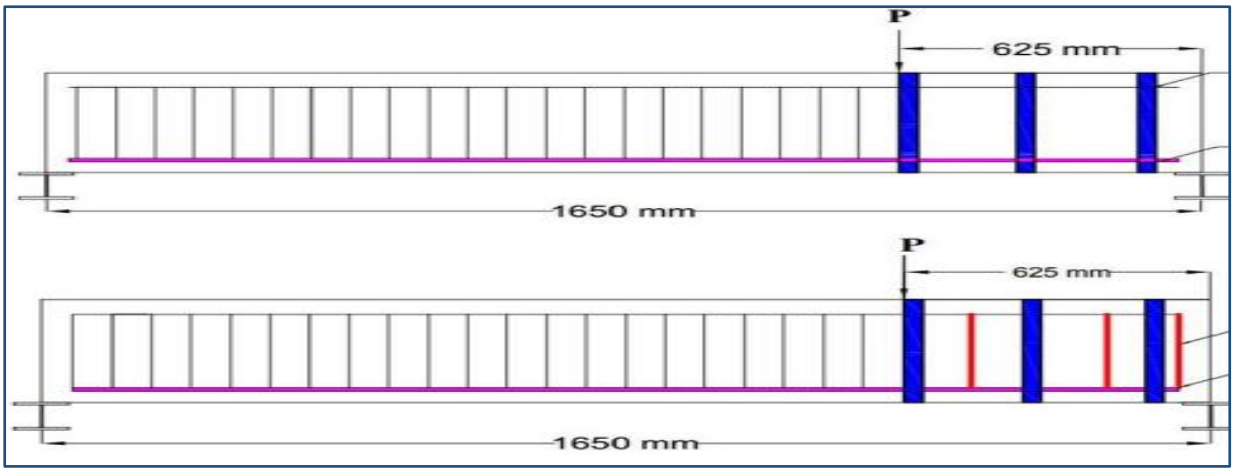

b-beams strengthened with CFRP at 90°

c-beams strengthened with CFRP at 45°

Continued Figure (2-7) Prestressed beams strengthening using CFRP [25]

Figure (2-8) Detailed of NSM CFRP shear strengthening [25]

NSM used strengthening of the PSC beams utilizing laminates of CFRP at 45˚improved the beam's shear capacity without and with vertical stirrups. It was also discovered that by constructing a proper NSM shear-strengthening scheme, the shear failure mode may be transformed into the flexural mode with increased ductility. The strengthened beams without stirrups using CFRP laminates with orientations 45˚ resulted in improvement of failure load and displacement by 52.0% and 34.4% respectively. Although NSM strengthening on beams with stirrups had only marginal improvement in strength, it was more effective in reducing the crack width and crack propagation. The strength improved by about 50% and 54%, respectively for 90˚and 45˚orientation of NSM laminates when compared to beams with no stirrups.

M. Abdullah et al. (2019) [26] studied the use of steel tendons as prestressed NSM reinforcement on PSC beams, tested beams' was dimensions had a width of (150)mm, the height of (300) mm, length of (3300) mm, an effective span of (3000) mm, and (1250) mm shear span. Seven prestressed beams have been evaluated. one as a control beam, the other one been strengthened by means of NSM steel strand without pre-stressing force, while the rest 5 specimens have been strengthened using NSM steel strands that have been pre-stressed to 30%, 40%, 50%, 60%, and 70% of strands' tensile capacity, respectively. One strengthening strand was used for each one of the strengthened beams. Figure (2-9) shows a pre-stressing technique for strengthening specimens. The prestressed concrete beams strengthening by NSM strands were very efficient.

The strengthened PSC beam with a 70% prestressed steel tendon outperformed the different strengthened beams, according to the results of the trial. When compared to the control beam, the first crack load, yield load, and ultimate load of the prestressed beam strengthened with a 70%prestressed steel tendon rose by 40%,57%, and 40 %, respectively.

Figure (2-9) Prestressing system for strengthening specimens [26]

2.2.3 Using External Post-Tensioned Technique

Since the 1990s, using external prestressing in applications involving either the construction of long-span beams or strengthening existing structures has become increasingly widespread. The external prestressing system has various benefits compared to the internal post-tension approach, with regard to the following: low friction losses in unbonded tendons, more cost-effective and simpler constructions, also more convenient and easier tendon inspection and replacement maintenance [27].

Reza Aram et al. (2008) [28] investigated the efficiency of prestressed CFRP strips for flexural strengthening by testing four prestressed concrete rectangular section beams have length (2.4) m with (150) mm width and (250) mm high, one beam was used as a reference beam. Evaluations were made of three prestressed concrete girders, and one has been bonded with a CFRP strip. The beams details have been displayed in Figure (2-10).

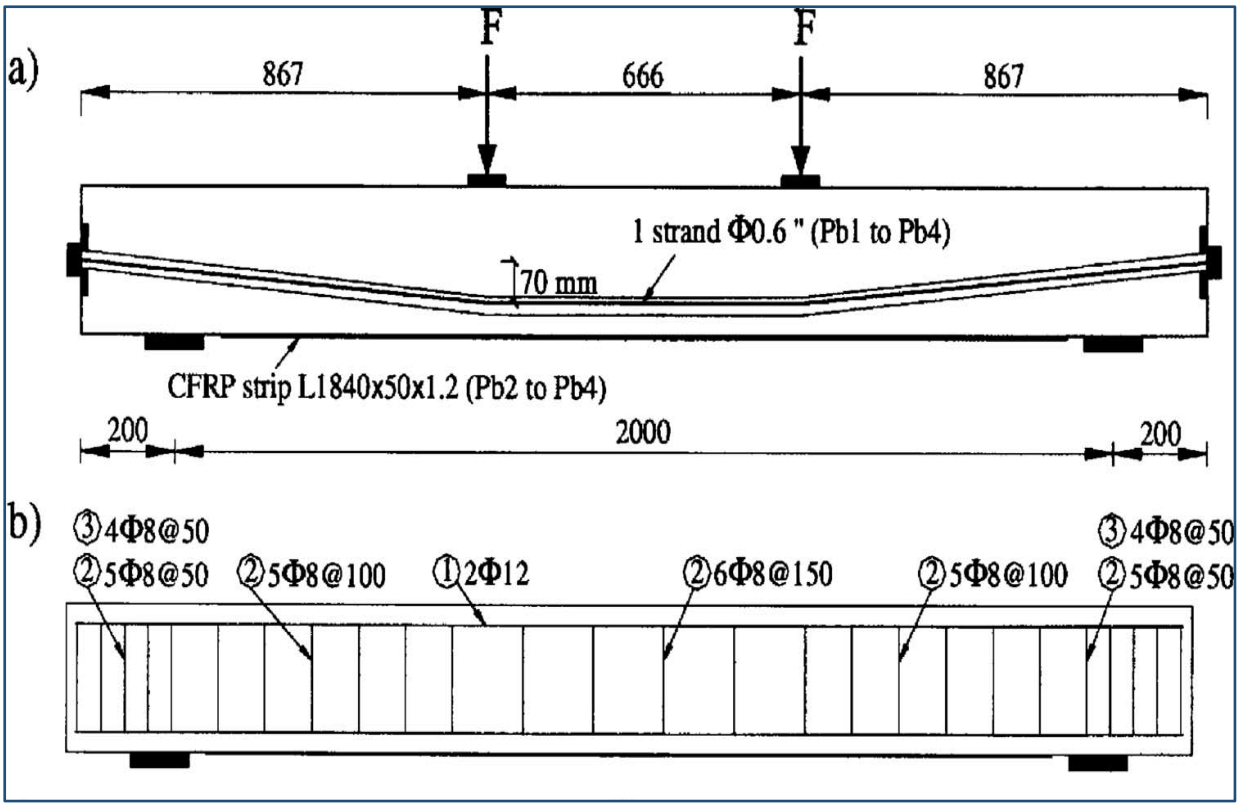

Figure (2-10) Beams details[28]

The findings of the experiment revealed that prestressing the strips had no effect on beam deflection or cracked width when compared to a non-prestressed instance. The failure load couldn't be increased and was decreasing. Furthermore, the deformation ductility has been visibly lower; such an approach might be more successful for large span beams, such as bridge girders, with small shear stresses from loading.

Allawi (2017)[29] surveyed experimentally strengthening prestressed concrete girders using the external post-tensioned approach. A total of four full-scale prestressed I-shape girders with a (1600) mm span have been built and tested up to failure under static and repeated loading.

As a result, a total of two girders have been strengthened externally with the use of the post-tensioned strands, whereas the other two girders have been left un-strengthened. The external prestressing scheme for strengthening is depicted in Figure (2-11).

The use of the external prestressing approach had led to the increase in cracking, yield, and ultimate moments attained 117.5%, 125.8%, and 118.1%, respectively and led to increase in the yield and ultimate moments under repeated loading as compared with reference girders by 128.4% and 116% for the studied cases, respectively.

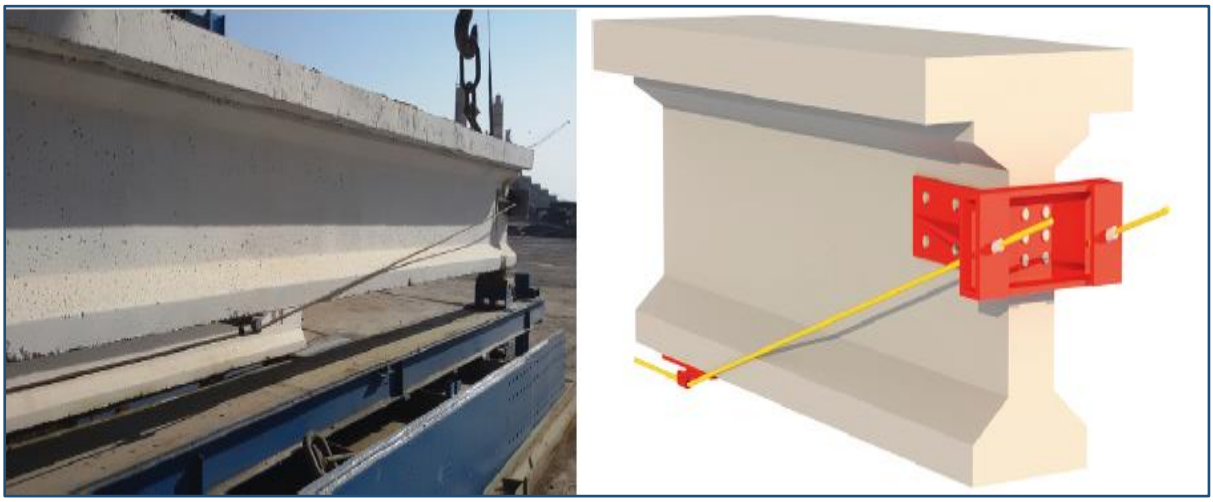

Figure (2-11) Girder detail and external prestressing scheme [29]

2.2.4 Using Fabric Reinforced Cementitious Matrix (FRCM) Systems

FRCM systems, which is also referred to as the mineral-based composite (MBC), textile-reinforced concrete (TRC), or textile-reinforced mortar (TRM), have only lately been brought into the construction sector as a viable alternative to FRPs. Fabric grids (which are made up of fibers like glass, carbon, and others) and a cementitious agent (mortar) serving as matrix and binder make up FRCM composites. Also, the matrix utilized in FRCM composites has a high thermal capacity and compatibility with the substrates of concrete in comparison with epoxy resin that is utilized in the FRPs. [19] The use of mortar instead of epoxy in the system enhances heat/fire resistance as well as compatibility with concrete substrate. By combining the benefits of lightweight glued CFRP-strips with extra concrete layers that have stronger bond qualities and reduced temperature

sensitivity, TRC offers a unique alternative for strengthening measures. Thin layers are available since the textile reinforcement doesn't need corrosion protection [30].

Hegger (2013) [30] tested two I-shaped prestressed concrete simply supported beams with dimensions length (6.5) m, high (0.7) m. I-shaped prestressed concrete beams strengthened by the TRC were tested under cyclic shear loading. Figure (2-12) depicts the use of textile reinforcement. According to the results used TRC provides a unique alternative for strengthening, Firstly, an increase of the shear fatigue strength can be obtained by strengthening the web with a TRC of about 51.5%. Secondly, the static shear capacity also increases due to the TRC strengthening about 47%.

Figure (2-12) Application of textile reinforcement [30]

Pino et al. (2017) [31] investigated the efficiency of FRCM and FRP for the repairing of the damaged prestressed concrete girders. Three different prestressed concrete girders were tested: one was the reference girder, the second girder strengthened by the FRP, the last girder retrofitted with FRCM as shown in Figure (2-13). Specifically, three prestressed concrete girders that had been

recovered from old bridge were used as test specimens. As a result, the reference girder reached its moment value of 4,320 KN.m, corresponding to 95% of its theory calculation capacity.

In spite of the fact that the girder didn't really fail during the test, it showed signs of flexural failure in the future. The test was terminated when the maximum load applied by the actuator was reached. The expected enhanced capacity for a girder reinforced with FRP was 4,690kN.m, and the FRP-strengthened girder achieved this Figure, which is higher than the girder's initial capacity of (4,170) kN m. This work indicates that fiber-reinforced plastic (FRP) as a reinforcing method may successfully restore flexural strength to damaged prestressed concrete girders in a controlled environment.

Finally, it was expected that the girder strengthened by FRCM would get a failure load 4,020kN.m after being strengthened. In the course of testing, damage occurred early as a result of deck faults originating from specimen deconstruction, at this time the test finished, and the resulting maximum moment was calculated to be 3,630 kN m. It's likely that the girder had reached the maximum capacity that had been predicted.

Figure (2-13) Application of FRCM system [31]

2.2.5 The Strengthening Using Aluminum Alloy Plates

Because of their excellent durability to corrosion effect, aluminum alloy plates ligament with magnesium phosphate cement are suggested a solution for reinforcing near sea structures that are subjected to extreme weather effects and effect of oil and gas platforms [32].

Chang et al. (2020) [32] studied the flexural behavior of simply supported prestressed concrete (C40) beams that are strengthened using aluminum alloy Plates. A total of six unbonded post-tensioned concrete specimens with different reinforcement ratios are subjected to static loads at first, the second step strengthened using AA plates as shown in Figure (2-14). The flexural strength and displacement ductility factor of the six specimens increased and decreased by an average of 14% and 34.14%, respectively.

Figure (2-14) Beams dimensions and strengthening scheme[32]

2.3 Slurry Infiltrated Fibrous Concrete (SIFCON)

Steel fiber-reinforced composites, which use a considerable amount of steel fibers, were first propositioned by Lankard in 1979 at the Engineering Research Institute in Mexico [33].

A new behavioral phenomenon, fiber lock, is observed in SIFCON, which is confirmed to be in charge of for stress-strain characteristics of the material. A combination of mechanical and frictional interlock and the matrix bond is thought to be responsible for the material's exceptional stress-strain capabilities. Mechanical and frictional interlock. SIFCON also has high range of strength as well as a high degree of ductility, which makes it a considerably superior material for structural constructions when unexpected loads are encountered during service operations [34].

SIFCON is a class of sophisticated materials used in constructions and is classed as such [35]. SIFCON has been utilized as a pavement overlay material, and it has also been employed in real construction as a material for the repair and renovation of concrete bridge decks, among other things. Another practical application of this material was the connecting of seismic-resistant reinforced concrete frames, which was another practical application of this material [36].

2.3.1 Materials and Mix Proportions of SIFCON

There are four main design factors that should be considered in a SIFCON product. These are slurry strength, fiber volume, fiber alignment, and type.

The modulus of elasticity, tensile strength, and compressive strength of the hardened slurry affect the behavior of the SIFCON composite. The fiber volume depends on the fiber type and the vibration effort needed for proper compaction. Smaller or shorter fibers may pack denser than longer fibers, and higher fiber volumes can be achieved with careful and sufficient vibration.

Fiber alignment also greatly affects the behavior of a SIFCON product. Fibers can be aligned parallel or perpendicular to the loading direction or can be placed randomly into the mold. The ultimate strength, residual strength, ductility, and energy absorption properties are all affected by the fiber alignment [16].

Steel fibers and cement-based slurry are the two most important constituent materials in SIFCON's construction.

A-Fibers

SIFCON researchers have looked into a wide range of fibers. Fibers with hook ends, crimped ends, surface deformations, and straight ends are examples of this[14].

Steel fibers with hooked ends have been employed in this study. The lengths of the fibers range from 30 mm to 60 mm. Various length-to-diameter ratios are available from 60-100. In the vast majority of applications. Fibers that have been crimped or straightened have also been used in various applications. When comparing straight fibers to deformed fibers, it is usually possible to include a greater volume proportion of straight fibers.

It was discovered from the results obtained that the geometry of fibers has a significant impact on the compressive, splitting tensile, modulus of elasticity, and toughness of material because the network of fibers formed and their density is dependent on the size and shape of the fibers. It was also deduced from empiricism results that combining long and short fibers gives premium results [37].

The pull-out peak load be higher when the embedded length of steel fiber is increased, the peak load of smooth steel fibers was smaller than hooked-end steel fibers and the debonding resistance of hooked-end fibers increased significantly higher than that of smooth steel fibers [38]. The mechanical

properties of SIFCON (compressive strength and splitting tensile strength) were increased with increase in volume fraction of steel fibers [34].

B-Matrix

SIFCON matrix has no coarse aggregates but a high cementitious content. It may contain fine or coarse sand and mineral admixture such as silica fume, fly ash and latex emulsions. So, the matrix of SIFCON is either cement paste or flowing cement mortar as opposed to regular concrete used in FRC [34].

The slurry of the SIFCON can be produced using mineral and chemical admixtures such as silica fume, fly ash, and high-range water-reducing admixture [superplasticizer (SP)] to improve the performance [36].

The use of (20 %) fly ash in combination with (10%) silica fume, as a replacement of cement, improves the workability, decreases the viscosity of SIFCON mortar, and reduces the dosage of HRWR as possible. Therefore, SIFCON mortar, having proper flowability and filling ability properties, can be produced with silica fume and/or fly ash replacement by using a proper dosage of HRWR [39].

2.3.2 SIFCON Preparation

SIFCON preparation process is special due to the high content of steel fiber. In FRC, the steel fibers are closely mixed with the wet concrete mix before mixing into shapes. Whereas, SIFCON is created through sprinkling fibers first into a mold till it is completely filled, as seen in Figure (2-15).

Fiber network is then infiltrated with cement-based slurry. Throughout the fiber installation process, external vibration may be applied, also it can apply as layer by layer under vibration to be ensured that the slurry was penetrated completely into the fiber pack.

Total fiber volume is a function of many parameters, such as fiber form, diameter and aspect ratio; orientation; packing method; mold size; and vibration range [40].

Figure (2-15) Fabrication process of the SIFCON specimens [41]

2.4 Previous Studies of Strengthening Members by SIFCON

Shannag et al. (2001) [42] examined the behavior regarding shear-deficient reinforced concrete (RC) beams which are repaired by SIFCON. The SIFCON was constructed using hooked steel fibers that have been diameter (0·5) mm, length of (30) mm, and fiber volume fraction of 8%.

They evaluated a total of fourteen simply supported reinforced concrete rectangular beams, each (2000) mm long and with a constant cross-section of (150) mm x (200) mm, utilizing externally applied SIFCON jackets with thicknesses of (20) mm and (25) mm, as indicated in the Figure (2-16), to increase the beams' shear capacity.

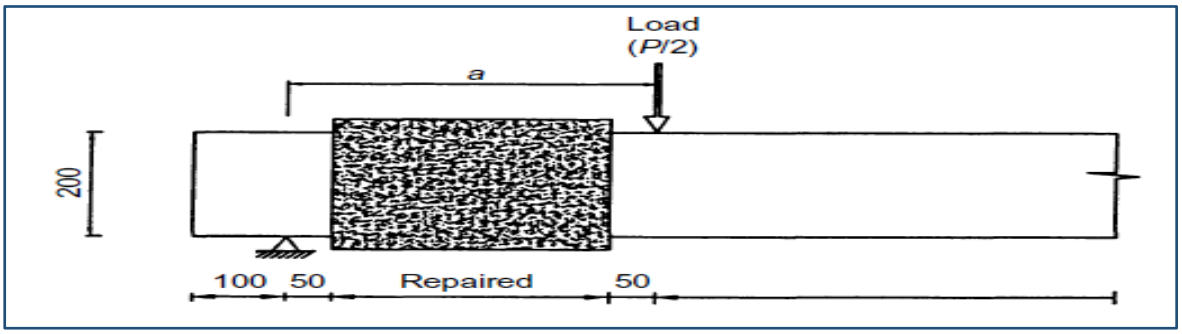

Figure (2-16) Jacket layout of repaired beams (dimension values in mm) [42]

The results indicated that all the beams failed in shear tests, and those repaired with SIFCON displayed an excellent shear capacity. The use of (25) mm thick SIFCON jacket as external shear reinforcement eliminated the brittle shear failure and increased the ultimate shear strength of the repaired beams from 25 to 55%.

Balamuralikrishnan (2015) [43] proposed an experimental approach for flexure retrofitting RC beams to rise the load ability that is related to SIFCON laminates that have been bonded directly to the bottom face of the beam through epoxy and tested under the compression loading. The beams dimensions, grouting and bonding method for SIFCON laminates are depicted in Figure (2-17).

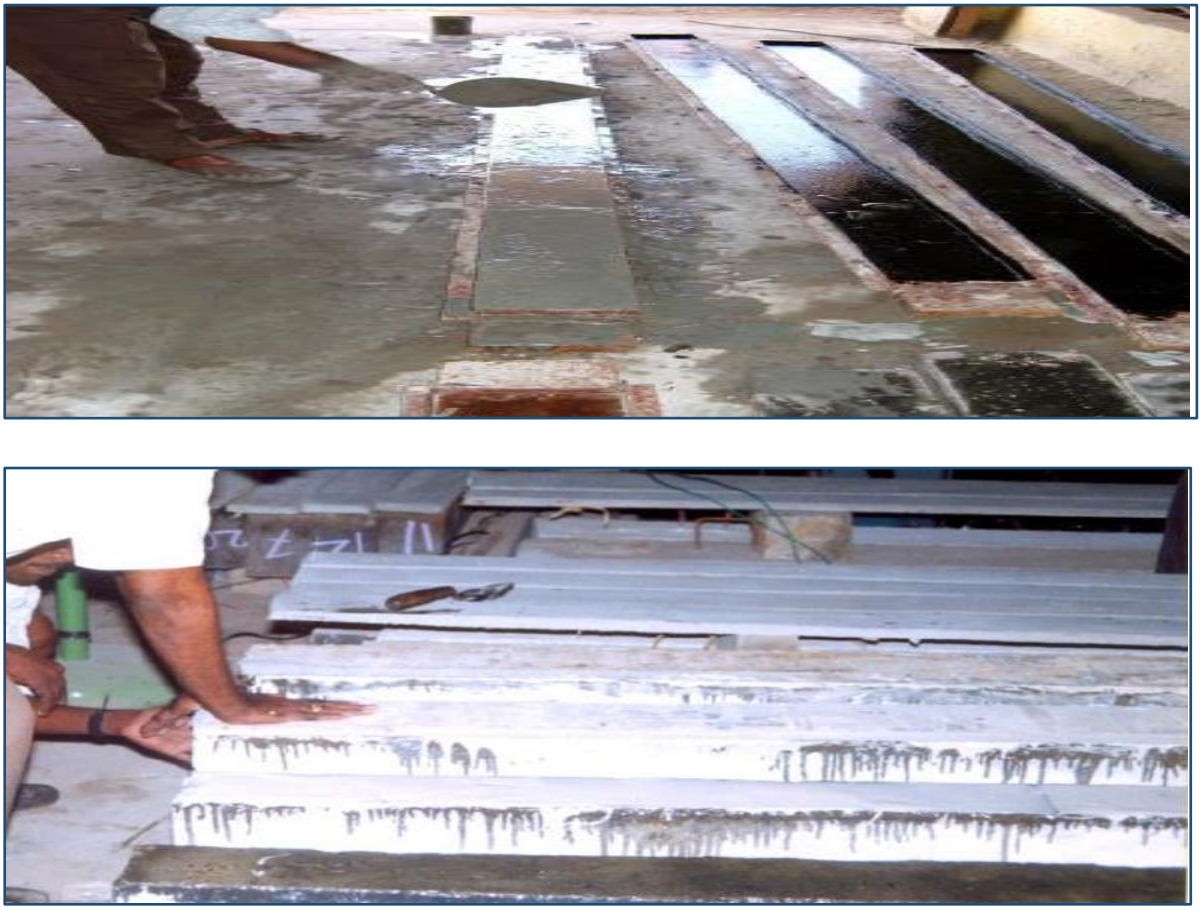

Figure (2-17) Grouting and bonding process of SIFCON laminates [43]

A total of four (250) mm depth, (125) mm width, (3200) mm length beams having a (3000) mm effective span were cast and tested in the lab. Laminates with a (125) mm width, depth of (25) mm and (2950) mm length were bonded between beam supports. A total of two beams have been retrofitted with laminates of SIFCON, while the rest two beams have been examined as baseline specimens under compression cyclic load.

For laminates with used discrete steel fibers aspect ratio of 70 and a volume fraction of 8 %, SIFCON strengthened beams show a flexural strength improvement of (68 to 70) %. Due to the existence of metal fibers, SIFCON strengthened beams have better ductility than control beams. With regard to the analyses of the RC beams that have been strengthened by externally-bonded laminates, a nonlinear finite element model implemented in ANSYS proved to be an adequate predictive tool. In addition, the numerical solution for SIFCON strengthened beams shows a 20% reduction in load-deflection variance in comparison with experimental results. It exhibits a reasonable level of agreement with the experimental findings.

Dhamak and Wakchaure (2015) [44] investigated the behavior of flexural RC beams related to concrete grade M20 with precast SIFCON laminates bonded directly to the beam through epoxy adhesives was investigated by the researchers. Twenty-one beams with dimensions of (150 x 300 x1800) mm have been cast and tested under the static load. The steel fibers used in this research for laminates have been hooked end steel fibers with an aspect ratio of 50 and a (0.6) mm diameter, with a fiber volume fraction of 7% and 10%. According to the findings, the first crack load for a 7% fiber volume is 53%, 37%, and 131% for the two-side face, bottom face, and three-side face, respectively, compared to the traditional control beam.

For a 10% fiber volume, the first crack load for the two side faces, bottom face, and three side faces is 67%, 51%, and 152%, respectively, compared to the

traditional control beam. For a 7% fiber volume, the ultimate load for the two side faces, bottom face, and three side faces is 147%, 80%, and 162%, respectively, compared with the traditional control beam. For 10% fiber volume, the ultimate load on the two-side faces, a bottom face, and three-side faces is 157%, 116%, and 185%, respectively, compared with the traditional control beam. We conclude that the use of 10% steel fiber and strengthened three-side faces gave the best results.

Sandansh et al.(2016) [45] investigated the flexural strengthening of RC beams by externally bonded SIFCON laminates that are bonded to the bottom face at the beam's soffit through epoxy and evaluated under two-point loading as shown in Figure (2-18).

A total of six beams with the width of (150) mm, depth of (230) mm, length of (1650) mm, two 10Ø mm at the top, two Ø12 mm at the bottom, and stirrup Ø6 mm @150 mm c/c M20 was the concrete grade utilized. A total of four SIFCON laminates with the width of 150 mm, depth of 25 mm, and length of 1550 mm were employed, each having a hook steel fiber diameter of 0.5 mm and an aspect ratio of 70, with two percentages of 6% and 8%. The results indicated that the strengthened beams had a 72.4% increase for laminates with a volume fraction of 8% and a 47% increase in flexural strength for laminates with a 6% volume fraction. The deflections were considerably decreased, resulting in an increase in the strengthened beams' stiffness.

Figure (2-18) Strengthened beam with SIFCON laminate [45]

Kumar and Sarathkumar (2017) [46] studied the flexural strengthening of the M30 RC beam with precast SIFCON laminate, externally bonded to RC beams' tension face as can be seen in Figure (2-19), beam dimensions of (1500) mm x (100) mm x (200) mm. As major reinforcement and shear reinforcement, 12 mm and 6 mm diameter bars are used, respectively. Steel fibers with 30 mm length and 0.5 mm diameter are used in a laminate with dimensions of (500) mm x (100) mm x (50) mm. The results referred to an enhancement in the flexural strength; at any given load level, the ultimate load capacity increased 26.3% compared with control beam, the strengthened beam's initial crack load has been found to be higher than the standard flexural beams and increased stiffness for the strengthened beam. In addition, the flexible epoxy system will prevent the bond line from breaking prior to the failure and will contribute entirely to SIFCON's structural resistance.

Figure (2-19) Attaching SIFCON laminate over the beam surface [46]

Venkatesh and Kannan (2018) [47] studied the flexural behavior of the conventional and GFRC beams strengthened by precast SIFCON laminates. beams dimension (100) mm x (100) mm x (500) mm, used for beams M20 grade concrete, tested as simply supported beams. For SIFCON used E type of glass fiber has a diameter (0.4) mm to product SIFCON, V_f equal to 7%. The flexural load of the conventional concrete beam with laminate is raised 7% than the beam without laminate. The failure load of the GFRC beam (0.05% V_f) with laminate

is increased up to 26% than the conventional beam. The failure load of the GFRC beam for (0.1% V_f) with laminate is increased up to 34% than the conventional beam.

Sisupalan et al. (2019) [48] tested nine RC and FRC beams to investigate the strength of thin precast SIFCON laminates that are bonded directly to the side faces and bottom face of the beam through epoxy adhesives as shown in Figure (2-20).The beam dimensions were (1000 x 100 x 120) mm, the laminates of sizes (1000 x 100x 20) mm and (1000 x 120 x 20) mm have been cast with 5% steel fibers and tested under a two-point bending test. M30 concrete grade was used. SIFCON laminates are made of 0.5 mm diameter hooked end fibers with a 60-aspect ratio.

(a)

(b)

Figure (2-20) Beam strengthened with (a) three face,(b) bottom face [48]

Results showed that using SIFCON laminates to strengthen FRC and RC beams resulted in a considerable increase in first crack load and the production of many finer cracks. Also, the ultimate load-carrying capacity that is related to RC beams with strengthened solely on the bottom face has

been 14% higher compared to that of typical RC beams, while with three faces strengthened it was shown to be 29% higher. In the case of FRC beams, strengthened beams were stronger. A single face strengthened beam had a 55% load-carrying capacity, whereas a three-face strengthened beam had a 133% load-carrying capacity more than controls.

Hameed et al. (2020) [49] studied the strengthening of concrete prisms using the various volume of hook-end steel fibers with a diameter of 0.6 mm and 50 aspect ratio have been utilized for casting the SIFCON layer (6, 7.5, & 9) % as shown in Table (2-1) that has been utilized for casting various thickness layers of SIFCON (15mm, 25mm, and 35mm) and the location of glued SIFCON layer (top, top & bottom, and jacking) on the strengthening of normal concrete grade M25 prisms are cast. Table (2-2) show prism's dimension and Table (2-3) explain the locations of the strengthening.

In all cases of strengthening the prisms' cross-section is constant, i.e., normal concrete prisms as well as the SIFCON laminate are glued to have a total composite section of (100mm x 100mm).

Table (2-1) Concrete mix proportions [49]

MIX	Cement kg/m^3	Sand kg/m^3	Gravel kg/m^3	w/c	%Steel fiber	%SP
normal	425	718	966	0.4	-	-
SIFCON1	900	900	-	0.3	6	1.6
SIFCON2	900	900	-	0.3	7.5	1.6
SIFCON3	900	900	-	0.3	9	1.6

Table (2-2) Prisms dimension [49]

Prism size (height x widths x length) mm		
bottom	Top+Bottom	Jacketing
85 x100 x400	70 x100 x400	85 x100 x400
75 x100 x400	50 x100 x400	75 x100 x400
65 x100 x400	30 x100 x400	65 x100 x400

Table (2-3) Location of SIFCON strengthen laminates [49]

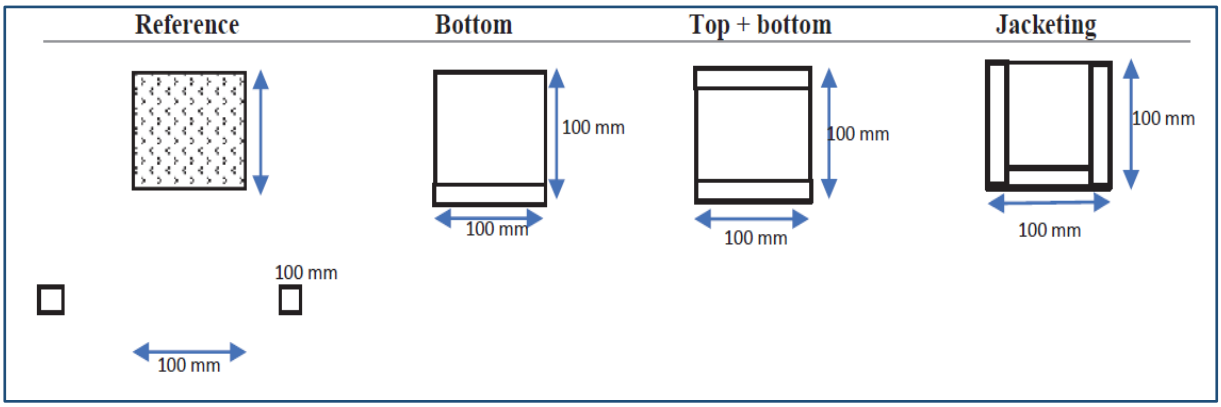

The results indicate that load-carrying capacity, flexibility, and hardness of the hybrid section are increased with the increase of the volume percentage of fiber and SIFCON layer thickness.

The maximal ultimate flexural loading for strengthened beam may be accomplished in jacketing case. For extra 9% of steel fiber, values have been 901%, 565%, and 1149 % of reference prism for 25 mm, 15 mm, and 35 mm thickness. The optimal toughness result has been obtained in cases of bottom and top hybrid section. They have been 2396, 1915, and 3259% of control prism for 7.50%, 6%, and 9% steel fiber contents. SIFCON ductility and normal concrete hybrid section have been significantly increased, in comparison with reference prism. The optimal results of the ductility might be achieved in the case of the

jacketing which is approximately 2.54 for 35mm SIFCON layer and 9% steel fibers.

Hameed et al. (2020) [50] studied the different methods to retrofit RC beams after loading them to about 60 % of their ultimate load in flexural and shear using the SIFCON layers. The thickness of the SIFCON layer used was (35) mm made using 9 % steel fiber. Figure (2-21) depicts the features of these beams as well as their reinforcing configuration.

Two methods were used to strengthen the bottom of beam specimens, a fresh SIFCON layer and a precast SIFCON layer. The strengthening by using a fresh SIFCON layer led to the rise in failure load is about (51) % compared to reference beam while the rise in failure load when using the precast SIFCON is than that use of the fresh SIFCON around (91) % compared the reference beam. The stiffness of the two processes is increased used fresh and precast layers had an of 23.81 kN/mm and 27.78 kN/mm, respectively.

For other methods using the jacketing method, strengthened beams with fresh and precast SIFCON layer, led to increased, ultimate load capacity compared with the bottom layer strengthening method. It was increased by 167%, 196% from the reference beam by using the fresh and precast jacketing, respectively. The stiffness of the two cases is practically identical in both circumstances. The value of stiffness is improved by 168% of that of the reference specimen. The strengthening method by using bolts led to a higher strength than the use of fresh SIFCON layer by about 26% and 11 % in both bottom and jacketing cases respectively.

For shear strengthening of beams that have experienced a shortage in shear resistance the strengthening by Jacketing SIFCON layers acts as an outer shear strengthening in the case of beams with a lack of shear resistance. Figures (22) to (24) show the application of strengthening methods.

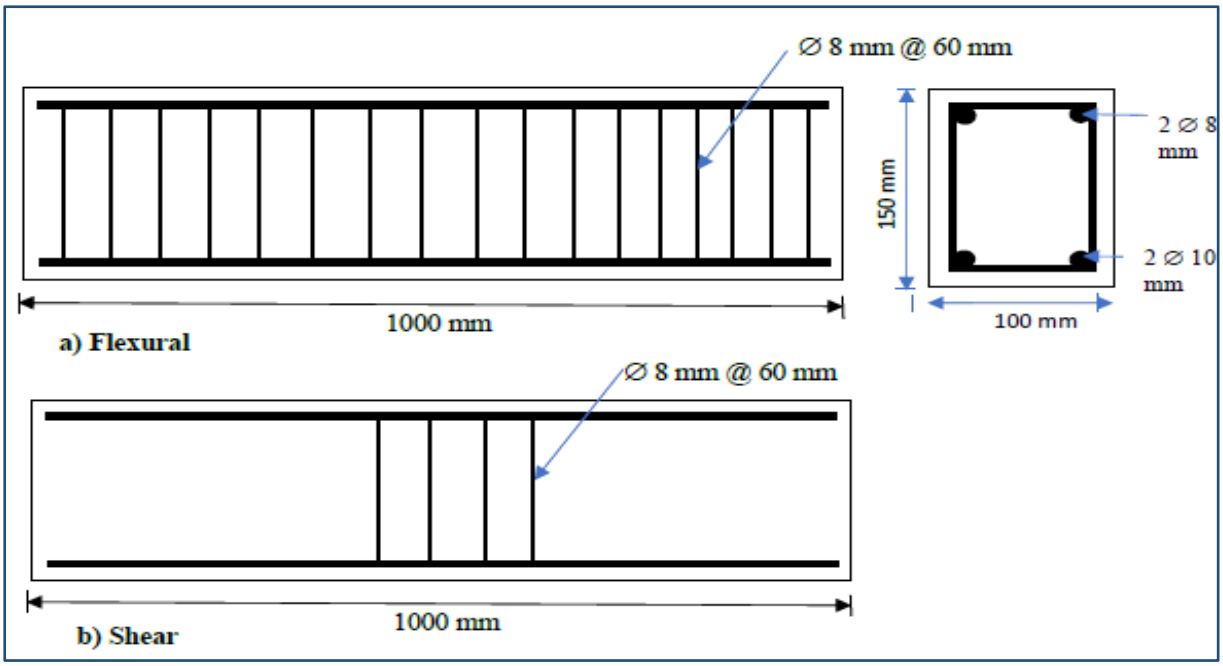

Figure (2-21) Details of flexural and shear failure beam[50]

Figure (2-22) Applied precast SIFCON layer[50]

Figure (2-23) Additional bolts are installed[50]

Figure (2-24) Jacketing of SIFCON layers[50]

2.5 Concluding Remarks

From the previous researches that are presented in this chapter, several remarks are concluded regarding the structural behavior of strengthening of prestressed concrete beams with a variety of the methods under flexural and shear and the behavior of the RC beam that has been strengthened with SIFCON laminates:

1-The limited number of studies of strengthening of continuous prestressed concrete beams and lack of enough experimental data of strengthening it, the researches in the literature studied the strengthening of simply supported prestressed beams strengthening with a variety of the methods using various materials.

2-Most researches over the past years were focused on investigating the structural behavior of simply supported RC beams with a normal strength concrete strengthened with SIFCON laminates.

3-All the research in the literature gave interest in studying RC beams' behavior strengthening by SIFCON laminate under the effects of static loads. The repeated load's effect has not been studied on the strengthened beams.

4- Only epoxy and fastening were used as a bonding method between the SIFCON laminates to strengthen the reinforced concrete beams, and no new bonding methods were tried.

CHAPTER THREE
EXPERIMENTAL PROGRAM

CHAPTER THREE

EXPERIMENTAL PROGRAM

3.1 General

The present chapter presents a description of an experimental program that was conducted to investigate the flexural and shear behavior of continuous prestressed concrete beams strengthened with precast SIFCON laminates under monotonic static and repeated loading. The load-carrying capacity, crack width, deflection, the modes of failure, toughness, redistribution of the moment of the beam and the bonding between the beams, and SIFCON laminates were investigated.

The experimental specimens consisted of twenty prestressed continuous concrete beams and sixty-six precast SIFCON laminates and a series of tests conducted on different materials to determine their physical-chemical properties. Also, different lab tests have been implemented to evaluate the physical-mechanical properties of the fresh and hardened concrete for HSC and SIFCON as compressive strength, splitting tensile strength and rupture modulus. Details of specimens' dimensions, longitudinal and transverse reinforcement, control tests for both fresh and hardened states of HSC, casting and curing, prestressing procedure, and testing setup and measuring instruments are also presented in this chapter. All specimens were cast and strengthened in Karbala Precast company; tests were carried out in Structural Laboratory at the University of Technology. Some of the properties of the materials were tested in the laboratories of the National Center for Constructional Laboratories and Research (NCCLR).

3.2 Description of Test Specimen

Twenty beam specimens with a (200×300) mm rectangular cross-section, (4300) mm length, and continuously supported on a (2000) mm clear span were fabricated, strengthened, and tested up to failure.

One prestressing strand seven-wire low-relaxation with (Φ15.24) mm a parabolic tendon profile. At the top and the bottom (2 Φ10) mm non-prestressing bars are used as longitudinal reinforcement.

Beams have been divided into two categories based on the behavior conditions the beams of flexure have been designed with additional strength in the utilized shear Φ (10) mm deformed mild steel bars stirrups at (100) mm c/c for ensuring the flexure failure, whereas shear beams that have been designed with no shear reinforcement in the maximum shear zone for ensuring shear failure. Simultaneously, two steel stirrups of the same diameter were used in the mid support zone to support the longitudinal bars and achieve the alignment and the correct location for the strand and longitudinal reinforcement in this zone. Moreover used Φ (10) mm deformed mild steel bars stirrups at (50) mm c/c in end zone (or end block). Specimen geometry is shown in Figure (3-1).

More details for beam specimens have been illustrated in Figures (3-2), (3-3), and (3-4). All the experimental beam specimens were designed according to **ACI 318-2019** [51] , **Design of prestressed concrete Nilson** [9] ,and **PCI Design Handbook 7th Edition 2014** [52] requirements (see Appendix A).

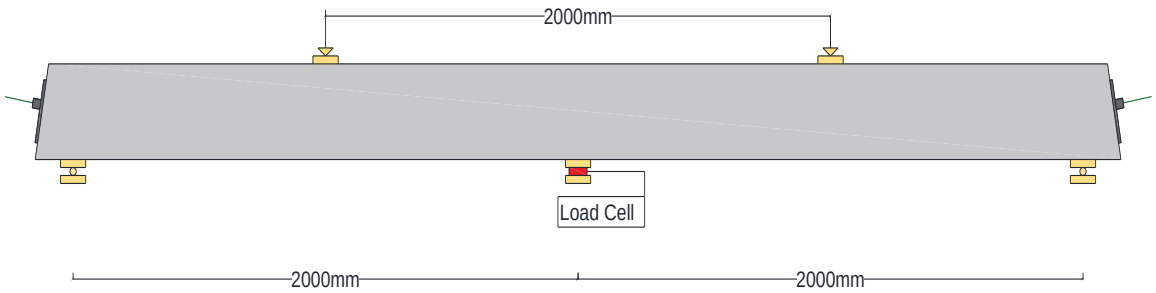

Figure (3-1) Geometry of test beam test setup, supports and load application

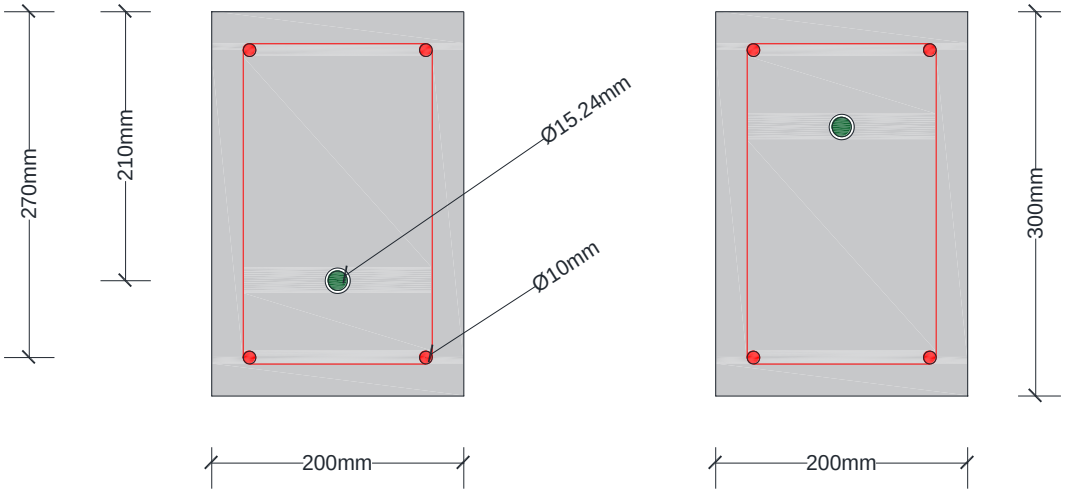

a- Beam section of sagging region b - Beam section of hogging region

Figure (3-2) Specimen dimensions rectangular cross-section

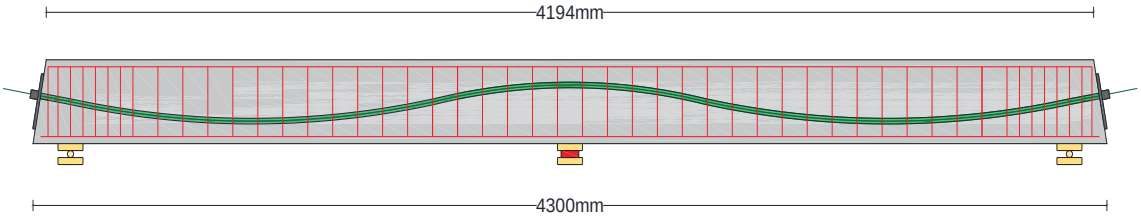

Figure (3-3) Reinforcement arrangement and tendon profile of flexure test beam

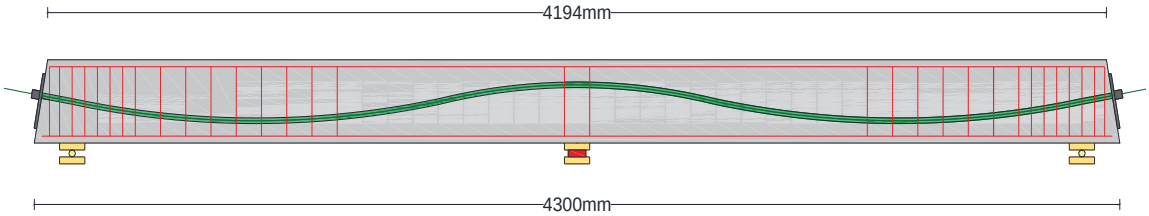

Figure (3-4) Reinforcement arrangement and tendon profile of shear test beam

3.3 Specimen's Categories

Twenty 4300 mm length continuous prestressed concrete beam specimens. They were divided into two identical categories, each consisting of ten specimens. The first category was studied flexural behavior; the second category was studied shear behavior. Each category consisted of two groups as follows: the first group consisted of beams tested under monotonic static loading, the second group consisted of beams tested under repeated loading; Figure (3-5) depicts a flow chart illustrating the experimental details of the specimens that were tested.

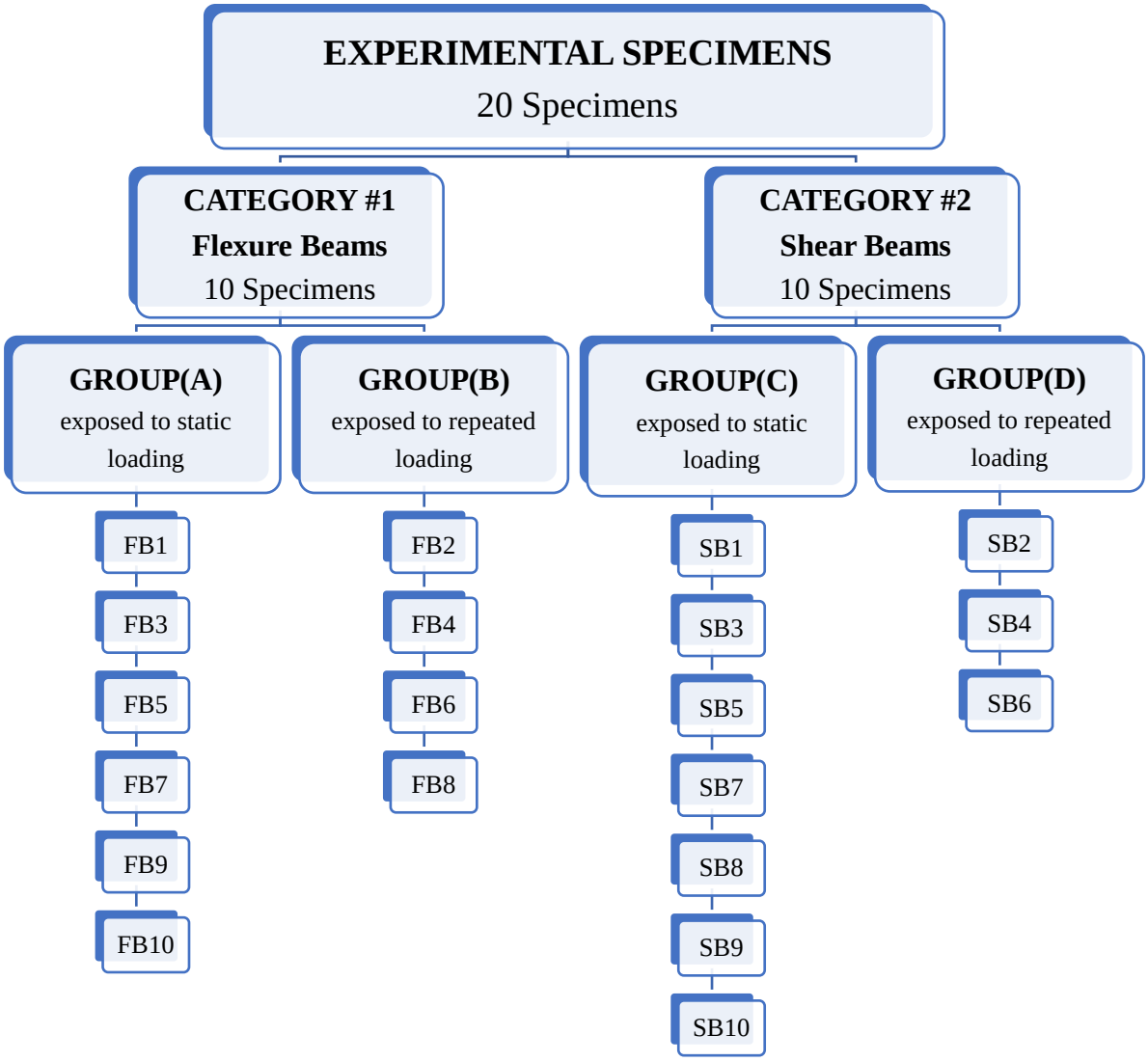

Figure (3-5) Flow chart of the experimental details of tested specimens

3.4 Specimens Identification

The beams were separated into two categories based on the beam behavior condition, which is described in detail in the Table (3-1). The categories were as follows:

Table (3-1) Beam specimen identification

Beam Name	The Describe
FB1	Control flexure beam under monotonic static loads.
FB2	Control flexure beam under repeated loads.
FB3	Flexure beam strengthened with precast SIFCON laminates: 2[200×1800×30] mm one at each sagging zone and [200×1600×30] mm at hogging zone glued by epoxy under monotonic static loads.
FB4	Flexure beam strengthened with precast SIFCON laminates: 2[200×1800×30] mm one at each sagging zone and [200×1600×30] mm at hogging zone glued by epoxy under repeated loads.
FB5	Flexure beam strengthened with precast SIFCON laminates: 2[200×1800×30] mm one at each sagging zone and [200×1600×30] mm at hogging zone. Glued by epoxy and bonded by end anchored steel plate under monotonic static loads.
FB6	Flexure beam strengthened with precast SIFCON laminates: 2[200×1800×30] mm one at each sagging zone and [200×1600×30] mm at hogging zone. Glued by epoxy and bonded by end anchored steel plate under repeated loads.
FB7	Flexure beam strengthened with precast SIFCON laminates: 2[200×1800×30] mm one at each sagging zone and [200×1600×30] mm at hogging zone. Glued by epoxy and bonded by U shape end anchored steel plate under monotonic static loads.

FB8	Flexure beam strengthened with precast SIFCON laminates: 2[200×1800×30] mm one at each sagging zone and [200×1600×30] mm at hogging zone. Glued by epoxy and bonded by U shape end anchored steel plate under repeated loads.
FB9	Flexure beam strengthened with precast SIFCON laminates: 2[200×1400×30] mm one at each sagging zone and [200×1600×30] mm at hogging zone glued by epoxy under monotonic static loads.
FB10	Flexure beam strengthened with precast SIFCON laminates: 2[200×1800×30] mm one at each sagging zone and [200×1200×30] mm at hogging zone glued by epoxy under monotonic static loads.
SB1	Control shear beam under monotonic static loads.
SB2	Control shear beam under repeated loads.
SB3	Shear beam strengthened with precast SIFCON laminates: 2[2100×300×30] mm one at each side face of the maximum shear zone, 2[975×200×30] mm at the lower face and [2100×200×30] mm at the upper face glued by epoxy under monotonic static loads.
SB4	Shear beam strengthened with precast SIFCON laminates: 2[2100×300×30] mm one at each side face of the maximum shear zone, 2[975×200×30] mm at the lower face and [2100×200×30] mm at the upper face glued by epoxy under repeated loads.
SB5	Shear beam strengthened with precast SIFCON laminates: 4[700×300×30] mm parallelogram shape two at each side face of the maximum shear zone, 2[700×200×30] mm at the lower face and [1400×200×30] mm at the upper face glued by epoxy under monotonic static loads.

SB6	Shear beam strengthened with precast SIFCON laminates: 4[700×300×30] mm parallelogram shape two at each side face of the maximum shear zone, 2[700×200×30] mm at the lower face and [1400×200×30] mm at the upper face glued by epoxy under repeated loads.
SB7	Shear beam strengthened with precast SIFCON laminates: 4[500×300×30] mm two at each side face of the maximum shear zone ,4[500×200×30] mm two at the lower face and two at the upper face glued by epoxy under monotonic static loads.
SB8	Shear beam strengthened with precast SIFCON laminates: 2[2100×300×30] mm one at each side face of the maximum shear zone glued by epoxy under monotonic static loads.
SB9	Shear beam strengthened with precast SIFCON laminates: 4[700×300×30] mm parallelogram shape two at each side face of the maximum shear zone glued by epoxy under monotonic static loads.
SB10	Shear beam strengthened with precast SIFCON laminates: 4[500×300×30] mm two at each side face of the maximum shear zone glued by epoxy under monotonic static loads.

*Note: The laminates whose shape is not mentioned are rectangular laminates.

3.5 Strengthening Schemes

The description of strengthening schemes is displayed in Figures (3-6) to (3-16).

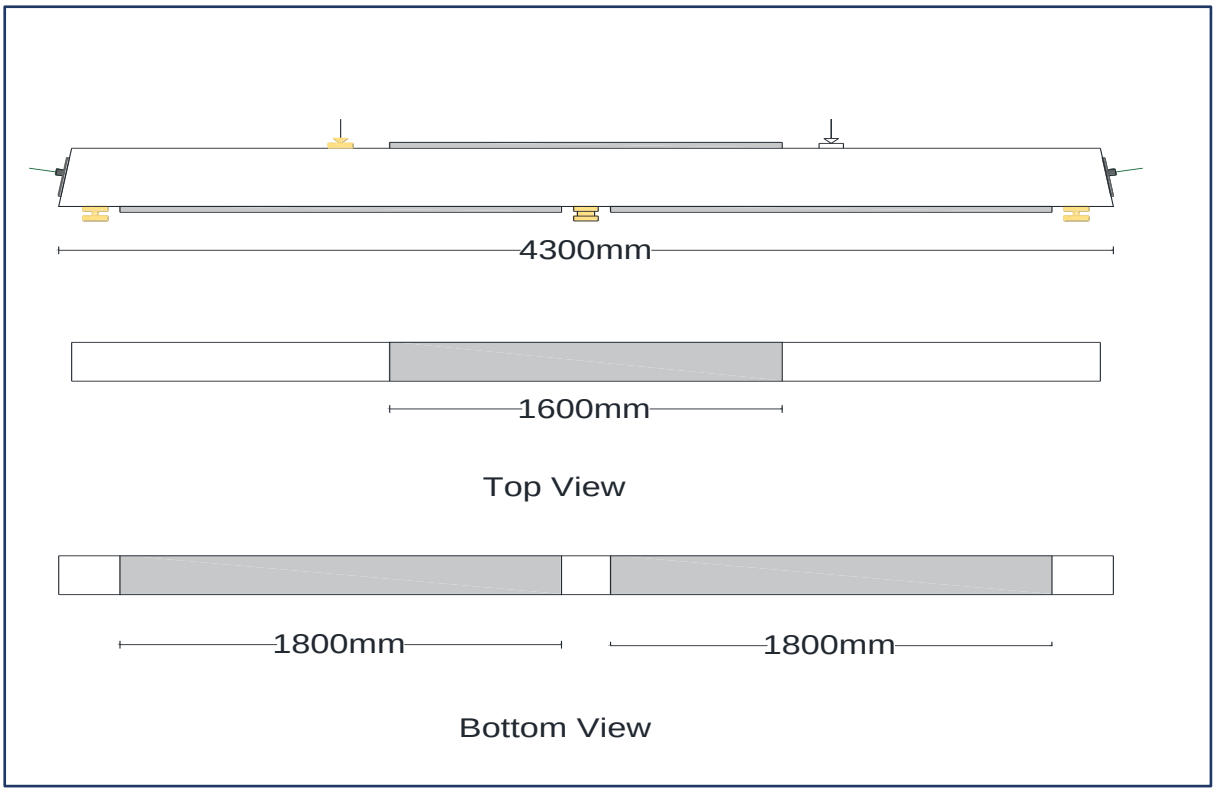

Figure (3-6) Flexure beam FB3 and FB4

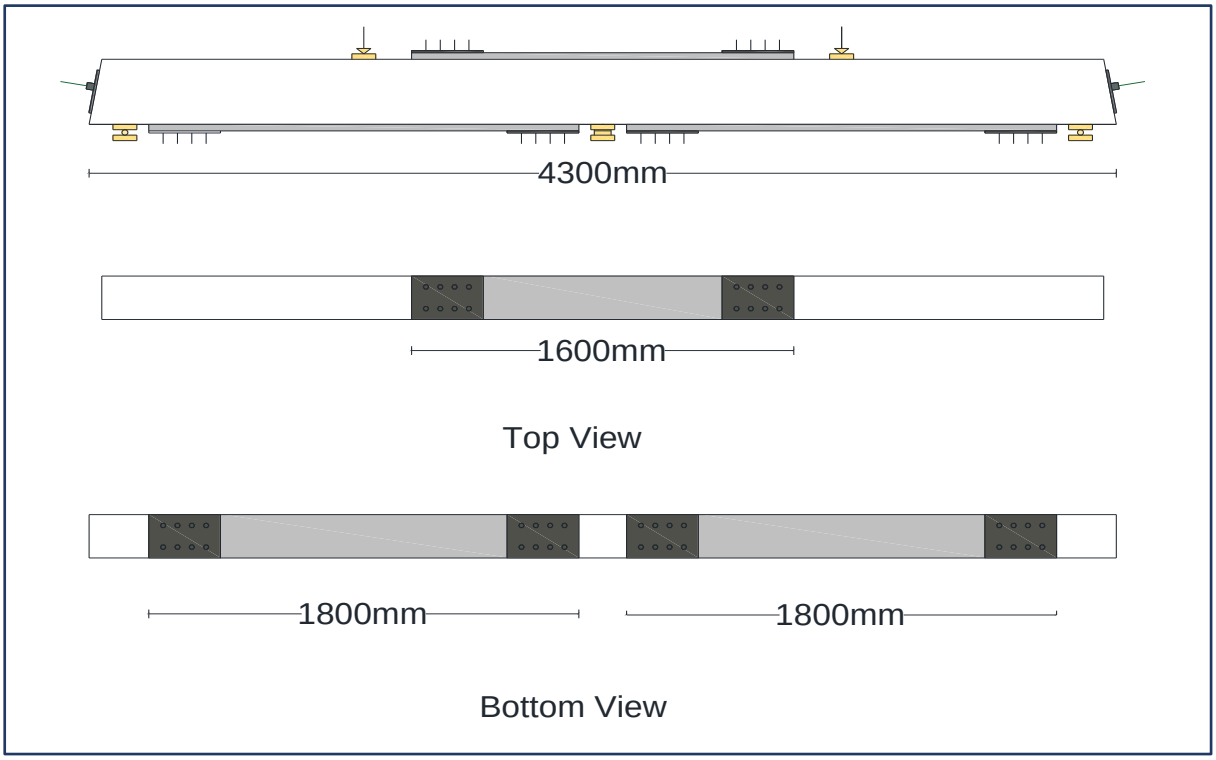

(a)

Figure (3-7) (a) Flexure beam FB5 and FB6 (b) End anchored steel plate

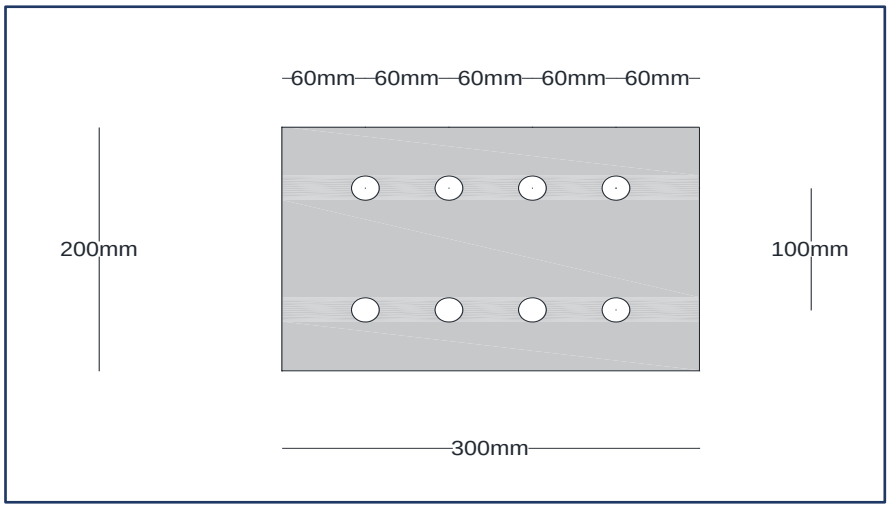

(b)

Continued Figure (3-7) (a) Flexure beam FB5 and FB6 (b) End anchored steel plate

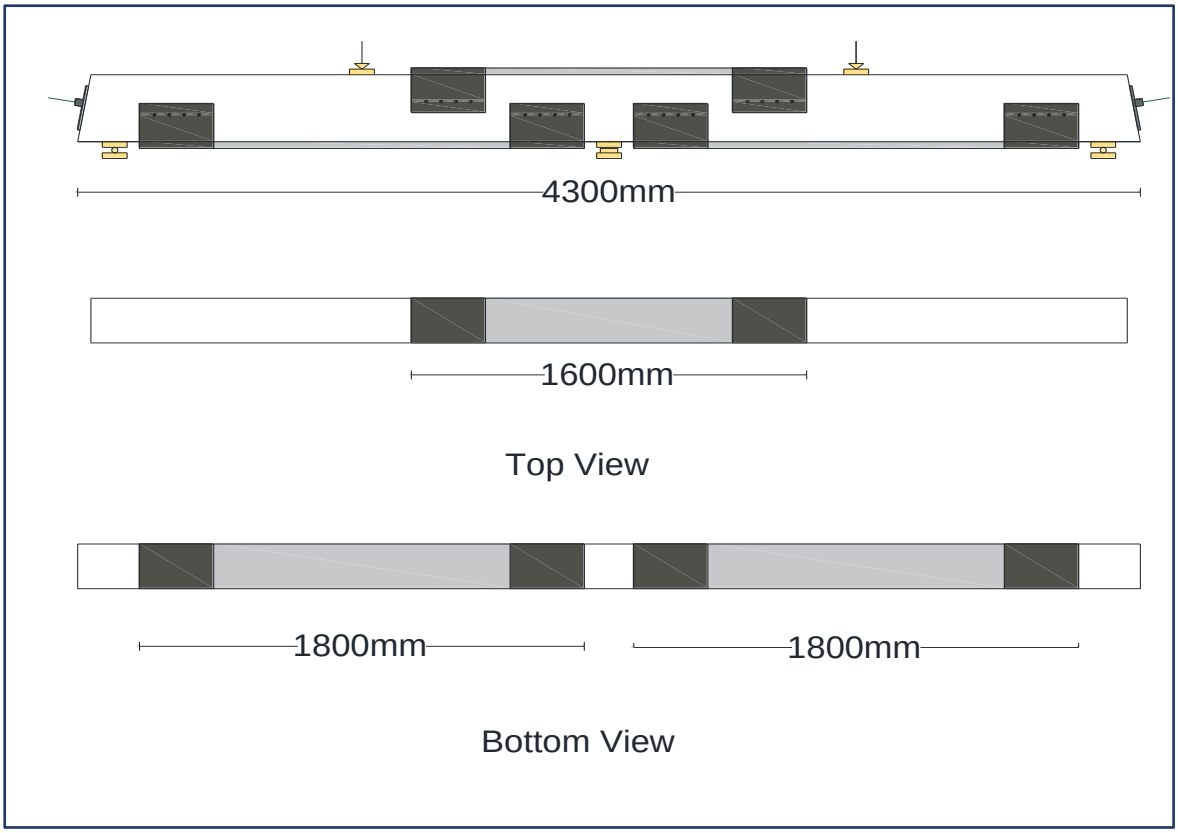

(a)

Figure (3-8) (a) Flexure beam FB7 and FB8 (b) Side view for the U shape end anchored steel plate

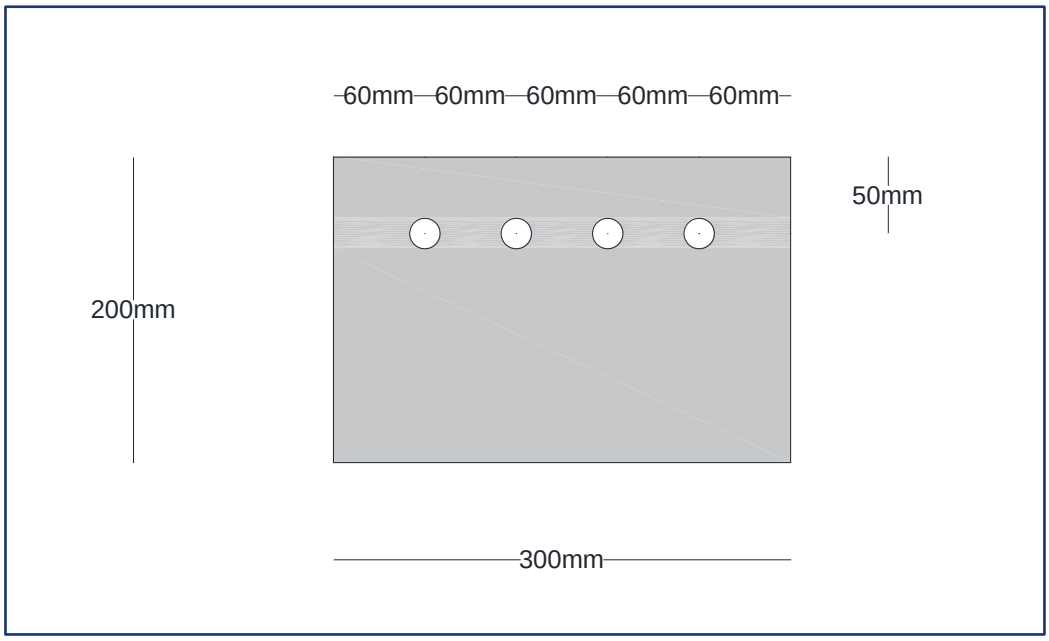

(b)

Continued Figure (3-8) (a) Flexure beam FB7 and FB8 (b) Side view for the U shape end anchored steel plate

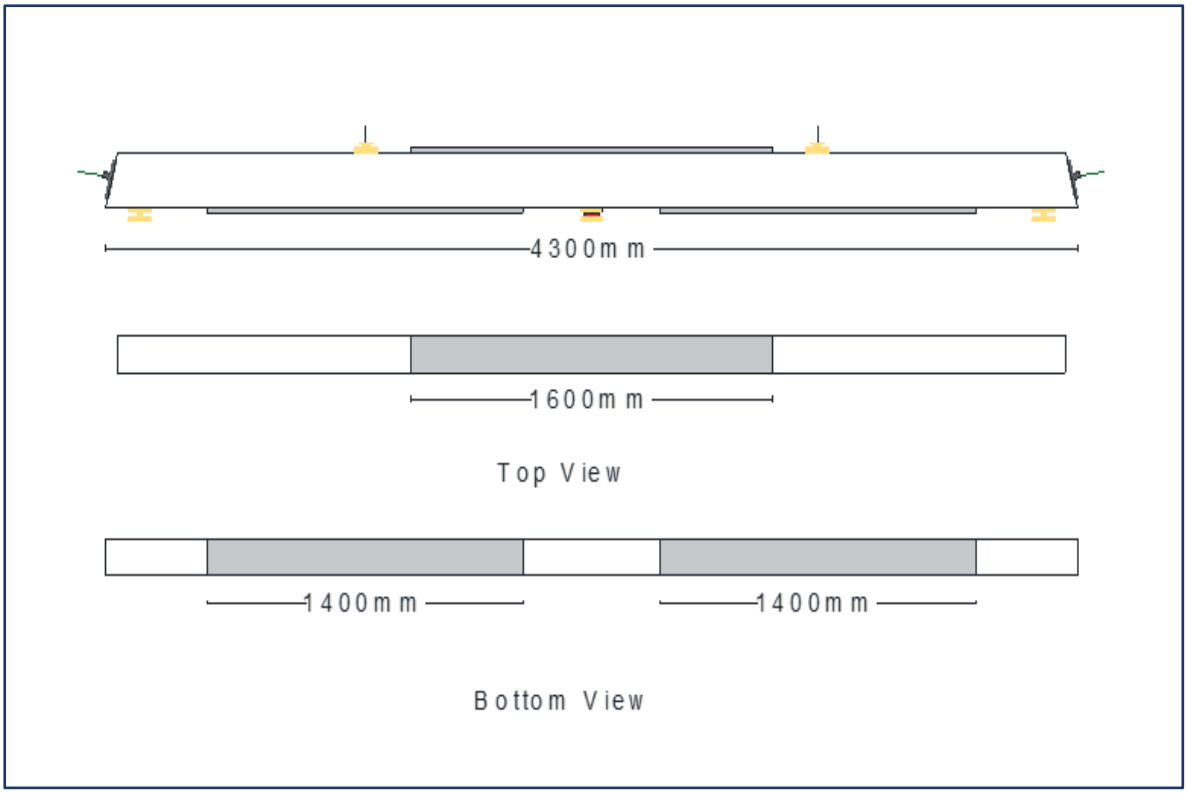

Figure (3-9) Flexure beam FB9

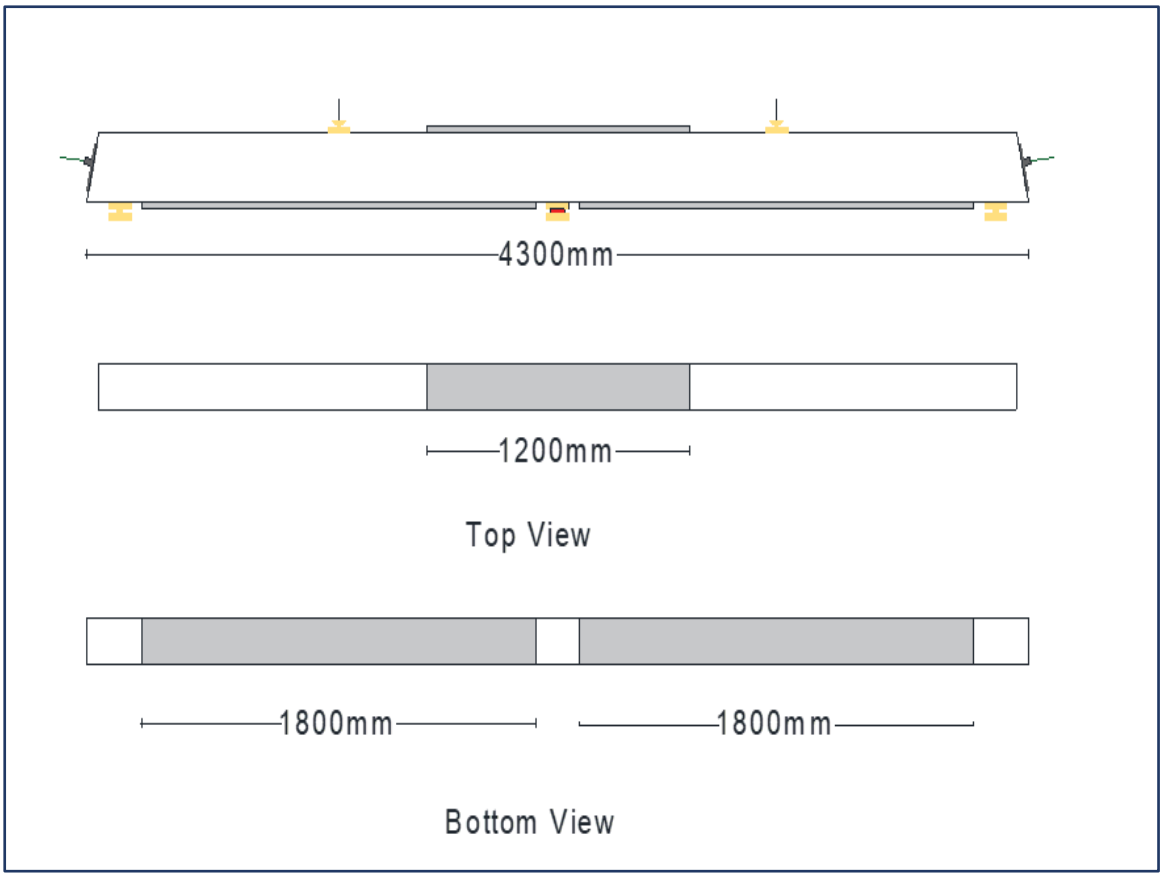

Figure (3-10) Flexure beam FB10

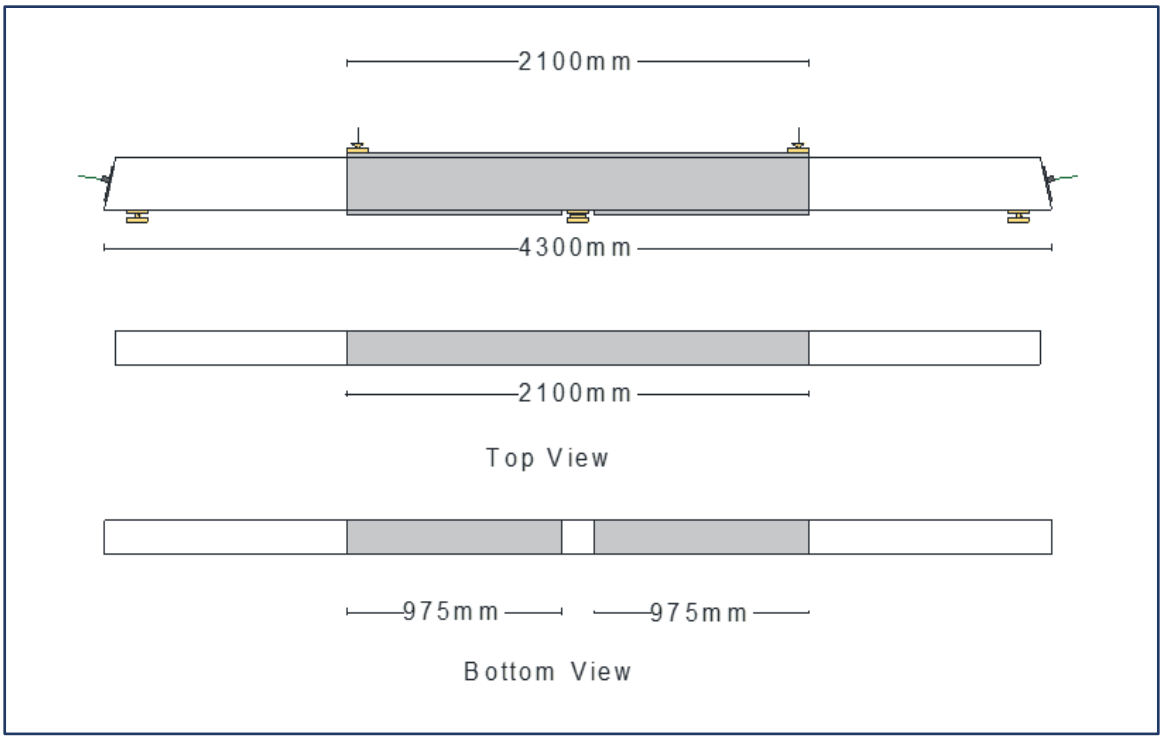

Figure (3-11) Shear beam SB3 and SB4

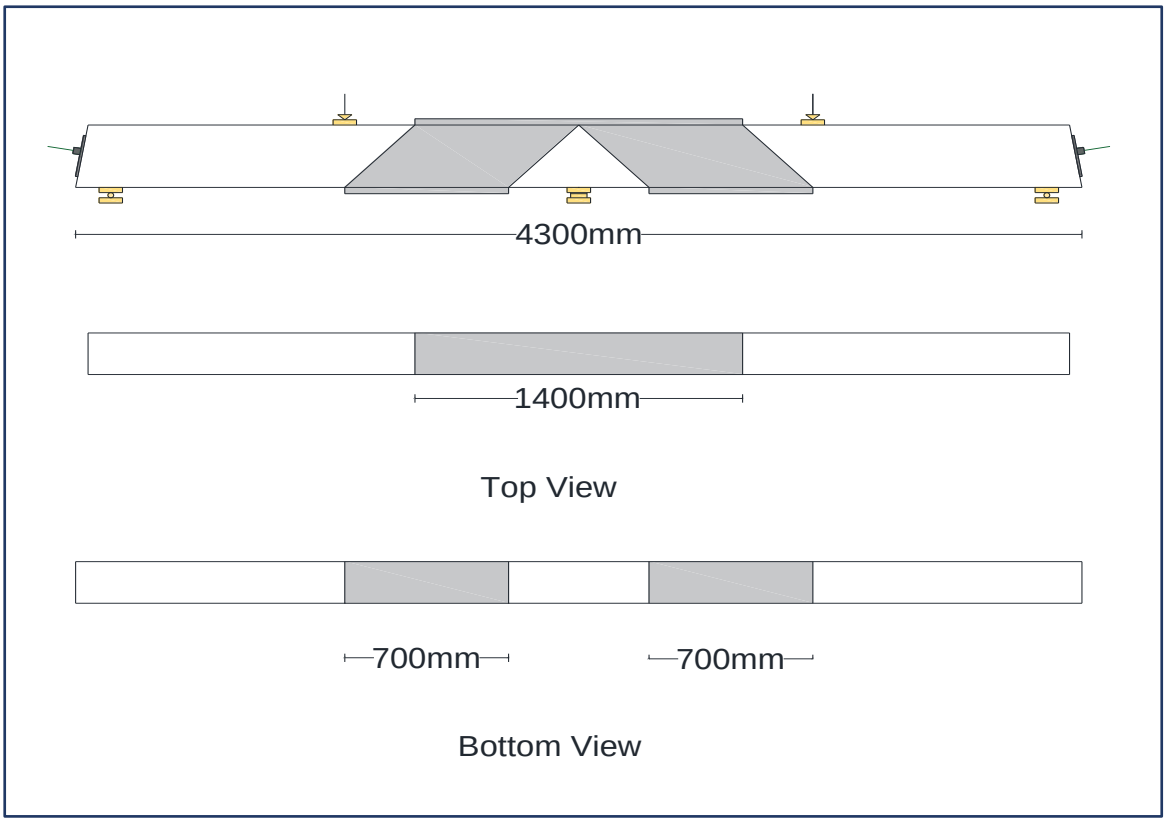

Figure (3-12) Shear beam SB5 and SB6

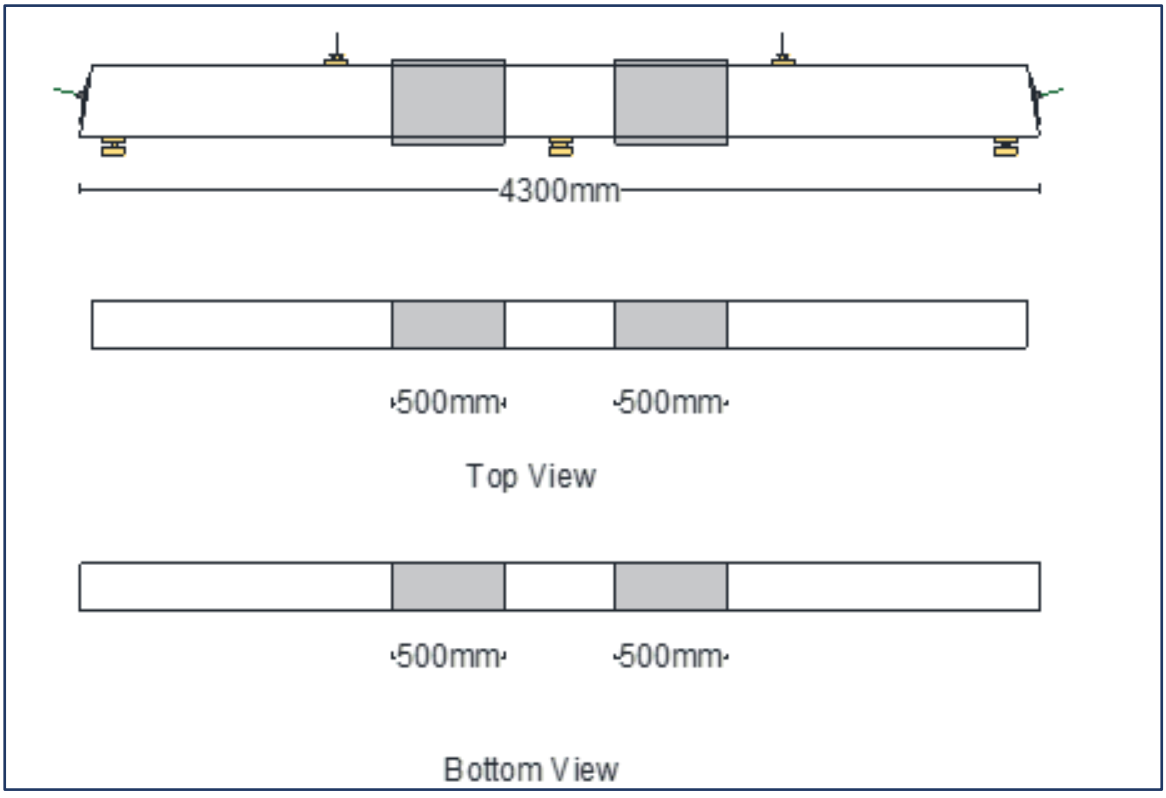

Figure (3-13) Shear beam SB7

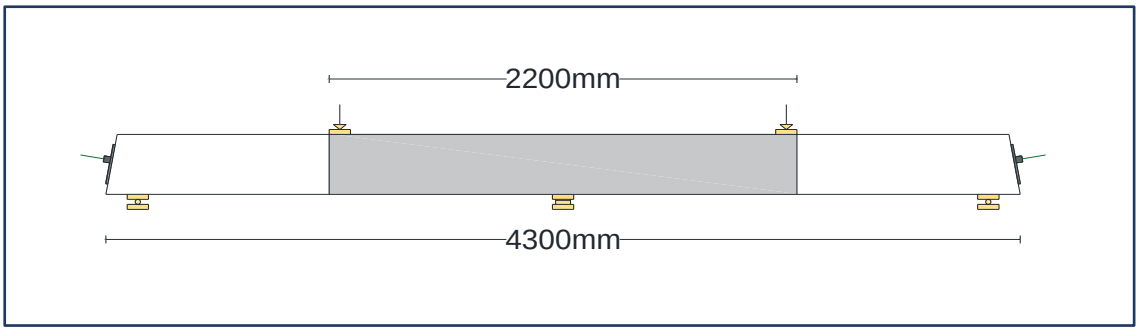

Figure (3-14) Shear beam SB8

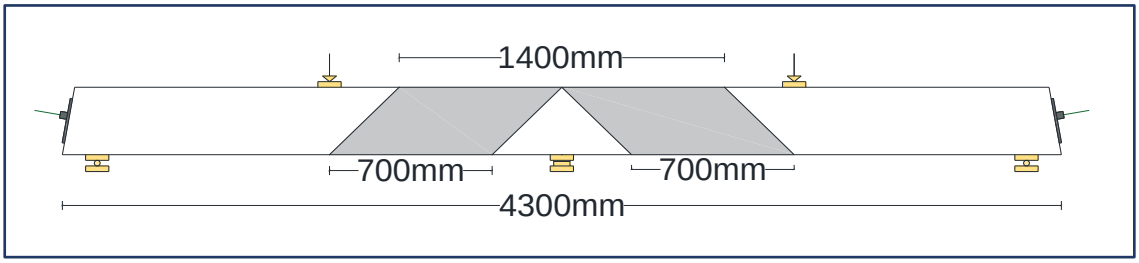

Figure (3-15) Shear beam SB9

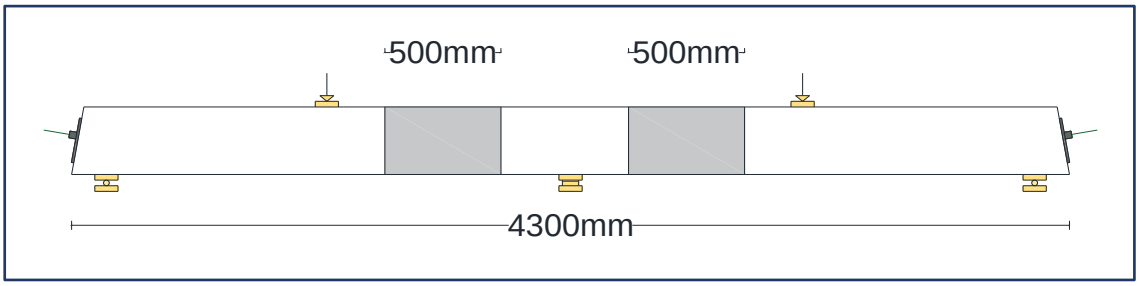

Figure (3-16) Shear beam SB10

3.6 Material Properties

This section describes the materials used in the manufacture of prestressed concrete beams and the precast SIFCON laminates.

3.6.1 Cement

OPC (Type I) has been utilized in the present study for HSC and SIFCON mixes. The chemical and physical properties of the cement, have been shown in Table (B-1) Appendix B. Those properties are approved with IQS No.5/1984 specifications of Portland cement.[53] as shown in Figure (3-17a).

3.6.2 Fine Aggregates

Fine aggregates were sieved on sieve No. 4 to discrete particles of a size larger than 4.75 mm for the HSC mix. At the same time, very fine sand (from the same type) with a maximal size of 600 μm (represent the size that has been utilized in the final selection mortar mix) has been utilized in the SIFCON mix.

In the SIFCON slurry, the significant requirement of the sand that has been utilized is its size; it must be sufficiently small for ensuring the full infiltration via dense fiber of steel with no clogging [54].Those properties are approved with ASTM C136 / C136M – 14 and IQS No.45/1984 standard tests, as listed in Tables (B-2) and (B-3) Appendix B [55] [56].

3.6.3 Coarse Aggregates

Natural rounded gravel (19 mm nominal size) was used for producing the HSC mix. Physical properties and sulphate content, along with the grading of coarse aggregates, were conducted as listed in Table (B-4) and (B-5) Appendix B. Gravel properties conform to IQS No.45/1984 standard test [56].

3.6.4 Silica Fume

Mega Add MS(D) (micro silica fume) which is a production of CONMIX LTD Company in U.A.E was used as a mineral admixture in producing HSC and SIFCON mixtures in this research. Properties of micro silica were obtained from the manufacture datasheet and presented in part (B-4) Appendix B. Those properties conform to the requirements of ASTM C1240 .15 standard specification [57]. As shown in Figure (3-17b).

3.6.5 Fly ash (FA)

Class F FA was utilized in the present investigation that has been a result of the combustion of coal through the electricity production in power station and contains less than 20% CaO. FA can be described as a glassy and fine powder

that is widely used as a cementitious and pozzolanic ingredient in hydraulic cement concrete ,the manufacture datasheet and presented in part (B-5) Appendix B conforms to the ASTM C618-10 requirement [58]. as shown in Figure (3-17c).

3.6.6 Chemical Admixtures

Sika ViscoCrete® 5930-L Figure (3-17) that is a third-generation high range water-reducing admixture (HRWRA), was used in producing SIFCON and HSC. It was used with a nominal dosage of (0.8–2)% liter by weight of cement) as recommended by the manufacturer. Sika ViscoCrete® 5930-L meets the requirements for SP in accordance with ASTM C494 / C494M 17 standard (ASTM C494 2015) The manufacturer's datasheet of these products is presented in part (B-6) Appendix B as shown in Figure (3-17d).

a-Cement b-Silica fume c-Fly ash d-SikaViscocrete-5930

Figure (3-17) Materials

3.6.7 Water

Clean poTable tap water was used in this study for washing the aggregates, mixing concrete batches, and curing all concrete specimens.

3.6.8 Steel Fiber

The steel fibers that have been utilized were hooked end with a (0.5) mm diameter and a (30) mm length. It’s supplied from Hebei YuSen Metal Wire Mesh

Co. in China and based on the requirements of the ASTM A 820/A 820 M-04[59]. Figure (3-18) illustrates hooked end steel fiber that has been utilized in the present study. According to the manufacturing company are explained Its shape and properties in part (B-7) Appendix B.

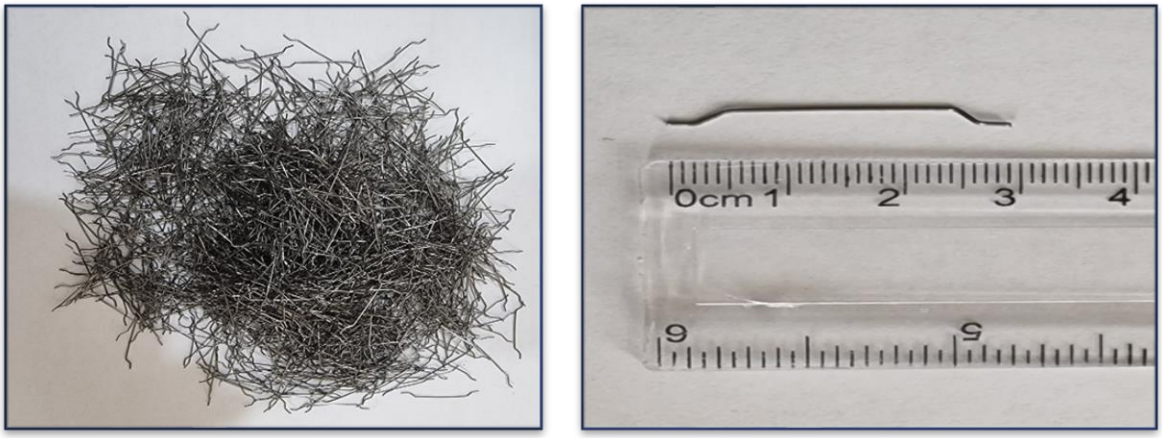

Figure (3-18) Hook steel fiber

3.6.9 Prestressing Reinforcement

Seven wire, grade 270, (Ø15.24 mm), low relaxation strand was used as post-tensioning prestressing reinforcement for all specimens and based on the requirements of the A416/A416M [60]. As shown in Figure (3-19), Table (B-6) shows the results of the test of used strands properties.

Figure (3-19) Strand Ø15.24 mm (7-wire)

3.6.10 Steel Bar Reinforcement

Deformed hot rolled mild steel bars diameters (10mm) for longitudinal reinforcement deformed bars was used in all specimens. The tensile test (for three specimens of steel bars) was done following ASTM A1064 / A1064M - 18a standard [61].The results are presented in Table (B-7) (Appendix B).

3.6.11 Plastic Duct

The plastic duct represents the most economical means to create a void for strands and will provide secondary corrosion protection with excellent behavior between strand and concrete. Plastic pipes (Ø 20 mm) that are usually used for in-house applications were used in producing the two-way piping systems are made from polypropylene random copolymer plastic and produced by Serene Plastik San. Tic. Ltd. (SERENEPLAST). Figure (3-20) shows the plastic duct.

Figure (3-20) Plastic duct

3.6.12 Steel Plate

Steel plates with the thickness (10 mm) were used as a bearing plate (End zone plate) of all beams and end anchor plate for strengthening some beams. Figure (3-21) illustrates the three types of steel plates used in this study. (Bearing plate, U shape end anchored steel plate, and end anchored steel plate).

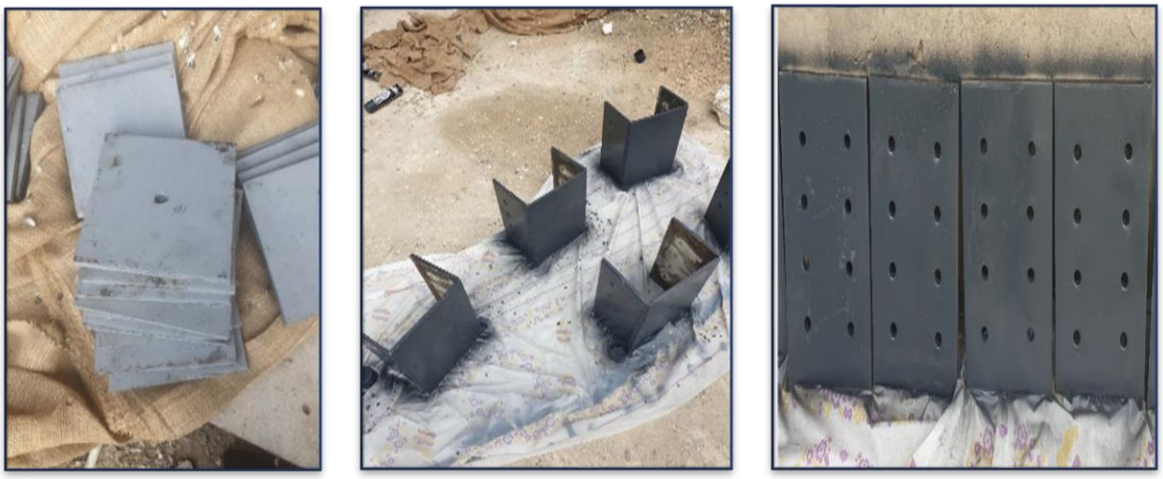

a- Bearing plate b- U shape end anchored steel plate c- End anchored steel plate

Figure (3-21) Steel plates

3.6.13Anchorage

Two-part single anchorage is used for longitudinal tendons in girders and bridges. In this type of anchorage, the wedge and conical anchor body introduce the pre-stressing force continuously into the member with the minimal front area through three load transverse planes. The separation of the anchor body and wedge plate makes it possible to insert the strand after casting the concrete. One wire strand single anchorage was used for all specimens in this study, as shown in Figure (3-22).

Figure (3-22) Single anchorage

3.6.14 Epoxy

Based on the bonding requirements, the following are the two types of epoxy used in this study:

1- Sikadur-331, a two-part epoxy resin, is utilized for attaching the precast SIFCON laminates to the prestressed concrete beam surfaces. The epoxy has been produced for manual mixing and applications. It has been manufactured by the Sika company, its details in (B-10). Figure (3-23 a) illustrates the product.

2- Sika Anchor Fix epoxy with the pourable consistency has been utilized to fill the holes of the bolts that have been utilized for fastening SIFCON layers by the prestressed concrete beams. It has been manufactured by Sika company; it has been illustrated in Figure (3-23b), its details (B-11).

(a) (b)

Figure (3-23) Epoxy (a) Sikadur-331 epoxy, (b) Sika Anchor Fix epoxy

3.6.15 Anchor Bolt

Each manufacturer has its own proprietary design for anchor bolts, and hence there are many different varieties available to choose from. All of them include a threaded end, to which a nut and washer can be added in order to support

an outside weight. Mechanical bolts and epoxy bolts are the only types of bolts that can be used after the concrete has been poured and allowed to set. Epoxy bolts are the strongest, but they are also the most difficult to install since the epoxy must be made to exact specifications, the hole must be extremely clean, and the set time must be closely monitored during the installation process. Used Φ10 mm anchor bolt chosen according to ACI Committee 355 report[62] as shown in Figure (3-24).

Figure (3-24) Anchor bolt

3.7 Molds Preparation

Ten steel molds have been made and utilized to cast prestressed concrete beams specimens and different size molds for cast SIFCON laminates, as can be seen from the Figure (3-25). The clear dimensions of the molds are (4300×200×300) mm. Before placing concrete, molds were coated with a thin oil film, and then the reinforcing cages were placed in the molds taking into consideration using PVC spacers to achieve the required concrete covers.

Figure (3-25) Steel molds

3.8 Reinforcement Details

Cutting the strand to the required length (i.e., one meter plus the length of the experimental beam specimen). Passing the strand through the PVC duct which was embedded in the mold before concrete casting, then formed as a three parabolic with the required dimensions. After that, the other longitudinal and stirrups reinforcing steel was delivered in the specified lengths and with the appropriate bends, as shown in Figures (3-26) to Figures (3-28).

Figure (3-26) Flexure beam reinforcement

Figure (3-27) Shear beam reinforcement

Figure (3-28) End zone reinforcement

3.9 Mix Design

Several trials of concrete mixes were conducted to determine the required proportionality between components where the mixing procedure was implemented according to ACI committee 211.4R,2008 [63]. Concrete mixes containing cement, Natural sand, crushed aggregate, mineral admix (Microsilica fume), and chemical admix (Sika Viscocrete-5930) have been utilized in producing the HSC. Mixture details are given in Table (3-2).

Table (3-2) Detail of HSC mixture

Mix	**Cement** Kg/ m^3	**Silica fume** Kg/ m^3	**Sand** Kg/ m^3	**Gravel** Kg/ m^3	**Water** Kg/ m^3	**HRWR % by wt. of binder**
HSC	495	55	686	1114	165	1.5%

To produce SIFCON many trials mixes were made in order to choose one mix to accomplish the optimum characteristics in the fresh and hardened states. However, the requirement for the fresh state was the mix fluidity and filling ability with no segregation or bleeding in the mortar. For SIFCON mortar used cement, fine sand, mineral admixture (20% FA +10% SF) replacement, by cement weight and chemical admixture (SikaViscocrete-5930) were used in the production of SIFCON with 11% V_f of hooked end steel fiber it was the maximum limit could apply in the molds, Table (3-3) shown the detail of SIFCON mix.

Table (3-3) Detail of SIFCON mixture

Mix	**Cement** kg/m^3	**SF** kg/m^3 **10%**	**FA** kg/m^3 **20%**	**Sand** kg/m^3	**Water** kg/m^3	**w/b*** **by wt.**	**V_f (%)**	**HRWR% by wt. of binder ****
SIFCON	619.5	88.5	177	885	265.5	0.3	11	2

*w/b= water/binder = water / (Cement +SF+FA)

**HRWR dosage was regulate to obtain similar flow diameter and adequate viscosity (without any bleeding and segregation)

3.10 Concrete Mix Preparation and Mixing Procedure

The process of mixing affects the quality of the concrete in the hardened state. The mixed material must be in uniform distribution and consistency in the concrete mix to reduce the weak spots within concrete specimens. For HSC used to product prestressing concrete beams mixing was performed by using a truck mixer. Figures (3-29) to (3-33) illustrate the casting procedure.

Figure (3-29) Placing reinforcement in molds

(a) (b)

Figure (3-30) The reinforcements in molds: (a)Flexure Beams (b) Shear Beam

Figure (3-31) Placing of concrete by truck mixers

Figure (3-32) The casting of concrete beam

For SIFCON, mortar needs sufficient mixing to obtain the required homogeneity, and a performance a rotary mixer, therefore, was utilized to mix the mortar. Mixing method procedures are summarized as follows:

1- The mixer was wetted before using.

2- The dry materials (cementitious materials and fine sand) are mixed first for about three minutes to get a uniform dry mix.

3- Two-thirds of the provided water was added to the rotary mixer. At the same time, one-third of the mixing water was mixed with the whole amount of HRWR (SikaViscocrete-5930L) for nearly one minute. Then, HRWR with one-third of mixing water was added to the mixer and mixed for nearly 10 minutes to obtain the wanted fluidity.

Figure (3-33) The casting of SIFCON laminate

3.11 Specimens Curing

HSC beams specimens, cubes cylinders and prisms cured with steam for a period of six hours after (three hours from casting). After 24 hours, the cast elements were removed from the forms then covered with a wet cloth for 28 days. SIFCON laminates cured 90 days.

For SIFCON laminates, specimens, cubes, cylinders and prisms after 48 hours of the cast elements were removed from the forms and cured in the water tank for 90 days. shown in Figures (3-34) to (3-36).

Figure (3-34) Curing

Figure (3-35) Precast SIFCON laminates

Figure (3-36) All prestressed beams

3.12 Fresh Properties of Hardened Concrete and SIFCON

3.12.1 Workability of HSC (Slump Testing)

The HSC Workability has been carried out by following the slump test process, which has been characterized in the ASTM C 143-15 [64].The w/c concrete has been adjusted to require equivalent slump (100mm ± 5mm).

3.12.2 SIFCON Matrix Flow Test

SIFCON matrix is defined as a slurry in terms of consistency. It must be flowable enough and have sufficient fineness to flow through the dense fiber network. The assessment of the workability of the SIFCON slurry is made by means of a flow test, according to ASTM C1437-15 [65]. The flow testing mold has been placed on the horizontal base plate, filling of the mold with slurry then the mold has been lifted right away and the slurry flowing freely. The flow has been computed as an increase in the average base diameter of mortar mass, represented as an original base diameter percentage. Figure (3-37) illustrates the slurry's flow test. All of the mixtures have been shown flow in a range of 180 ± 5%. Such consistency has been found suitable for achieving good infiltration for the slurry in dense fiber networks with no blockages and bleeding.

Figure (3-37) The mini slump flow test for SIFCON mortar

3.13 Mechanical Properties of Hardened Concrete and SIFCON

3.13.1 Compressive Strength

The cubical compression test was directed following BS 1881-Part 116. [66] using concrete cubes of (10× 10 × 10) cm (for SIFCON) and (15×15× 15) cm (for HSC). Concrete specimens were cured and prepared. This test was carried out by applying compression utilizing a hydraulic machine with a 2000kN capacity, as can be seen from the Figure (3-38). The cubical compressive strength (f_{cu}) for each batch was estimated at 28 days and 90 days age as the average of the compressive strength of three concrete cubes (Eq. 3-1).

$$f_{cu} = \frac{P}{A} \quad \text{..... (3-1)}$$

where:

P: denotes the peak load (N)

A: represents the specimen cross-sectional area (mm^2)

f_{cu}: represents the cubical compressive strength (MPa)

Figure (3-38) Compressive test of a cubical specimen

3.13.2 Splitting Tensile Test

This test was conducted for all batches using concrete cylinders of (15×30) cm (for HSC) and (10×20) cm (for SIFCON) following ASTM C496 / C496M–17 specification [67]. A hydraulic compression machine with 2000 kN capacity was used, as can be seen from the Figure (3-39). Finally, this test has been terminated when the tested cylinder has been broken into two halves with a longitudinal crack. The splitting tensile strength for each batch was computed at 28 days as the mean of splitting tensile strength of three cylinders (Eq. 3-2).

$$f_{ct} = \frac{2P}{\pi dL} \quad \text{..... (3-2)}$$

where:

f_{ct}:represents the splitting tensile strength (MPa)

d: represents the diameter of the cylinder (mm)

P: represents the peak load (N)

L: represents the length of the cylinder (mm)

Figure (3-39) A typical tensile test

3.13.3 Flexural Tensile Test (Modulus of Rupture)

The flexural tensile test was conducted for each batch based on ASTM C78 /C78M –18 standard tests. For each batch, three (10×10×40) cm simply supported concrete beams were tested under one-line load with the use of a hydraulic machine that has a 150 kN capacity as illustrated in Figure (3-40). When a specimen has been broken into two parts, the testing has been terminated. The flexural strength of each specimen was determined using the following equations adapted from ASTM C 78 / C 78M –18 standard testing [68].

Case 1: The fracture initiated within the middle third:

$$f_r = \frac{2PL}{bd^2} \quad \text{(3-3)}$$

Case 2: The fracture occurs outside the middle third by less than 5% of the length of the span:

$$f_r = \frac{3Pa}{bd^2} \quad \text{(3-4)}$$

where: f_r: modulus of rupture (MPa), L: span length c/c (mm), P: peak load (N), d: average depth (mm), b: average width (mm), a: The average distance between the line of the fracture and the nearest support is measured in millimeters.

Case 3: The fracture takes place outside middle third by over 5% of the length of the span; the testing should be disregarded.

Figure (3-40) A typical flexure test

3.14 Prestressing Process

For prestressed concrete beams, after attaining the age of (28) days for concrete, the prestressing process has been done according to the following sequences:

1-Attaching the end bearing steel plates at the ends of the beam then passing the grips at the ends of the strands.

2-Starting the prestressing process for the strands which were tensioned from one end. Accordingly, the strand was stressed to about (10%) then completed to 100% of the required prestressing.

The single-strand jack and the other prestressing accessories are employed to apply to prestress tensile force to the strand as shown in Figure (3-41). Single strand (mono wire) jack, operated by a motor-driven hydraulic pump with pressure, is graduated from 0-600 bars (1bar=1kgf/cm2).

Specifically, according to ACI-318M-19, For all beams the prestressing force of (147.28) kN is applied gradually with an increase in gauge pressure in three stages as per the manufacturer's obligation of single strand hydraulic-jack.

Prestressing Level 0.55 f_{pu}

$f_{pj} = 0.55 \times 1895 = 1042.25$ Mpa

Jacking force p_j=147.28KN

The ram area of single -pull jack =42 cm

Jack pressure = $\frac{\text{prestressing force}}{\text{ram area}} = \frac{147.28\times100\text{kgf}}{42\text{ cm}}$ =350.6 bar

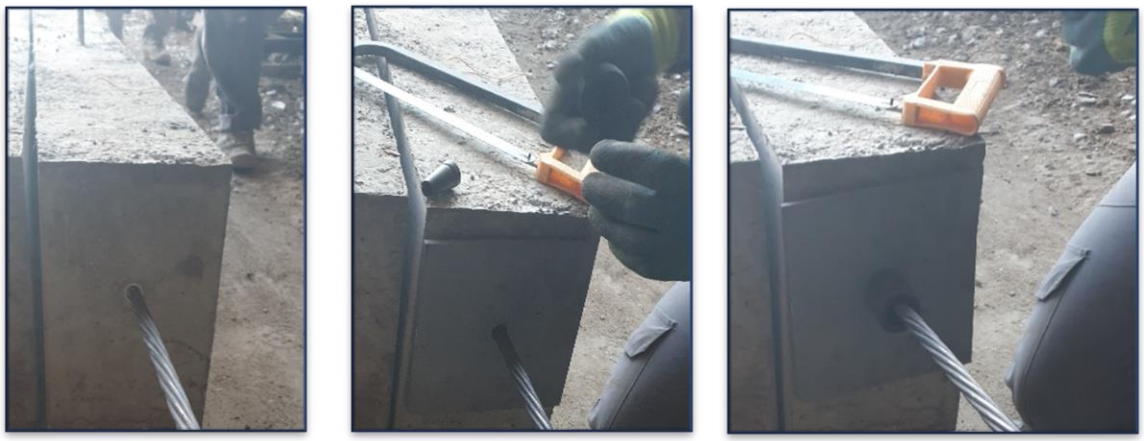

(a)

(b) (c)

Figure (3-41) Prestressing Process: (a) attaching the end bearing steel plates and anchorage, (b) Jacking Machine, (c) Strand Jacking.

3.15 Application of Strengthening Technique

3.15.1 Smoothing of Beam and SIFCON Laminate Surfaces

Before installing the SIFCON laminate, it was important to keep the beam surface-level clean and free from dust. For this purpose, A hand grinding machine was used to smooth the rough surface of the beam. Also, the SIFCON laminate surface was smoothened, as shown in Figure (3-42).

Figure (3-42) Smoothing of laminate with hand grinding machine

3.15.2 Cleaning of Beam and SIFCON Laminate Surface

After smoothing the surface of the beam and SIFCON laminate, it was thoroughly cleaned with a hand blower machine. It was necessary to clean the laminates and beams surfaces; because epoxy would work properly if the laminates and beams surfaces were free from dust, debris, water when applicable, oil, grease and other contaminants.

3.15.3 Installation of Precast SIFCON Laminates by Epoxy

A layer of Sika-331 epoxy paste coat form (8 mm thickness) has been applied to the bonding faces and secured together; the composite beam has been left for 14 days in order to allow the epoxy to cure, Figure (3-43).

Figure (3-43) Installation of precast SIFCON laminates

3.15.4 Installation of End Steel Plate

Due to the Insertion of the bolt into concrete, drilling is important to step in retrofitting work. Before drilling the existing rebar, the location was detected by a reinforcement scanning machine, Figure (3-44), and marked by marker pencil. The locations of the holes are determined, then drilled (60 mm) with a drill and cleaned with a fine wire brush. Air is used to clean the hole from dust and the remains of concrete. The vacuum is injected with Sika Anchor Fix epoxy, then the screw is placed, and after 24 hours, the iron plates are fixed, and the anchor is closed. The installation of the two types of end steel plate is shown in Figure (3-45).

Figure (3-44) Reinforcement scanning machine

Figure (3-45) Installation of end steel plate

Continued Figure (3-45) Installation of end steel plate

3.16 Testing Rig

The test has been carried out using a closed-loop hydraulic rig with a (200) metric ton capacity actuator and load control capability. Two load cells calibrated to (2000 kN) full capacity was equipped to the testing rig. This rig is available at the structural engineering laboratory of the civil engineering department at the University of Technology, as shown in Figure (3-46). Before testing, the specimens were painted with white emulsion to facilitate crack detection easily and precisely. Also, the positions of supports, applied load, LVDT and strain gauges were marked. Finally, the strain gauges wires were connected to the data logger unit.

Figure (3-46) Testing machine

3.17 Measurements and Instrumentations

To study the flexural and shear behavior of the beam specimens, the following instruments are used to record the deflection, crack width and the strain in concrete at each loading increment:

3.17.1 Deflection Measurement

The linearly variable differential transformers LVDT use in this study to measure the vertical deflections at two points, each one located at mid of each span, located at sections exactly under the point loads as shown in Figure (3-47).

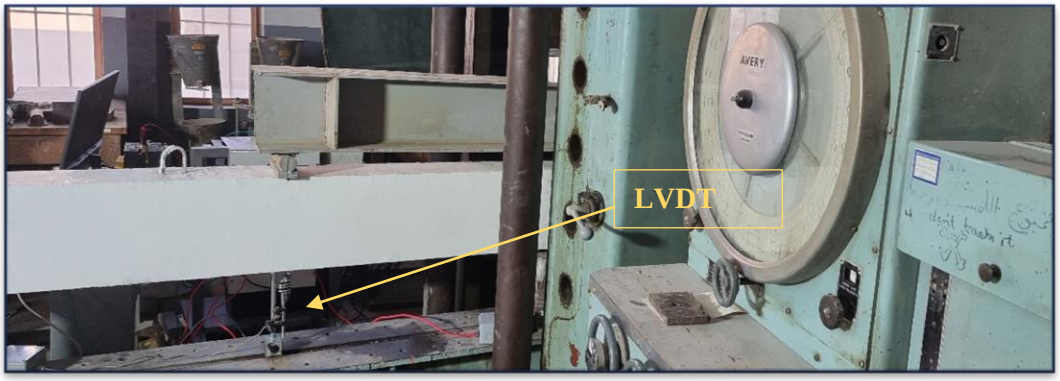

Figure (3-47) LVDT position

3.17.2 Strain Measurements

A uniaxial electrical resistance strain gauge with a length of (60) mm was used for measuring the strain in the concrete of pre-wired strain gauges of (120Ω) resistance, (TML company, Japan), which have been utilized in all tests as shown in Figure (3-48), details of strain gauges have been shown in Table (3-4).

Table (3-4) Strain gauges in detail

MODEL	Size (mm)		Gauge Factor	Gauge Material	Setting Location
	L	W			
PL-60-11-3L	60	10	2.08±1%	Polyester wire	Concrete Surface

Figure (3-48) Wired electrical resistance strain gauges

3.17.3 Installation of Strain Gauge on the Concrete

Following the cleaning of all of the surfaces, gauges have been installed based on:

1- The determination of the exact strain gauge locations.

2-Smoothing concrete surface at those locations by using coarse grinding paper.

3- Cleaning places thoroughly with a cotton material that includes a small Acetone amount.

4- Putting CN-Y adhesive fluid on gauge and after that, evenly spreading and putting a gauge on the concrete surface and keeping the pressing it for approximately 1 min for ensuring that it has been well pasted. Which has been illustrated in Figure (3-49).

5- Ultimately, gauges have been numbered for the purpose of designating their location.

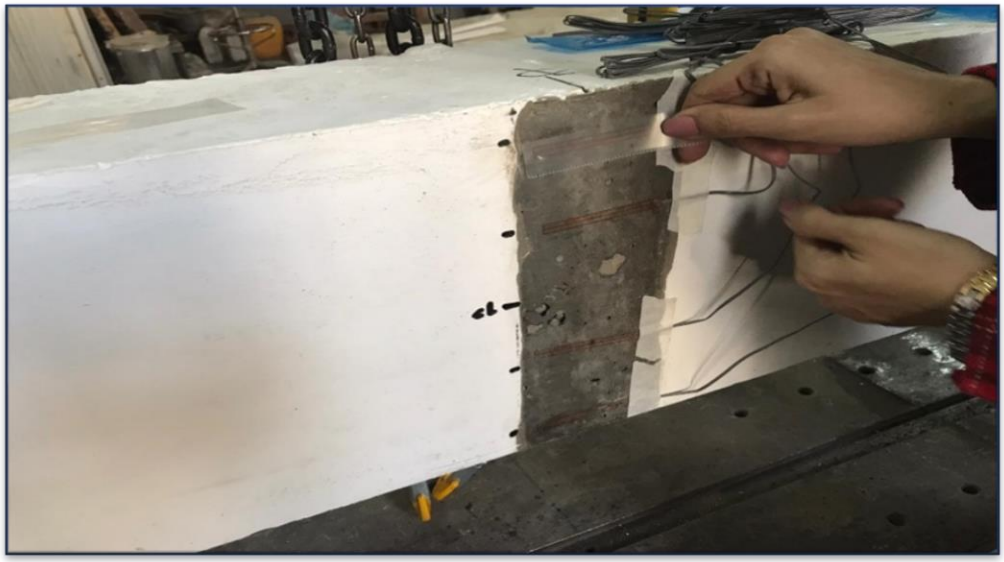

Figure (3-49) Installing strain gauges on concrete

3.17.4 Strain Gauge Indicator (data logger)

The multichannel strain gauge data logger of NIC Jaipur - DAQ-MC-USB which has been illustrated in Figure (3-50) has been used. The total number of channels in the device is (24). The operating software of the strain indicator provides the capability to record 1000 readings every one second.

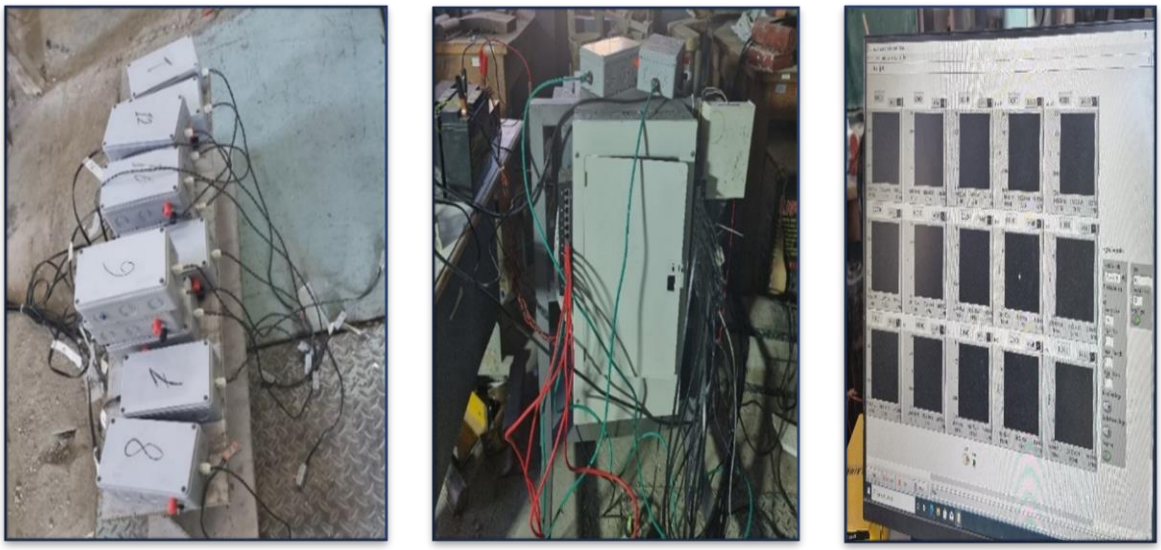

Figure (3-50) Strain gauges data logger

3.17.5 Crack Width Measurement

Used Digital Concrete Crack Width meter to measure the crack width at the face of the beams, as shown in Figure (3-51). This device consists of a monitor and Probe (camera), lighting fixtures, work constantly regardless of light changes, and an automatic crack width interpretation directly to the values of the crack width that have been shown on the screen.

Figure (3-51) Crack width measurement

3.17.6 Slip Measurement

The slip of the prestressing steel due to slip between grip and strand for specimen with unbonded strand was measured through the static and repeated tests. Linearly variable differential transformer (LVDT) was attached to the specimen end to measure the movement if occur in the prestressed strand. The LVDT was fixed to the strand and oriented horizontally along the strand axis. The sensing bar was supported directly on the end face, as shown in Figure (3-52).

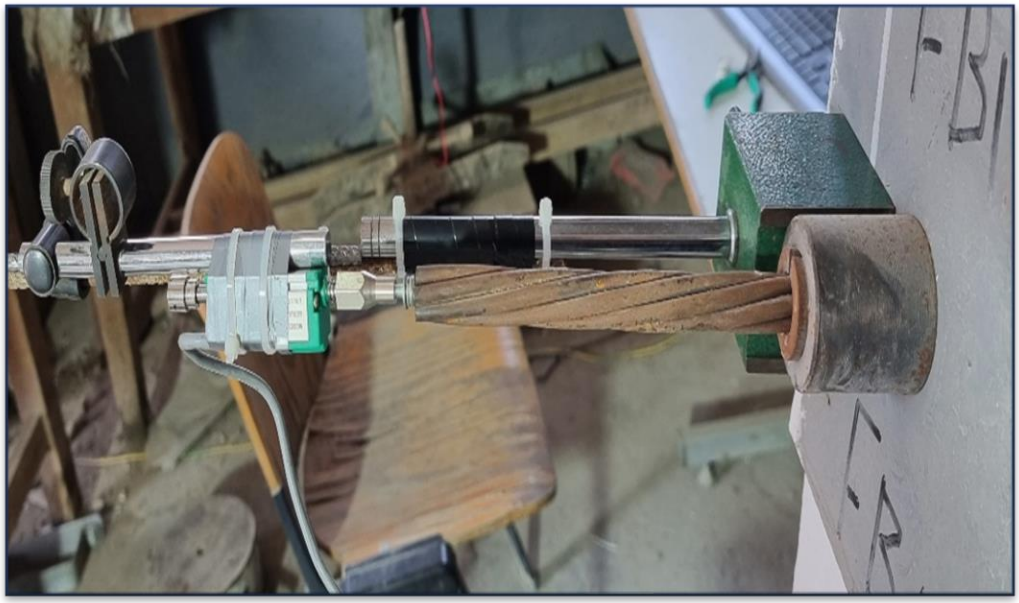

Figure (3-52) Slip measurement

3.18 Test Setup

The beam specimens were supported on three steel supports; two allowed horizontal and angular movement of the specimens simulated as roller supports. One allowed angular movement only of the specimens simulated as hinge supports.

The line load was transmitted to the specimen through a rigid steel beam using two loading steel rods of (50 mm) diameter to avoid stress concentration at the contact area of the beam specimen. Steel plates of (200x100x20) mm were used under the loading steel rods and above the supports. Used the two-point load at the middle of each span of the beam specimen with a distance two-meter between them.

3.19 Testing Procedure for Beam Specimens

3.19.1 Monotonic Static Loading

Before starting the test, the specimen was loaded to about 5 kN and then unloaded. The reason for that is to make the specimen sTable and also to prevent

any possibility of twisting. The strain and dial gauges were attached to their specific locations. The strain gauges were connected to the data acquisition system and then calibrated. After that, applied the static loading with increments which ranged from approximately 2.5% to 5% of the ultimate load.

The data acquisition logger readings of strain gauges were recorded and automatically saved to a personal computer. The time consuming for testing one specimen under static loading on average was between 2 to 4 hours, depending on the load capacity of each tested specimen. Through the test, deflections, crack's width, concrete strains across the depth of section, and strand slip were recorded at each loading increment. At the end of the test, the ultimate load capacity was recorded, and the specimen was dismantled for more inspection.

3.19.2 Repeated Loading

The repeated loading test, as shown in Figure (3-53), was carried out in three stages as follows:

1- Stage 1: the minimal and maximal cyclic loads and have been taken as 40% to 60% of ultimate loading, as it has been observed from the static loading test of the specimen. The load was applied statically by increments equal to (5%) of the ultimate static load until reaching and then unloaded to by the same increments. Ten loading and unloading cycles between and have been implemented. The deflections, strains in concrete, crack widths, and strand slip were recorded for each loading increment.

2- Stage 2: following ten loading cycles, the load has been released to 0 The residual deflections, strains in concrete, and strand slip were recorded.

3- Stage three: in this stage, the specimen was tested statically until failure with an increment equal to approximately 5% of the ultimate load as observed from the monotonic static loading test. The whole repeated load test took an average of 8 to 10 hours. Figure (3-54) show all tested beams.

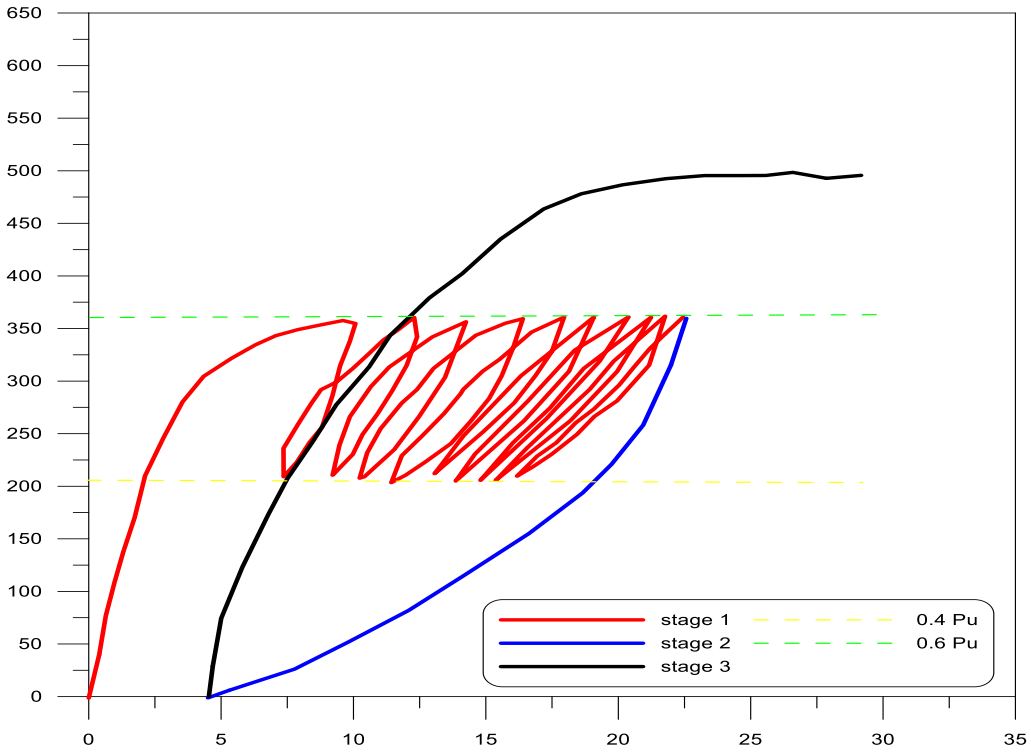

Figure (3-53) Repeated loading test stages

Figure (3-54) All tested beams

CHAPTER FOUR

EXPERIMENTAL RESULTS AND DISCUSSION

CHAPTER FOUR

EXPERIMENTAL RESULTS AND DISCUSSION

4.1 General

A summary and discussion of the outcomes of the experimental work described in chapter three are presented in this chapter. In the beginning, high strength concrete (HSC) properties and slurry infiltrated fibrous concrete (SIFCON) are described.

After that, the results of the experimental work of twenty (4300) mm length continuous unbonded post-tensioned HSC beams specimens. They were divided into two identical categories, each consisting of ten specimens.

The first category was studied flexure behavior; the second category was studied shear behavior. Each category consisted of two groups as follows: the first group consisted of beams tested under monotonic static loading, the second group consisted of beams tested under repeated loading. Beams were cast, strengthened, and tested under concentrated loading at the mid of each span up to failure.

The behavior of the tested specimens is discussed about load versus deflection at mid-span at each span, toughness, crack patterns, failure modes, maximum crack width, cracking and ultimate load capacities with failure, load versus strains in the concrete, and redistribution of moments of the tested specimens.

4.2 Properties of Concrete Mixtures

The hardened properties of high strength concrete (HSC) and slurry infiltrated fibrous concrete (SIFCON) mixtures obtained by testing control specimens at the age of 28 and 90 days are documented in the Table (4-1).

Table (4-1) Concrete mixes hardened state properties

Mix Name	**Compressive Strength (MPa)**		**Tensile Strength (MPa)**		**Modulus of Elasticity* (GPa)**
	28days	**90 days**	**28 days**		**28 days**
	f_{cu}	f_{cu}	f_{ct}	f_r	E_c
SIFCON	139.611	151.951	23.87	39.29	56.00 [69]
FB mix	76.638	87.781	5.34	5.91	32.895
SB mix	78.365	94.025	5.98	6.07	33.187
**ACI363R-97($E_c = 3320\sqrt{f_c'} + 6900$)*					

4.3 General Behavior of Prestressed Concrete Beams Under Monotonic Static Loading

Thirteen continuous unbonded post-tensioned beams specimens were divided into two categories: flexural [Group A] and shear [Group C] tested under monotonic static loading. The cracking and ultimate load-carrying capacities, the proportional ratios of loads, and failure mode of the tested prestressed concrete beams at central support (hogging region) and mid-span (sagging region) are supplied in the next paragraphs; a summary of the tested beam under monotonic static loading are recorded in a Table (4-2).

Table (4-2) Summary of the tested beam under monotonic static loading

Group	Beam Name	P_{cr} [KN] Central support	P_{cr} [KN] Mid span	P_u [KN]	Ultimate Deflection (mm)	α	Failure Mode
A	FB1	247.1	261.9	438.2	17.8	56.4	Flexure failure-concrete crushing
	FB3	395.3	401.1	629.3	7.9	62.8	Concrete crushing, SIFCON debonding &rupture
	FB5	499.7	500.6	667.6	9.9	74.8	Concrete crushing &SIFCON rupture
	FB7	488.9	491.1	687.7	10.7	71.1	Concrete crushing & SIFCON rupture
	FB9	385.9	399.2	600.6	8.3	64.3	Concrete crushing, SIFCON debonding &rupture
	FB10	392.3	406.6	600	9.7	65.4	Concrete crushing, SIFCON debonding &rupture
C	SB1	238.9	241.4	413.3	19.9	57.8	Shear failure-concrete crushing
	SB3	-	491.5	605.3	11.9	81.2	Concrete crushing, SIFCON debonding &rupture
	SB5	328.1	302.1	492.9	12.2	61.2	Concrete crushing, SIFCON debonding &rupture
	SB7	310.9	318.3	501.7	19.4	62	Crushing of concrete
	SB8	-	359.2	524.3	12.5	68.5	SIFCON rupture
	SB9	316.3	295.5	475	11.9	62.2	Crushing of concrete
	SB10	299.1	302.9	455.7	16.8	65.6	Crushing of concrete

$$\alpha = \left[{}^{P_{cr}}/_{P_u} \right] \times 100\%$$

Where : P_{cr} : Cracking load , P_u : Ultimate load

4.3.1 General Behavior of Flexure Beams [Group A]

This group consists of six prestressed concrete beams specimens to study the flexural behavior under monotonic static load for the strengthened beams. One unstrengthened as a reference beam and five strengthened with precast SIFCON laminates in hogging and sagging regions to study two parameters the first, length of the laminate, and chose the optimal length in sagging and hogging regions, the second study the feasibility of the new bonding methods which used first once to bonding precast SIFCON laminate with the beam.

» FB1

This unstrengthened prestressed concrete beam specimen is considered as a reference beam for the other test beams that are designed to fail in flexure and subjected to monotonic static loading.

At a cracking load (247.1kN), the first visible flexural crack appeared at the central support (the maximum moment region) about (56.4%) of the ultimate load. By slightly increasing the load, the limited number of existing cracks grew wider. Then, on further load increases, the cracks occurred under the load points (mid-span region) at the load of (261.9 kN), as an individual crack in each span.

The flexural cracks at the mid-span changed their direction and propagated towards the nearest loading point, which was called flexure-shear crack. Beam FB1 reached an ultimate load capacity at (438.2 kN) with the mode flexure failure the concrete crushing as shown in Figure (4-1); The relationship between the load-deflection response at mid of each span is depicted in Figure (4-2).

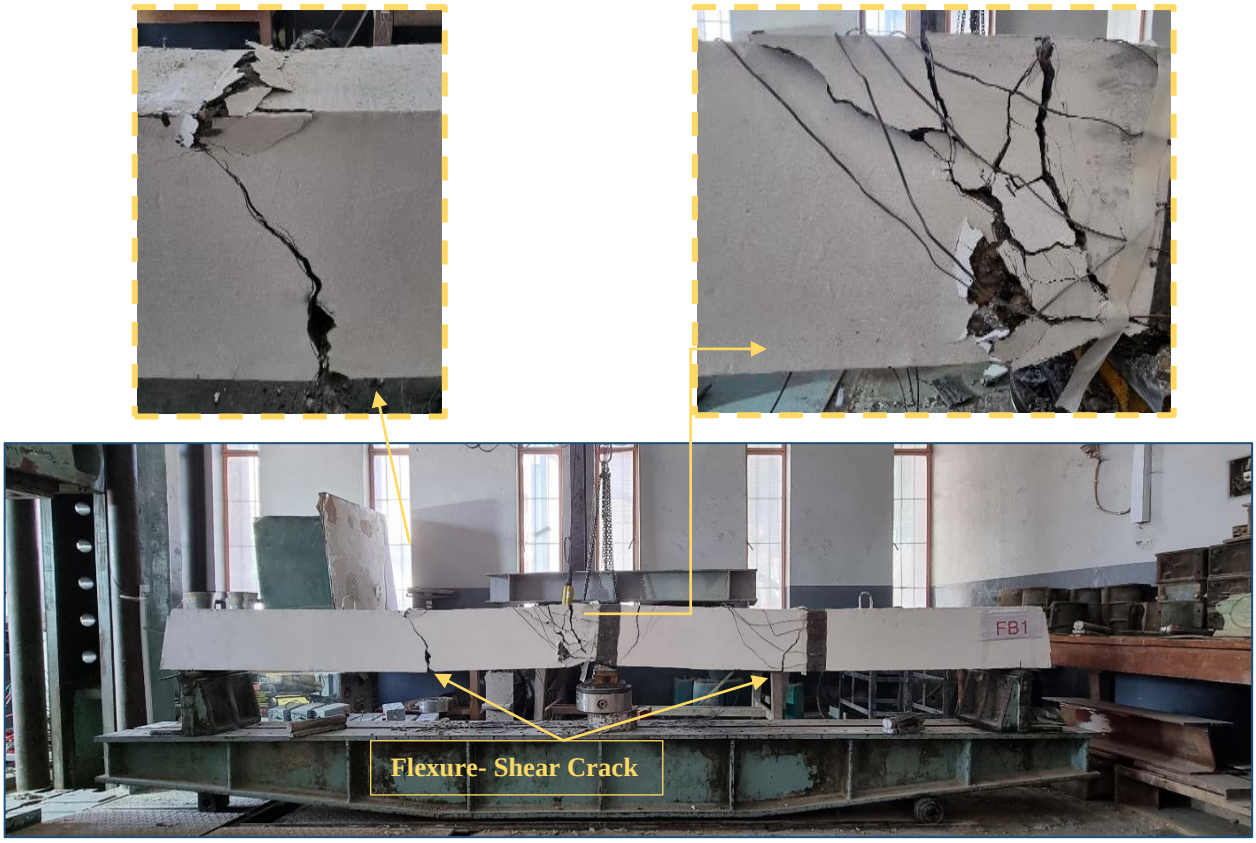

Figure (4-1) Failure of beam FB1

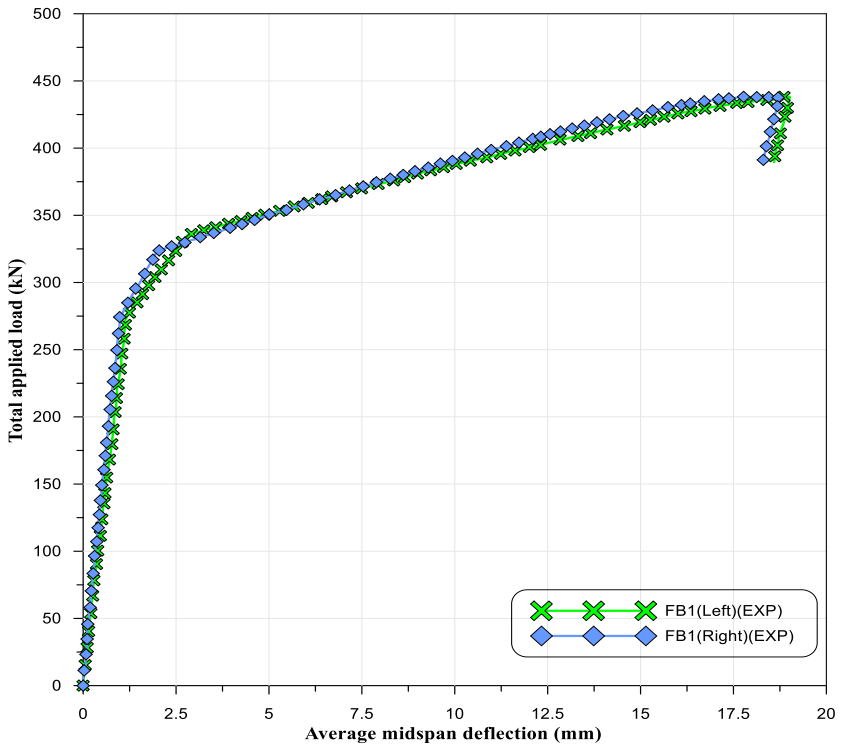

Figure (4-2) Load deflection curves of the FB1 tested beam

»FB3

This prestressed concrete beam specimen was strengthened with precast SIFCON laminates glued by epoxy resin that have a length to span ratio (0.8) at the central support region (hogging region) and (0.9) at mid-span regions (sagging regions); the details of strengthened FB3 beam specimen are shown in Figure (3-6).

When the applied load arrives (395.3kN) of (62.8% of ultimate load), the first crack appearance at the hogging region (central support region), by increasing load gradually, at a load of (401.1 kN), another crack occurs at the sagging region (mid-span region). The cracking load at the central support and the mid-span increased significantly compared to the reference beam FB1.

After more applied loads, the separation happened at the end of the (SIFCON) laminate at the hogging region. Then, a rupture in the (SIFCON) laminate occurred in the middle of the sagging region.

Increased the number of cracks in the sagging region more than the reference beam FB1 but less than cracks number at the hogging region. At load (629.3 kN) FB3 beam failure with concrete crushing, rupture SIFCON laminate in the mid-span, and debonding on the SIFCON laminate at the hogging region, as shown in Figure (4-3).; as well as hearing distinctive sounds during the separation and rupture of the laminates. The relationship between the load-deflection response at each mid-span is depicted in Figure (4-4).

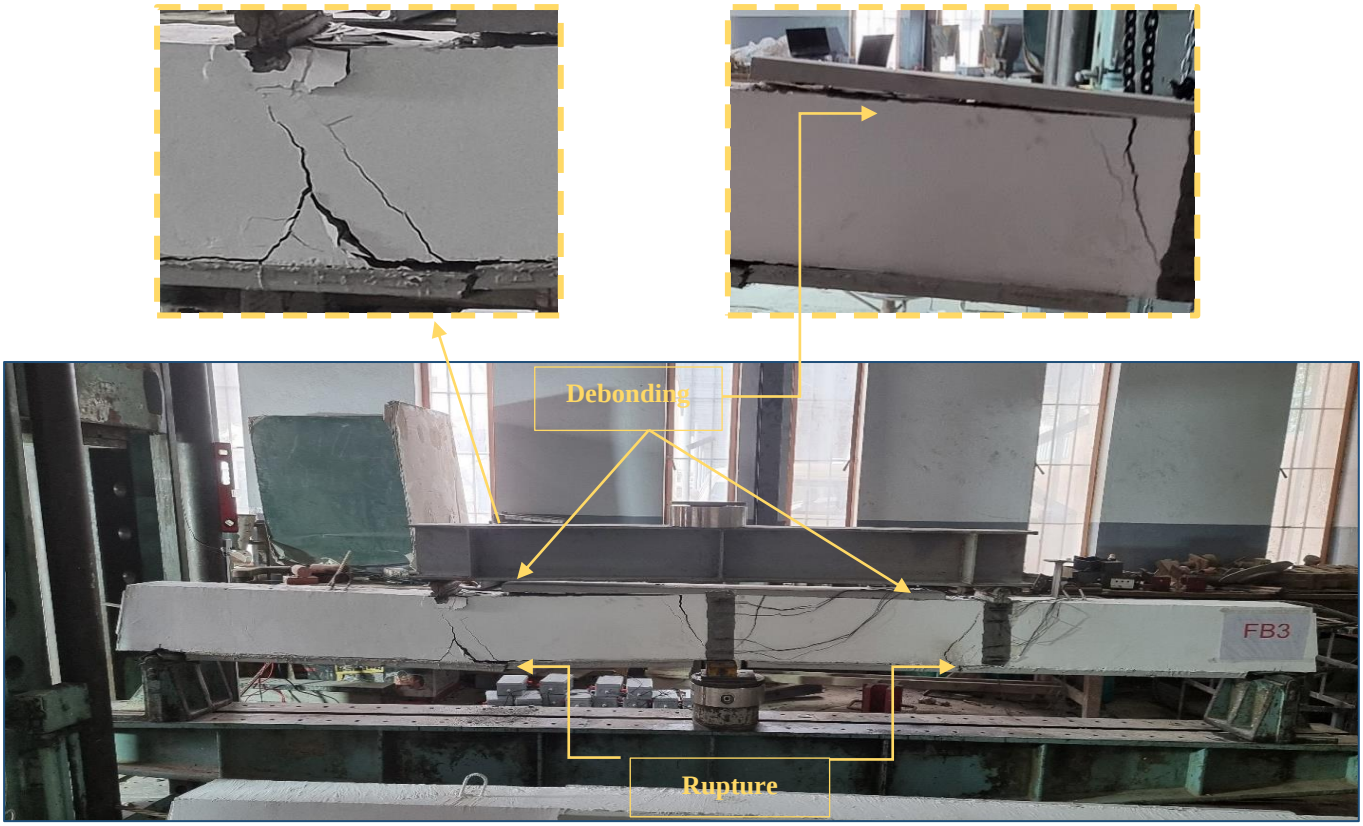

Figure (4-3) Failure of beam FB3

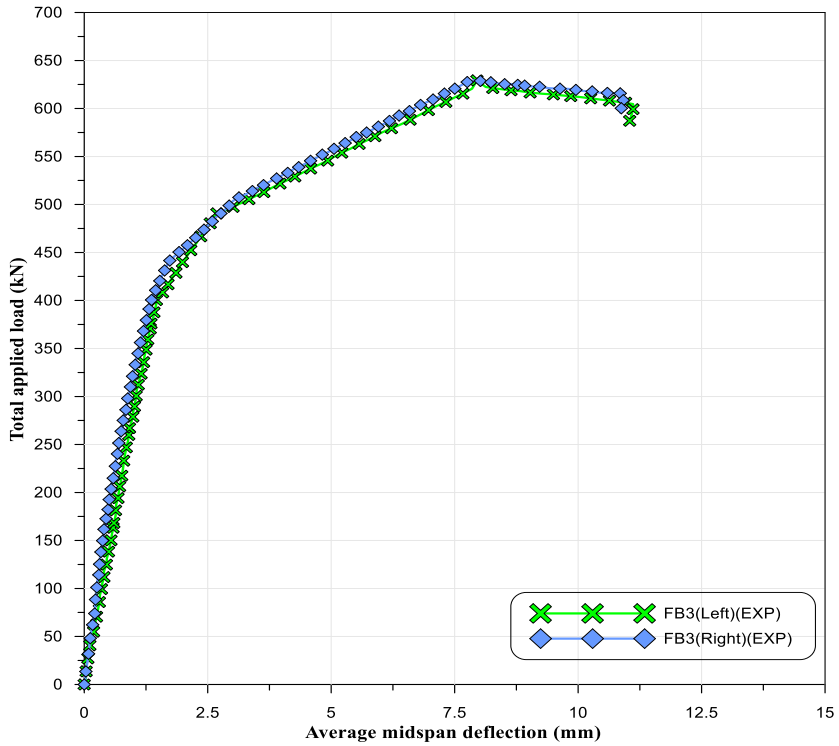

Figure (4-4) Load deflection curves of the FB3 tested beam

»FB5

Strengthening techniques employed for this prestressed concrete beam specimen FB5 were identical to those used for FB3 and the addition of two rectangle shape anchored end steel plates in each laminate ends to designate its advantage compared to only epoxy resin bonding, the details of the strengthened FB5 beam specimen are shown in Figure (3-7).

The first crack occurred at the central support at the cracking load (499.7kN) of (74.8% of ultimate load). By increasing load, the first crack occurred at the mid-span at the load of (500.6 kN). The cracking load at the central support and the mid-span increased significantly compared to FB1 and FB3.

As the applied loads increased, the number of cracks increased at the central support and mid-span regions. The failure was initiated at the hogging region, and laminate debonding propagated toward mid-span. But the end anchored steel plate prevented the separation from occurring at the laminate ends, as happened in FB3.

With increasing loads was visually observed, a crack was concentrated on the laminate. Beam FB5 reached an ultimate load at (667.6kN) with the mode of failure crushing of concrete, rupture of SIFCON laminate at mid-span with a few cracks around the mechanical anchorages at ends of SIFCON laminates as shown in Figure (4-5); Midspan load-deflection responses for each span are depicted in Figure (4-6).

Figure (4-5) Failure of beam FB5

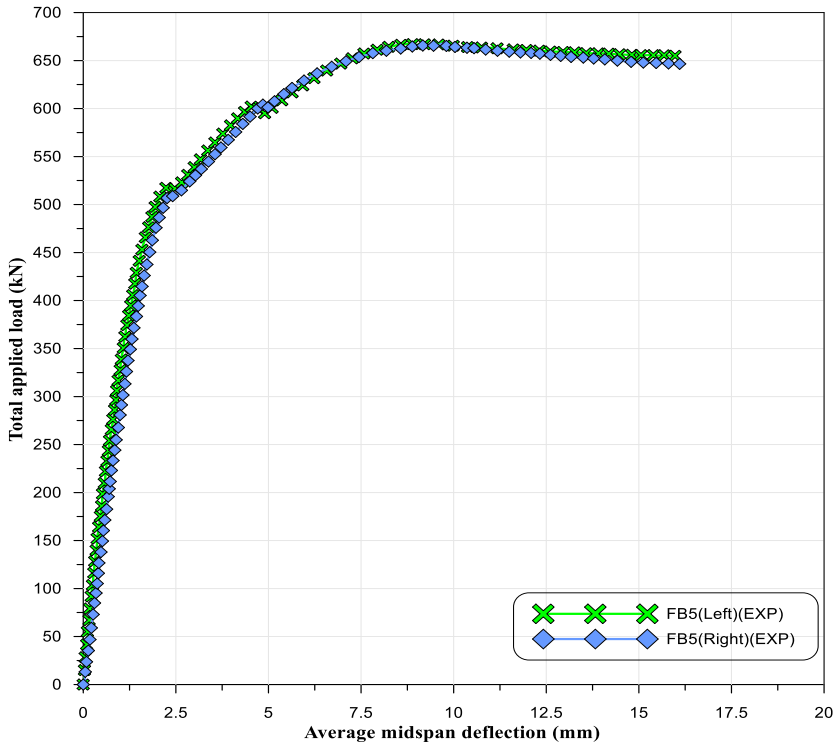

Figure (4-6) Load deflection curves of the FB5 tested beam

»FB7

Strengthening techniques employed for this prestressed concrete beam specimen FB7 were identical to those used for FB3 and the addition of two U shape anchored end steel plates in the ends of each laminate to designate its advantage compared to only epoxy resin bonding, the details of the strengthened FB7 beam specimen are shown in Figure (3-8).

The first crack occurred at the central support at the cracking load (488.9kN) of (71.1% of ultimate load). By increasing load, the first crack occurred at the mid-span at a load of (491.1 kN). The cracking load at the central support and the mid-span increased significantly compared to FB1and FB3.

It was clearly seen that a crack appeared to be concentrated on the laminate as the load increased. Beam FB7 reached an ultimate load at (687.7kN) with the mode of failure crushing of concrete, rupture of SIFCON laminate. The use of precast SIFCON laminate allowed the beam to maintain its current condition as shown in Figure (4-7).

It did not happen any separation of the SIFCON laminates from the surface of the beam due to the presence of U shape end anchored steel plate. This indicates the effectiveness of this method by maintaining the stability of the ends of the laminates from separating so that they rupture in the middle under the influence of the applied force. Midspan load-deflection responses for each span are depicted in Figure (4-8).

Figure (4-7) Failure of beam FB7

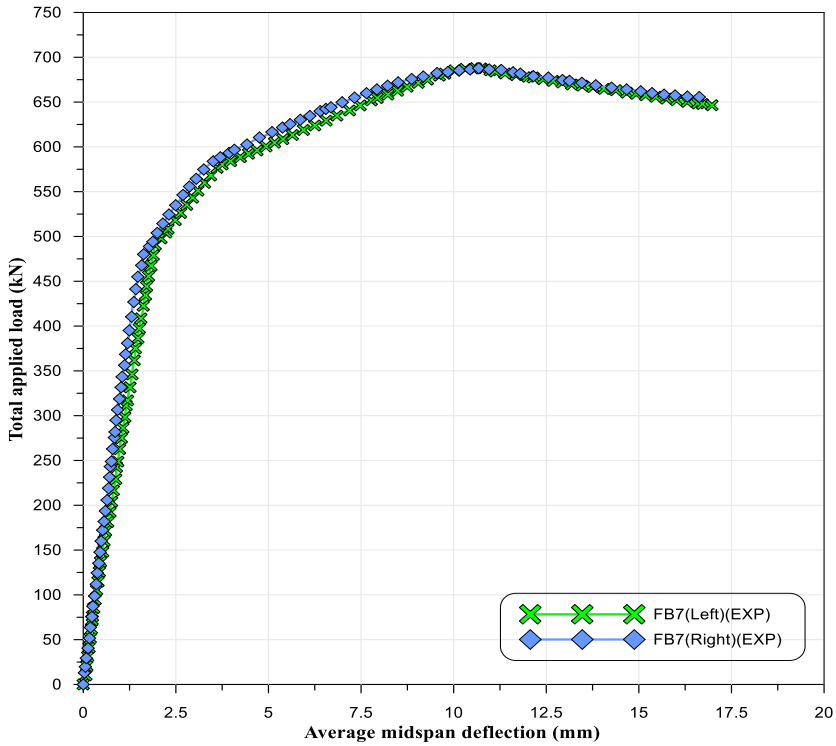

Figure (4-8) Load deflection curves of the FB7 tested beam

»FB9

This prestressed concrete beam specimen was strengthened with precast SIFCON laminates glued by epoxy resin that have a length to span ratio (0.8) at the central support region (hogging region) and (0.7) at mid-span regions (sagging regions), the details of the strengthened FB9 beam specimen are shown in Figure (3-9). The first crack occurred at the central support at the cracking load (385.9kN) of (64.3% of ultimate load). By increasing load, the first crack occurred at the mid-span at the load of (399.2 kN). The cracking load at the central support and the mid-span increased significantly compared to FB1 but less than FB3. The failure initiated at the sagging region laminate end and debonding was along with the laminate/adhesive interface at sagging laminate ends and propagated toward mid-span and rupture in the hogging region laminate. Beam FB9 reached an ultimate load at (600.6kN) with the mode of failure crushing of concrete, rupture of SIFCON laminate at central support region, and laminate debonding initiated at the end of the laminate at sagging region (inverse FB3) as shown in Figure (4-9); Midspan load-deflection responses for each span are depicted in Figure (4-10).

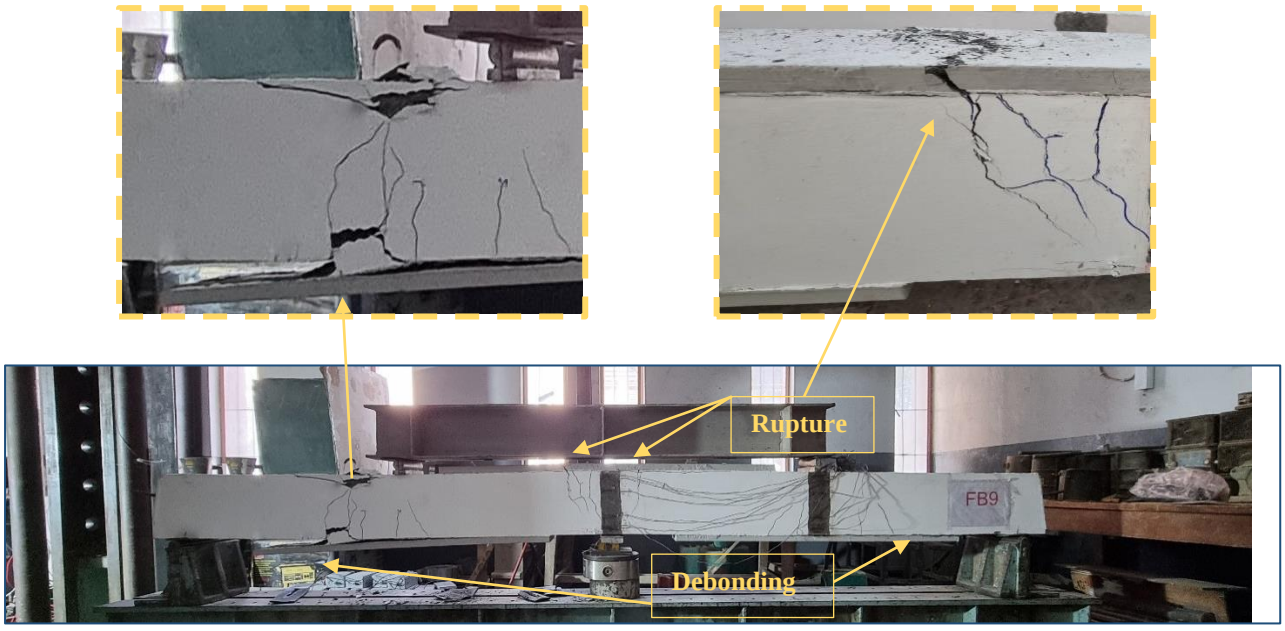

Figure (4-9) Failure of beam FB9

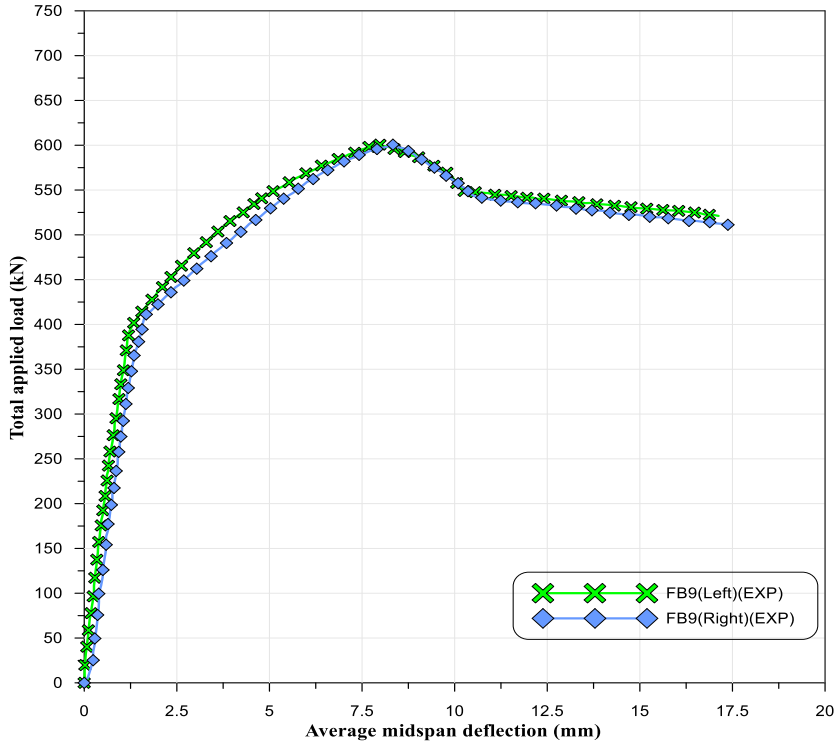

Figure (4-10) Load deflection curves of the FB9 tested beam

»FB10

This prestressed concrete beam specimen was strengthened with precast SIFCON laminates glued by epoxy resin that have a length to span ratio (0.6) at the central support region (hogging region) and (0.9) at mid-span regions (sagging regions), the details of the strengthened FB10 beam specimen are shown in Figure (3-9).

The first crack occurred at the central support at the cracking load (392.3kN) of (65.4% of ultimate load). By increasing load, the first crack occurred at the mid-span at the load of (406.6 kN). The cracking load at the central support and the mid-span increased significantly compared to FB1.But less than FB3 at the central support. The failure initiated at the hogging region where debonding the laminate ends (same FB3), with increasing loads was visually observed a crack was concentrated on the laminate at mid-span. Beam FB10 reached an ultimate load at (600kN) with the mode of failure crushing of

concrete, rupture of SIFCON laminate at mid-span, and debonding laminate initiated at the end of the laminate as shown in Figure (4-11); Midspan load-deflection responses for each span are depicted in Figure (4-12).

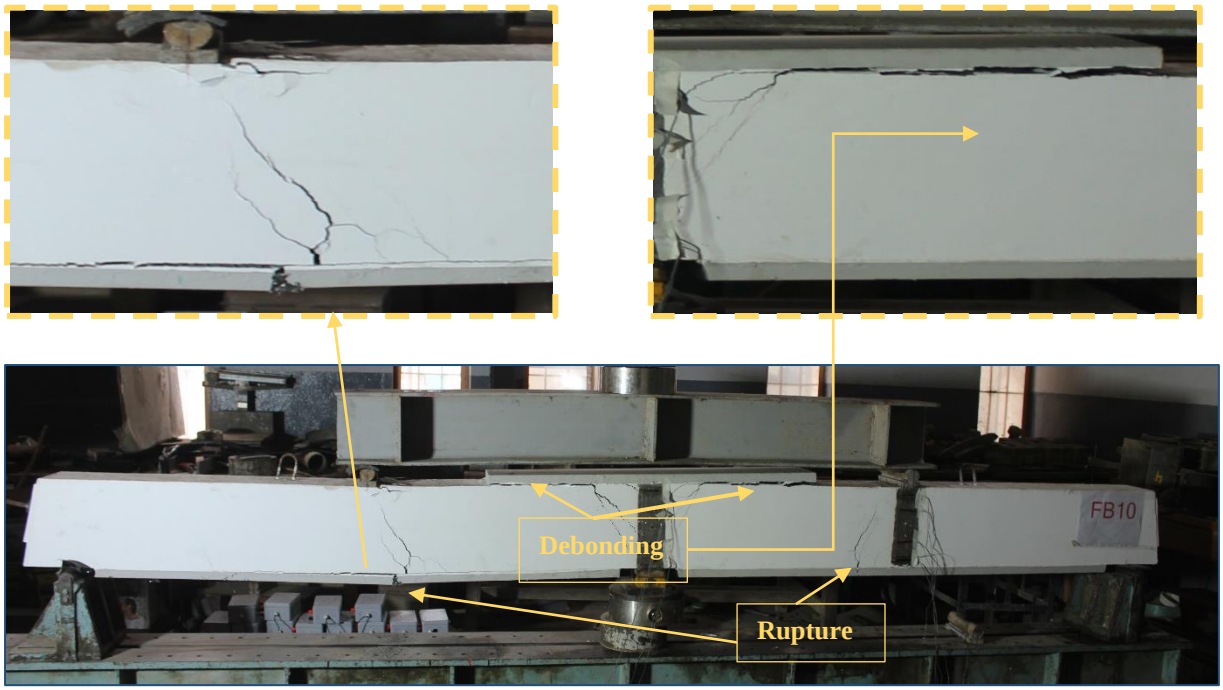

Figure (4-11) Failure of beam FB10

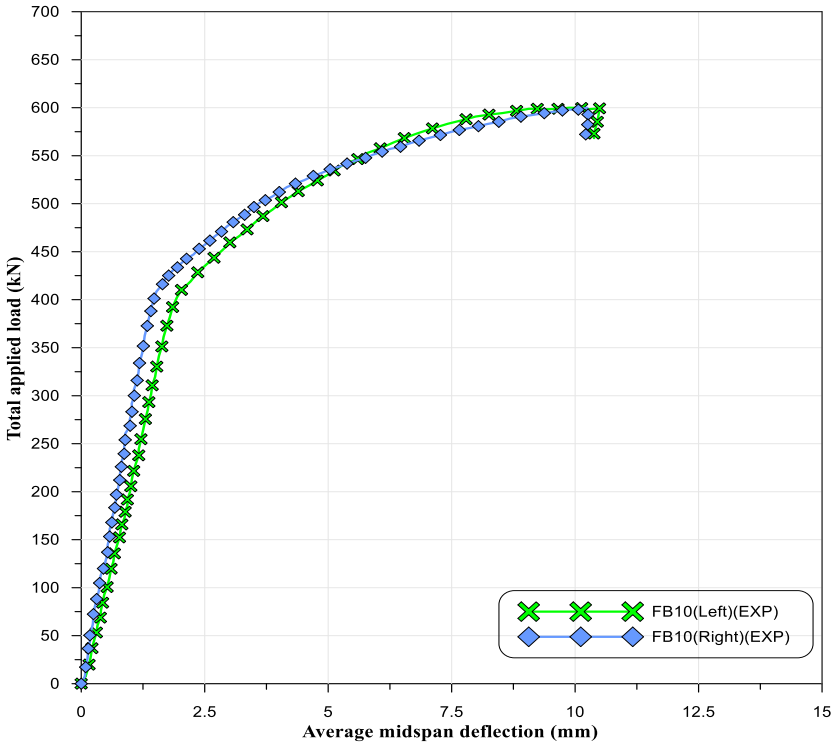

Figure (4-12) Load deflection curves of the FB10 tested beam

4.3.2 The Feasibility of The Flexural Strengthening by Using the Different Lengths of The Laminates

From the results in section (4.3.1) four beams and different lengths of precast SIFCON laminates were used for strengthening the sagging and hogging regions for comparison in this section of the study. FB1unstrengthened beam, FB3, FB9, and FB10 strengthened beams with the precast SIFCON laminate that has the length to span ratio (0.8,0.9), (0.8,0.7), and (0.6,0.9) in hogging and sagging regions respectively that glued by epoxy resin. Figure (4-13) compares the load-deflection curves s of beams FB1, FB3, FB9 and FB10, and the following are observed:

- Generally, this strengthening is effective in delaying the first crack appearance time of the tested beams. The first crack load increased with ratio (60%), (56.2%) and (58.8%) respectively for the beam FB3, FB9, and FB10 compared with the reference beam FB1.
- Increased the ultimate load capacity of the tested beams, the results explain that the enhancement in flexural capacity has reached (43.6%), (37.1%) and (36.9%) respectively for the beam FB3, FB9, and FB10 compared with the reference beam FB1.
- Precast SIFCON laminates significantly reduced mid-span deflection at ultimate load for strengthened beams; the deflection decreased with ratio (55.6%), (53.3%), and (45.5%) respectively for the beam FB3, FB9, and FB10 compared with the reference beam FB1.
- Regarding the effect of the length of laminates, an increase in the first crack appearance time, and ultimate flexural strength is achieved with the increase of the length of laminates. That means the FB3 beam has the optimal length of precast SIFCON laminate

from the three beams used in the comparison. However, all the laminate lengths used helped strengthen prestressed concrete beams.

- The bonding by epoxy resin succeeded in flexural strengthening prestressed concrete beams and stopped the sudden failure, but it can't prevent the debonding of the laminates ends.

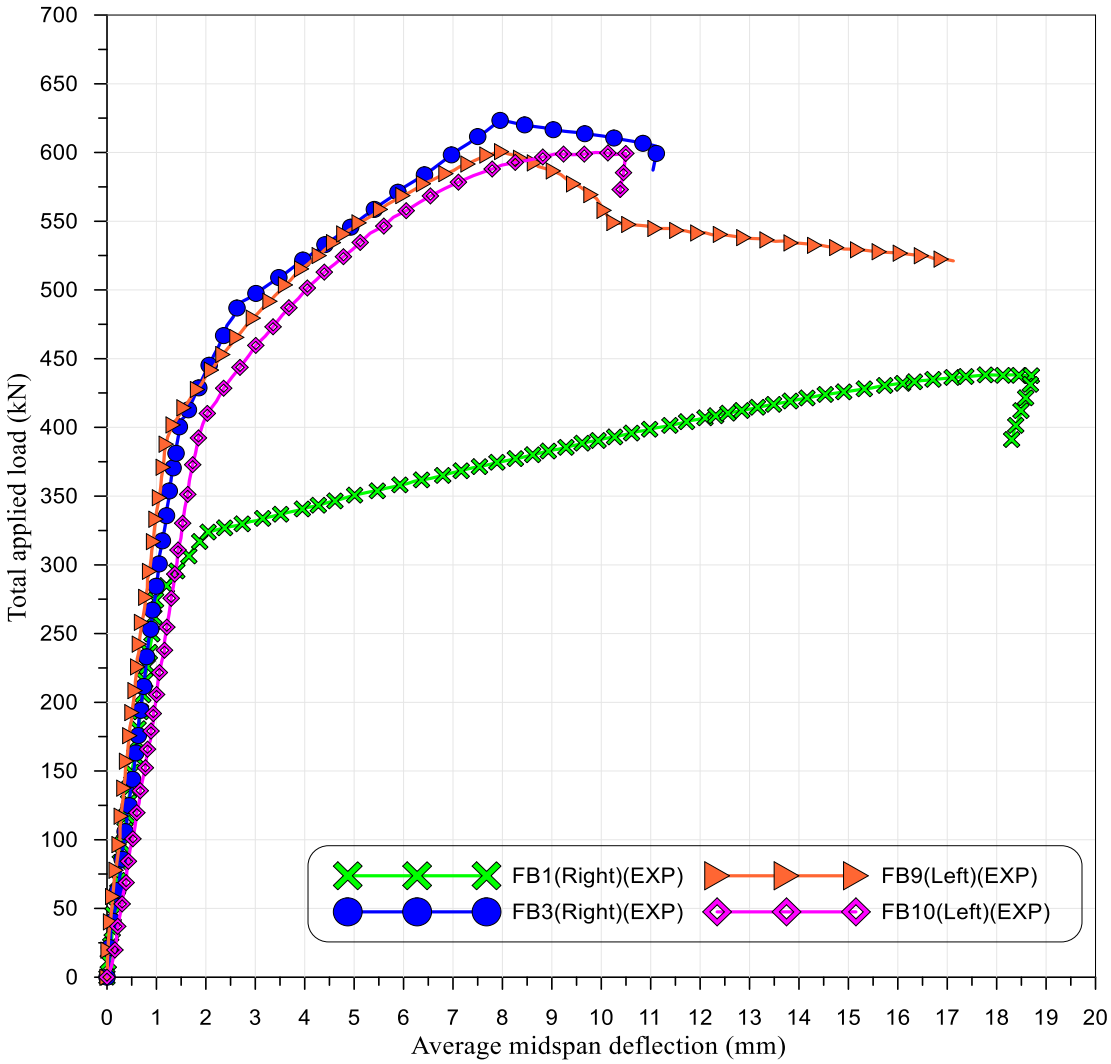

Figure (4-13) Load deflection curves of the FB1, FB3, FB9 and FB10 tested beams

4.3.3 The Feasibility of The Flexural Strengthening with The Different Bonding Methods

In order to examine the effect of the different bonding methods for precast SIFCON laminates with the beams and their effectiveness in strengthening, four beams are taken FB3, FB5, and FB7 in addition to the reference beam FB1.

In section 4.3.2, the optimal length of precast SIFCON laminate glued externally by epoxy resin was chosen. Strengthening solved a sudden deterioration but resulted in independent failures in epoxy resin was used to bind the precast SIFCON laminate especially on the ends. Therefore, two shapes of end anchored steel plate were suggested to bind SIFCON laminates in addition to epoxy resin. Figure (4-14) shows the load-deflection curves of specimens that strengthen by precast SIFCON laminates using three bonding methods (using epoxy or the two shapes of the end anchored steel plate) and compared to each other, and the following are observed:

- The strengthening with the use of all the bonding methods leads to a delay in the first crack appearance time. The first crack load increased with ratio (60%), (102.2%) and (97.8%) respectively for the beams FB3, FB5 and FB7 compared with the reference beam FB1, and reached (26.4%), and (23.6%) respectively for the beams FB5, and FB7 compared with beam FB3.

- The results explain that the strengthening increased the ultimate load capacity, it has reached (43.6%), (52.4%), and (57%) respectively for the beam FB3, FB5 and FB7 compared with the reference beam FB1, and reached (6.1%), and (9.3%) respectively for the beams FB5, and FB7 compared with beam FB3.

- Precast SIFCON laminates significantly reduced mid-span deflection at ultimate load for strengthened beams, the decrease in deflection (55.6%),

(44.3%), and (39.8%) respectively for the beam FB3, FB5, and FB7 compared with the reference beam FB1, and the use of the two types of end anchored steel plate increased in the deflection (25.3%) and (35.4%) respectively for the beam FB5 and FB7 compared with beam FB3.

- The three methods used to bind the precast SIFCON laminates with the prestressed concrete beams were very efficient, but anchored end steel plates solved the problem of the separation in the ends of laminates. The U shape anchored end steel plates showed more efficiency in preventing any separation of the SIFCON laminates from the surface of the beam then followed by the rectangular shape anchored end steel plates.

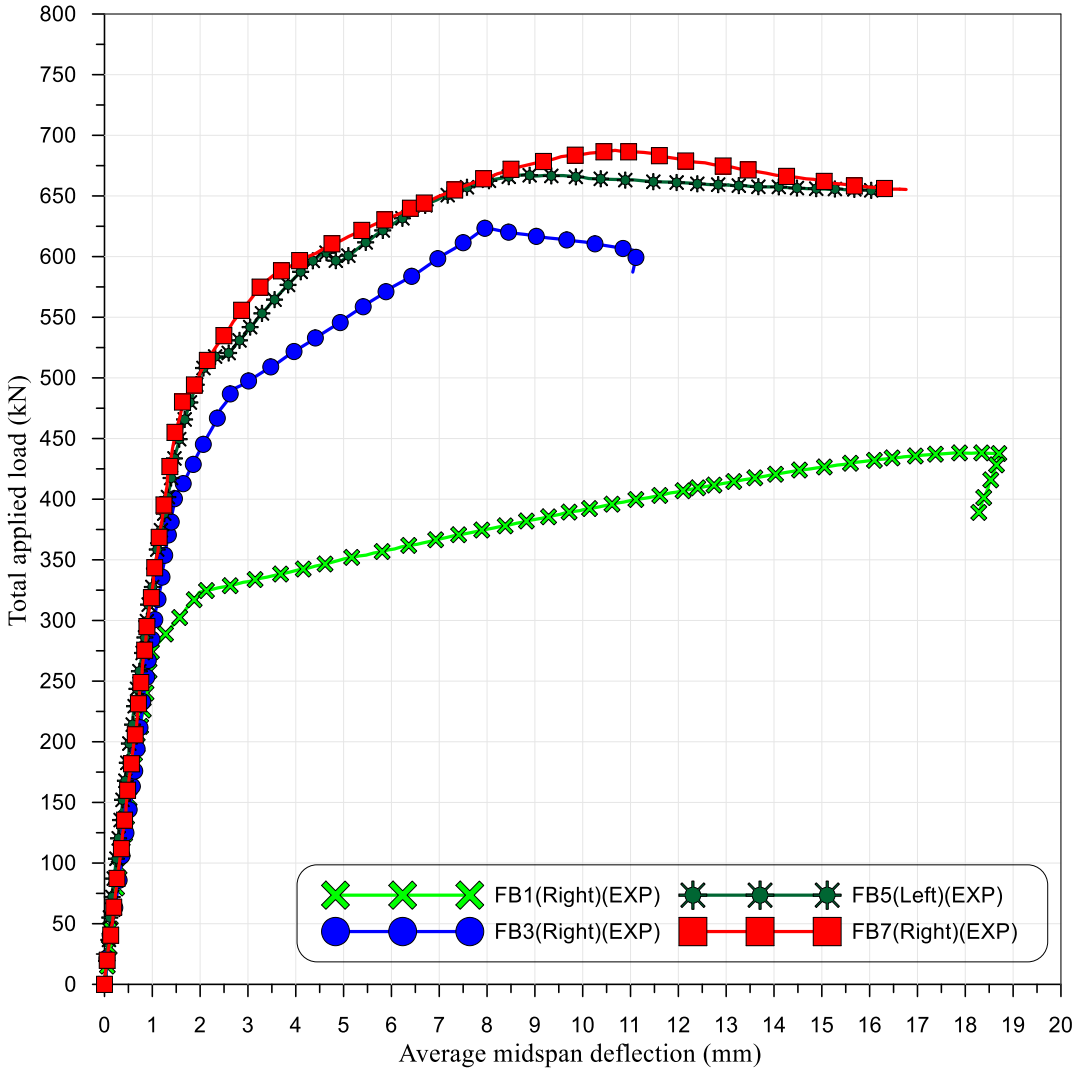

Figure (4-14) Load deflection curves of the FB1, FB3, FB5 and FB7 tested beams

4.3.4 General Behavior of Shear Beams [Group C]

This group consists of seven prestressed concrete beams specimens to study the shear behavior under a monotonic static load for the strengthened beams. One unstrengthened as a reference beam and six strengthened with precast SIFCON laminates with different patterns at the maximum shear region to study two parameters. The first is the effectiveness of the different wrapping patterns of the laminate. The second is the comparison between full and partial wrapping of the beams by precast SIFCON laminates.

» SB1

This unstrengthened prestressed concrete beam is considered as a reference beam for the other test beams that are designed to fail in shear and subjected to monotonic static loading.

When the load was applied in small increments, The beam began to develop flexural cracks and shear cracks as a result of the loading. The flexural cracks ceased to form as shear cracks began to mature at a specific load level. The shear crack started at the point of applying the load and propagated italicized towards the mid support. The first flexural and shear cracks appeared simultaneously at a force of (238.9kN) at the cracking load (Pcr) of (57.8% of ultimate load) at the central support region, followed by another crack at the mid-span region at a load of (241.4 kN), at the high loading stages, diagonal cracks became much wider.

This beam failed in shear by means of diagonal tension and hearing distinctive sounds during the cracking. This type of shear failure is characterized by a large diagonal shear crack that develops with the further load. It extends gradually until it reaches its critical point where it finally fails without warning; The maximum shear resistances were (413.3kN), as shown in Figure (4-15).

Figure (4-16) shows the relationship between the load-deflection response at mid of each span.

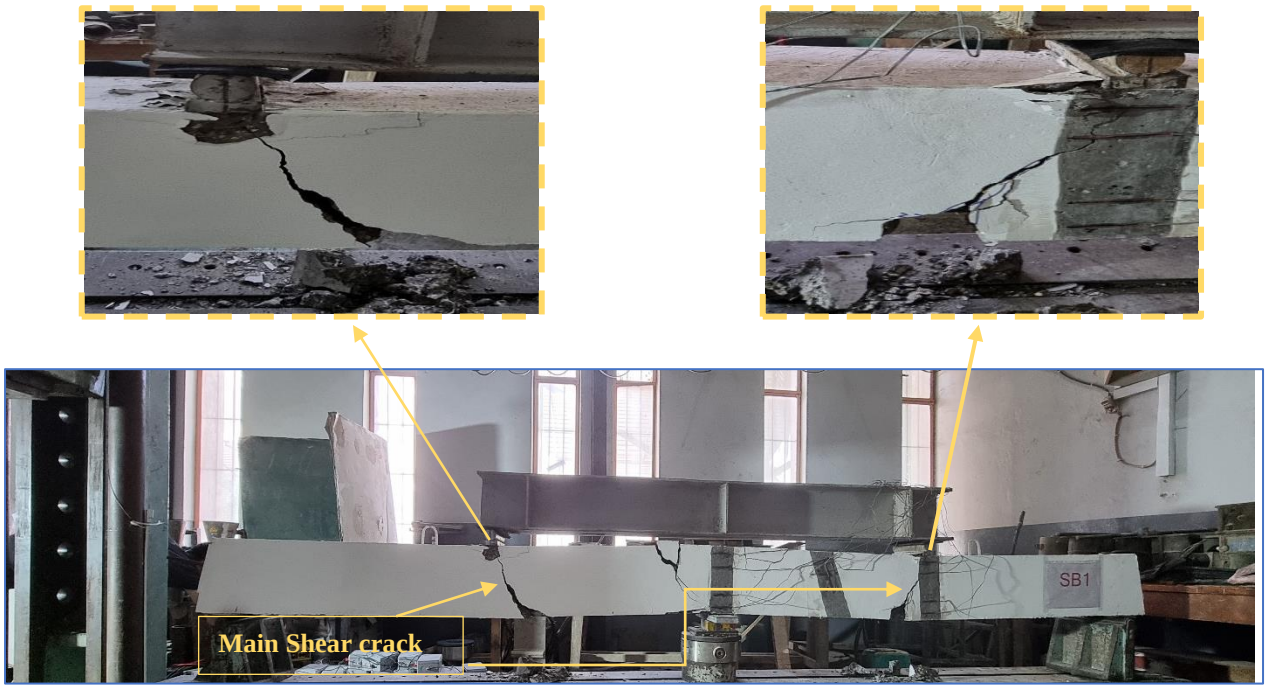

Figure (4-15) Failure of beam SB1

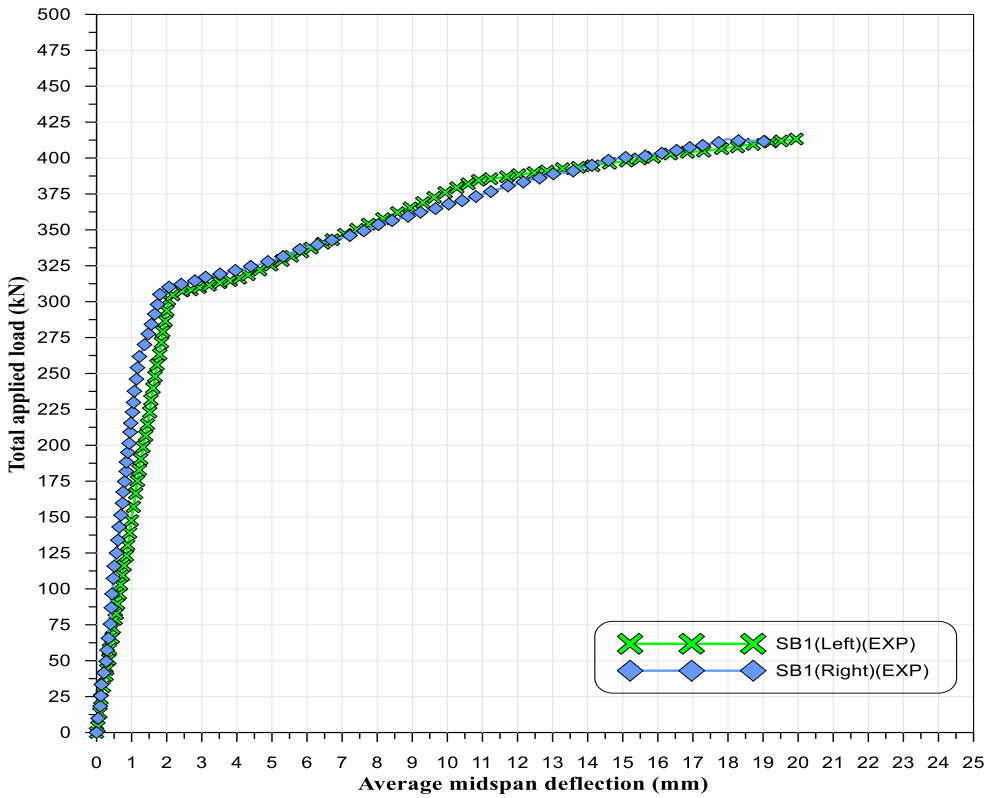

Figure (4-16) Load deflection curves of the SB1tested beam

» SB3

This prestressed concrete beam was strengthened full wrapping (the two sides, top, and bottom face) by precast SIFCON laminates at the maximum shear region with the use of precast SIFCON laminates glued by epoxy resin; the details of the strengthened SB3 beam specimen are shown in Figure (3-11).

When the load was incrementally applied, there were no visible shear cracks at the central support region because it is covered with SIFCON laminate. The first flexure crack appeared at the mid span region beside the laminates at the force of (491.5 KN), at the cracking load (Pcr) of (81.2% of ultimate load). The cracking load increased significantly compared to SB1.

With the increased loads, the separation initiated at the end of the SIFCON laminate at the bottom then, a rupture in the SIFCON laminate at two middle of sides and top and hearing distinctive sounds during the separation and cracking of the laminates.

Beam SB3 reached an ultimate load at (605.3kN) with the mode of failure rupture of SIFCON laminate at the central support region, and bottom laminate debonding. Debonding was along with the laminate/adhesive interface (i.e., adhesive remained attached to the concrete soffit), part of concrete cover, and part of the steel reinforcement as shown in Figure (4-17); Figure (4-18) shows the relationship between the load-deflection response at mid of each span.

This strengthening pattern prevents any shear crack from appearing in the prestressed beam specimen.

Figure (4-17) Failure of beam SB3

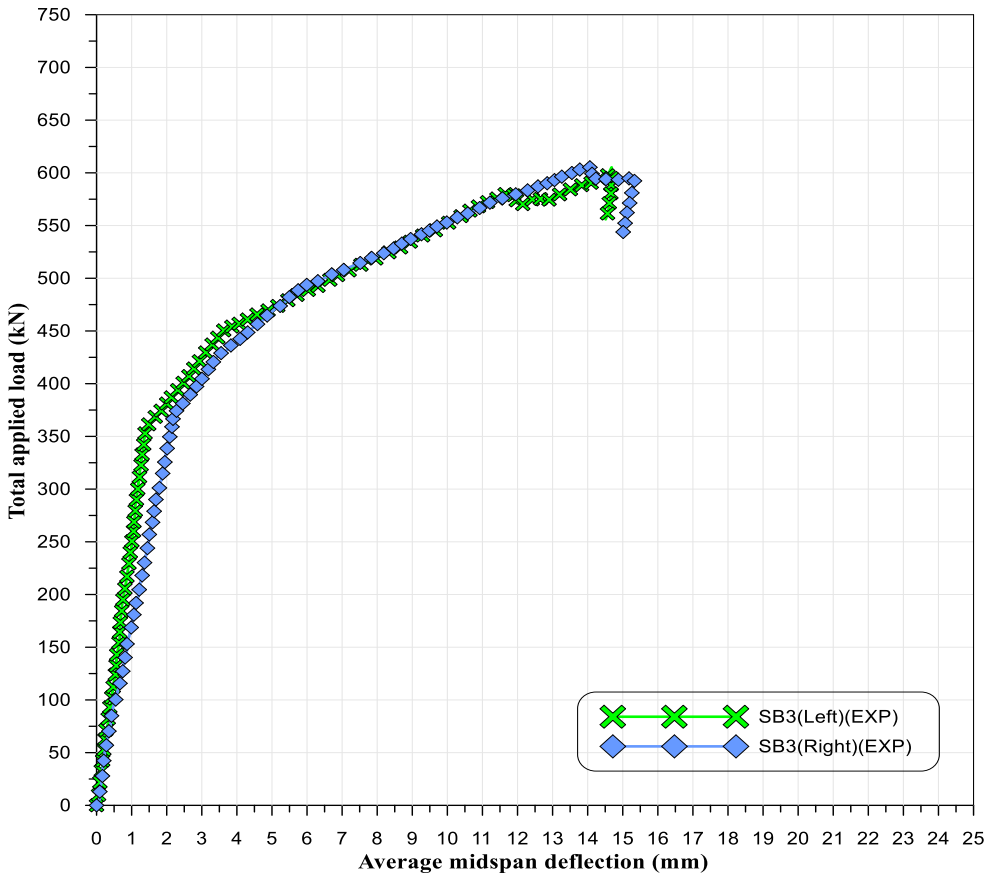

Figure (4-18) Load deflection curves of the SB3 tested beam

» SB5

This prestressed concrete beam was strengthened full wrapping the two sides (parallelogram shape), top, and bottom face by precast SIFCON laminates at the maximum shear region with the use of precast SIFCON laminates glued by epoxy; the details of the strengthened SB5 beam specimen are shown in Figure (3-12).

When the load was incrementally applied, the first flexural crack appeared at the mid-span region beside the laminates at the force of (302.1 kN). At the cracking load (Pcr) of (61.2% of ultimate load) at (328.1 kN), shear cracks are visible at the central support region. The cracking load at the central support and the mid-span increased significantly compared to SB1.

At high loading stages, the vertical flexural cracks in the mid-span region propagated towards the loading point and increased the width shear crack in the central support region, while SIFCON laminates prevented shear cracks in the mid-span. With the increased loads, a rupture in the SIFCON laminate at the top.

Beam SB5 reached an ultimate load at (492.9kN) with the mode of failure rupture of the top SIFCON laminate at the central support and debonding the top laminate, it did not happen any separation in SIFCON laminate at the insides and bottom, but SIFCON laminate helped the beam to hold its current state. As shown in Figure (4-19), Figure (4-20) shows the relationship between the load-deflection response at mid of each span. This strengthening pattern prevents any shear crack under the loading point region from appearing in the beam specimen.

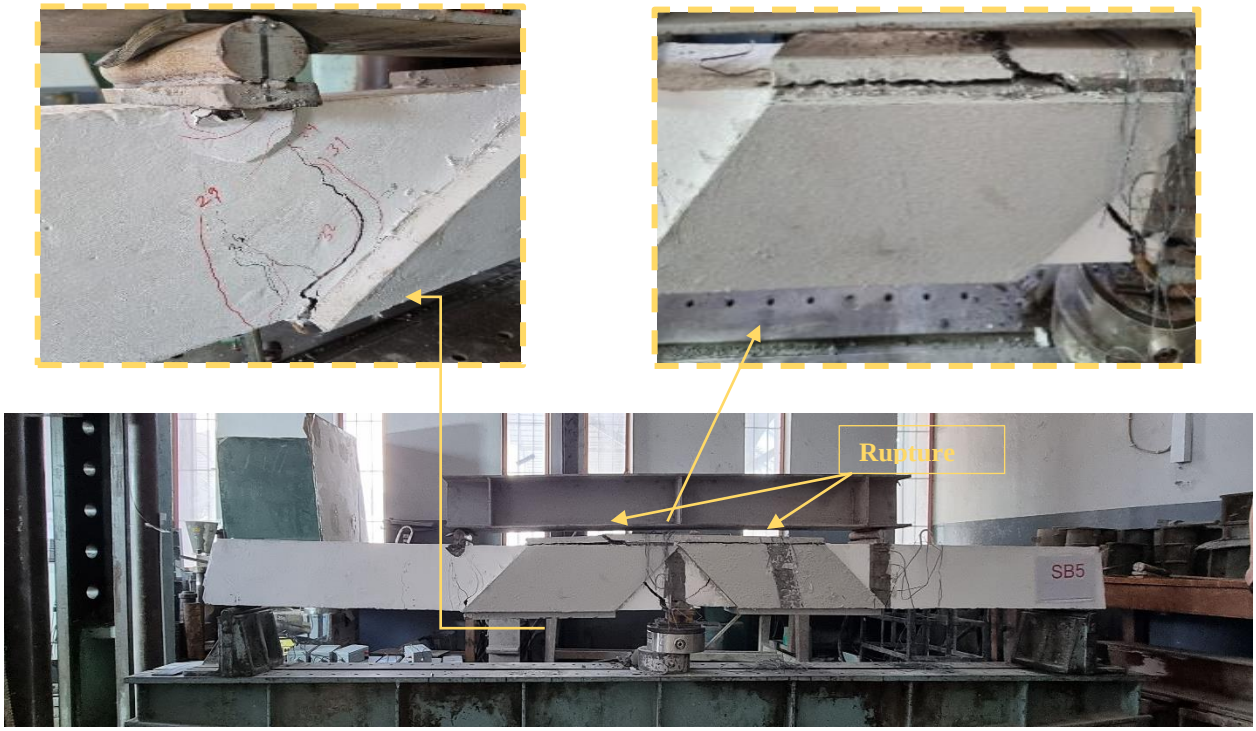

Figure (4-19) Failure of beam SB5

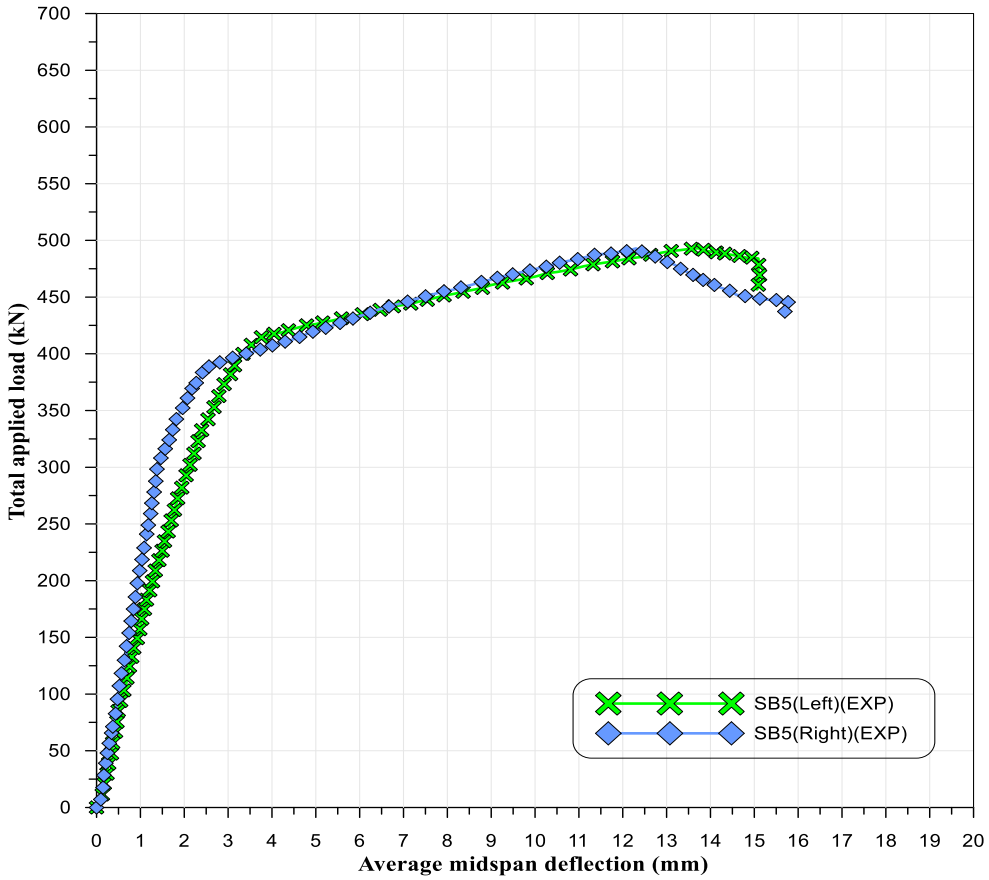

Figure (4-20) Load deflection curves of the SB5 tested beam

» SB7

This prestressed concrete beam was strengthened full wrapping (the two sides, top, and bottom face) with precast SIFCON laminates at the maximum shear region laminates glued by epoxy with small dimensions compared to that used with SB3 beam; the details of the strengthened SB7 beam specimen are shown in Figure (3-13).

When the load was incrementally applied, the beam started to develop flexural cracks, flexure-shear cracks at mid-span region, shear cracks in the central support region. The shear crack in the central support region propagated italicized towards the central support.

The first flexural cracks appeared of (310.9 kN) at the central support region the cracking load (Pcr) of (62 % of ultimate load), followed by another crack at the mid-span at a load of (318.3 kN). The vertical flexural cracks propagated towards the loading point at high loading stages and develop the shear cracks in the central support.

This beam failed in concrete crushing at mid-span. It fails without warning; The maximum shear resistances were (501.7kN). The cracking load at the central support and the mid-span increased remarkably compared to SB1; this strengthening pattern prevents shear failure in the mid-span and converts it to flexure-shear failure and doesn't happen is any debonding and rupture in SIFCON laminate as shown in Figure (4-21); Figure (4-22) shows the relationship between the load-deflection response at mid of each span.

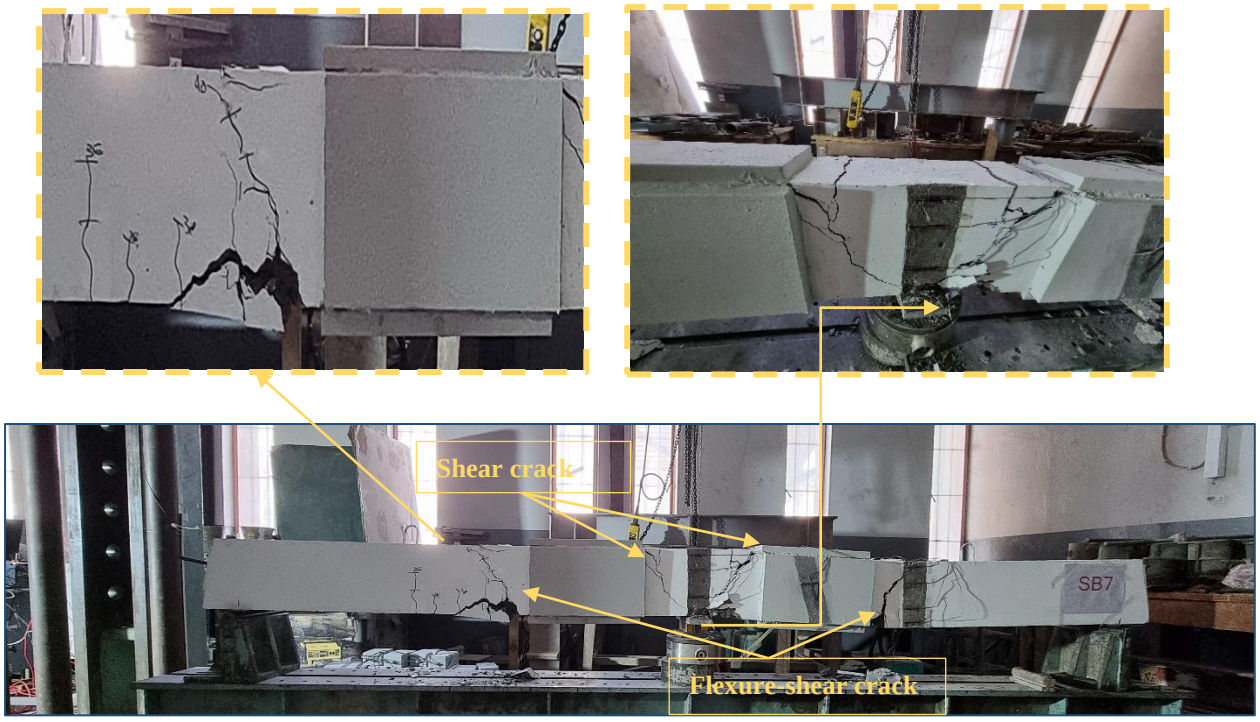

Figure (4-21) Failure of beam SB7

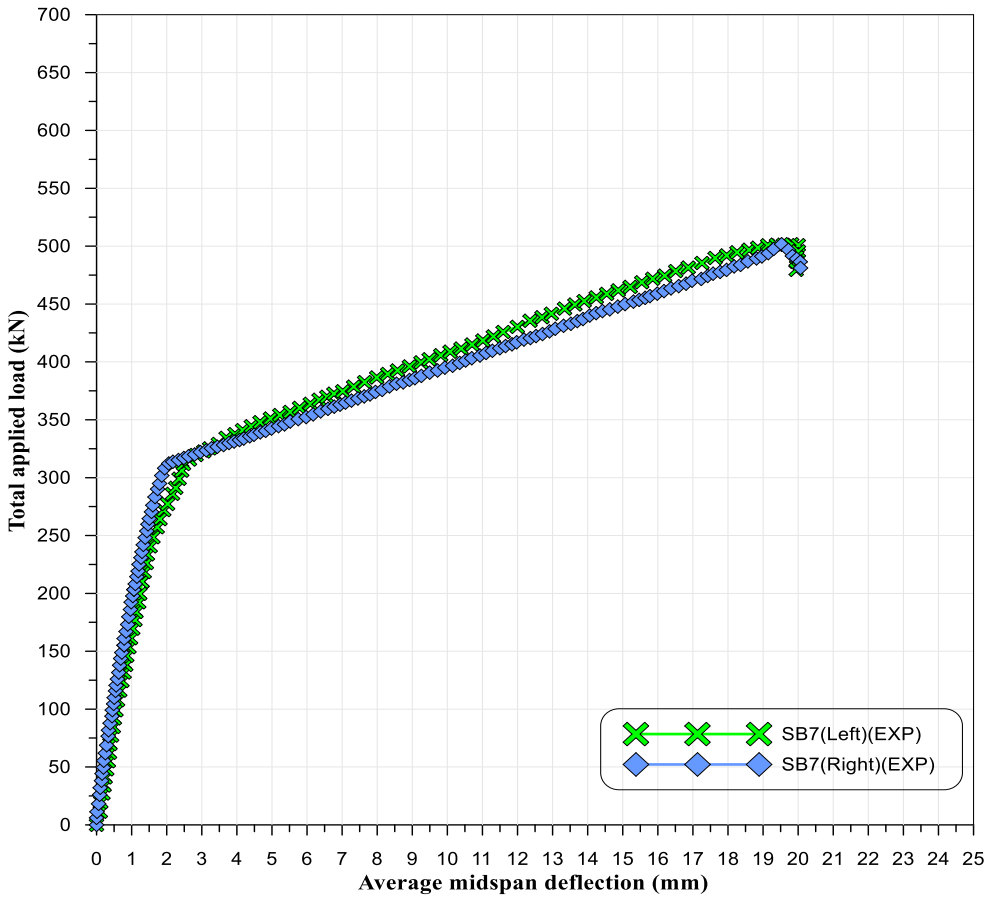

Figure (4-22) Load deflection curves of the SB7 tested beam

» SB8

This prestressed concrete beam was strengthened by precast SIFCON laminates similar to SB3 but partial wrapping (the two lateral faces only) at the maximum shear region with the use of precast SIFCON laminates glued by epoxy, the details of strengthened SB8 beam specimen shown in Figure (3-14).

When the load was incrementally applied, there were no visible shear cracks in the central support region because it is covered with SIFCON laminate. The first flexural crack appeared at the middle span region beside the laminates at the force of (359.2kN) at the cracking load (Pcr) of (68.5% of ultimate load). The cracking load increased significantly compared to SB1 but less than SB3.

At high loading stages, the cracks appear in the top surface of the beam in the central support region, the vertical flexural cracks in the mid-span region propagated towards the loading point. With the increased loads, a rupture in the SIFCON laminate at two middles of sides and hearing distinctive sounds during the cracking of the laminated beam SB8 reached an ultimate load at (524.3kN) with the mode of failure rupture of SIFCON laminate at the central support as shown in Figure (4-23) the ultimate load increased significantly compared to SB1 and less than SB3, Figure (4-24) shows the relationship between the load-deflection response at mid of each span.

Figure (4-23) Failure of beam SB8

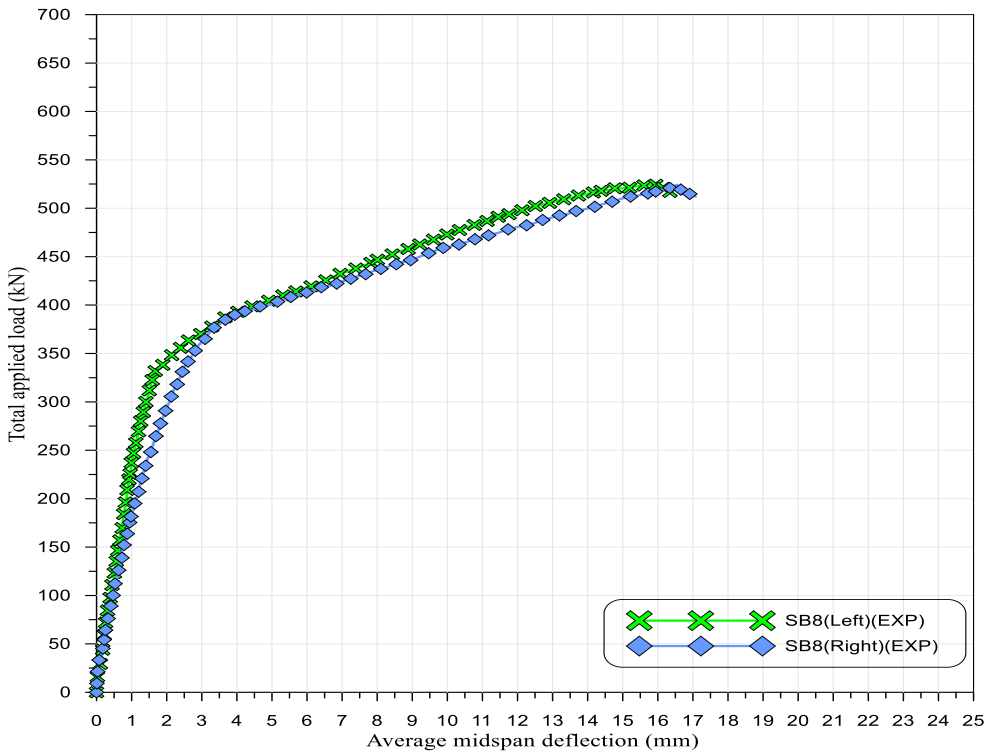

Figure (4-24) Load deflection curves of the SB8 tested beam

» SB9

This prestressed concrete beam was strengthened by precast SIFCON laminates similar to SB5 but partial wrapping (the two lateral faces only) at the maximum shear region with the use of precast SIFCON laminates glued by epoxy, the details of strengthened SB9 beam specimen shown in Figure (3-15).

When the load was incrementally applied, the first shear crack appeared at the mid span region beside the laminates at the force of (295.5 kN) at the cracking load (Pcr) of (62.2% of ultimate load).

Then at (316.3 kN) shear cracks visible at the central support region. The cracking load at the central support and the mid-span increased significantly compared to SB1.

At high loading stages, the cracks appear in the top surface of the beam in the central support region and the shear cracks in the mid-span region propagated towards the loading point.

With the increased load's beam SB9 reached an ultimate load at (475kN) with the mode of failure crushing of concrete, it fails without warning; it did not happen any separation in SIFCON laminate at the insides. But SIFCON laminate helped the beam to hold its current state. As shown in Figure (4-25), Figure (4-26) shows the relationship between the load-deflection response at mid of each span.

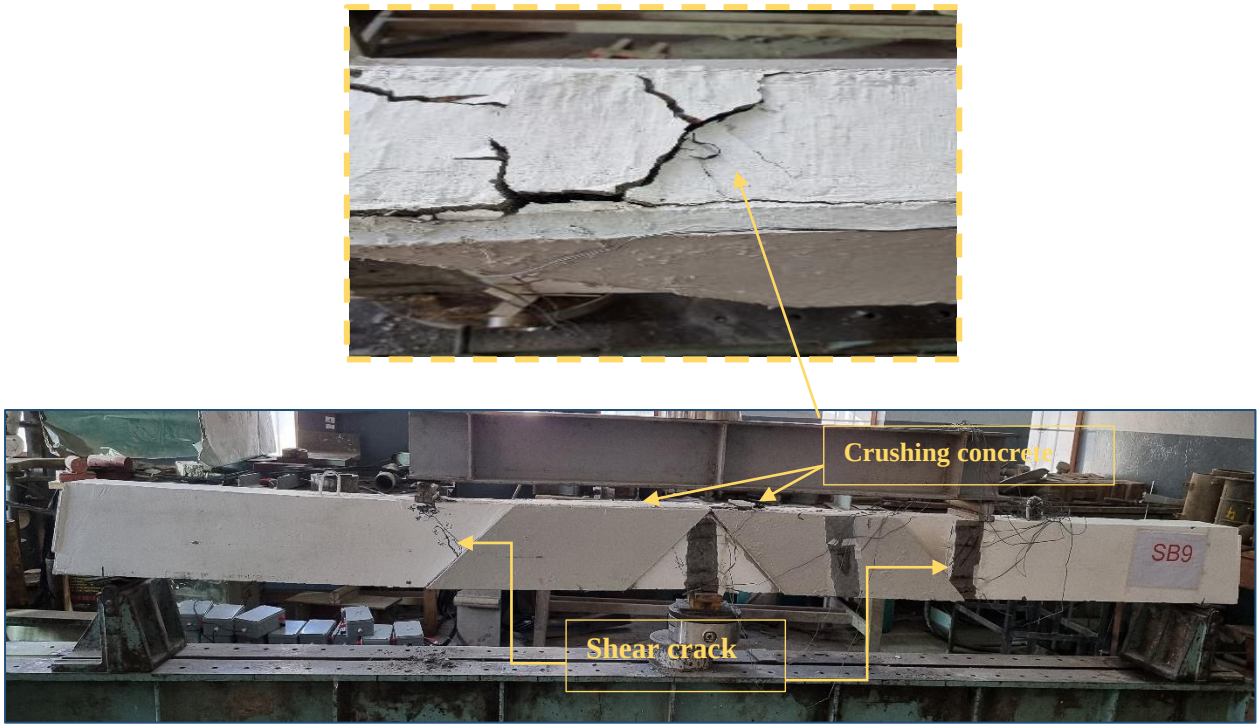

Figure (4-25) Failure of beam SB9

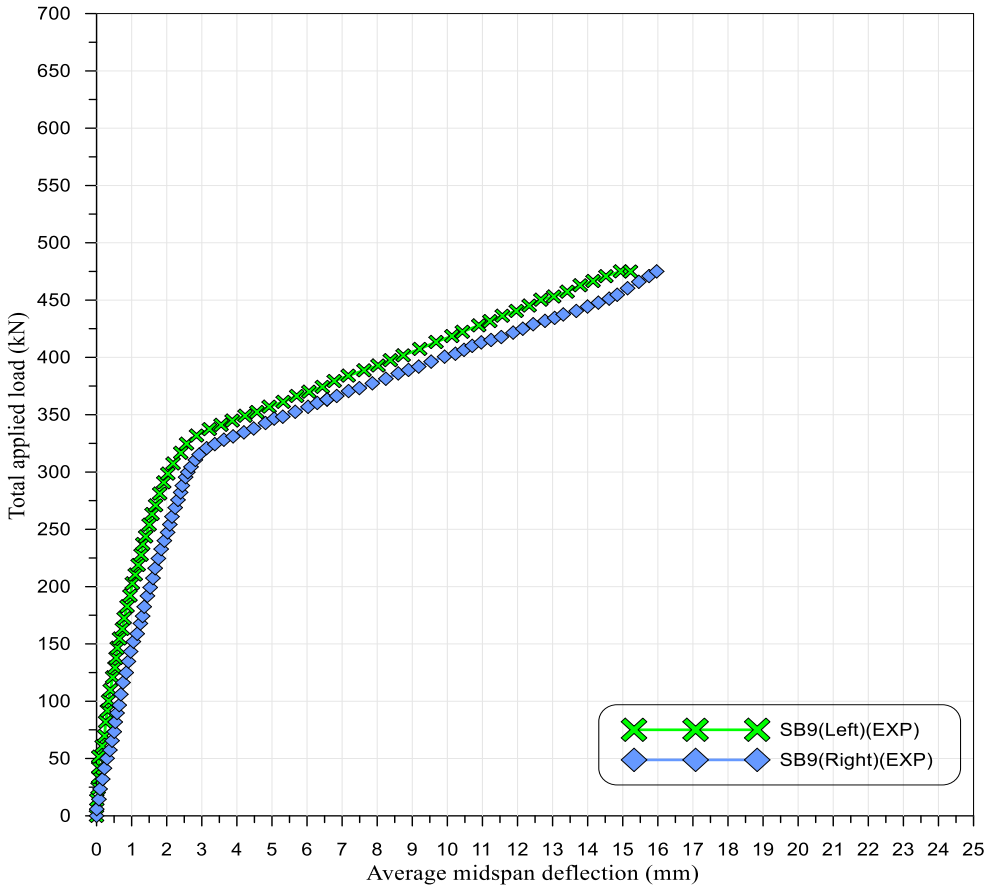

Figure (4-26) Load deflection curves of the SB9 tested beam

» SB10

This prestressed concrete beam was strengthened similar to SB7 but partial wrapping (the two lateral faces only) at the maximum shear region with the use of precast SIFCON laminates glued by epoxy, the details of strengthened SB10 beam specimen shown in Figure (3-16).

When the load was incrementally applied, the first flexural cracks appeared at the central support region in the cracking load (Pcr) of (299.1kN) of (65.6 % of ultimate load), followed by another crack at the mid-span at a load of (302.5 kN).

With increasing load, the beam started to develop flexure-shear cracks in the mid-span region, shear cracks in the central support region. The shear crack in the central support region propagated italicized towards the central support.

The vertical flexural cracks propagated towards the loading point at high loading stages and developed the shear cracks in the central support.

This beam failed in concrete crushing at mid-span. It fails without warning; the maximum shear resistances were (455.7 kN) the cracking load at the central support and the mid-span increased significantly compared to SB1; this strengthening pattern reduces the sharpness of the shear failure in the mid-span and converts it to flexure-shear failure and doesn't happen any debonding and rupture in SIFCON laminate as shown in Figure (4-27); Figure (4-28) shows the relationship between the load-deflection response at mid of each span.

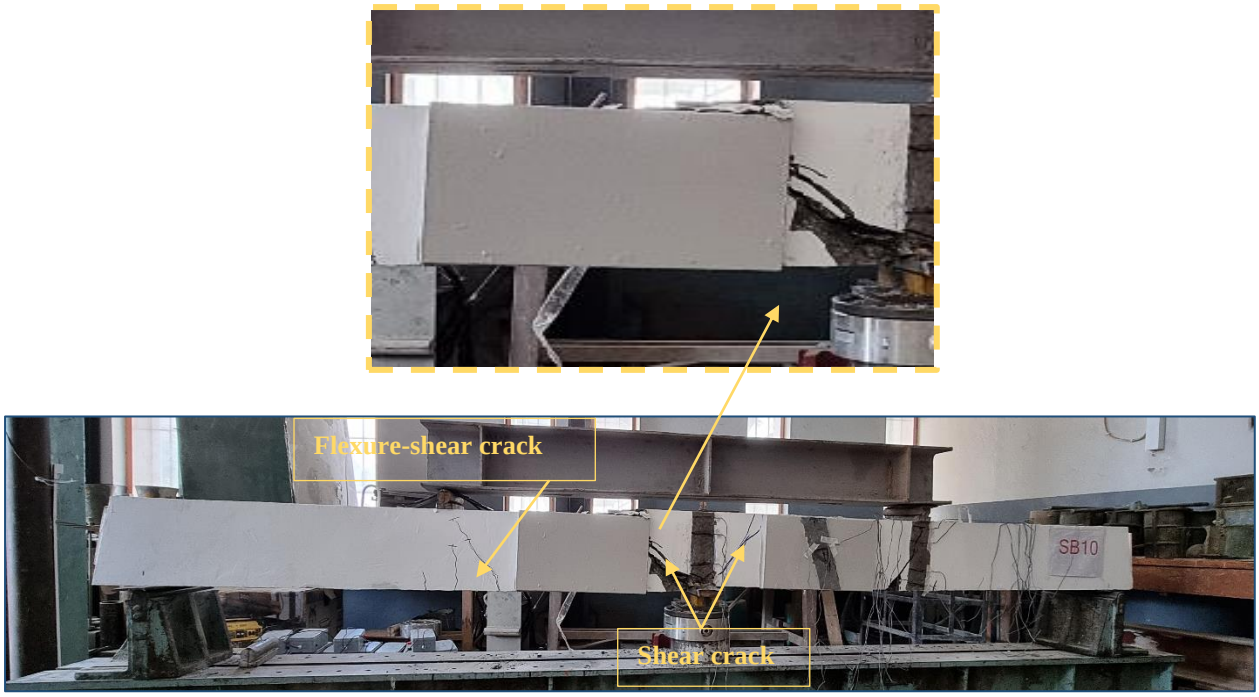

Figure (4-27) Failure of beam SB10

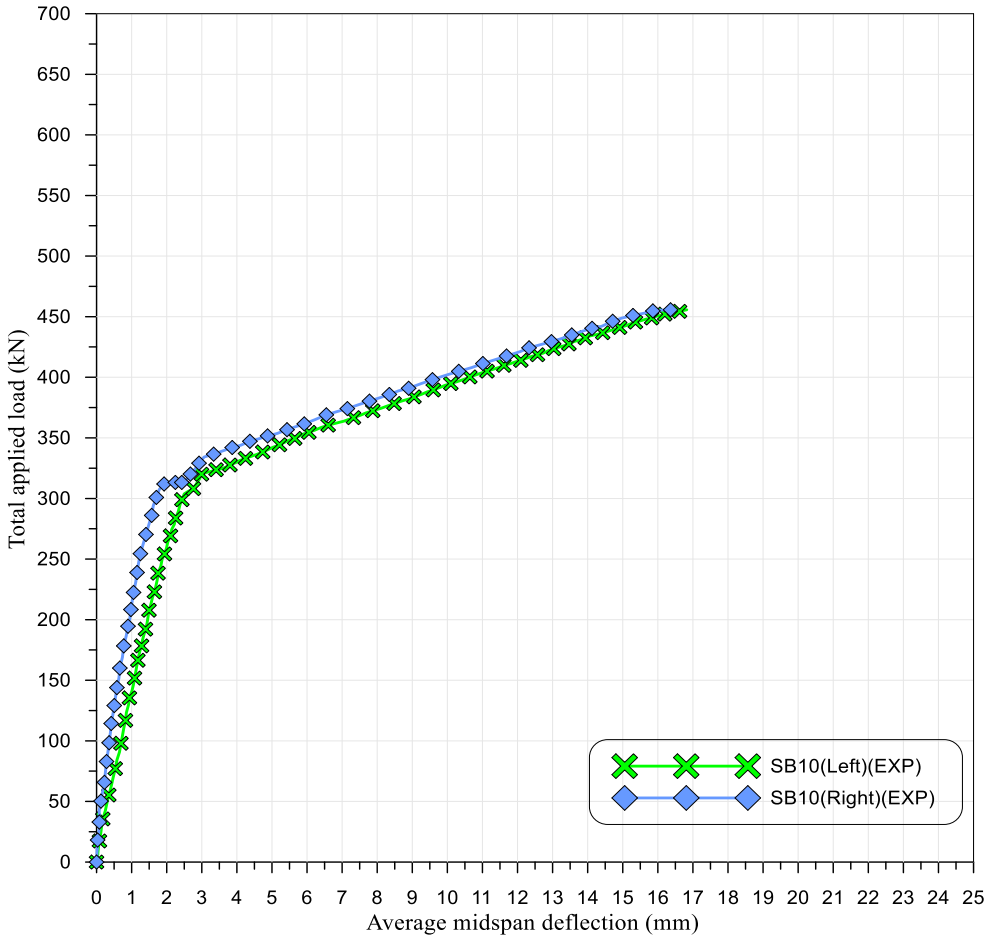

Figure (4-28) Load deflection curves of the SB10 tested beam

4.3.5 The Feasibility of The Shear Strengthening by Using the Different Pattern of The Laminates

Seven prestressed concrete beams with six different patterns of the precast SIFCON laminates glued by epoxy resin were used for strengthening the maximum shear regions for comparison in this section of the study.SB1 unstrengthened beam, SB3, SB5, SB7, SB8, SB9, and SB10 strengthened beams with the precast SIFCON laminate that have patterns shown in Figures (3-11) to (3-16) from the results in section (4.3.4). Figure (4-29) compares between the load deflection curves of beams above, and the following are observed:

- Generally, all the shear strengthening patterns that used is effective in delaying the first crack appearance time of the tested beams, the first crack load increased with ratio (105.7%), (26.4%), (30.1%), (50.4%), (23.7%) and (25.2%) respectively for the beam SB3, SB5, SB7, SB8, SB9, and SB10 compared with the reference beam SB1.
- Increasing the ultimate load capacity of the tested beams, the results explain that the enhancement in shear capacity has reached (46.5%), (19.3%), (21.4%), (26.9%), (14.9%) and (10.3%) respectively for the beam SB3, SB5, SB7, SB8, SB9, And SB10 compared with the reference beam SB1.
- Reduction of the mid-span deflection at the ultimate load due to the application of SIFCON laminates, the decrease in deflection (40.2%), (38.6%), (2.5%), (37.1%), (40.2%) and (15.5%) respectively for the beam SB3, SB5, SB7, SB8, SB9, and SB10 compared with the reference beam SB1.
- For SB9 and SB10, although strength was increased by gluing precast SIFCON laminates to the two faces, the behavior has

deteriorated, and the specimen failed abruptly without showing any warning.

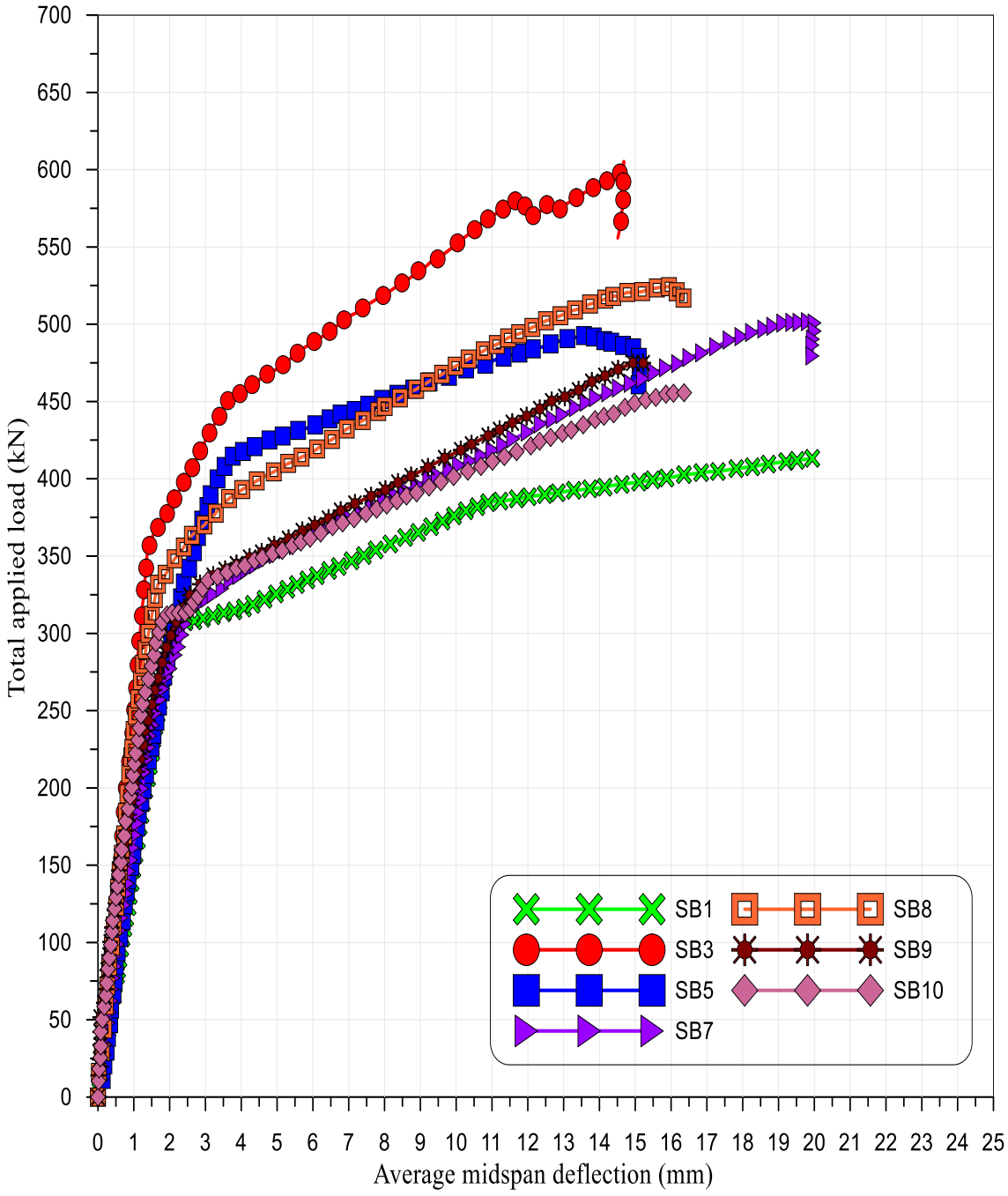

Figure (4-29) Load deflection curves for beams SB1, SB3, SB5, SB7, SB8, SB9, and SB10

4.3.6 The Feasibility of Full and Partial Wrapping on The Shear Strengthening

Regarding the effect of full and partial wrapping of precast SIFCON laminates, it was a comparison between six prestressed concrete beams that have similar strengthen patterns full and partial wrapping: (SB3, SB8), (SB5, SB9) and (SB7, SB10). Figures (4-30) to (4-32) compare between the load-deflection curves of tested beams strengthened by using the full and partial wrapping and reference beam SB1, and the following are observed:

- Delay the appearance of the first crack for the beams strengthened full wrapping the first crack load increased with ratio (36.8%), (2.2%) and (4%) respectively for the beam SB3, SB5, and SB7 compared with the similar pattern but partial wrapping beams SB8, SB9, and SB10 respectively.
- Increasing the ultimate load capacity of the tested beams, (15.4%), (3.8%) and (10.1%) respectively for the beam SB3, SB5, and SB7 compared with the similar pattern but partial wrapping beams SB8, SB9, and SB10 respectively.
- Increasing and decreasing the mid-span deflection at the ultimate load due to applying SIFCON laminates according to the strengthening pattern. Decreased in deflection (4.8%) for the beam SB3 compared with SB8 and increased the deflection (2.5%) and (15.5%) for SB5, and SB7 compared with the similar pattern with partial wrapping beams for SB9, and SB10 respectively.

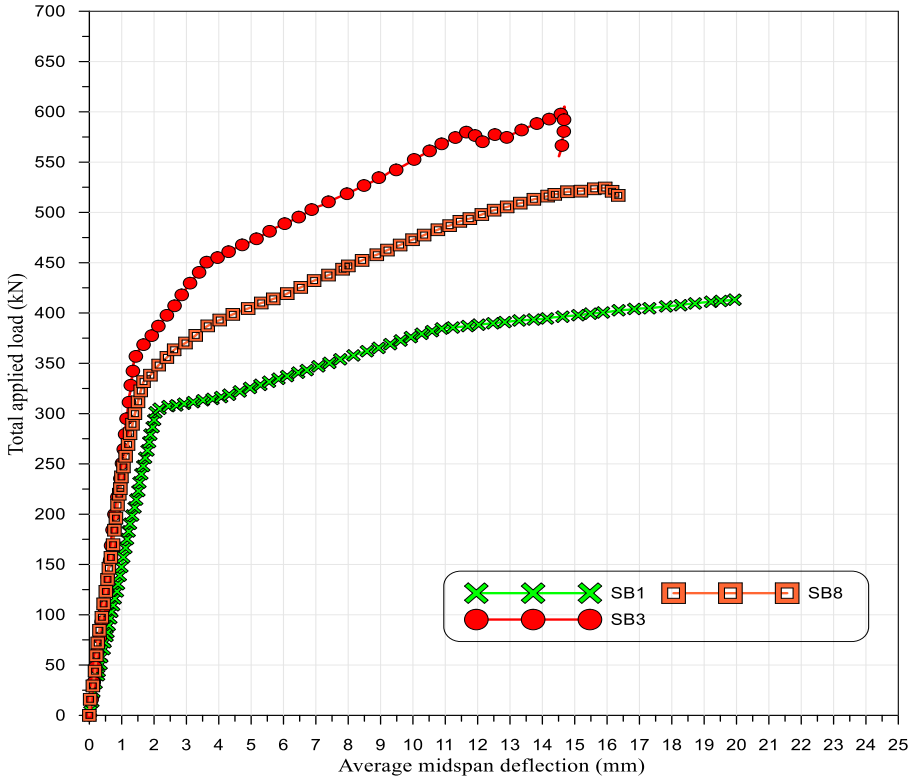

Figure (4-30) Load deflection curves for beams SB1, SB3 and SB8

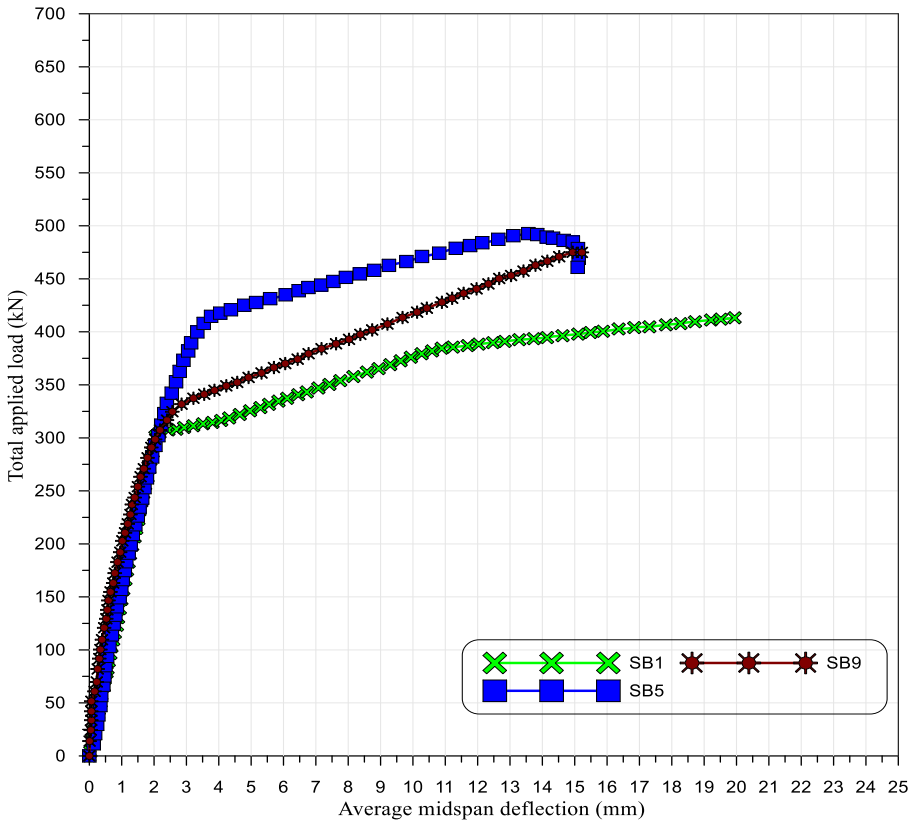

Figure (4-31) Load deflection curves for beams SB1, SB5 and SB9

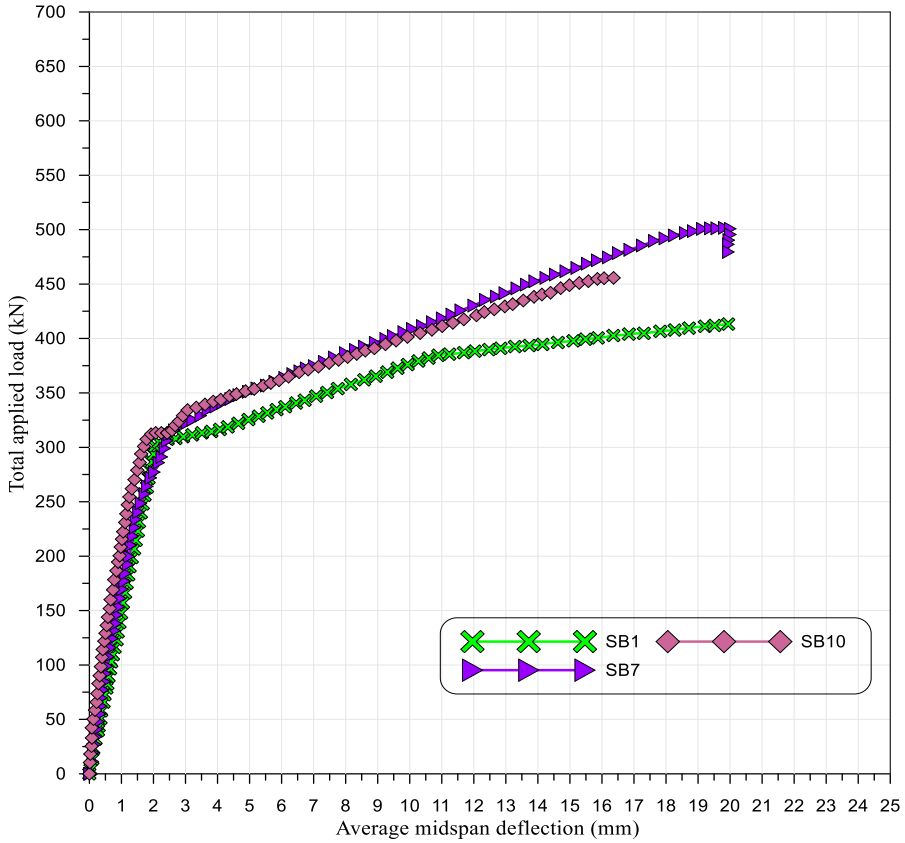

Figure (4-32) Load deflection curves for beams SB1, SB7 and SB10

4.4 General Behavior of Prestressed Concrete Beams Under Repeated Loading

The second part of the experimental program includes testing seven prestressed concrete beams specimens were divided into two categories: flexural [Group B] and shear [Group D] tested under repeated loading.

The current study adopted ten cycles with the loading range varied between (40%) to (60%) of the ultimate load produced from the monotonic static loading test. The testing procedure has been conducted according to the steps mentioned in section (3.19.2). The cracking and ultimate load-carrying capacities and types of failure mode of the tested beams at the central support and the mid-span are provided in the next paragraphs.

4.4.1 General Behavior of Flexure Beams [Group B]

This group consists of four prestressed concrete beams specimens to study the flexural behavior of the tested beams under repeated loading.

One unstrengthened as a reference beam and three strengthened with precast SIFCON laminates in hogging and sagging regions to study the effect of repeated loading on the tested beams specimens.

»FB2

This prestressed concrete beam is unstrengthened considered as a reference beam for the other test beams that are designed to fail in flexure and subjected to the repeated loading.

The first visible flexure crack occurred at the central support (maximum moment region) at the cracking load (243.8 kN) at the first cycle of the loading by a little increasing the load the limited number of existing cracks grew wider, on further load increases the cracks occurred under the load points at the mid-span at a load of (258.1 kN).

Beam FB2 reached an ultimate load at (430.6kN) with a flexure mode of failure (crushing of concrete) as shown in Figure (4-33). Figure (4-34) shows the relationship between the load-deflection response at mid of each span.

Compared with the previous reference specimen FB1, it can be noticed that FB2 has the same behavior but cracks increased at the mid-span region due to the repeated loading, which caused a reduction in the beam the ultimate load.

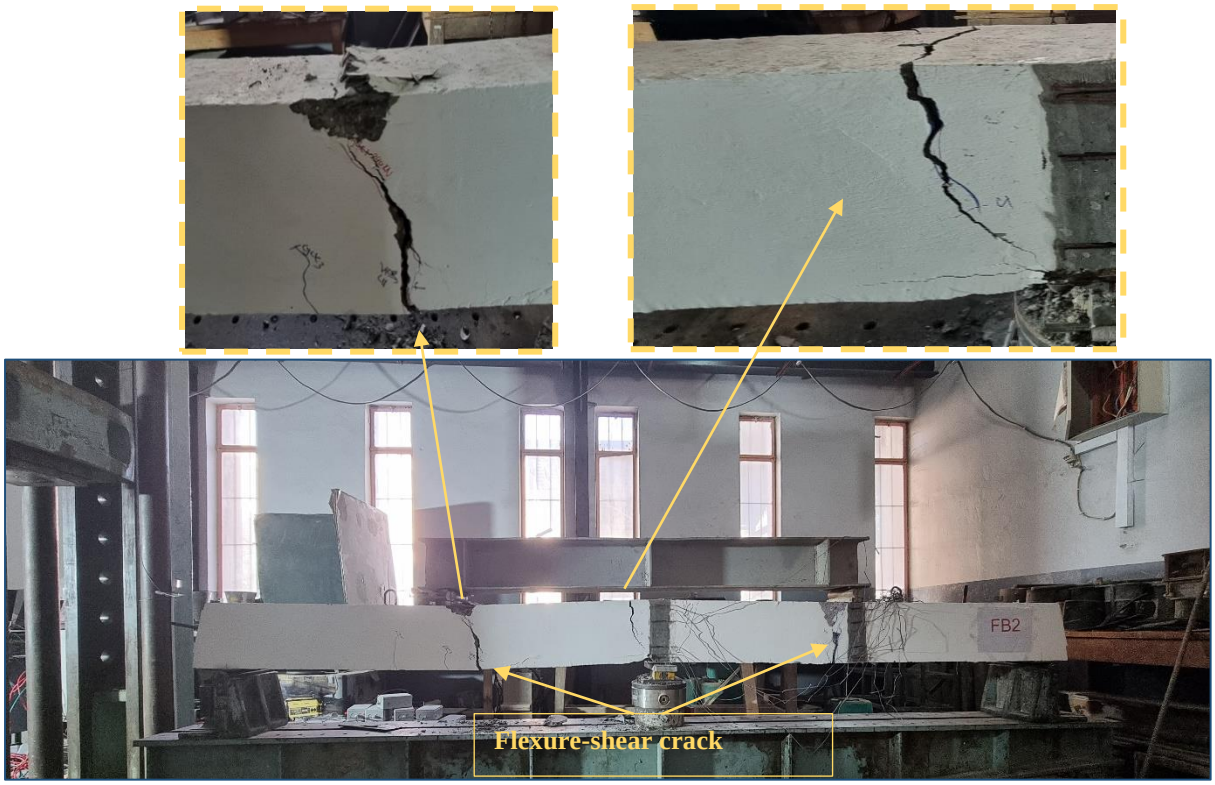

Figure (4-33) Failure of beam FB2

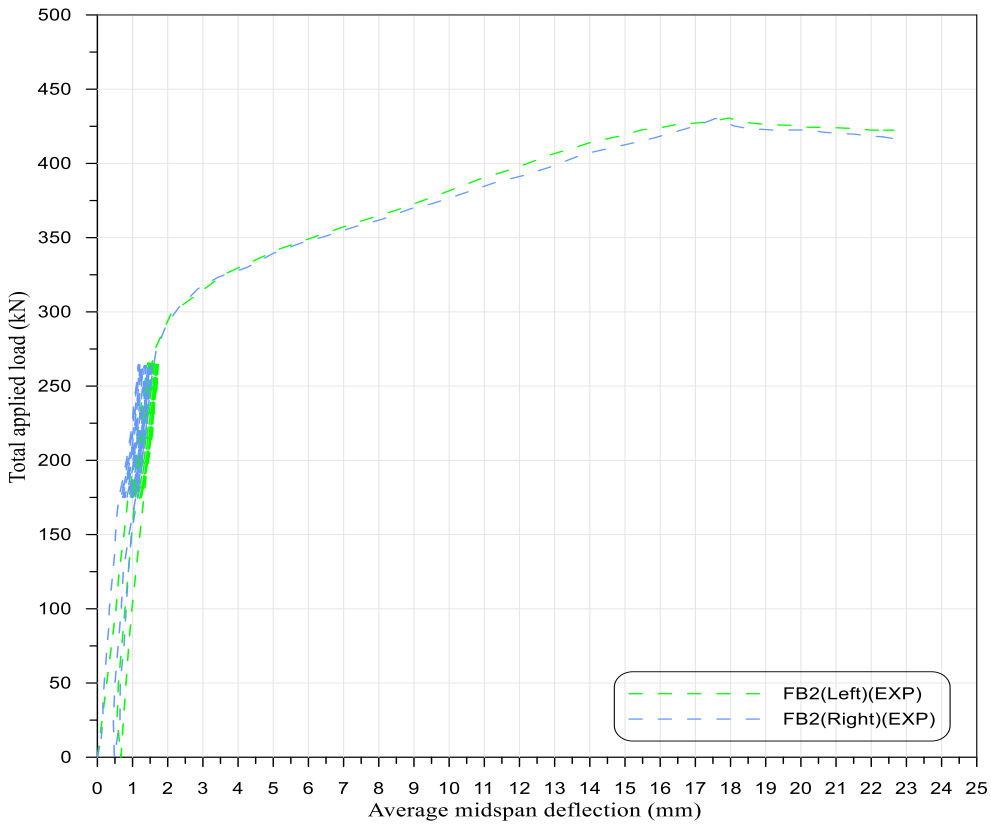

Figure (4-34) Load deflection curves of the FB2 tested beam

»FB4

This prestressed concrete beam is completely the same as FB3 and subjected to the repeated loading. The first crack occurred at the central support at the cracking load (351.1kN) at the second cycle of loading by the increasing load the first crack occurred at the mid-span at the load of (356 kN).

The FB4 beam reached an ultimate load at (592.3kN) with crushing of concrete, rupture SIFCON laminate in the mid-span and central support region, as shown in Figure (4-35). Figure (4-36) shows the relationship between the load-deflection response at mid of each span.

Compared with the previous reference specimen FB3, it can notice that FB4 has the same behavior but the difference in the beam failure before debonding the SIFCON laminate and cracks increased at mid-span due to the repeated loading, which caused a reduction in the beam the ultimate load.

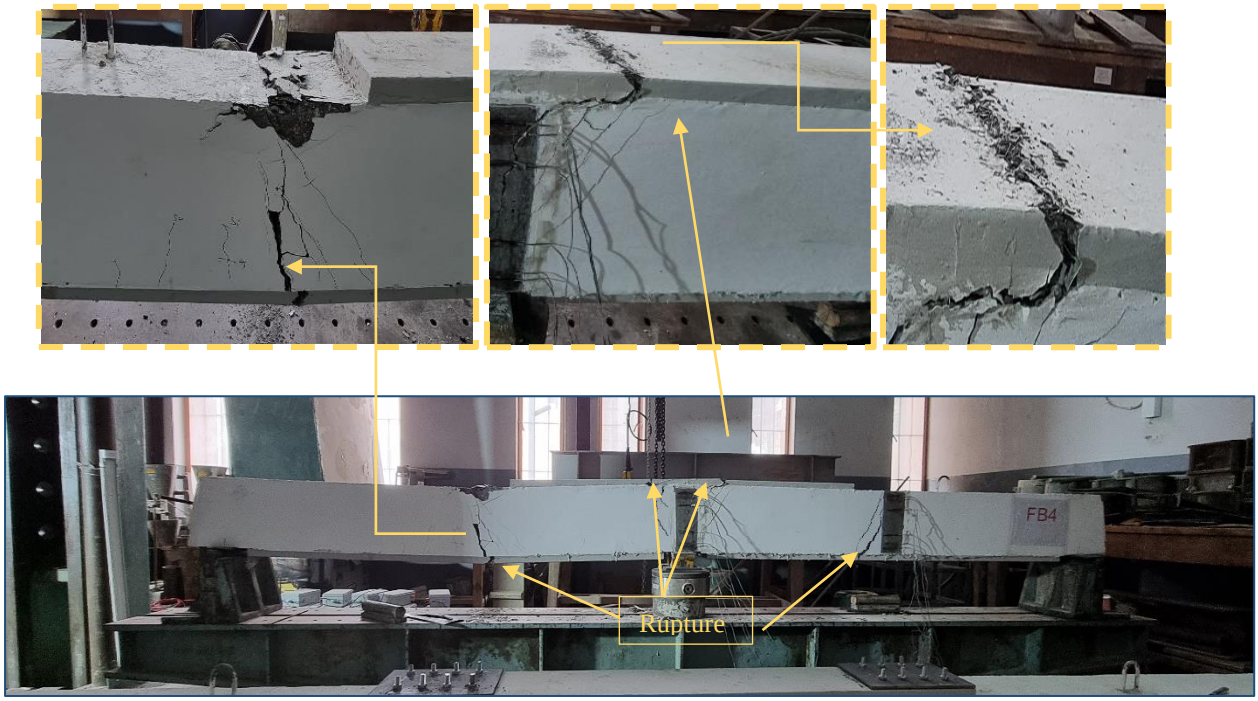

Figure (4-35) Failure of beam FB4

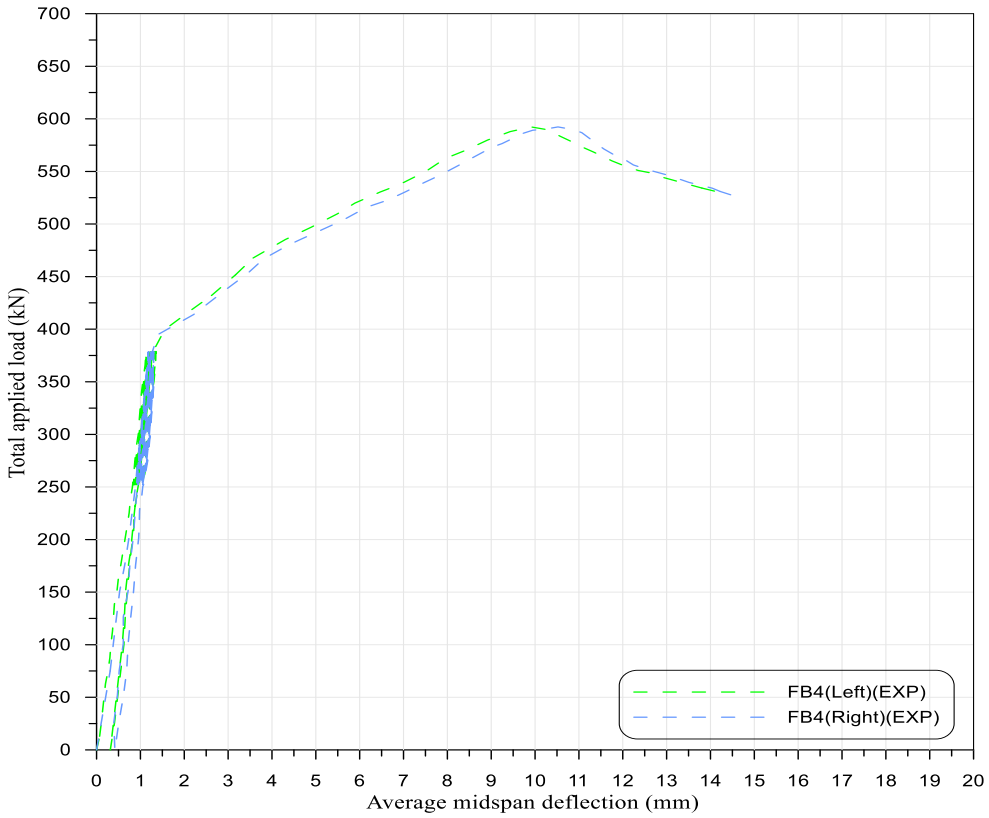

Figure (4-36) Load deflection curves of the FB4 tested beam

»FB6

This prestressed concrete beam is completely the same as FB5 and subjected to the repeated loading. The first crack occurred at the central support at the cracking load (312.2kN) at the third cycle.

By increasing load, the first crack occurred at the mid-span at a load of (320.1kN). Beam FB6 reached an ultimate load at (661.8 kN) with the mode of failure crushing of concrete, and rupture in SIFCON laminate sagging region in addition pull part of concrete at last stage of loading and rupture in SIFCON laminate at hogging region as shown in Figure (4-37); Figure (4-38) shows the relationship between the load-deflection response at mid of each span.

Compared with the previous reference specimen (FB5), it can be noticed that the first flexural cracks increased in mid-span and formed early due to the

repeated loading, which caused a reduction in the ultimate load and debonding happened after rupturing in SIFCON laminate at sagging region.

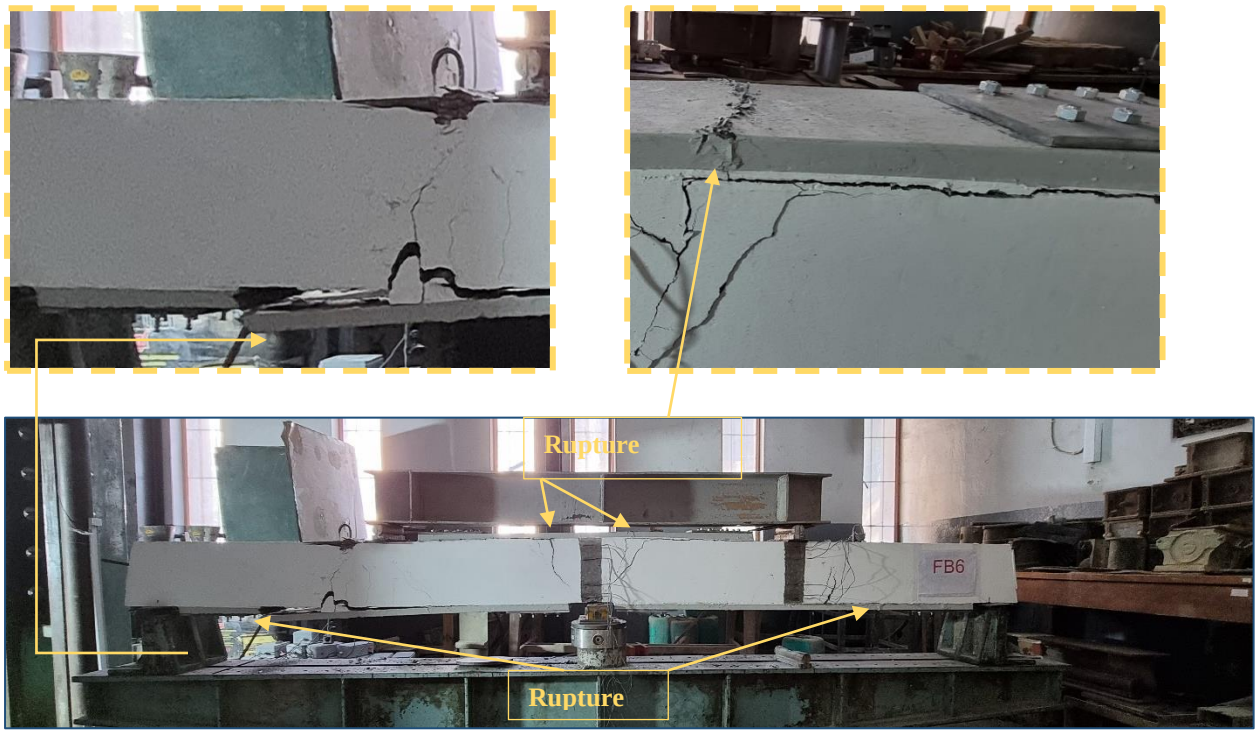

Figure (4-37) Failure of beam FB6

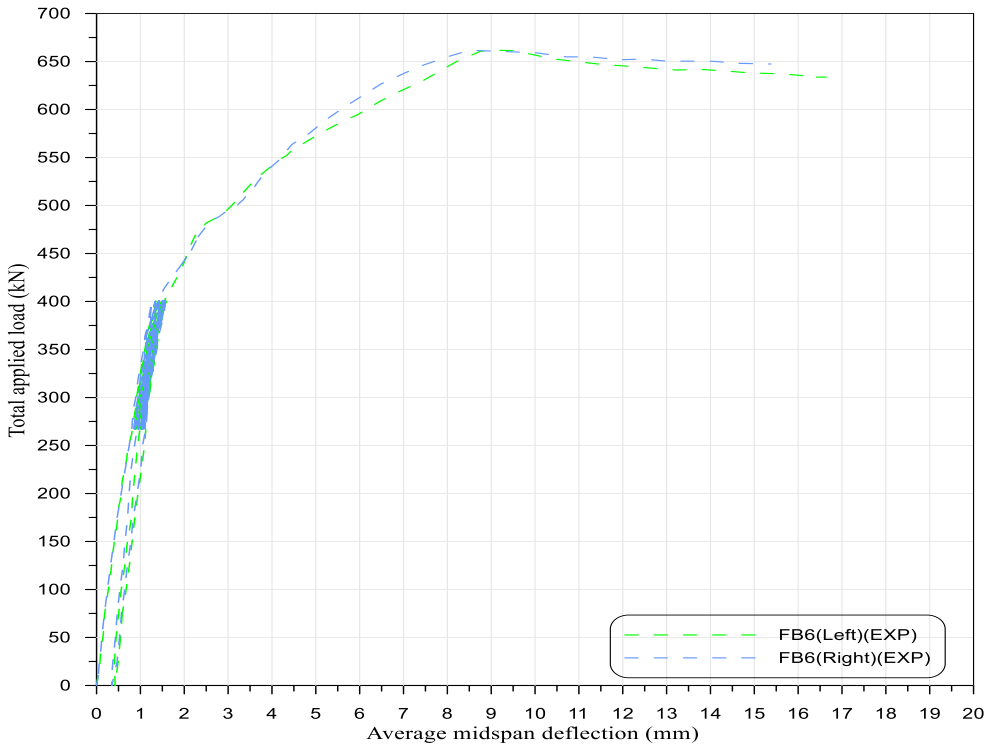

Figure (4-38) Load deflection curves of the FB6 tested beam

»FB8

This prestressed concrete beam is completely the same as FB7 and subjected to the repeated loading. The first crack occurred at the central support at the cracking load (387.1kN) at the third cycle of loading; by increased load, the first crack occurred at the mid-span at the load of (390.5 kN).

Beam FB8 reached an ultimate load at (681.8 kN) with flexure mode of failure crushing of concrete and rupture of SIFCON laminate, as shown in Figure (4-39). Figure (4-40) shows the relationship between the load-deflection response at mid of each span.

Compared with the previous reference specimen (FB7), it can be noticed that increase in flexural cracks in mid-span due to the repeated loading, which caused a reduction in the ultimate load.

Figure (4-39) Failure of beam FB8

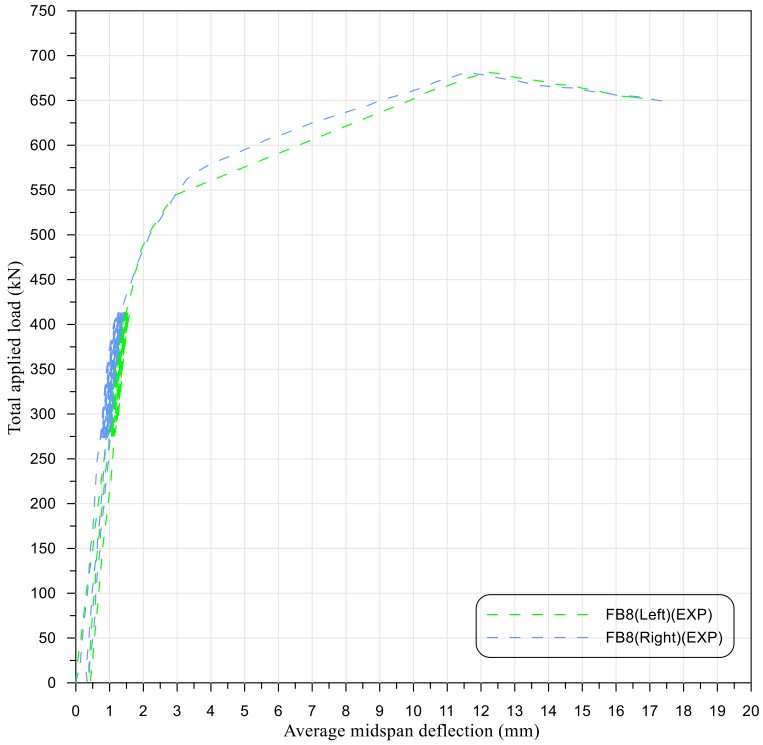

Figure (4-40) Load deflection curves of the FB8 tested beam

4.4.2 General Behavior of Shear Beams [Group D]

This group consists of three prestressed concrete beams specimens to study the shear behavior of tested beams under the repeated load. One unstrengthened as a reference beam and two strengthened with precast SIFCON laminates with different patterns in the maximum shear region to study the effects of repeated loading.

»SB2

This unstrengthened prestressed concrete beam is considered as a reference beam for the other test beams that are designed to fail in shear and subjected to the repeated loading.

When the load was incrementally applied, the beam started to develop flexural cracks and shear cracks. The shear crack started at the point of applying the load and propagated italicized towards the mid support. The first flexural and shear cracks appeared simultaneously at a force of (240.5kN) at the first cycle of

loading at the central support region, followed by another shear crack at the mid-span at a load of (248.1 kN).

This beam failed in shear by means of diagonal tension and hearing distinctive sounds during the cracking. The maximum shear resistances were (397.3kN), as shown in Figure (4-41). Figure (4-42) shows the relationship between the load-deflection response at mid of each span.

Compared with the previous reference specimen SB1, it can be noticed that SB2 has the same behavior but a decrease in failure loading due to the repeated loading, which caused a reduction in the ultimate load.

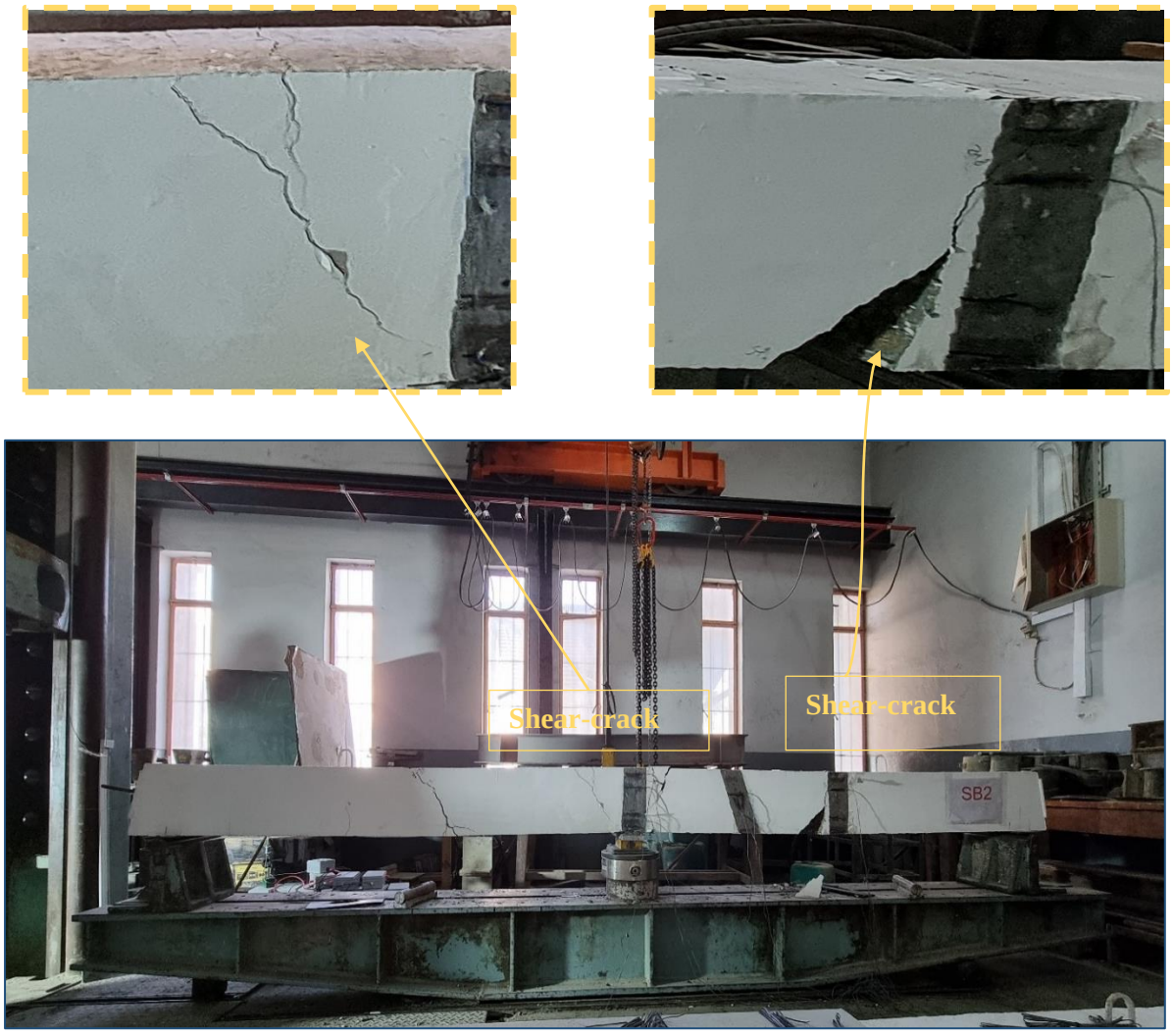

Figure (4-41) Failure of beam SB2

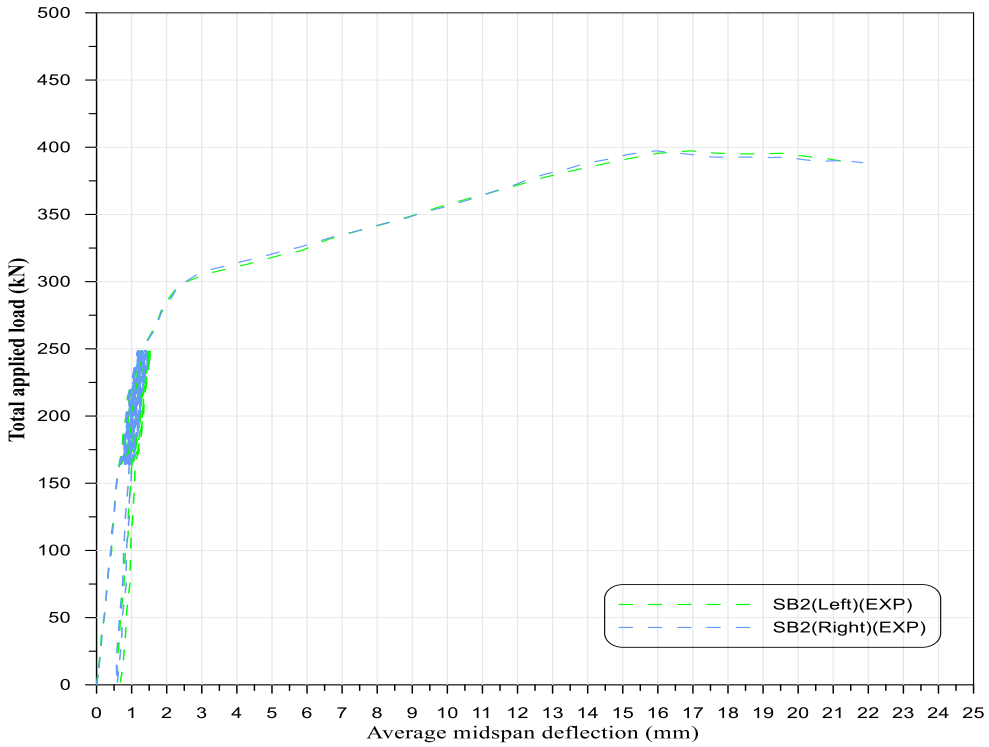

Figure (4-42) Load deflection curves of the SB2 tested beam

»SB4

This prestressed concrete beam is completely the same as SB3 and subjected to the repeated loading. The first flexural crack appeared at the middle span region beside the laminates at the force of (350.2 kN) at the third cycle of loading.

Beam SB4 reached an ultimate load at (589.2 kN) with the mode of failure crushing of concrete at mid-span region and rupture of SIFCON laminates at the central support region as shown in Figure (4-43), Figure (4-44) shows the relationship between the load-deflection response at mid of each span.

Compared with the previous reference specimen SB3, it can be noticed that SB4 has the same behavior but the lower laminates are not debonding as it happened in the SB3 beam and a decrease in failure loading due to the repeated loading, which caused a reduction in the ultimate load.

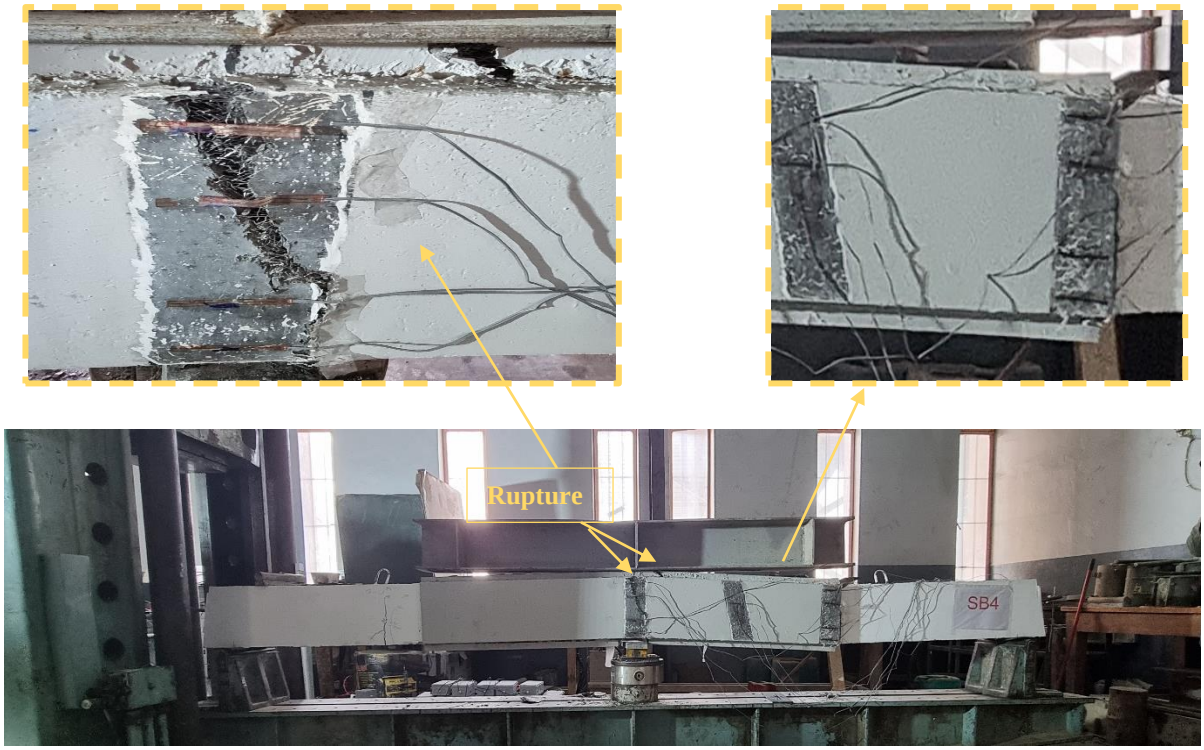

Figure (4-43) Failure of beam SB4

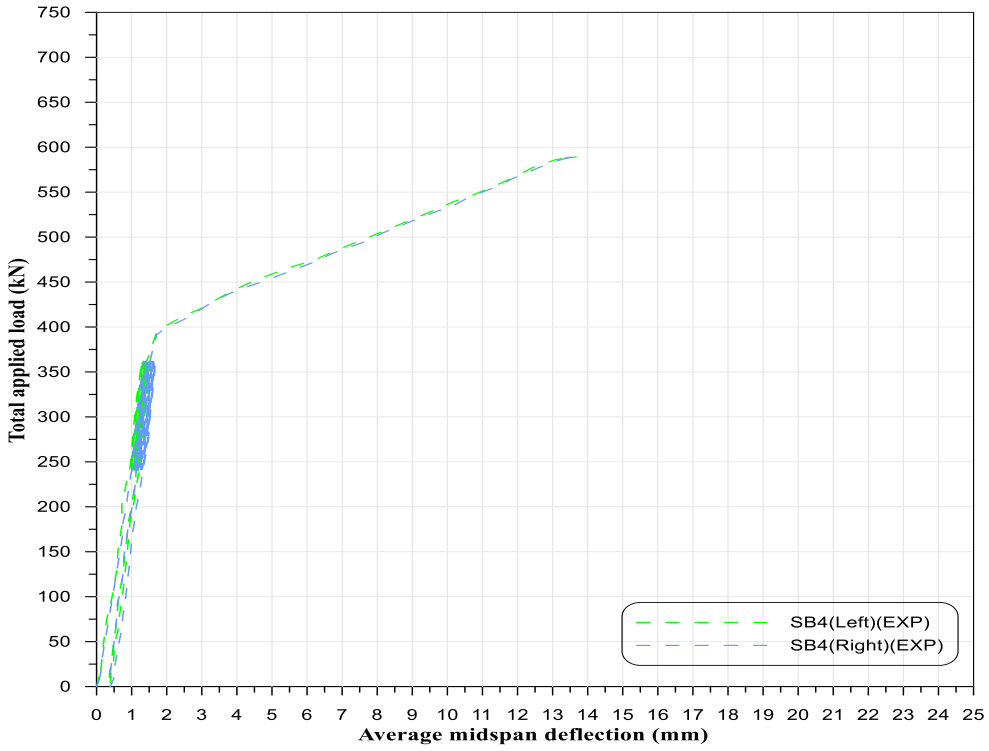

Figure (4-44) Load deflection curves of the SB4 tested beam

»SB6

This prestressed concrete beam is completely the same as SB5 and subjected to repeated loading. When the load was incrementally applied, the first flexural crack appeared at the mid-span region beside the laminates at the force of (292.5kN) at the first cycle, shear cracks are visible at the central support region at (295kN). With the increasing loads, a debonding in the SIFCON laminate at the top.

Beam SB6 reached an ultimate load at (481.9kN) with the mode of failure crushing concrete and debonding of the top laminate as shown in Figure (4-45), Figure (4-46) shows the relationship between the load-deflection response at mid of each span. Compared with the previous reference specimen SB5, it can be noticed that SB6 has the same behavior, but a decrease in failure load due to the repeated loading and the beam SB6 arrive to failure before rupturing in the SIFCON laminates.

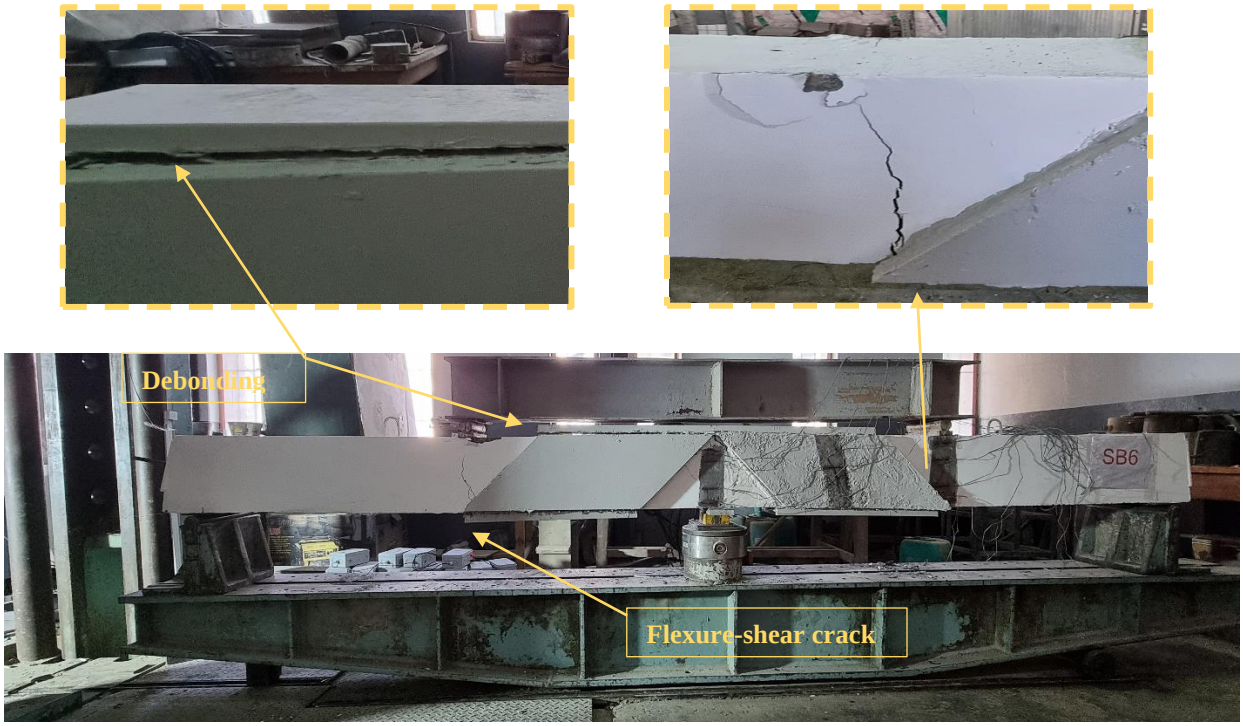

Figure (4-45) Failure of beam SB6

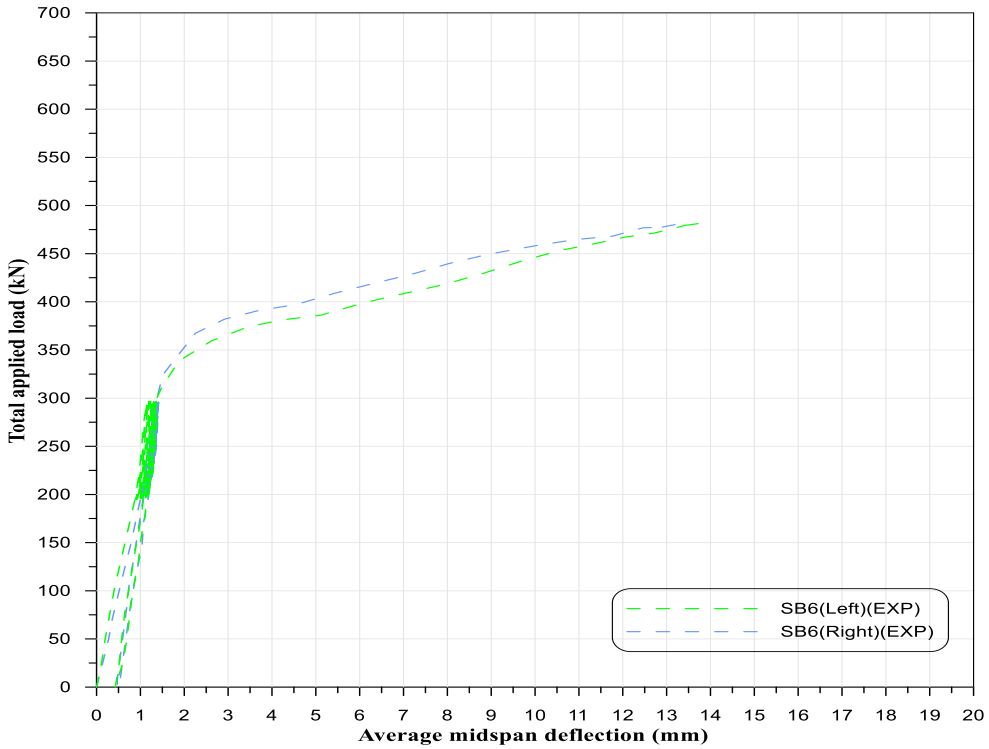

Figure (4-46) Load deflection curves of the SB6 tested beam

4.4.3 Comparative Study: Monotonic Static and Repeated Loading

In this section, a comparison of the flexural and shear behavior of the prestressed concrete beams specimens tested under monotonic static loading (group A and C) and the specimens subjected to repeated loading (group B and D) .

The goal of this comparison is to investigate the effect of repeated loading on the characteristics of prestressed concrete specimens that are externally strengthened with precast SIFCON laminates.

This comparison involves load-deflection curves, first and ultimate loading, ultimate deflection. Figure (4-47) to (4-53) includes the load-deflection curves for the specimens under monotonic static loading and for counterpart specimens but after exposing them to ten cycles of repeated loading.

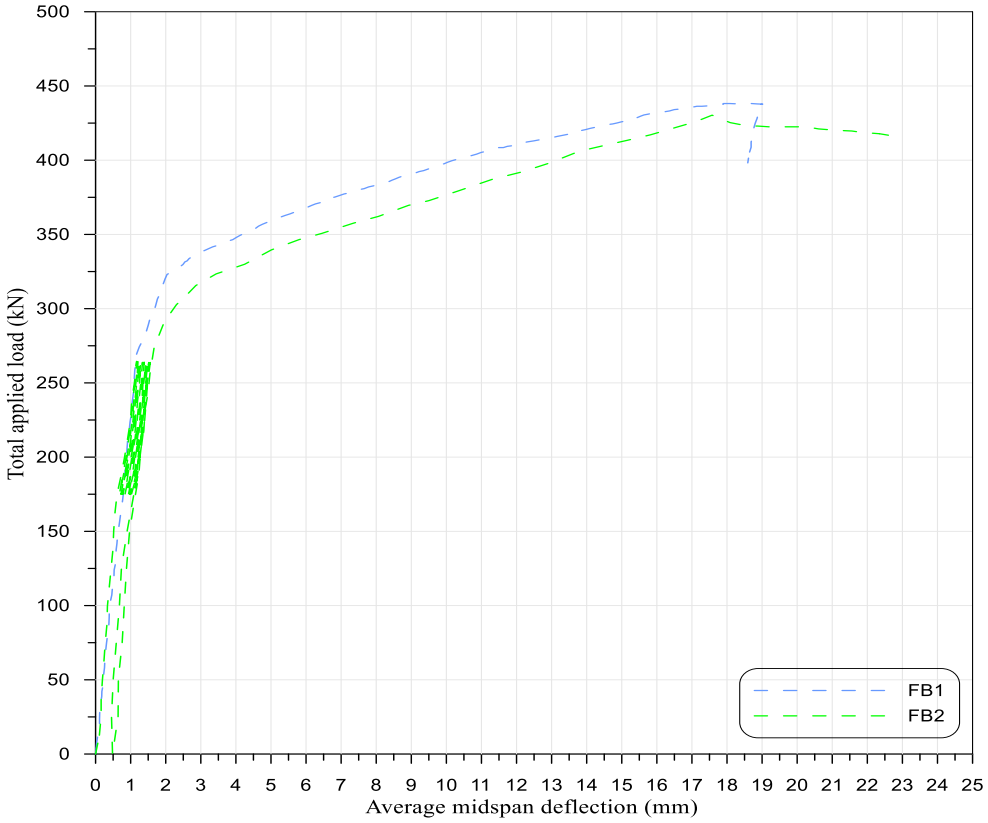

Figure (4-47) Load deflection curves of the FB1 and FB2 beam

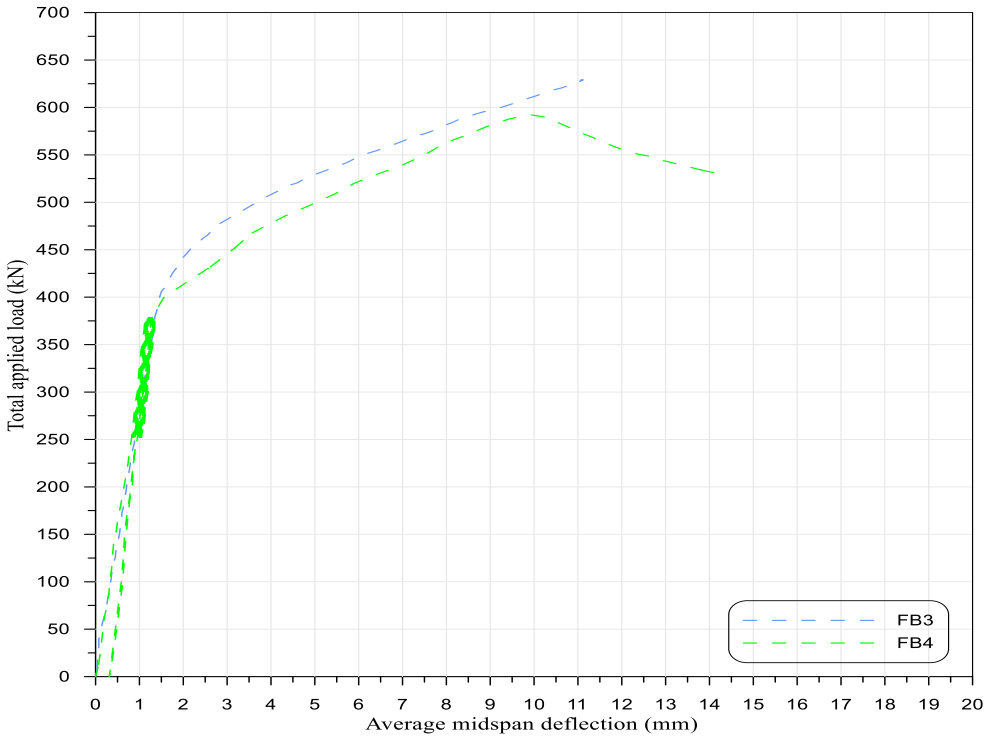

Figure (4-48) Load deflection curves of the FB3 and FB4 beam

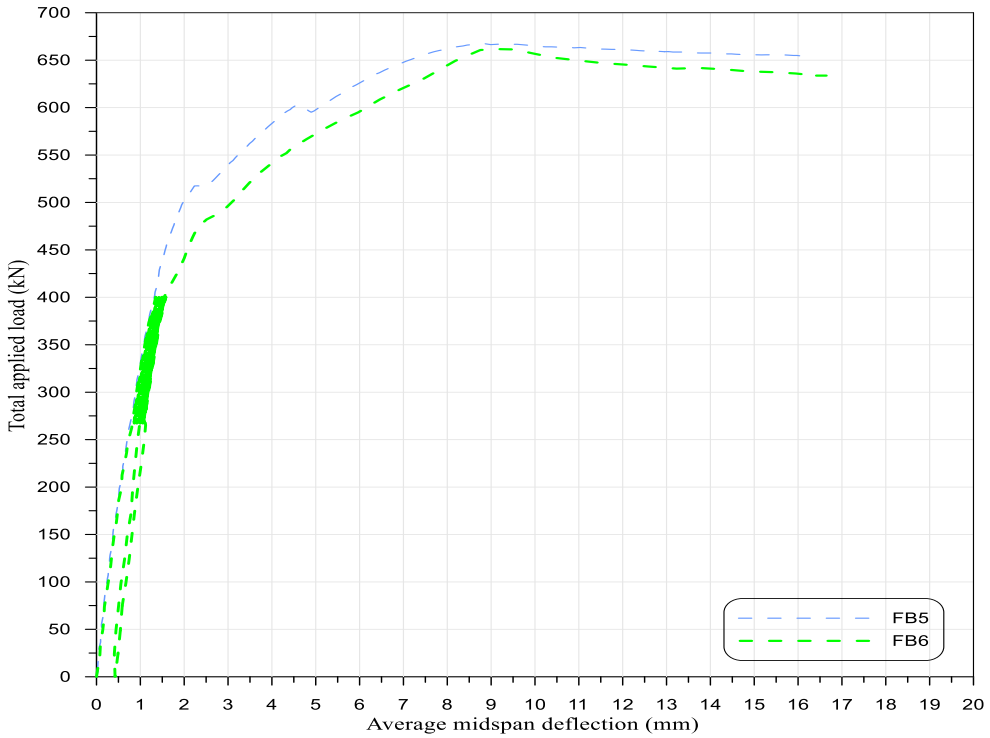

Figure (4-49) Load deflection curves of the FB5 and FB6 beam

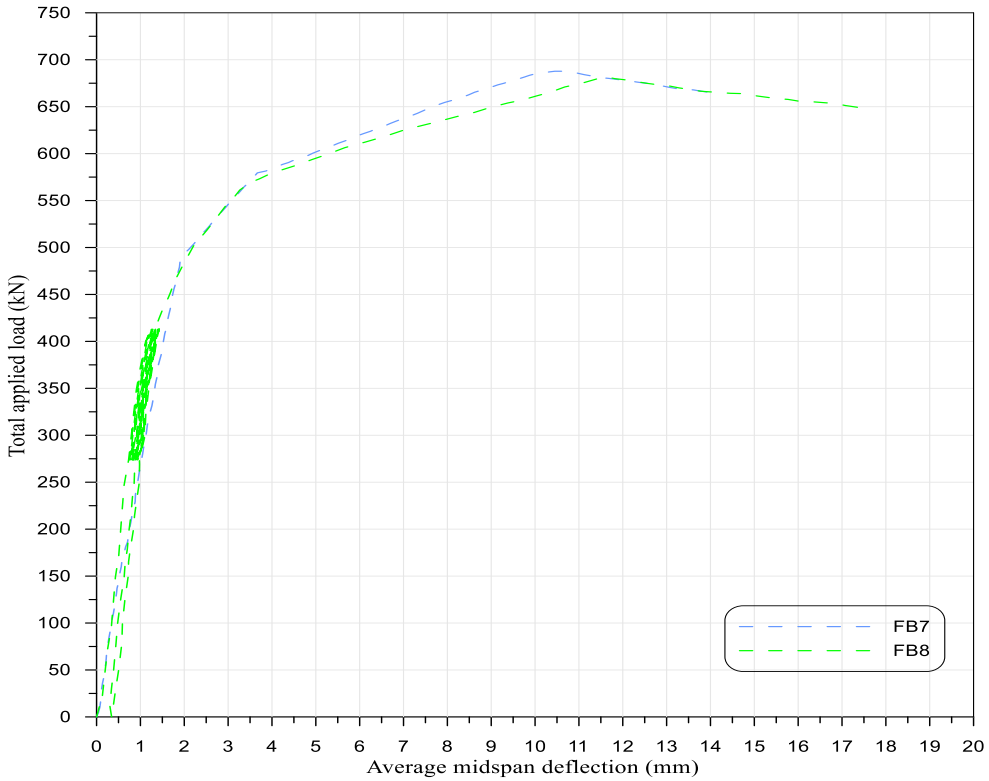

Figure (4-50) Load deflection curves of the FB7 and FB8 beam

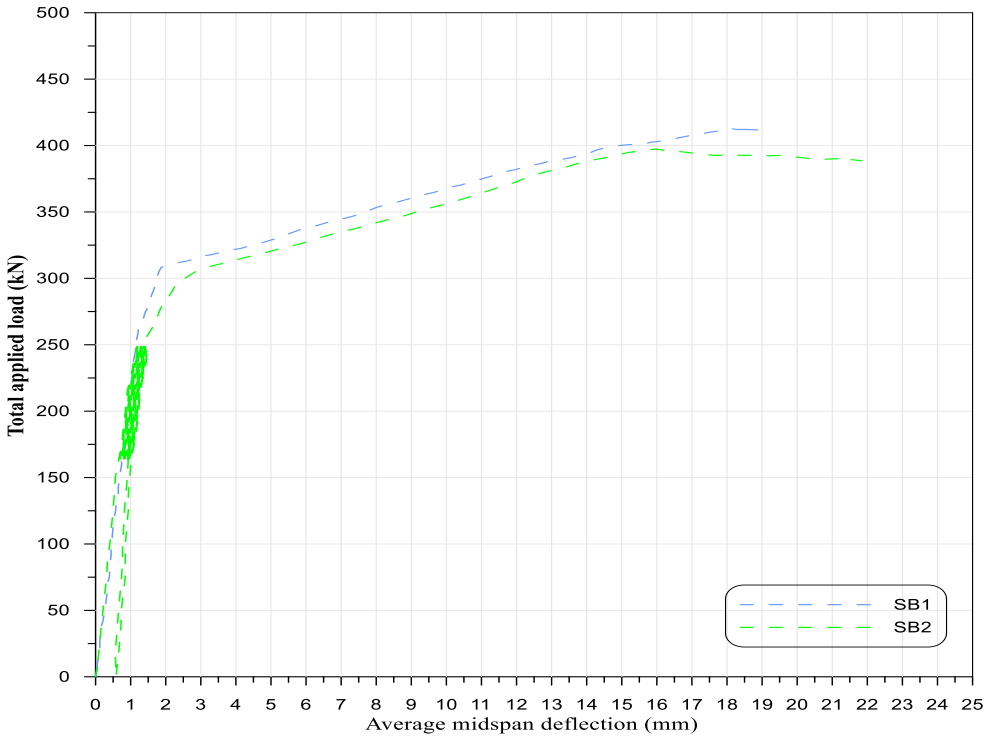

Figure (4-51) Load deflection curves of the SB1 and SB2 beam

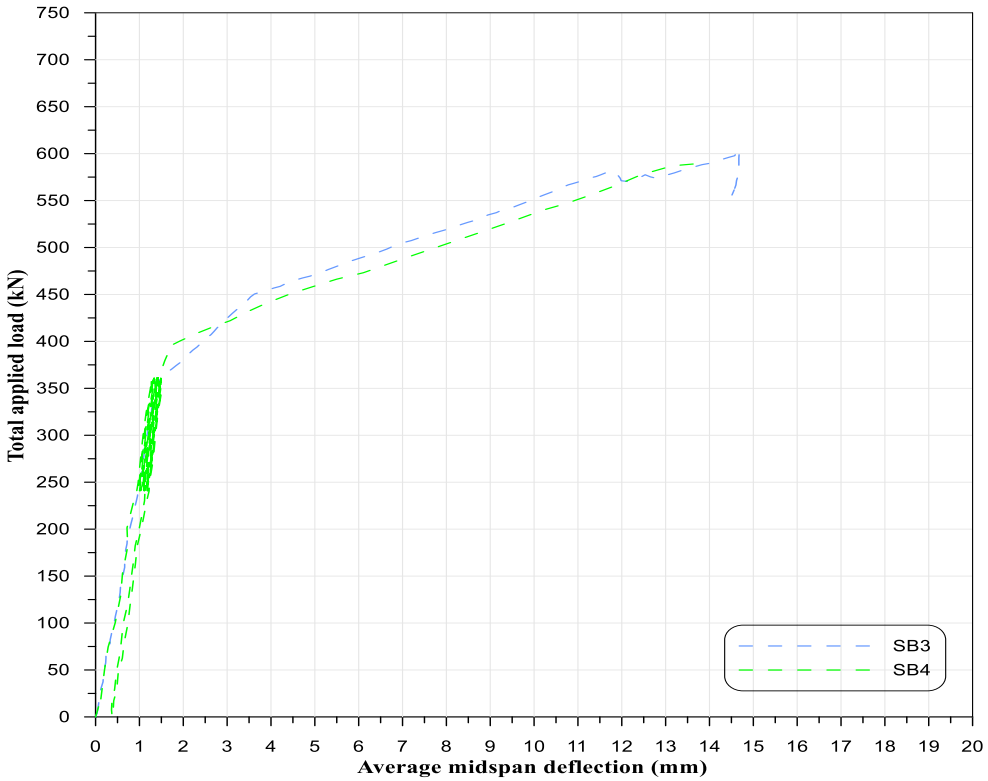

Figure (4-52) Load deflection curves of the SB3 and SB4 beam

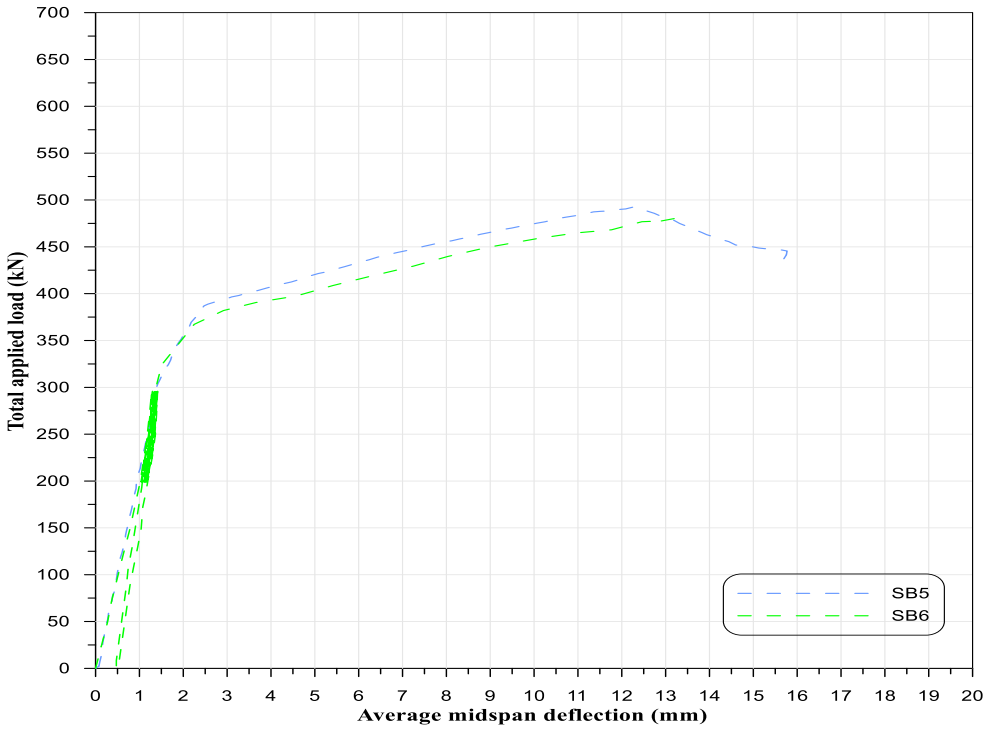

Figure (4-53) Load deflection curves of the SB5 and SB6 beam

Table (4-3) Ultimate load-carrying capacities, ultimate deflections and ratios for beams under static and under repeated loading

Beam	P_u **(St) kN**	P_u **(Re) kN**	$P_u\,(\mathbf{St})/P_u\,(Re)$	Δ_u**(St) (mm)**	Δ_u**(Re) (mm)**	$\Delta_u\,(\mathbf{St})/\Delta_u(Re)$
FB1	438.2			17.8		
FB2		430.6	1.017		17.5	1.017
FB3	629.3			7.9		
FB4		592.3	1.062		9.9	0.797
FB5	667.6			9.9		
FB6		661.8	1.008		11.1	0.891
FB7	687.7			10.7		
FB8		681.8	1.008		11.6	0.922
SB1	413.3			19.9		
SB2		397.3	1.040		15.9	1.251

Continued Table (4-3) Ultimate load-carrying capacities, ultimate deflections and ratios for beams under static and under repeated loading

Beam	P_u **(St) kN**	P_u **(Re) kN**	P_u (St)$/P_u$ (Re)	Δ_u**(St) (mm)**	Δ_u**(Re) (mm)**	Δ_u (St)$/\Delta_u$(Re)
SB3	605.3		1.027	11.9		1.144
SB4		589.2			10.4	
SB5	492.9		1.022	12.2		0.931
SB6		481.9			13.1	
P_u : Ultimate loading (kN), St: Static, Re: Repeated, Δ_u:Ultimate deflection (mm)						

Table (4-3) illustrates ultimate load-carrying capacities and ultimate deflections ratios for both specimens' categories. From this Table (3-4) and from Figure (4-47) to (4-53), the following observations can be noticed:

- Decreasing the flexure ultimate load capacity of the tested beams, the results explain that has reached (1.73%), (5.87%), (0.87%) and (0.86%) respectively for the beam FB2, FB4, FB6 and FB8 compared with the reference beams FB1, FB3, FB5 and FB7.

- Decreasing the shear ultimate load capacity of the tested beams, the results explain that has reached (3.86%), (2.66%) and (2.22%) respectively for the beam SB2, SB4, and SB6 compared with the reference beams SB1, SB3, and SB5.

- Reduction of the mid-span deflection at the ultimate load due to application repeated load cycles for unstrengthened reference beams for flexure and shear categories is reduced (1.6%) and (20.1%) for FB2 and SB2 compared with FB1 and SB1.

- Increasing of the mid-span deflection at the ultimate load for the whole flexure strengthened beams under repeated load, the increase in deflection

(25.3%), (12.1%), and (8.4%) respectively for the beam FB4, FB6, and FB8 compared with the reference beams FB3, FB5, and FB7.

- Decreasing and increasing of the mid-span deflection at the ultimate load for the shear strengthened beams under repeated load according to strengthening pattern, the decrease in deflection (12.6%) for the beam SB4 compared with the beams SB3 and increased in deflection (7.3%) for SB6 compared with the beams SB5.

4.5 Toughness

The toughness (Ut) of a substance is recognized as the ability of a material to absorb energy. Specifically, it has to do with the mix of strength and ductility.

When it comes to continuous beams and other statically indeterminate structures, ductility and energy absorption capacity are critical consideration, particularly applicable to constructions subjected to cyclic or repeated loads because the rotation of the plastic hinges facilitates the redistribution of moment forces .“ Flexure toughness can be defined as the area under the load-deflection curve that has been determined”[70]. Table (4-4) contains the toughness values for all of the beams that were tested.

Table (4-4) Toughness for all beams under monotonic static loads

Group	Beam	Toughness (N.m)	%Increase over FB1 reference beam
A	FB1	7144.925	0
	FB3	5601.056	-21.607
	FB5	9505.862	33.043
	FB7	9897.486	38.524
	FB9	8708.214	21.879
	FB10	5096.380	-28.671

Continued Table (4-4) Toughness for all beams under monotonic static loads

Group	Beam	Toughness (N.m)	%Increase over FB1 reference beam
C	SB1	6650.320	0
	SB3	7470.443	12.332
	SB5	6602.077	-0.725
	SB7	7841.191	17.906
	SB8	6975.996	4.897
	SB9	5662.439	-14.854
	SB10	6033.877	-9.269

Under monotonic static loads, we can see that strengthening the prestressed beams with precast SIFCON laminates led to increasing the toughness by about (33%), (38.5%), and (21.9%), for beams FB5, FB7, and FB9, also (12.3%), (17.9%), and (4.9%) for beams SB3, SB7, and SB8 respectively, compared with the reference beam for each group.

According to the results in the Table (4-4), Figure (4-54), and Figure (4-55), the strengthening of the prestressed beams by precast SIFCON laminates for the group (A) where the bonding between laminates and beam use epoxy only of beams FB3, and FB10 caused reduced toughness while an increased toughness in beam FB9. At the same time, when adding anchored end steel plates increased toughness in beams FB5 and FB7 compared with the reference beam FB1. We find that the bonding with epoxy and end steel anchorage plates generally show a ductile behavior.

For group (C), the shear strengthening increases the toughness for beams SB3 and SB7, when using the full wrapping, gave a higher toughness ratio compared with parts for the same scheme that partial wrapping.

This trend might explain the fact that the capability of the strengthening by precast SIFCON laminates led to the transfer of the emerging loads, and as a reason, the maximum load and the area of the load-deflection curve rose.

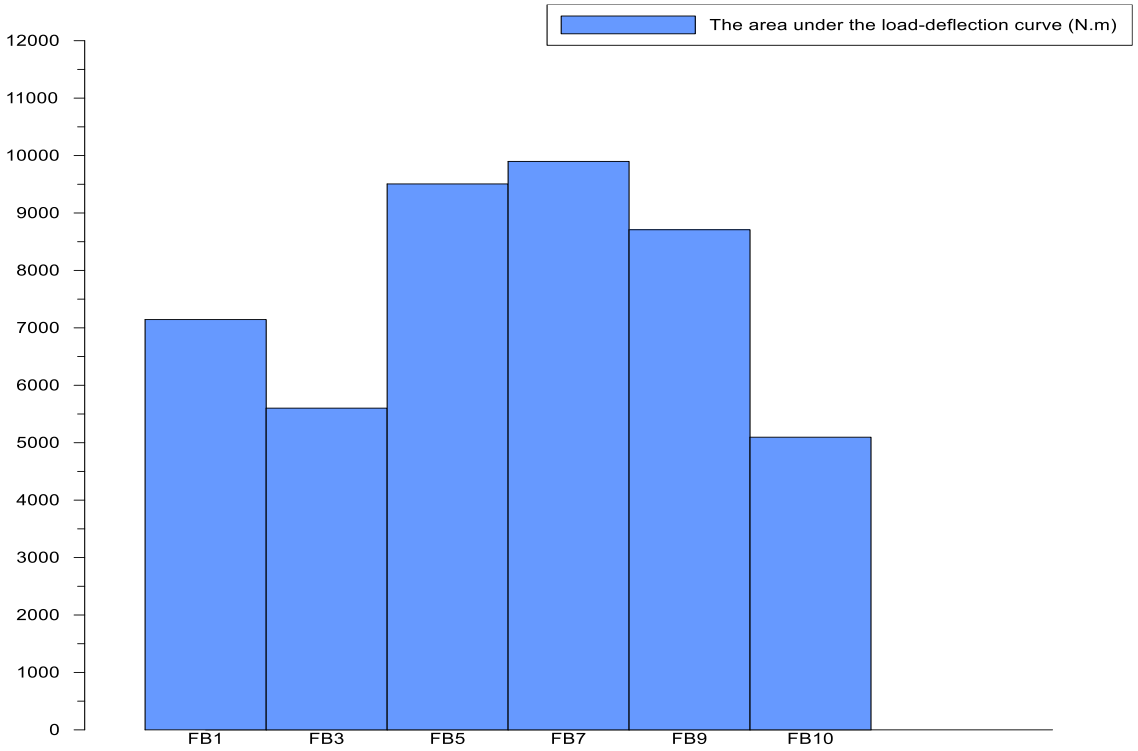

Figure (4-54) Effect of the flexure strengthening on toughness

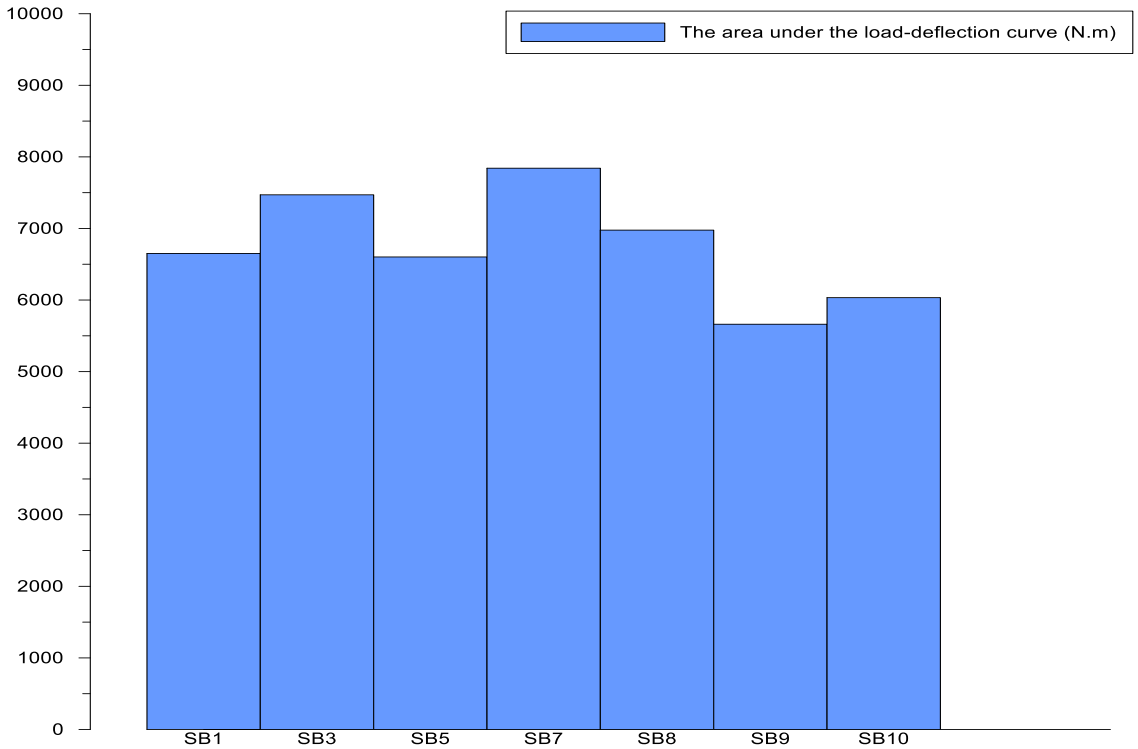

Figure (4-55) Effect of the shear strengthening on toughness

4.6 Load and Moment Redistributions

Figures (4-56) and (4-57) describe the relationship between the total applied load and the central support response for all beams, respectively.

Because the beams are considered to be statically indeterminate, the load cell was utilized to measure the central support response, which was then used to compute the real internal forces at any segment along the beam. To summarize the ultimate moments and ratio of moment redistribution (β) obtained using Eq. (4-1) at the central support and mid span region, respectively, in a Table (4-5), the following values are given:

$$\beta = \frac{M_e - M_E}{M_e} \times 100 \qquad \text{..... (4-1)}$$

Where: M_e: the elastic bending moment,

M_E: the experimental bending moment

Table (4-5) Moment redistribution for all beams

			At central support (M-)			**At mid span (M+)**		
Beam	P_u**(kN)**	**R* (kN)**	M_E **(kN.m)**	M_e **(kN.m)**	**β**	M_E **(kN.m)**	M_e **(kN.m)**	**β**
FB1	438.2	297.1	77.9	82.1	5.08	70.5	68.4	-3.05
FB2	430.6	291.2	75.8	80.7	6.04	69.7	67.2	-3.63
FB3	629.3	421.1	106.4	117.9	9.74	104.0	98.3	-5.85
FB4	592.3	395.4	99.2	111.0	10.63	98.4	92.5	-6.37
FB5	667.6	445.9	112.1	125.1	10.45	110.8	104.3	-6.27
FB6	661.8	441.3	110.4	124.0	11.03	110.2	103.4	-6.61
FB7	687.7	459.1	115.2	128.9	10.65	114.3	107.4	-6.39
FB8	681.8	454.4	113.5	127.8	11.19	113.6	106.5	-6.72
FB9	600.6	401.9	101.5	112.6	9.78	99.3	93.8	-5.87
FB10	600.0	402.2	102.2	112.5	9.16	98.9	93.7	-5.49

*R: Ultimate reaction of mid support, Pu: Ultimate failure load

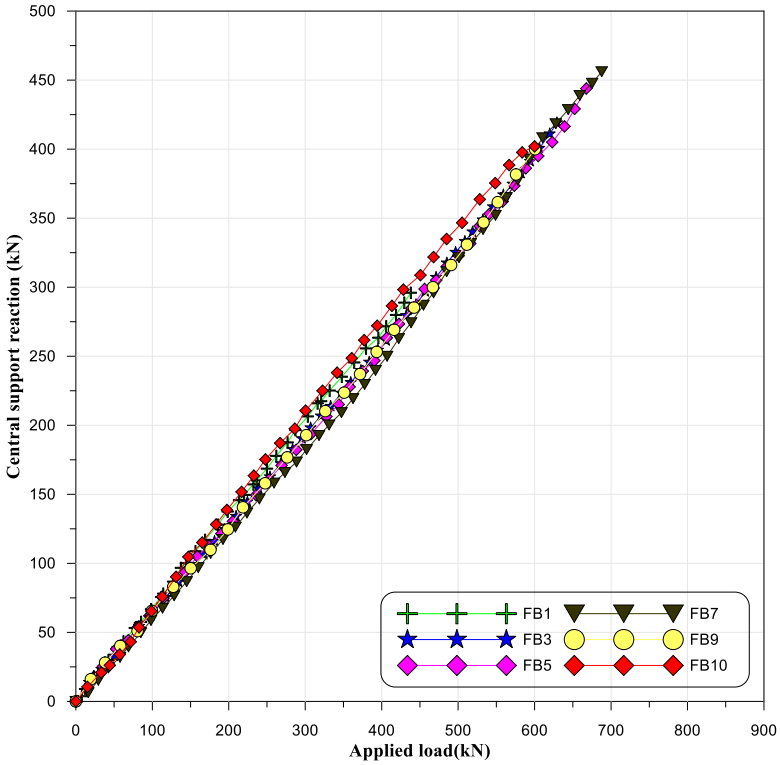

Figure (4-56) Internal supported reaction for tested beam group (A)

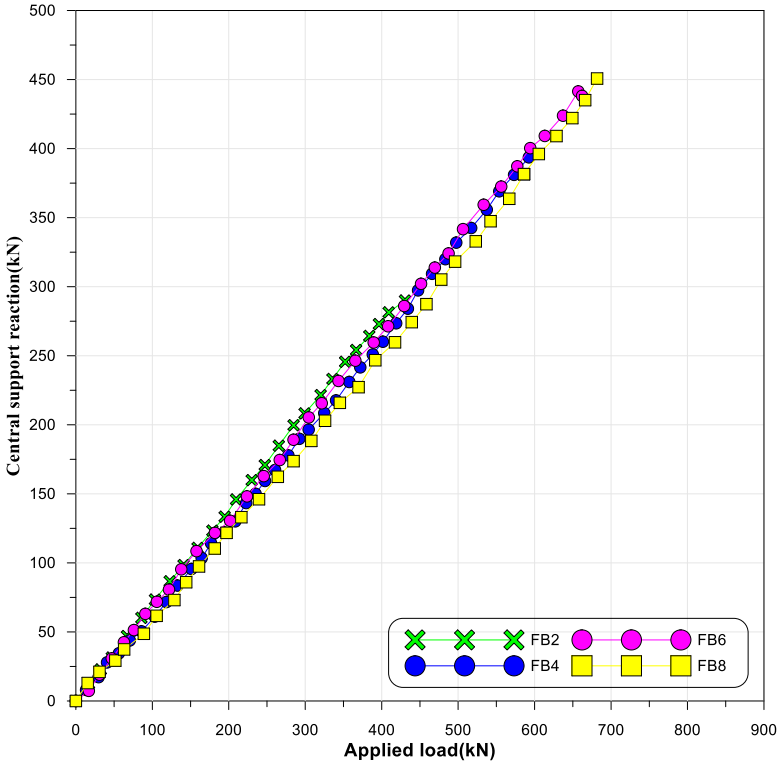

Figure (4-57) Internal supported reaction for tested beam group (B)

4.6.1 Effect of Flexural Strengthening on Moments Redistribution

According to the results in a Table (4-5), it is clear that the FB1 beam under monotonic static loads had a moment redistribution ratio of (5.08) for a negative moment and (3.05) for a positive moment.

Moreover, the strengthened beams with monotonic static loading conditions show significant growth in moment redistribution, because of the increased strength and ductility offered by applied precast SIFCON laminates in the hogging region.

FB3, FB5, FB7, FB9, and FB10 had moment redistribution ratios of (9.74, 10.45, 10.65, 9.78 and 9.16) % at the central support and (5.85, 6.27, 6.39, 5.87 and 5.49) % at mid-span, respectively.

However, it is clear that there is an improvement in moment redistribution with an increase in the laminate length and using the anchored steel plate. Figures (4-58) to (4-63) present the experimental and elastic moments at tested beams.

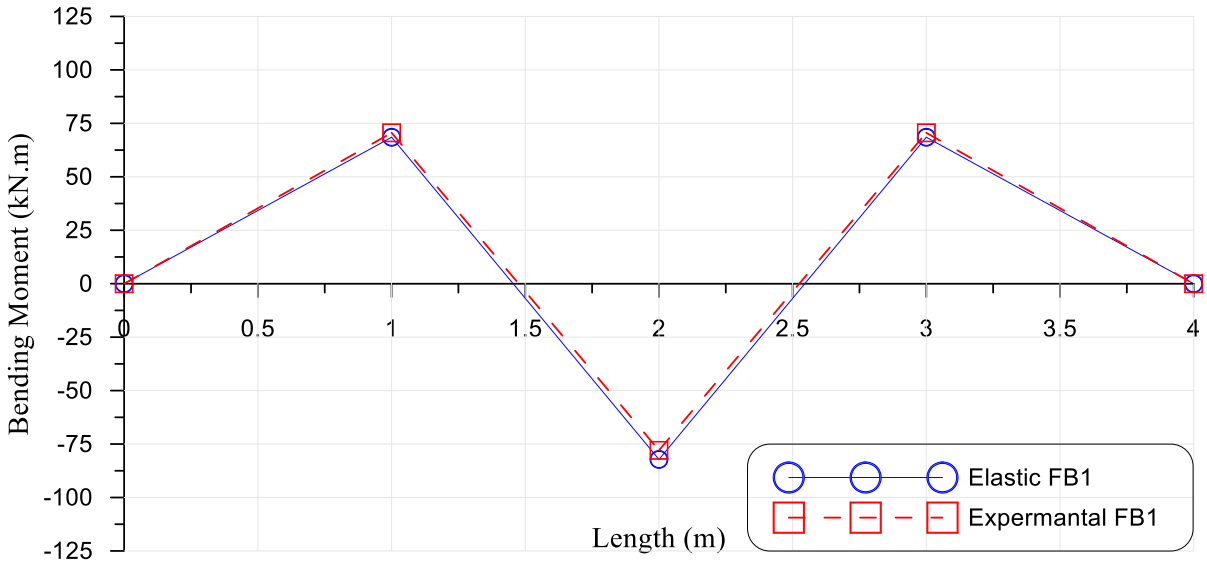

Figure (4-58) The ultimate moments for tested beam FB1

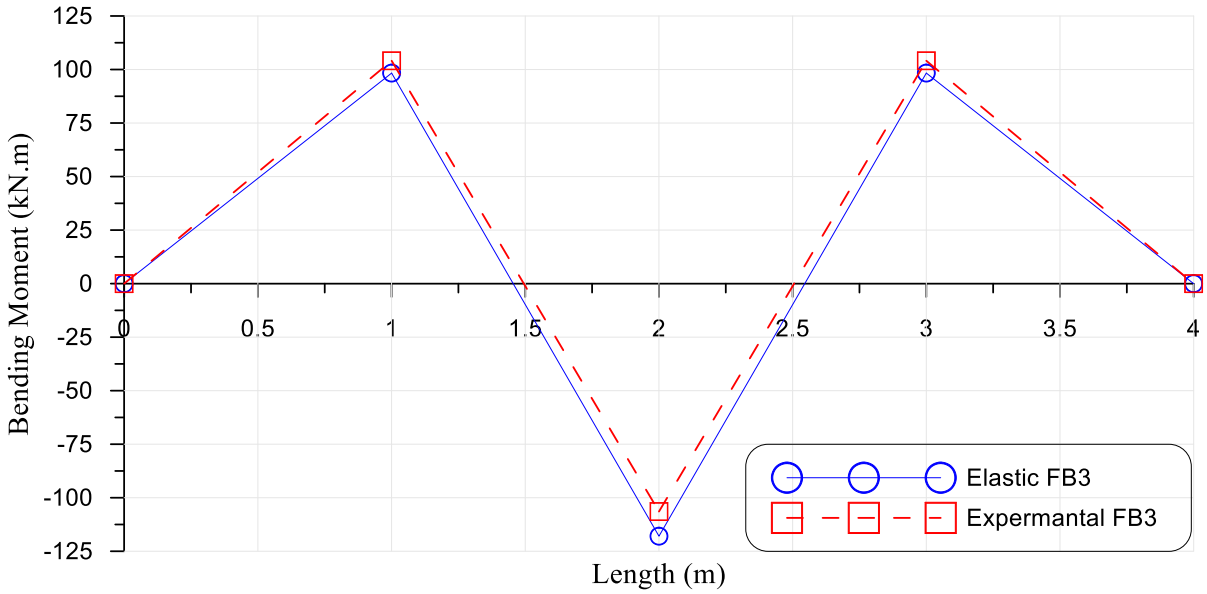

Figure (4-59) The ultimate moments for tested beam FB3

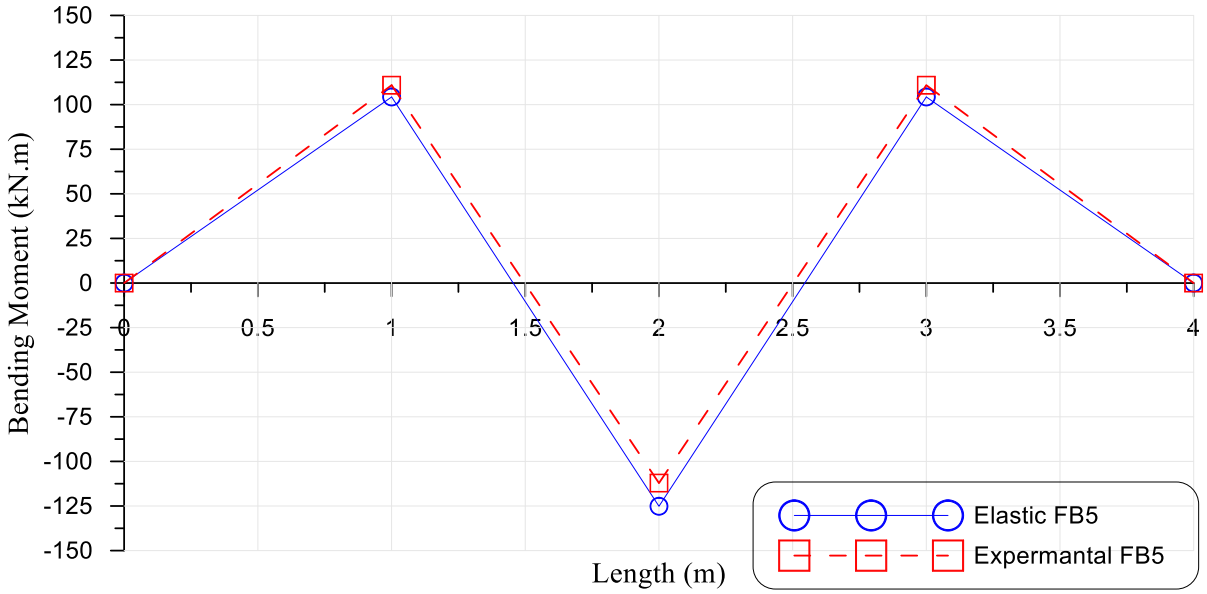

Figure (4-60) The ultimate moments for tested beam FB5

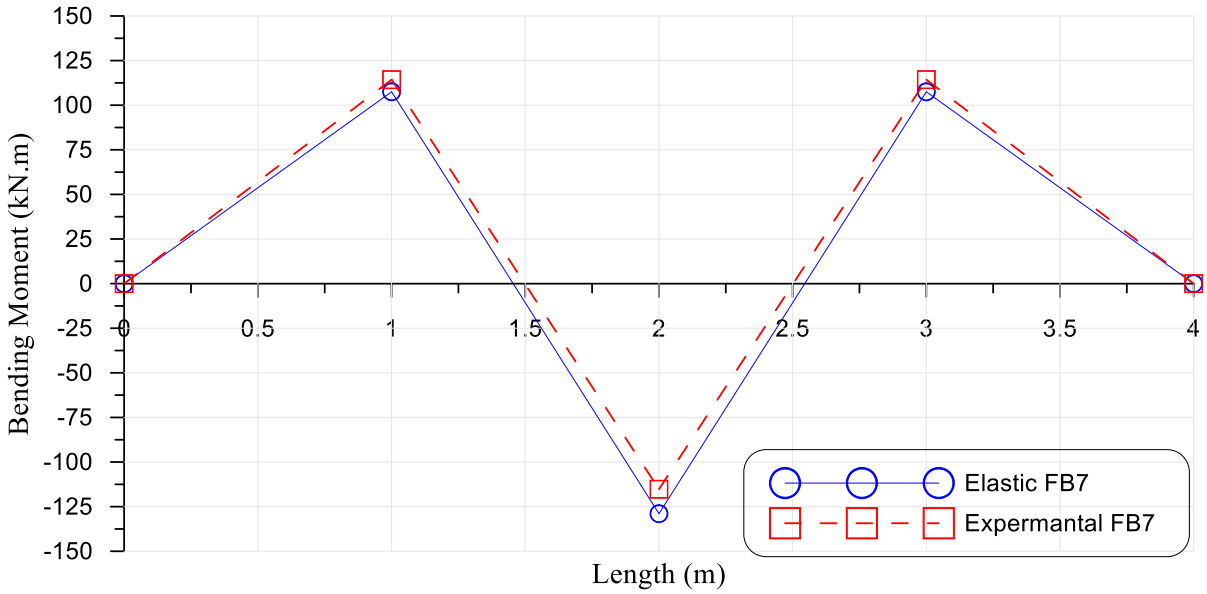

Figure (4-61) The ultimate moments for tested beam FB7

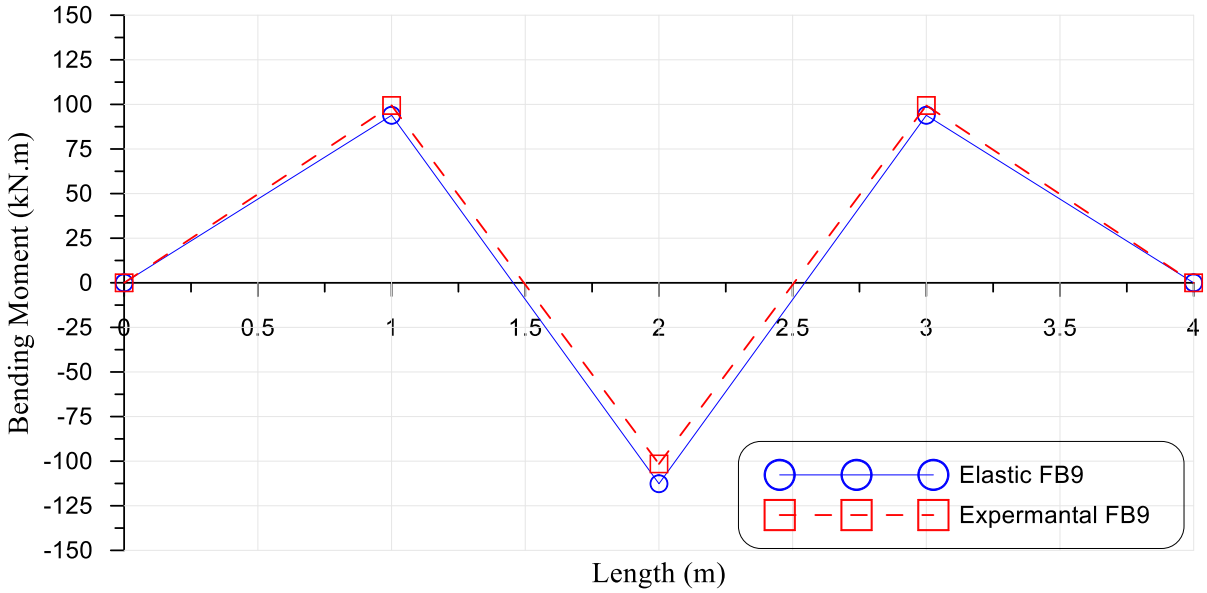

Figure (4-62) The ultimate moments for tested beam FB9

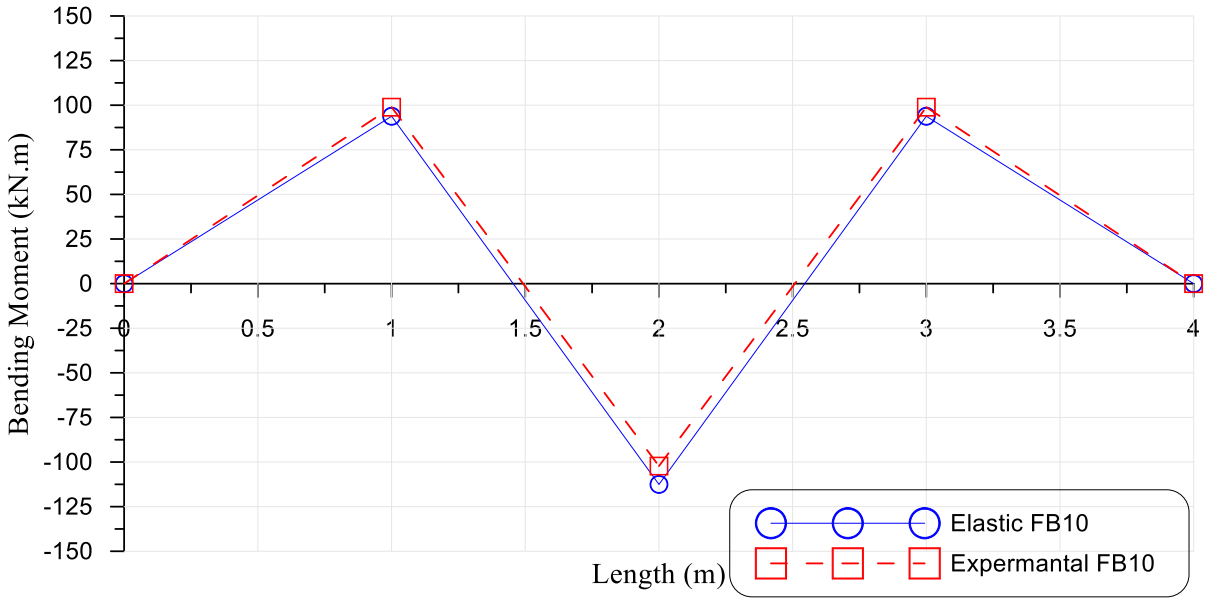

Figure (4-63) The ultimate moments for tested beam FB10

4.6.2 Effect of Repeated Loading on Moments Redistribution

To investigate the influence of the repeated loads on the moment's redistribution, Figures (4-64) to (4-67) plotted for comparison the elastic and experimental ultimate moments for tested beams after ten cycles of loading and unloading range varied between (40%) to (60%) of the ultimate load, for the beams FB2, FB4, FB6, and FB8.

According to the results in the Table (4-5), it is clear that the FB2 beam under repeated loads had a moment redistribution ratio of (6.04) for a negative moment and (3.63) for a positive moment.

Moreover, the strengthened beams with static loading conditions show significant growth in moment redistribution. FB4, FB6, and FB8 had moment redistribution ratios of (10.63,11.03 and 11.19) % at the central support and (6.37,6.61and 6.72) % at mid-span, respectively.

By comparing the results for beams under repeated loads to beams under monotonic static loads, it was observed that it is clear an increase in the moment redistribution ratio.

The ratio for moment redistribution of negative moments for FB2, FB4, FB6, and FB8 increased by about 18.87%, 9.03%, 5.54%, and 5.02% compared with similar beams FB1, FB3, FB5 and FB7 under static loading conditions.

Figure (4-68) compared the ultimate moments at the central support of beams under repeated loads with the ultimate elastic moments and the moments at central support for the identical beams under monotonic static loads, respectively.

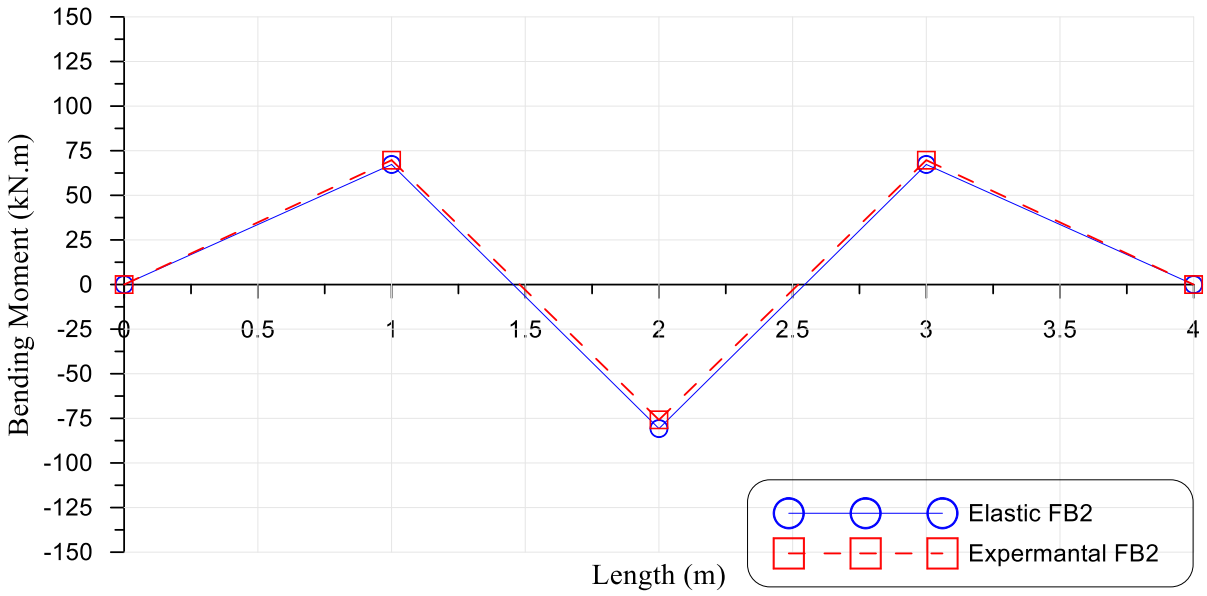

Figure (4-64) The ultimate moments for tested beam FB2

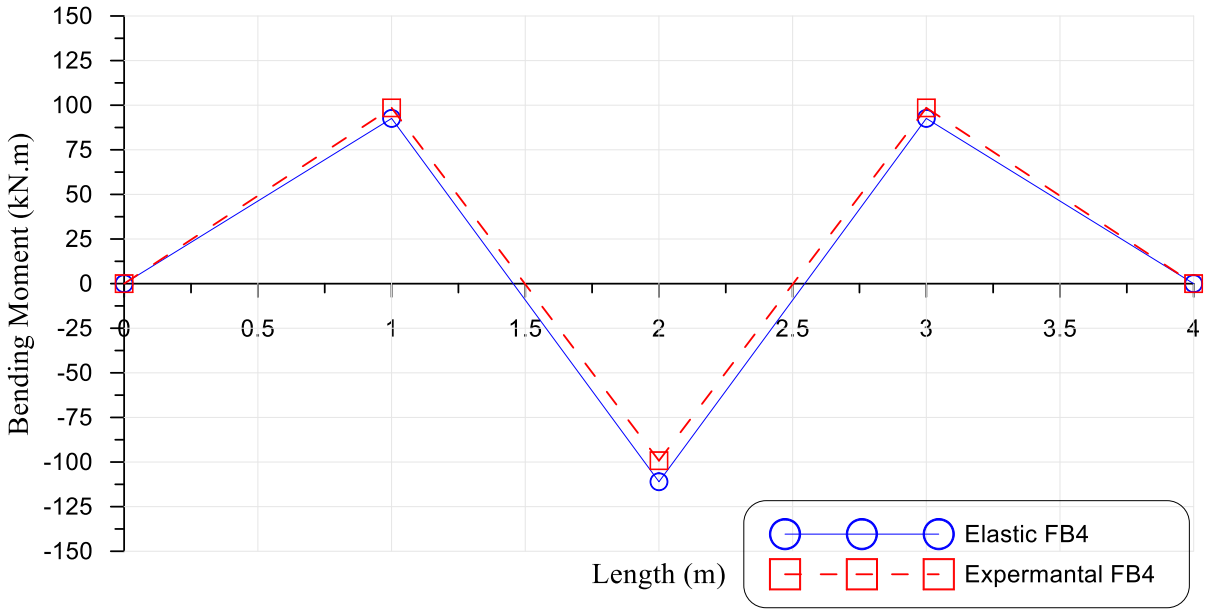

Figure (4-65) The ultimate moments for tested beam FB4

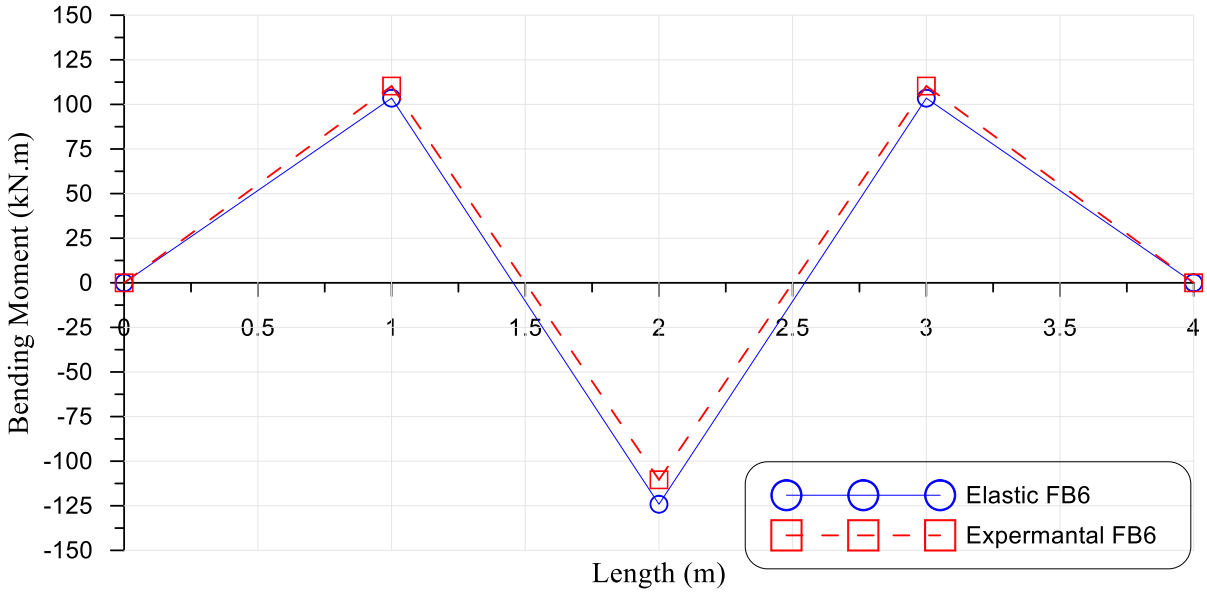

Figure (4-66) The ultimate moments for tested beam FB6

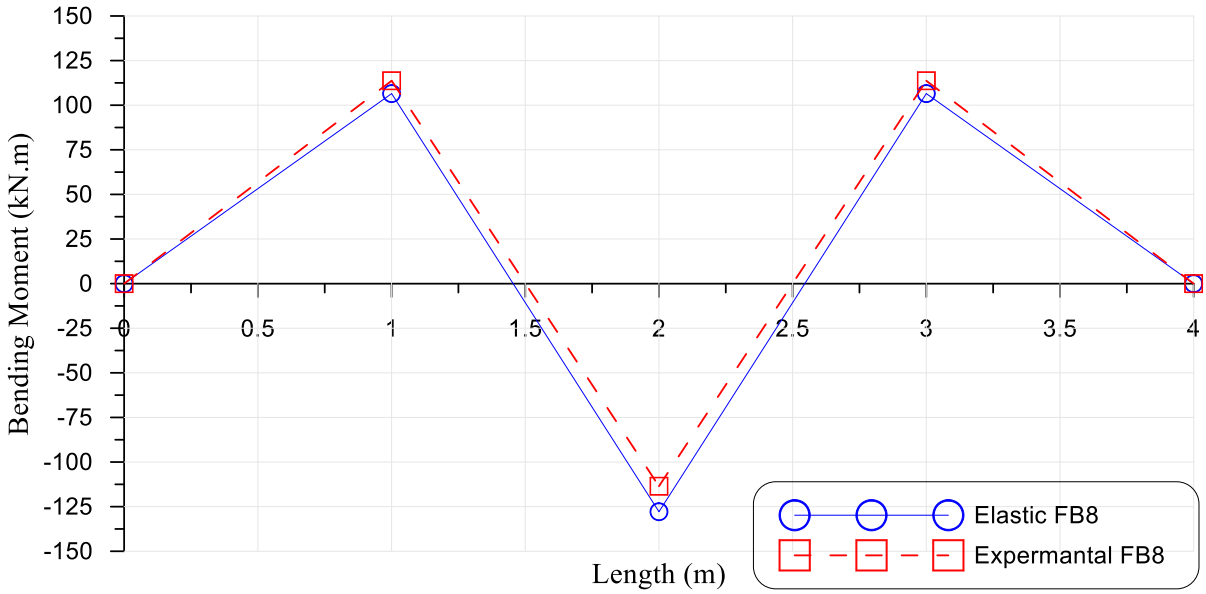

Figure (4-67) The ultimate moments for tested beam FB8

Figure (4-68) Ultimate negative moments at central support under monotonic static and repeated loads

4.7 Cracking Behavior

Primary cracks are initiated in the central support region after that in mid-span. As the applied loading increased, additional cracks would appear. It noticed that the number of cracks would be stabilized at a loading range of 80 % of the ultimate load. The crack widths were measured and recorded throughout the test at every load increment using a digital concrete crack width meter.

4.7.1 Effect of The Strengthening in Crack Width

Figures (4-69) and (4-70) represent the indication of crack width with increasing load of the groups (A) and (C), respectively. Through a close and in-deep look at the above Figures, the following conclusions may be drawn:

- The first crack does not give the maximum crack width for the tested prestressed concrete beams; the first crack appears at the central support region then appears in the mid-span region but the maximum crack occurs in the mid-span region for most tested beams. For this, the evolution of the crack width was recorded with the applied loads for the cracks at the central support and mid span regions as shown in Figures (4-66) to (4-67).
- For flexure beams group (A), compared between beams without strengthening and beams strengthened with precast SIFCON laminates, it has been found that the strengthening has resulted in a reduction in the crack width in the central support and mid-span regions. To put it another way, the crack behavior was enhanced.
- For shear beams group (C), the strengthening also gives a good reduction in crack width especially strengthening full wrapping.

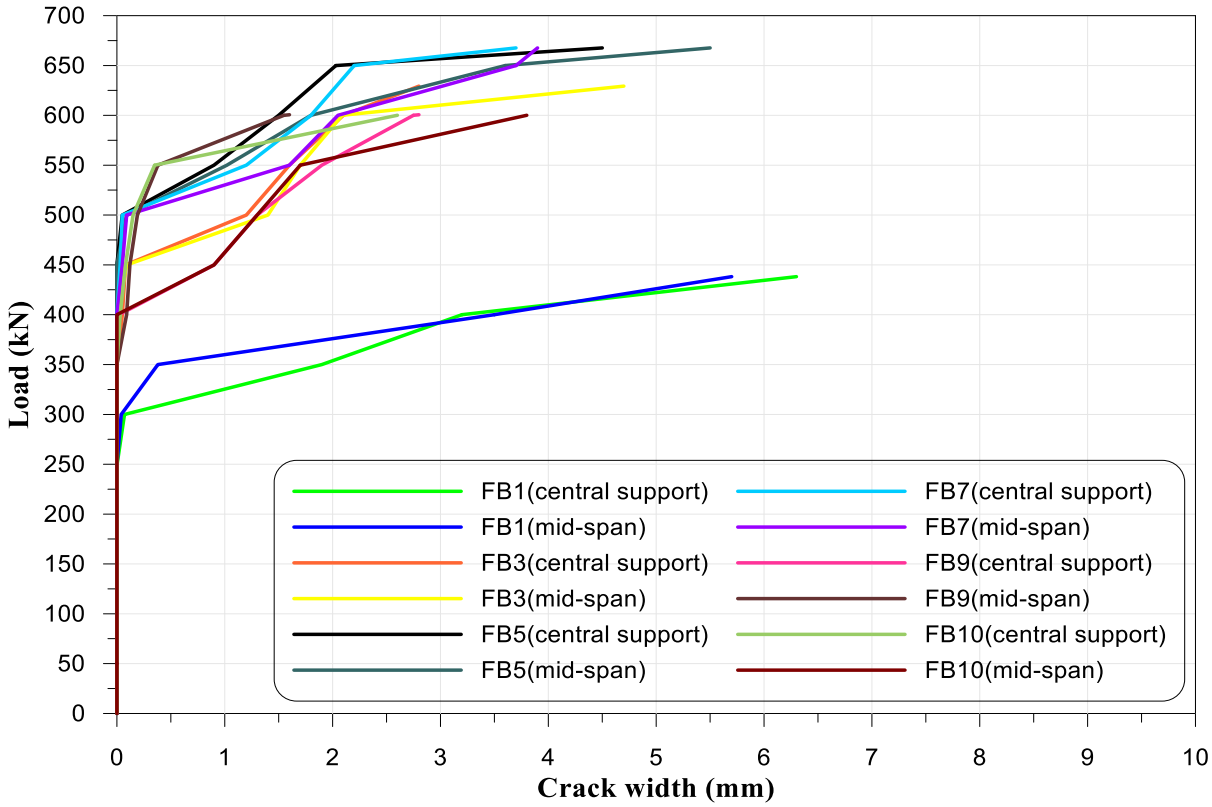

Figure (4-69) Indication of crack width with increasing load of group (A)

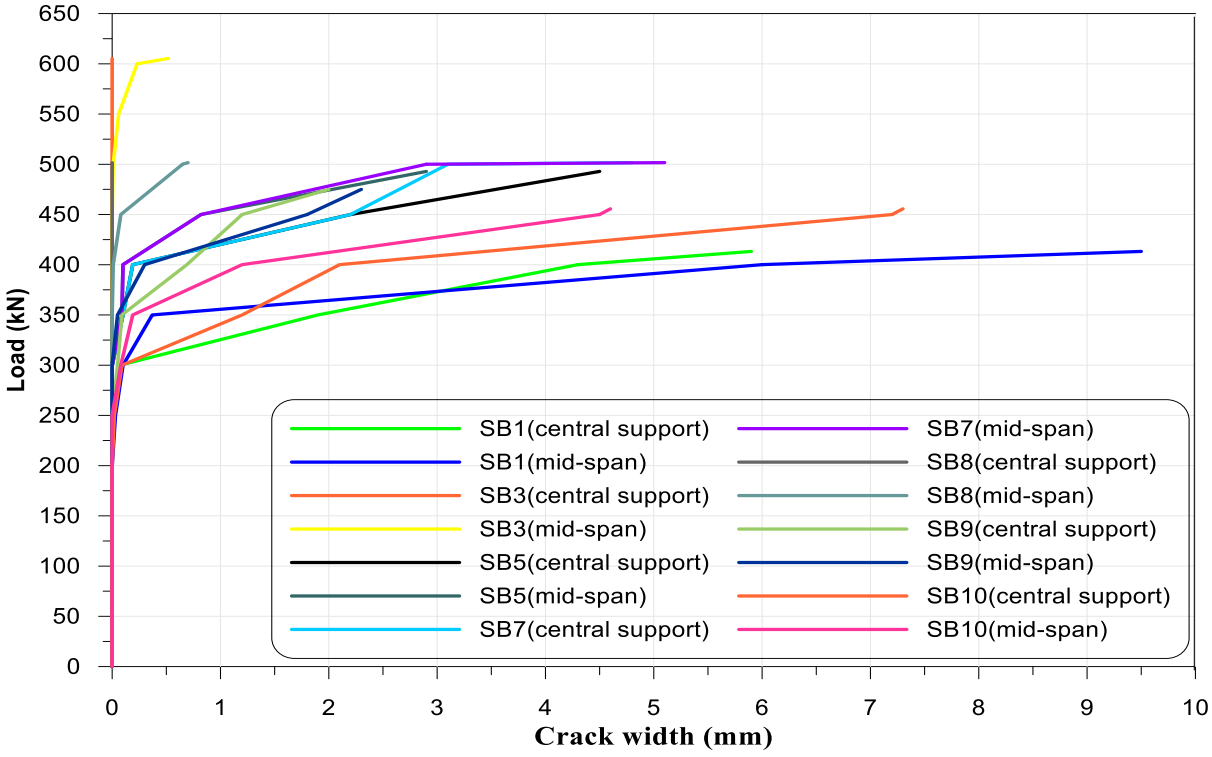

Figure (4-70) Indication of crack width with increasing load of group (C)

4.7.2 Effect of The Repeated Loading in Crack Width

A comparison between the specimens tested under monotonic static loading from (group A and C) and the specimens subjected to repeated loading from (group B and D) will be conducted. The goal of this comparison is to investigate the effect of repeated loading on the crack width. Figure (4-71) to (4-74) includes the comparison between maximum crack width for the specimens under monotonic static loading and for counterpart specimens but after exposing them to limited cycles of repeated loading, the following are possible conclusions:

- In predominantly, a decrease in crack width for beams in both groups (B) and (D) is due to great new cracks that happened due to applied cycles of repeating load and the decrease of ultimate load.
- No significant effect on the number of cracks, crack propagation, or the increasing number of cracks in the specimen during the exposure to limited repeated loading, and the increasing number of cracks in the specimen during the exposure to limited repeated loading was very limited.

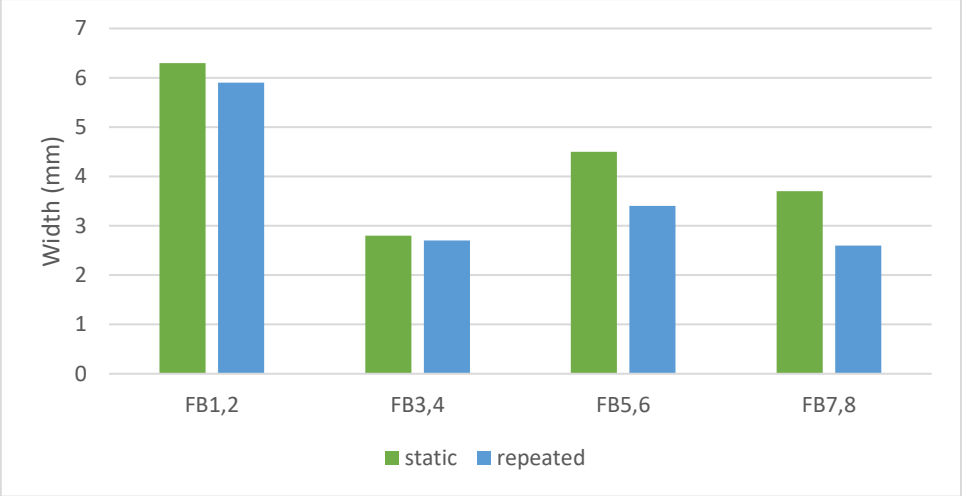

Figure (4-71) Maximum crack width for the groups (A and B) at the central support

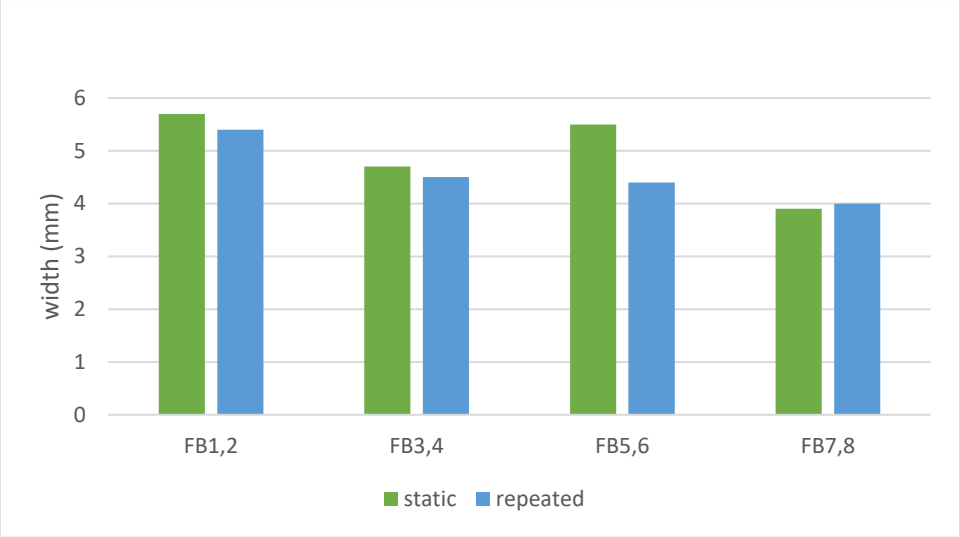

Figure (4-72) Maximum crack width for the groups (A and B) at mid-span

Figure (4-73) Maximum crack width for the groups (C and D) at central support

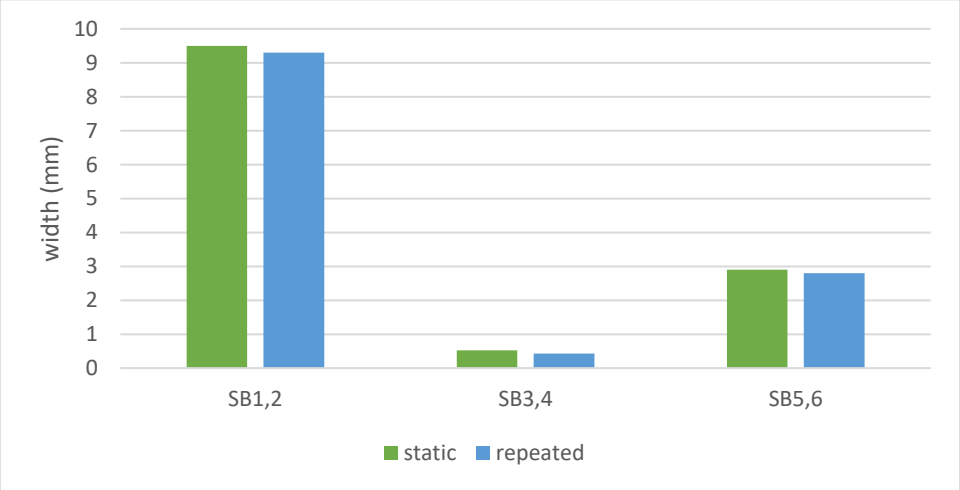

Figure (4-74) Maximum crack width for the groups (C and D) at mid-span

4.8 Load Versus Strains in Concrete for Flexural Beams Category

The compressive strain at the extreme top and bottom side of the concrete surface by taking many locations in sagging and hogging regions for each specimen was monitored and recorded automatically for each load increment up to failure.

4.8.1 Extreme Concrete Compressive Strains at Sagging Region Under Monotonic Static Loading

Figure (4-75) shows the strains of the concrete surface at the top and bottom of the mid-span region (sagging region). The FB1 beam exhibited more rapid strain than the strengthened beams beam.

Maximum strain equals to [(4894 με) at the bottom and (-4647με) at the top] at 430.185 kN. FB1 has the highest strain value, which is significantly greater than the ACI318R-19 recommended value was recorded for FB1 beams while the strengthened beam recorded less than the value.

Not only were the strands unbonded, but also the strength the results indicate that the provisions of A_s and A'_s2Φ10 and stirrup, Φ10@10 cm, were capable of affecting the confinement. For the strengthened beams, the concrete compressive strain independent of the SIFCON laminates arrangement remains more or less linear up to the beam's failure and is not significantly affected by concrete cracking or yielding of the tensile steel. These results demonstrate that the strengthening strategy reduced the strain in the compressive region of concrete. Thus, externally bonded SIFCON laminates may also be utilized to reduce the compressive stresses in the concrete, in addition to acting as an additional tensile reinforcement. As seen from the curves that the FB1 and strengthened beams behaviors at the bottom were with well agreement till reaching load (325kN) approximately at bottom region but it is doing not agree at top region.

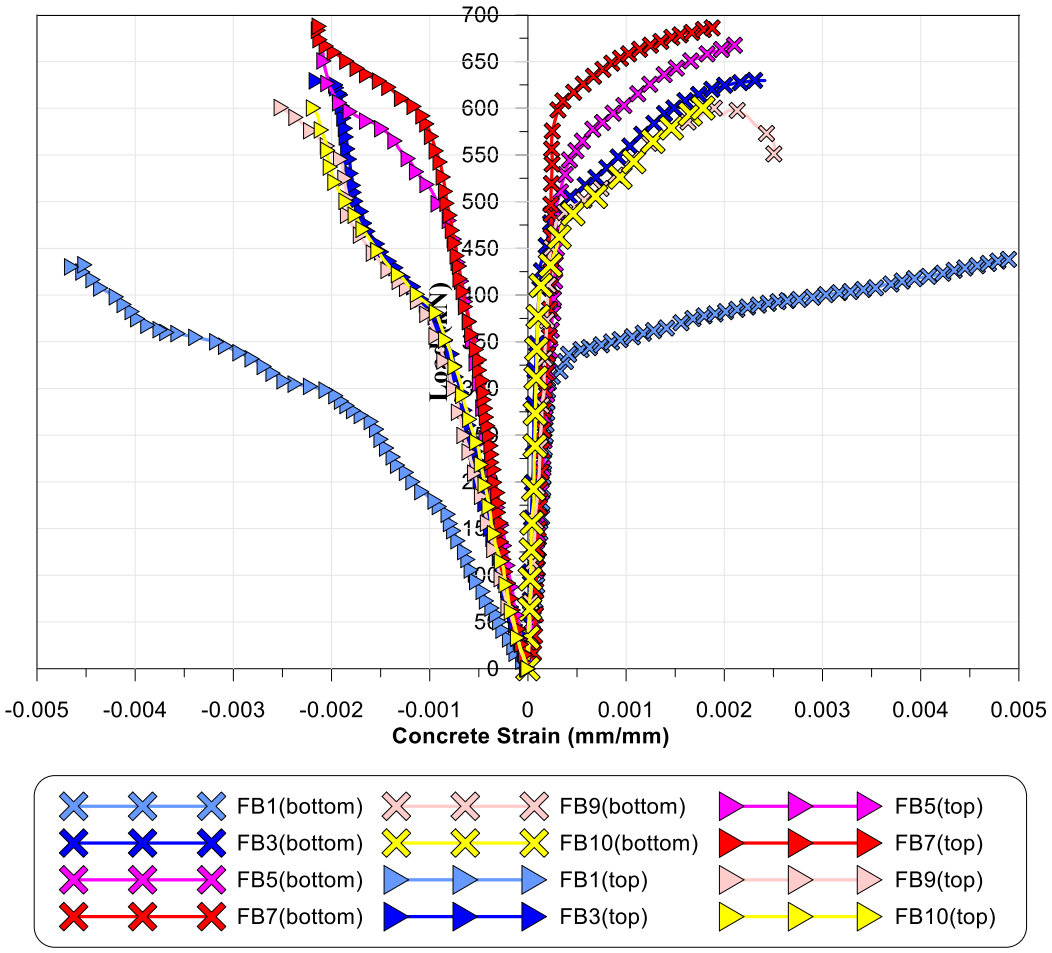

Figure (4-75) Load versus strain on concrete surface at the sagging region

4.8.2 Extreme Concrete Compressive Strains at Hogging Region Under Monotonic Static Loading

Load versus strain on a concrete surface at the hogging region readings curves of group (A) beams are shown in Figure (4-76). The highest strain value is for the FB1 reference beam with a value of (-2760με) which is considered within the suggested value in ACI 318R-19, at the bottom and (3887με) at the top was recorded for FB1 beams while the strengthened beam recorded less than the value.

These results demonstrate that the strengthening strategy reduced the strain in the compressive region of concrete. Thus, externally bonded SIFCON laminates may also be utilized to reduce the compressive stresses in the concrete,

in addition to acting as an additional tensile reinforcement. As seen from the curves that the FB1 and strengthened beams behaviors were with well agreement till reaching load (250 kN) in top strains and (330 kN) in bottom strains approximately. The FB1 beam exhibited more rapid strain than the strengthened beams beam.

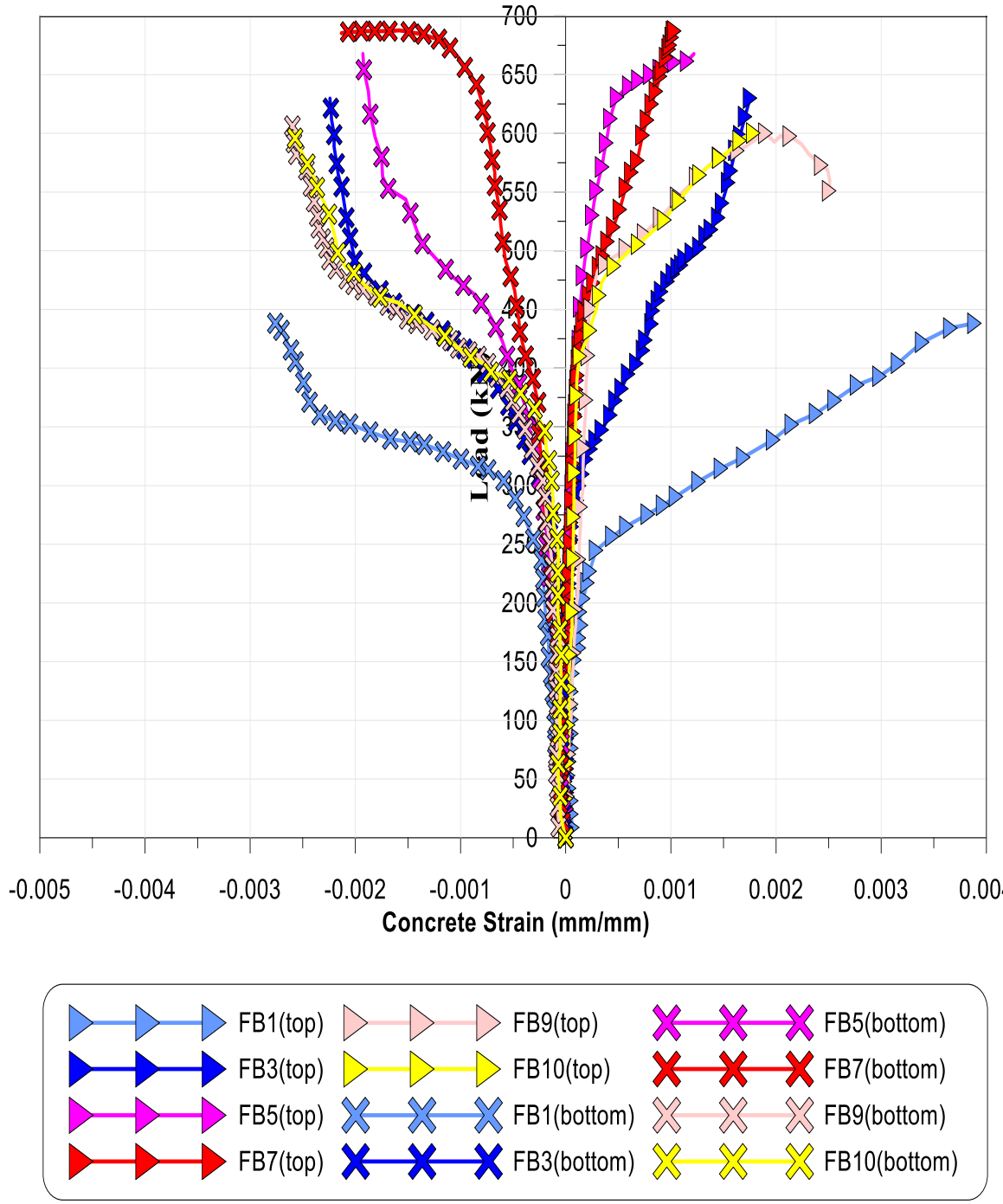

Figure (4-76) Load versus strain on concrete surface at the hogging region

4.9 Load Versus Strains in Concrete for Shear Beams Category

The compressive strain at the extreme top, bottom, and slant between them at the side of the concrete surface by taking many locations in mid-span and central support regions for each specimen was monitored and recorded automatically for each load increment up to failure.

4.9.1 Extreme Concrete Compressive Strains at Sagging Region under Monotonic Static Loading

Figure (4-77) shows the strains of the concrete surface at the top and bottom of the mid-span region. The SB1 beam exhibited more rapid strain than the strengthened beams beam. Maximum strain equals to [(3042 με) at the bottom and (-3859 με) at the top] at 413.2 kN. The highest strain value is for SB1 which is considerably higher than the suggested value in ACI318R-19 was recorded for SB1 beams while the strengthened beam recorded less than the value.

For the strengthened beams, the concrete compressive strain independent of the SIFCON laminates arrangement remains more or less linear up to the beam's failure and is not significantly affected by concrete cracking or yielding of the tensile steel. These results demonstrate that the strengthening strategy reduced the strain in the compressive region of concrete. Thus, externally bonded SIFCON laminates may also be utilized to reduce the compressive stresses in the concrete.

As seen from the curves that the SB1 and strengthened beams behaviors at the bottom were with well agreement till reaching load (200kN) at top and (325kN) at bottom approximately.

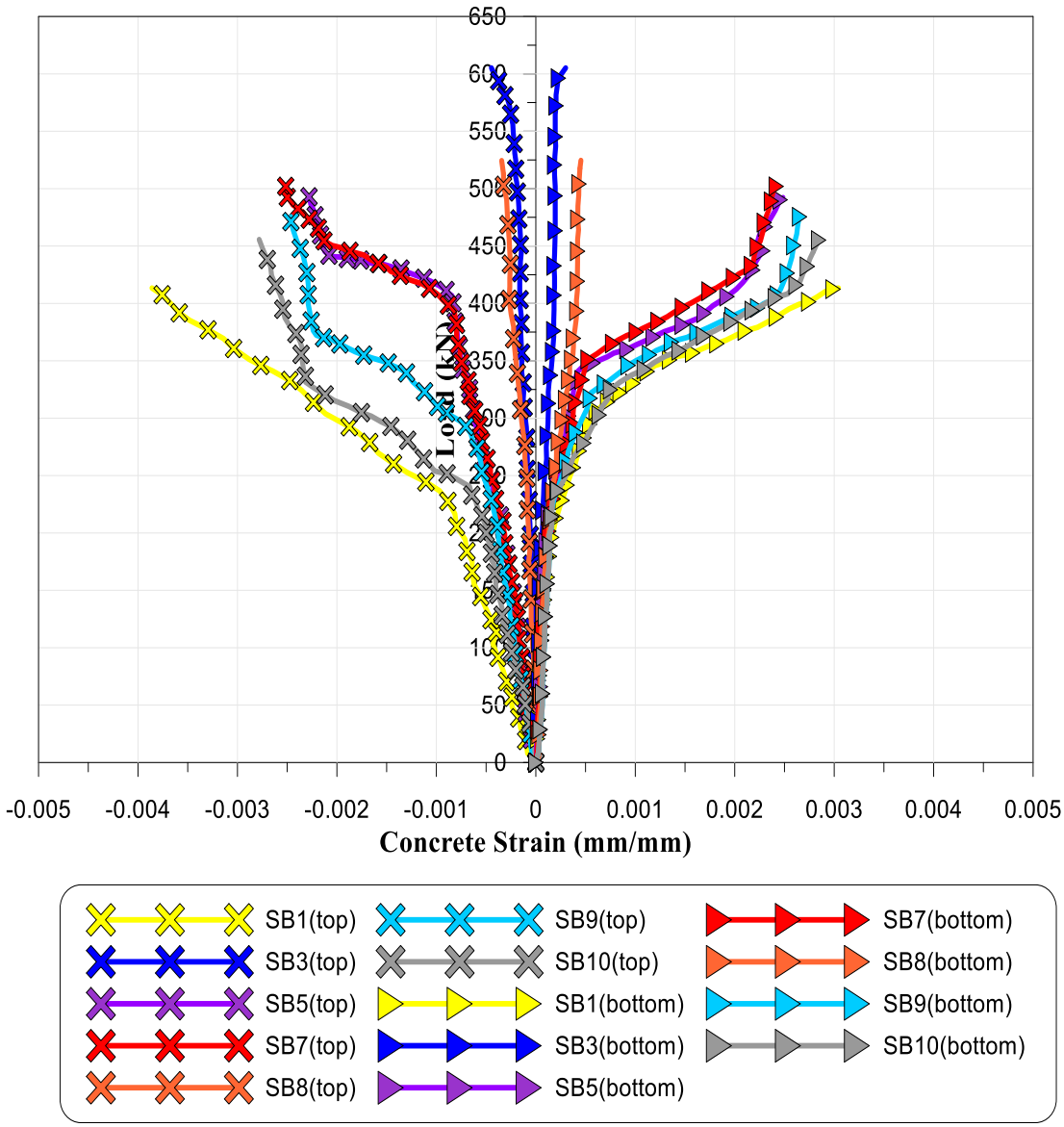

Figure (4-77) Load versus strain on concrete surface at the sagging region

4.9.2 Extreme Concrete Compressive Strains at Hogging Region Under Monotonic Static Loading

Load versus strain on a concrete surface at the hogging region readings curves of group (C) beams are shown in Figure (4-78).

The highest strain value is for the FB1 reference beam with a value of (3490με) at the top and (-2653με) at the bottom it is within the limit that suggested in ACI 318R-19.

These results demonstrate that the strengthening strategy reduced the strain in the compressive region of concrete. Thus, externally bonded SIFCON laminates may also be utilized to reduce the compressive stresses in the concrete.

As seen from the curves that the SB1 and strengthened beams behaviors were with well agreement till reaching load 250 KN in top and bottom strains approximately. The SB1 beam exhibited more rapid strain than the strengthened beams beam.

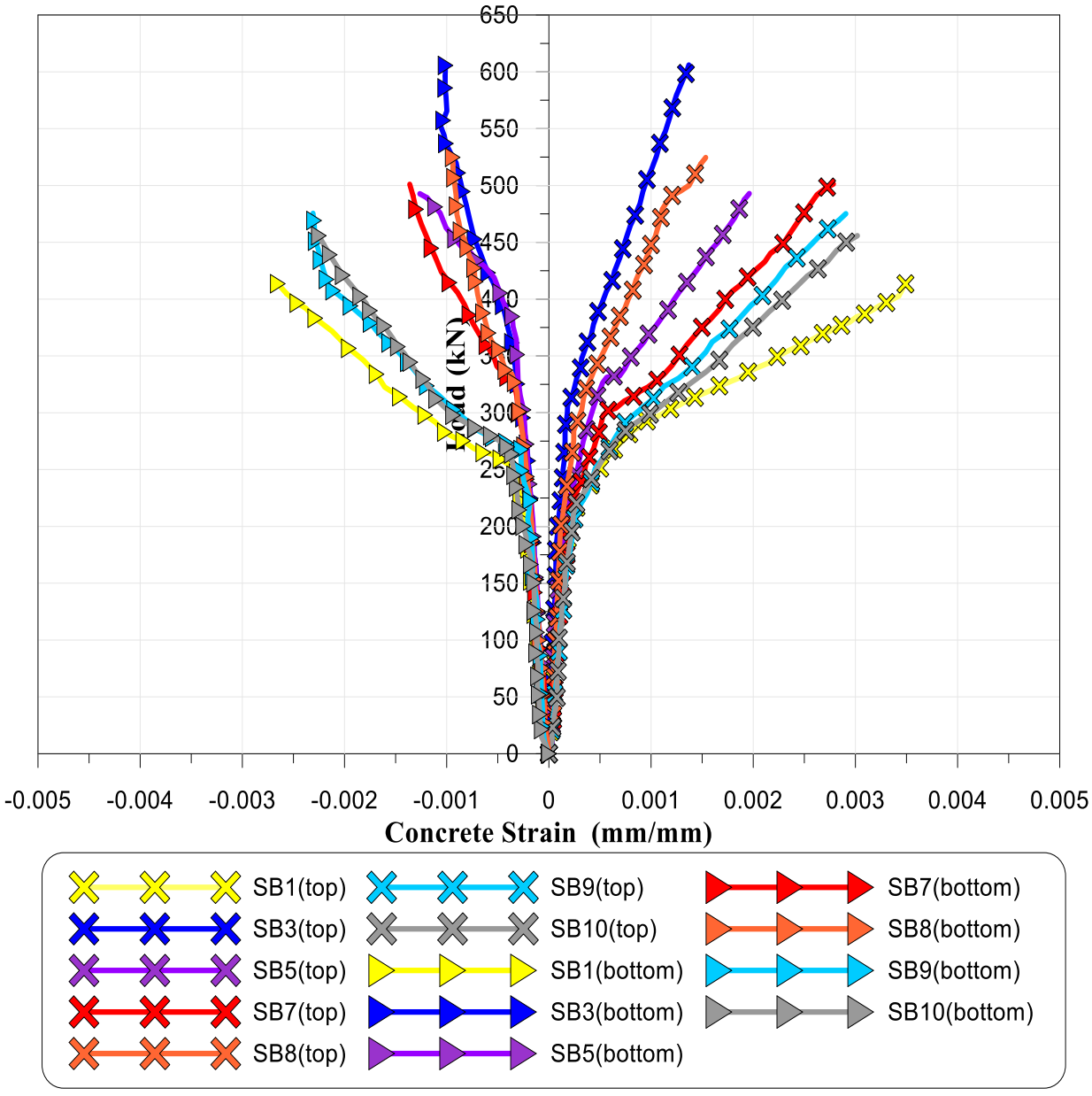

Figure (4-78) Load versus strain on concrete surface at the hogging region

4.9.3 Extreme Concrete Compressive Strains at Sloping Region Under Monotonic Static Loading

Load versus strain on a concrete surface at sloping region (slope 45° between central support and load point line extension) readings curves of group (C) beams are shown in Figure (4-79).

The highest strain value is for the SB1 reference beam with a value of (-288με) which is considered within the suggested value in ACI 318R-19. These results demonstrate that the strengthening strategy reduced the strain in the compressive region of concrete. Thus, externally bonded SIFCON laminates may also be utilized to reduce the compressive stresses in the concrete.

As seen from the curves that the SB1 and strengthened beams behaviors were with well agreement were their move parallel to each other. The SB1 beam exhibited more rapid strain than the strengthened beams beam.

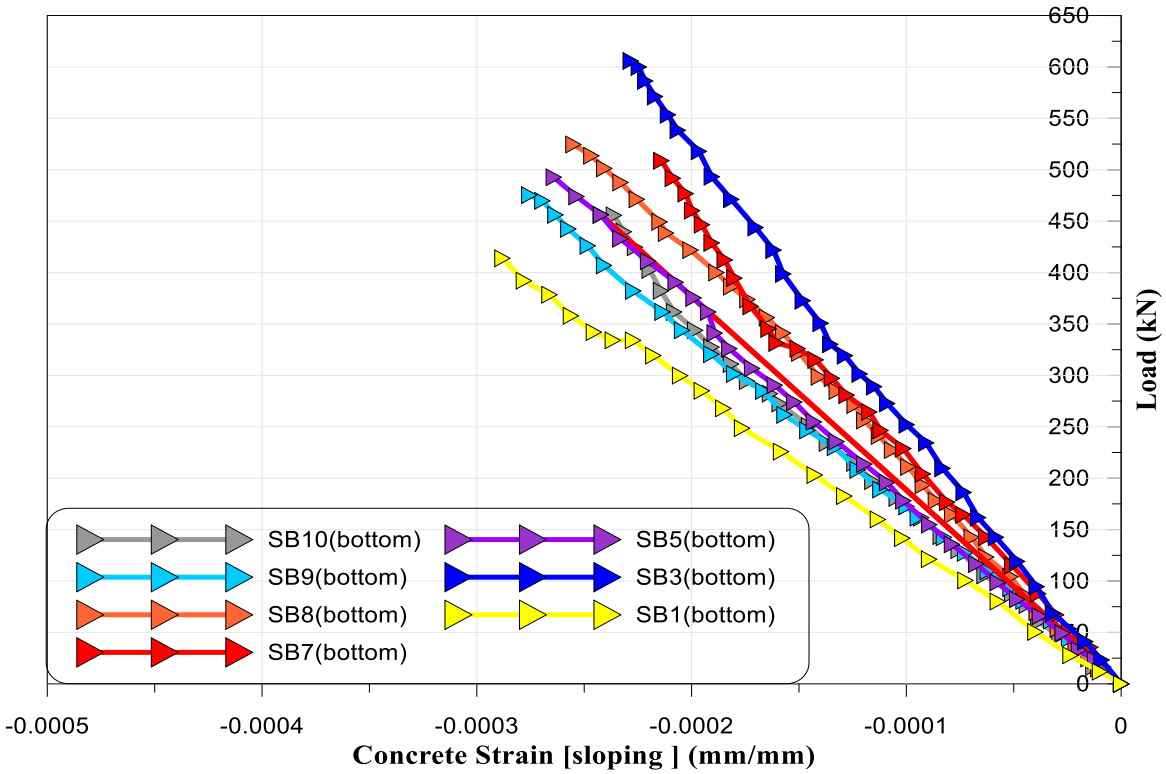

Figure (4-79) Load versus strain on concrete surface at the sloping region

4.10 Mode of Failure and Slipping Strand

For specimens tested under monotonic static loading, as illustrated in section (4-3), three types of failures may occur depending on the type of specimen category and strengthening.

Two types of failure related to the SIFCON laminates were observed through the experimental tests of the specimens; debonding, and rupture SIFCON laminates. The third type, where the failure was due to steel yielding followed by crushing of concrete failure.

It was observed that the mode of failure for each specimen subjected to repeated loading was exactly the same mode of failure for the counterpart specimen under monotonic static loading. Table (4-2) can be applied to define the mode of failure of specimens.

It should be noted that no slip between strands and concrete was recorded for all the specimens, and also no fracture of any type of reinforcement was observed.

Except for the SB3 beam specimen when debonding in SIFCON laminate happened did pull and cut a part of the concrete cover, with a part of the ordinary steel reinforcement.

In addition, no rupture of the prestressed strands in any specimens was noticed throughout all static and repeated loading tests.

CHAPTER FIVE

FINITE ELEMENT MODELING

CHAPTER FIVE

FINITE ELEMENT MODELING

5.1 General

A numerical simulation is performed in this analysis to expand the experimental investigation by using the most practical parameters. The Finite Element Model (FEM) that is developed by using ABAQUS software is described in this chapter. ABAQUS is a program of finite elements for evaluating the behavior of solids and structures under external loads. Both static and dynamic problems can be analyzed by using ABAQUS. It can model a wide range of shapes (2D and 3D) with a library of advanced and extensive materials and elements. Also, it can contact solids [71]. In this study, ABAQUS is used for modeling the unbonded post-tensioned prestressed beams strengthening with SIFCON laminates response when subjected to monotonic static and repeated loads.

5.2 Finite Element Modeling

A three dimensions finite element model is used to simulate the continuous rectangular section beams in the present study to analyze these beams under the influence of static and repeated loads.

ABAQUS software version -2019 was used to model rectangular section prestressed continuous beam with regard to load-deflection relation, ultimate load capacity, crack propagations.

Moreover, the parametric study of several variables such as loading type (applied distributed loads and comparing the behavior with the concentrated loads at the middle of spans), using different concrete strength and applied the repeated load with various level of the ultimate load were also examined using this software.

5.2.1 Element Selection

In order to model the concrete beam, strand, steel plates and SIFCON laminates. C3D8R (8-node continuum 3-dimensional element with reduced command integration) and C3D10(10-node quadratic tetrahedron) For complex shapes with holes is used as shown in Figure (5-1) a and Figure (5-1) b. This element is capable of modeling material and geometrical nonlinearities in addition to large deformations[71]. Each node in these elements has three translational degrees of freedom. The reduced integration technique which is adopted by ABAQUS for solid and shell elements was selected to reduce higher order solid requirements without impacting the accuracy of recorded responses. Hourglass problems which are normally happened with continuum linear solid elements are taken into account for this element type. Whereas, the 2-nodes linear 3D truss element called (T3D2) available in ABAQUS is unitized for steel reinforcement modeling (see Figure (5-1) c).

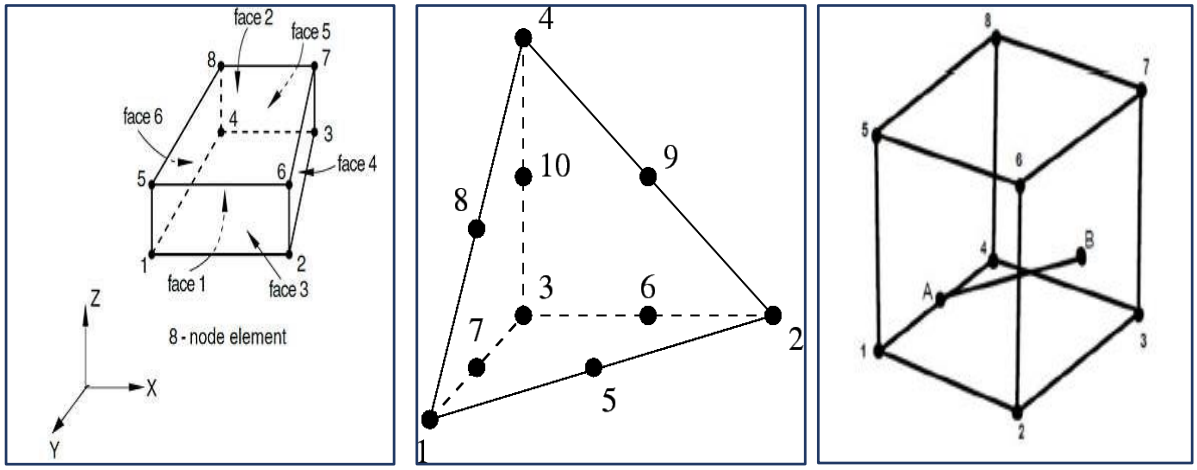

a. C3D8 b.C3D10 c.T3D2

Figure (5-1) The geometry ABAQUS elements that used in this study[40]

5.2.2 Modeling of Materials and Elements in ABAQUS

In order to simulate the specimens, modeling for the used materials which are concrete (HSC and SIFCON), ordinary steel, and prestress strand. In the

ABAQUS program, the material specifications data are entered in stages according to the behavior of the material where the first stage is elasticity and then the plasticity stage. For the elastic stage passion ratio and elasticity modulus for material are used in the present analysis. For plasticity, ABAQUS provides several models depending on the material behavior after the elastic stage. In the present analysis, the Concrete Damaged Plasticity model is used for concrete and plastic for reinforced bars. While only the elastic stage is used to simulate the steel plates. Then select mesh size convergence, represent the boundary conditions and loading steps modeling and modeling of the interaction between all parts of the model. The detailed explanation is in Appendix (C).

5.3 Calibration of the Fabricated FE Model

In this section, several comparisons are made with the experimental results.

5.3.1 Load-Deflection Relation

To test the applicability of the results for the numerical model, responses of load to mid-span deflection obtained from the study of finite elements were compared with experimental tests for twenty specimens. The objective of testing the results of the ABAQUS program by comparing them with the practical results is to ensure the accuracy of the results for the parametric studies that will be investigated using the ABAQUS program.

The load to mid-span relations for the examined beams are shown in Figure (5-2) for beams tested under static loads and Figure (5-3) for beams subjected to repeated loads ten cycles of (0.4) P_u to (0.6) P_u and then loaded up to failure. These Figures usually indicate a good agreement between the finite element analyzes curves and the experimental curves. Also, the deformable shape for the beams simulated in ABAQUS can be shown in Figure (5-4).

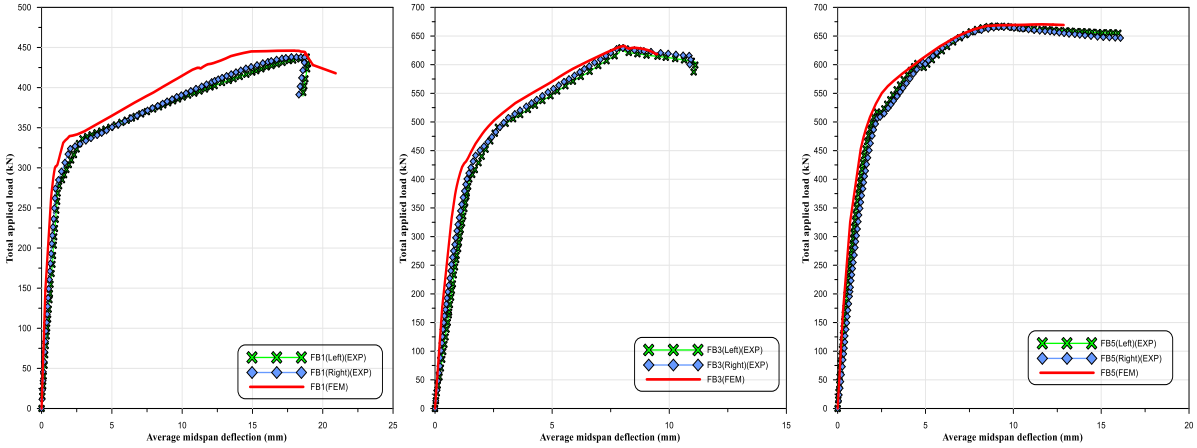

FB1 FB3 FB5

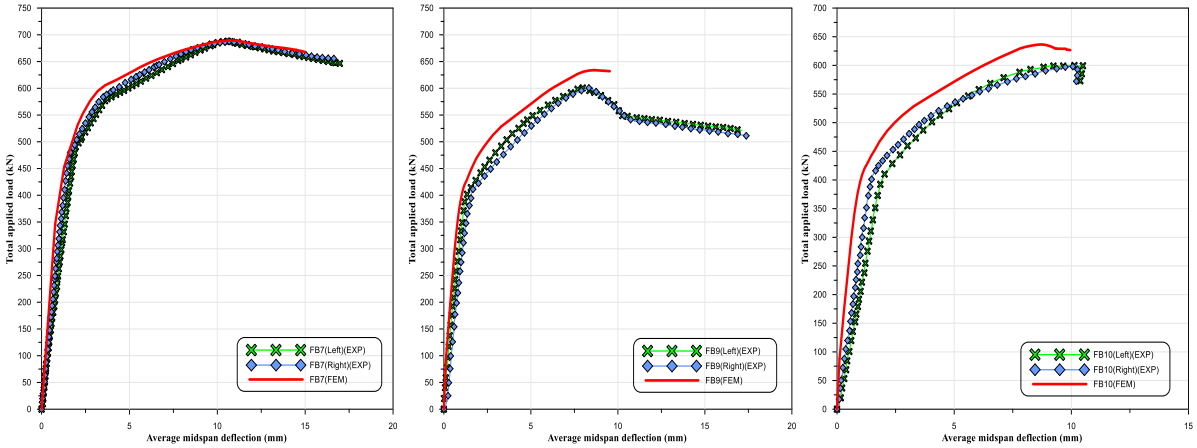

FB7 FB9 FB10

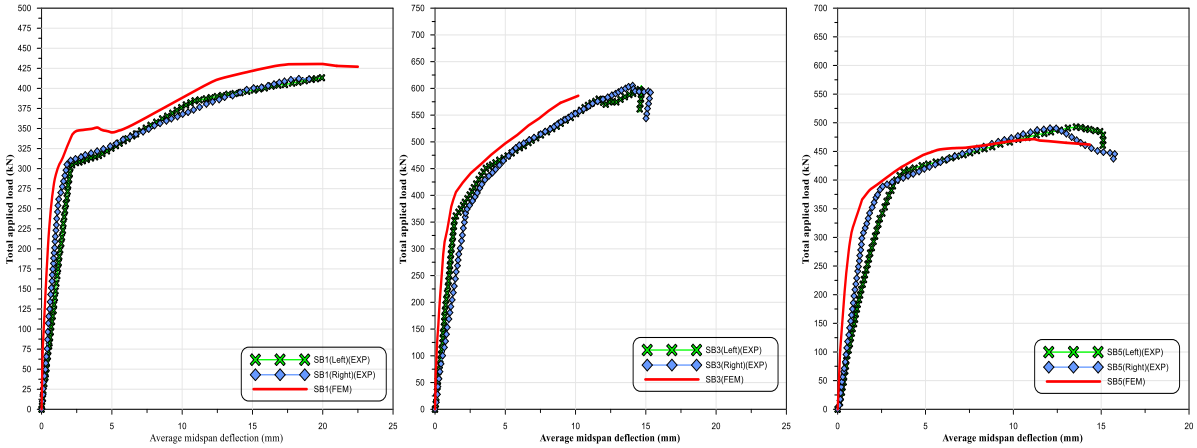

SB1 SB3 SB5

Figure (5-2) Exp. and FEM load-deflection curves groups (A) and (C)

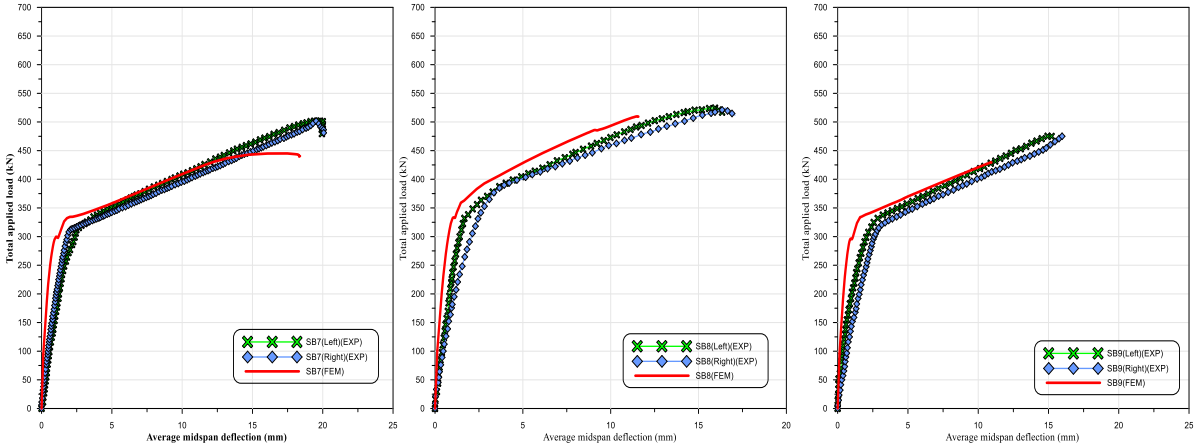

SB7 SB8 SB9

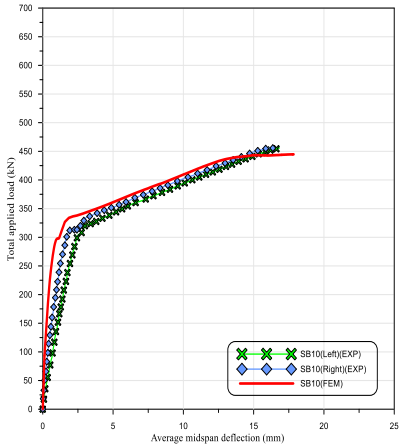

SB10

Continued Figure (5-2) Exp.and FEM load-deflection curves groups (A) and (C)

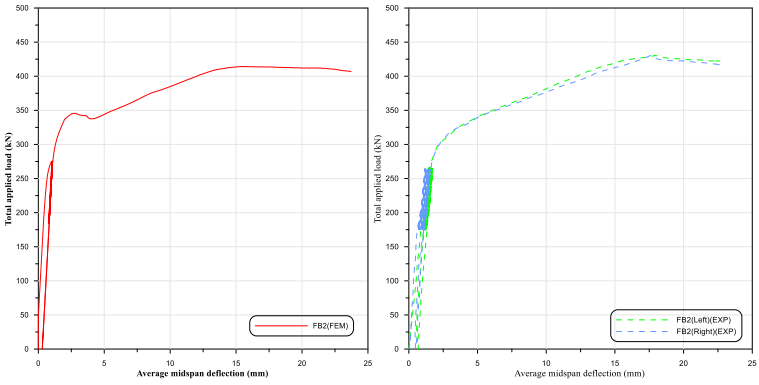

FB2 -FEM FB2-Exp.

Figure (5-3) Exp. and FEM load-deflection curves groups (B) and (D)

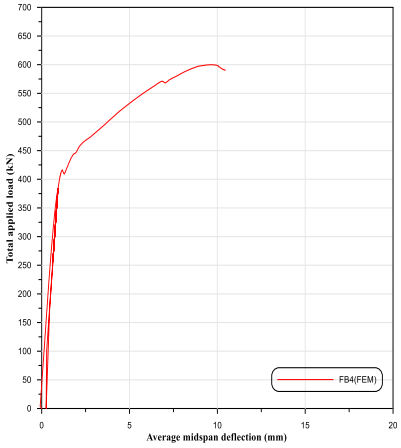

FB4 -FEM

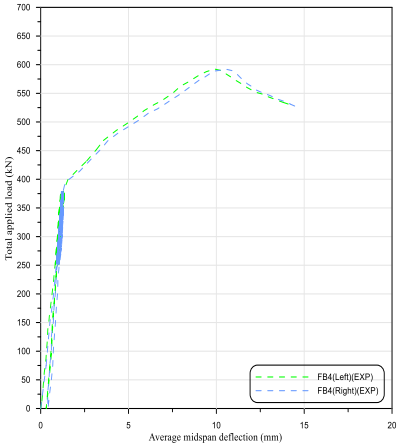

FB4-Exp.

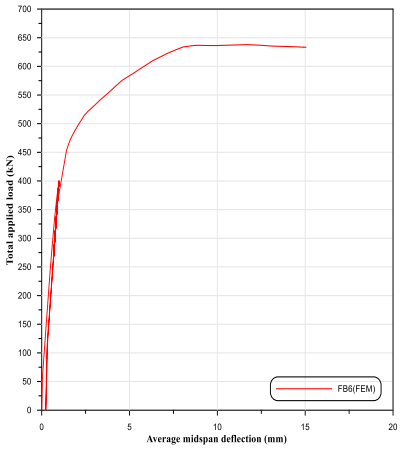

FB6 -FEM

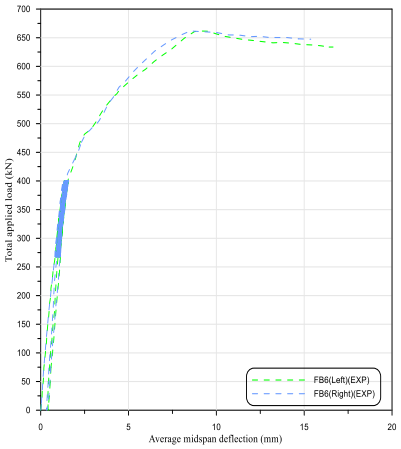

FB6-Exp.

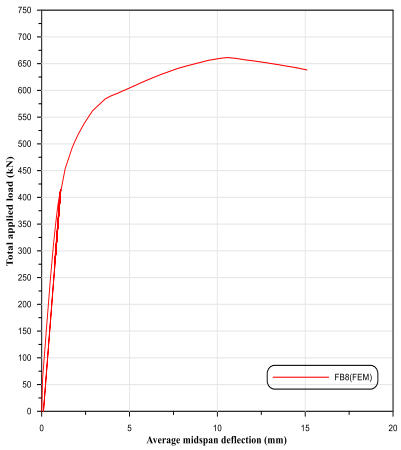

FB8 -FEM

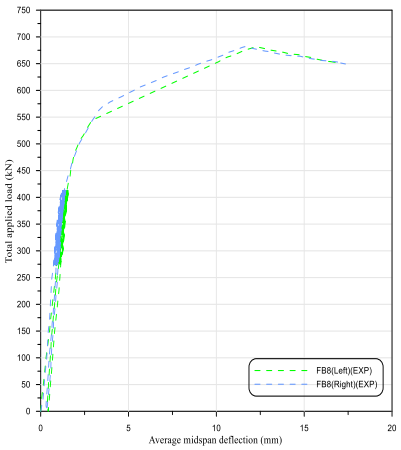

FB8-Exp.

Continued Figure (5-3) Exp. and FEM load-deflection curves groups (B) and (D)

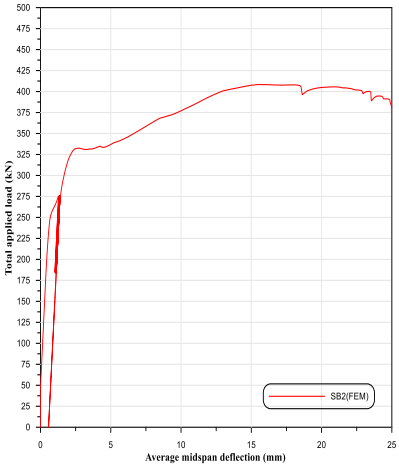

SB2 -FEM

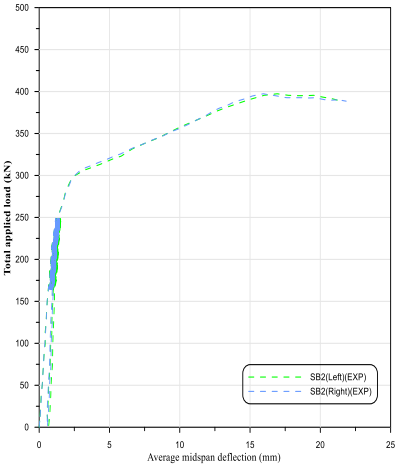

SB2-Exp.

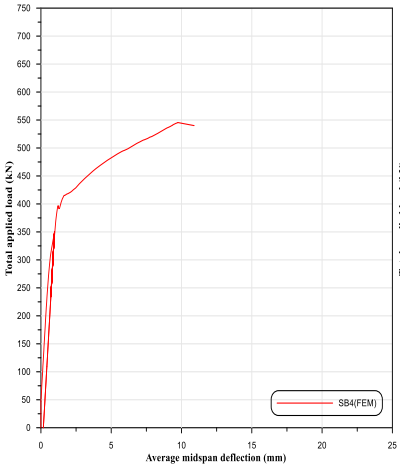

SB4 -FEM

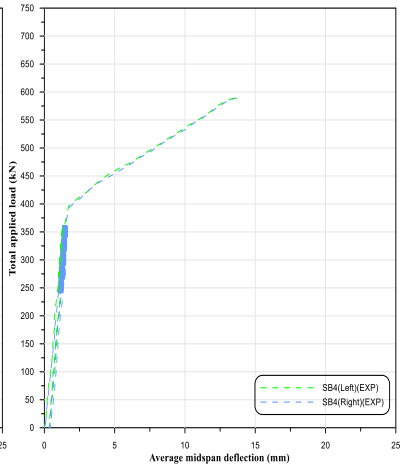

SB4-Exp.

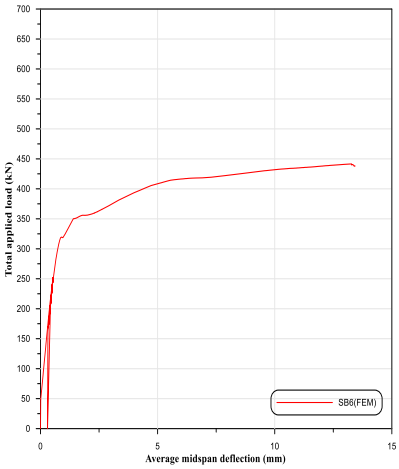

SB6 -FEM

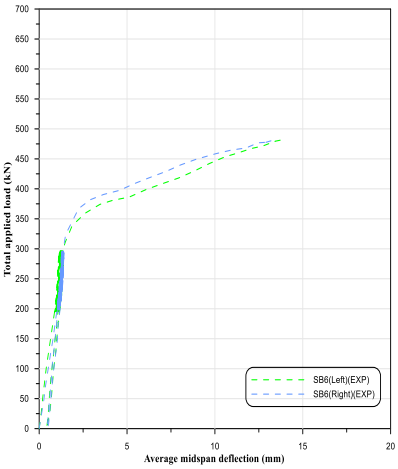

SB6-Exp.

Continued Figure (5-3) Exp. and FEM load-deflection curves groups (B) and (D)

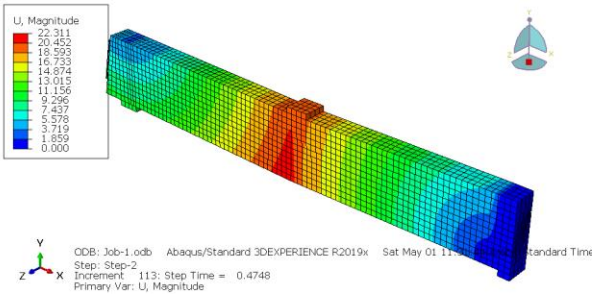

FB1

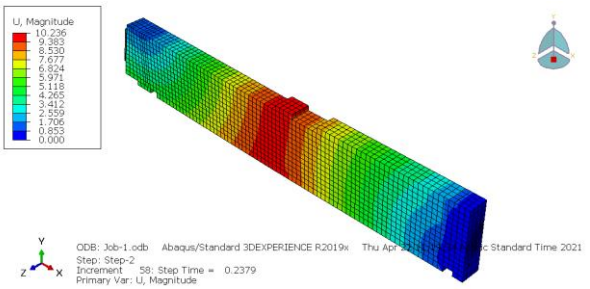

FB3

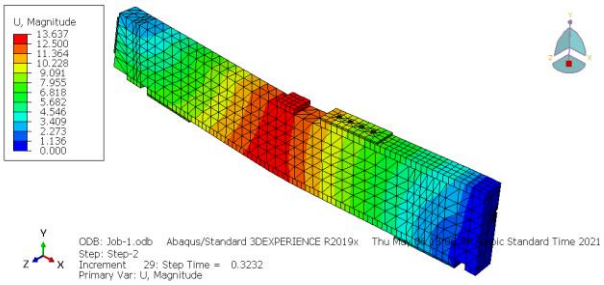

FB5

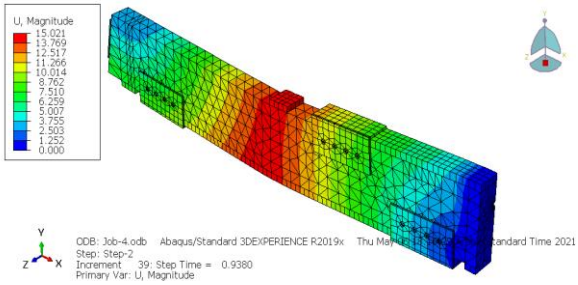

FB7

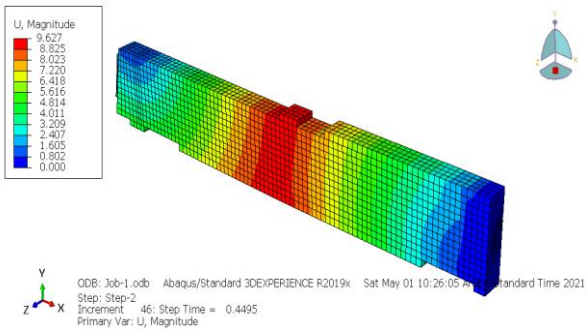

FB9

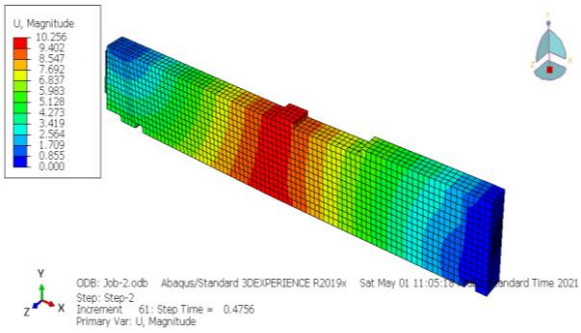

FB10

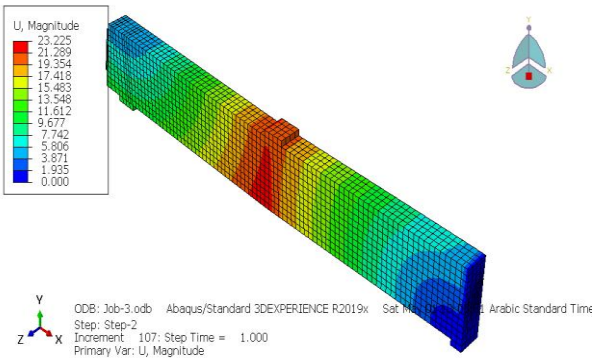

SB1

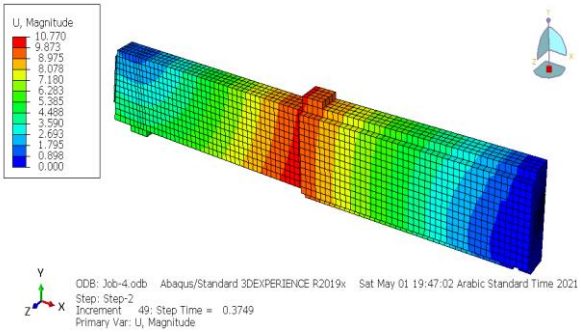

SB3

Figure (5-4) Vertical numerical deflection of all beams

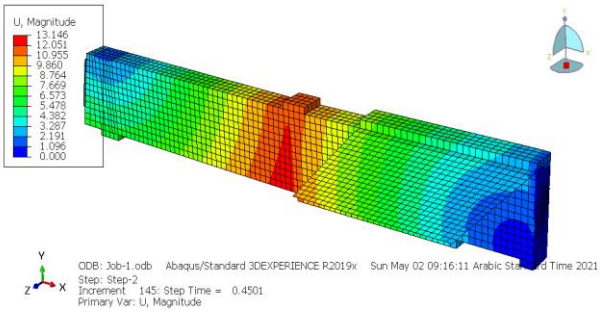

SB5

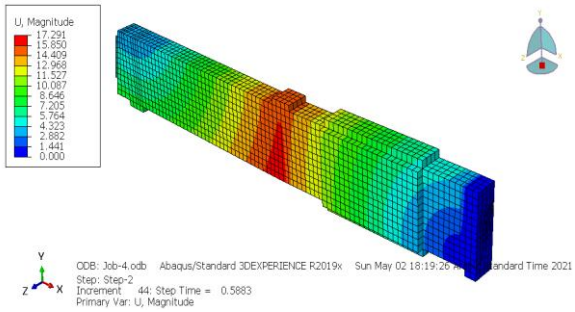

SB7

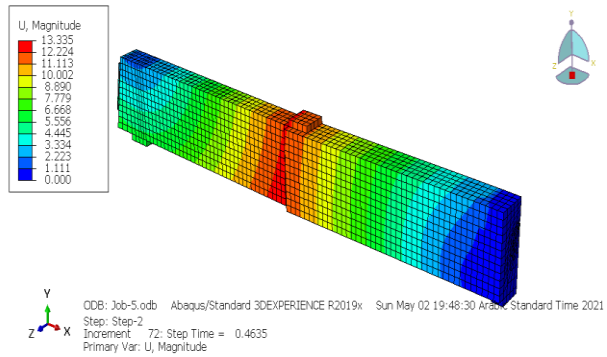

SB8

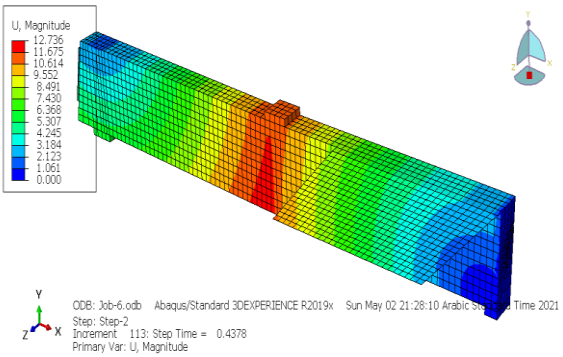

SB9

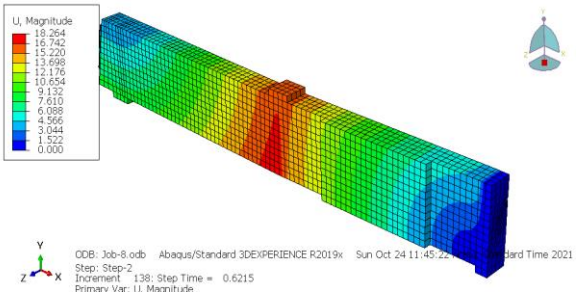

SB10

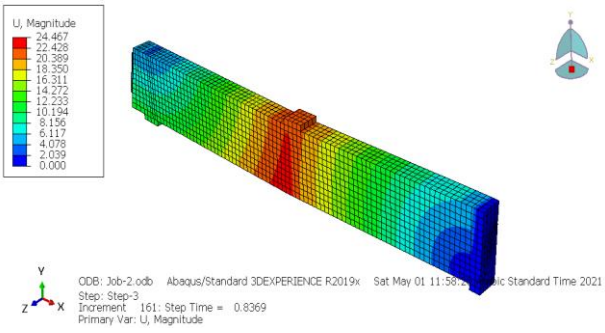

FB2

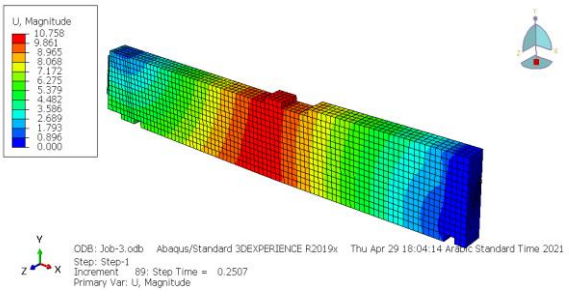

FB4

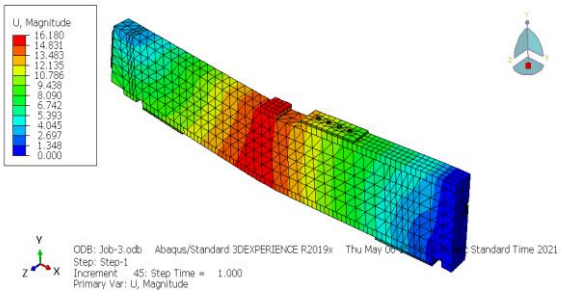

FB6

Continued Figure (5-4) Vertical numerical deflection of all beams

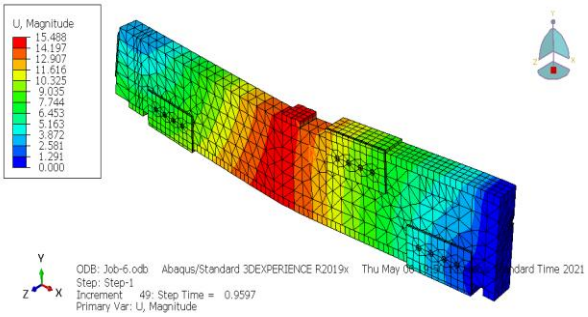

FB8

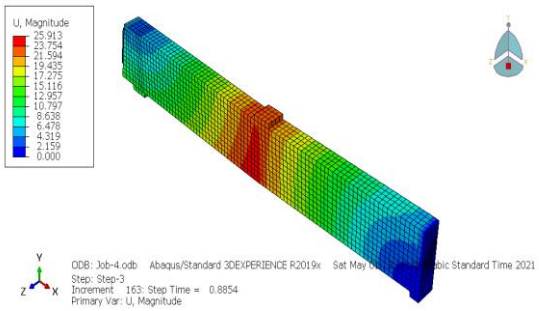

SB2

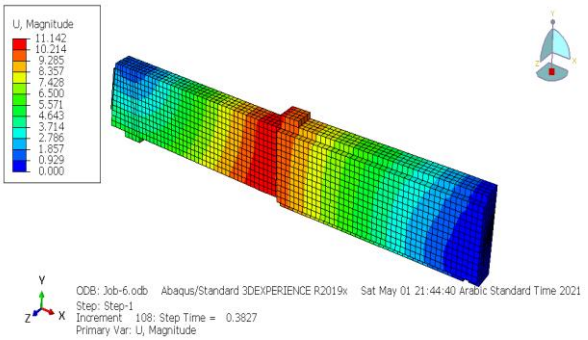

SB4

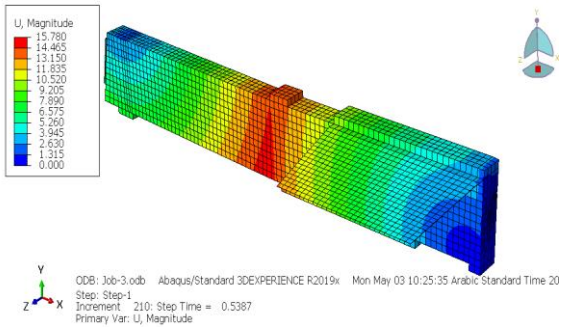

SB6

Continued Figure (5-4) Vertical numerical deflection of all beams

Table (5-1) Comparison between experimental and numerical values of ultimate load capacity and maximum deflection for tested beams

Group	Beam	Ultimate load capacity (kN)			Max. deflection (mm)		
		Exp.	Num.	Num./Exp.	Exp.	Num.	Num./Exp.
A	FB1	438.2	446.0	1.017	17.8	18.0	1.012
	FB3	629.3	632.7	1.005	7.9	8.1	1.025
	FB5	667.6	670.4	1.004	9.9	10.6	1.075
	FB7	687.7	689.2	1.002	10.7	10.8	1.009
	FB9	600.6	633.9	1.055	8.3	8.6	1.039
	FB10	600	636.4	1.060	9.7	8.9	0.926

Continued Table (5-1) Comparison between experimental and numerical values of ultimate load capacity and maximum deflection for tested beams

Group	Beam	Ultimate load capacity (kN)			Max. deflection (mm)		
		Exp.	Num.	Num./Exp.	Exp.	Num.	Num./Exp.
C	SB1	413.3	430.4	1.041	19.9	19.6	0.987
	SB3	605.3	586.2	0.968	11.9	12.2	1.026
	SB5	492.9	471.4	0.956	12.2	11.1	0.917
	SB7	501.7	445.1	0.887	19.4	17.4	0.901
	SB8	524.3	509.6	0.972	12.5	11.5	0.920
	SB9	475	429.3	0.903	11.9	10.8	0.913
	SB10	455.7	444.7	0.975	16.8	17.7	1.058
B	FB2	430.6	414.2	0.962	17.5	15.4	0.880
	FB4	592.3	599.9	1.012	9.9	9.6	0.970
	FB6	661.8	637.9	0.963	11.1	12.3	1.117
	FB8	681.8	661.349	0.970	11.6	10.5	0.912
D	SB2	397.3	408.3	1.027	15.9	15.4	0.972
	SB4	589.2	545.5	0.925	10.4	9.7	0.936
	SB6	481.9	441.5	0.916	13.1	13.2	1.014

Table (5-1) explains a comparison between the experimental and numerical values for ultimate load capacities and ultimate deflections for all the tested beams specimen. These values indicated that the difference between the ultimate experimental load capacities and that obtained by ABAQUS is less than (9.6%). At the same time, the biggest difference in maximum deflection values between the theoretical and practical results was not to exceed (11.9%).

It is essential to note from the presented Figures (5-2) and (5-3) that in the elastic region of the finite element, the loading deflection response is stiffer than the experimental ones. The FE model has multiple factors which can result in the simulated beams being higher in stiffness. The most noticeable influences are that of:

- The concrete is considered to be homogeneous material in the FEA model but it was actually a heterogeneous material.
- The concrete micro-cracks that formed as a result of handling and drying shrinkage, make the stiffness of the actual concrete beams be reduced, however in the FEA model, these effects were not included.
- It is assumed that there is an ideal bond between concrete and the reinforced bars in the FE analysis. However, this assumption can't be reached in the actual study.
- Bonding by epoxy is subjected to many factors, including humidity, temperature, and quality of installation. Still, in the program, it represents an ideal bonding without don't take into consideration these factors. This is an essential cause of the difference between numerical the experimental results.

5.3.2 Distribution of Von Mises Stress at Reinforcement Bars

Von Mises stresses for the 7-wires steel strands and ordinary reinforcement bars at the ultimate load which was obtained numerically by ABAQUS were presented in Figure (5-5). It’s clear that stress for the 7-wires steel strand dominant along with the beams, steel main reinforcement bars in the maximum moment's zones (both the mid-span region and the central support region) is reached to the ultimate value stresses.

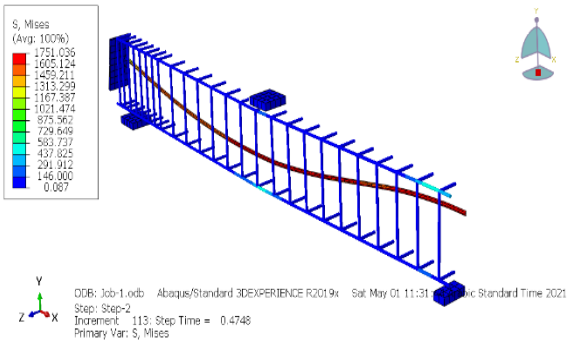

FB1

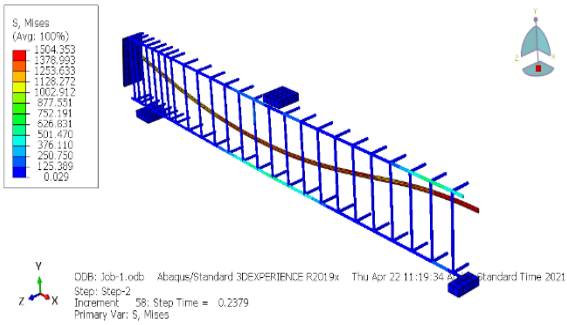

FB3

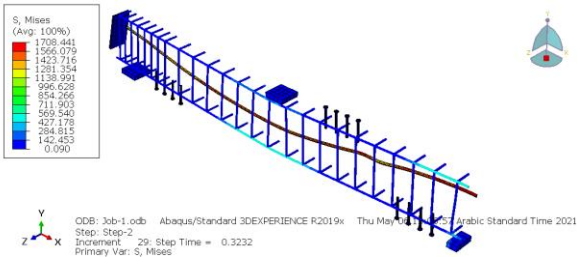

FB5

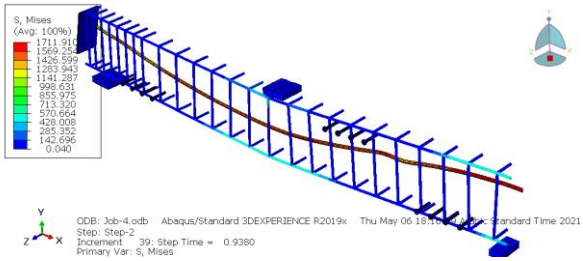

FB7

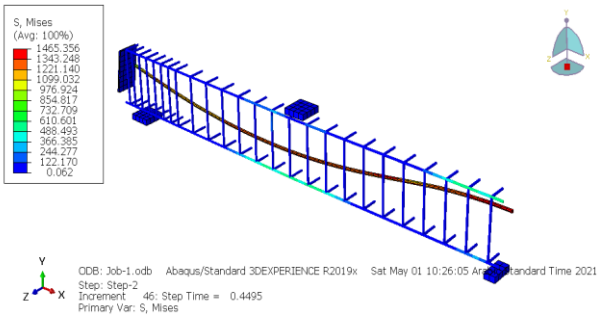

FB9

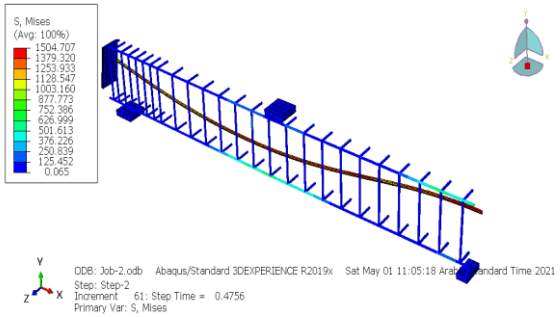

FB10

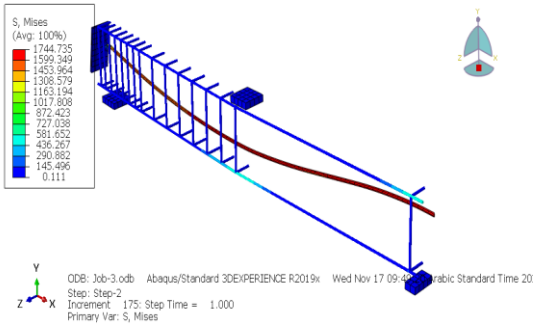

SB1

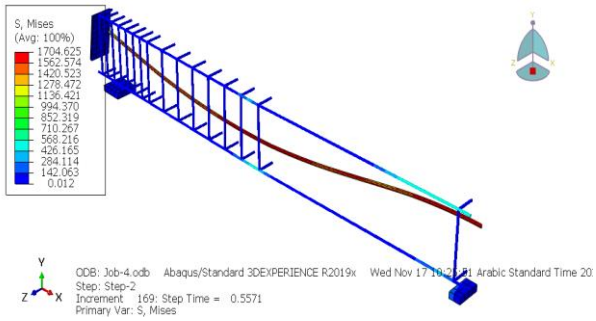

SB3

Figure (5-5) The strand and reinforcement bars stresses of all tested beams

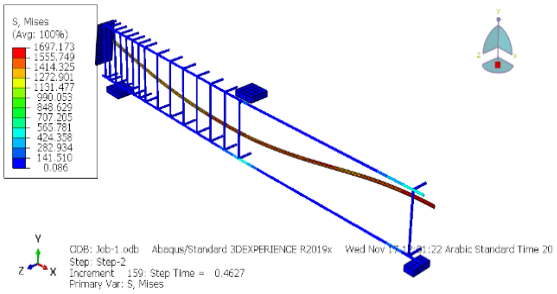

SB5

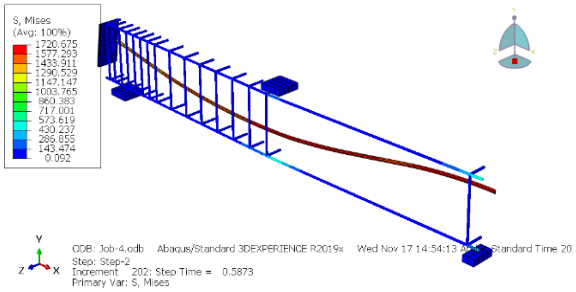

SB7

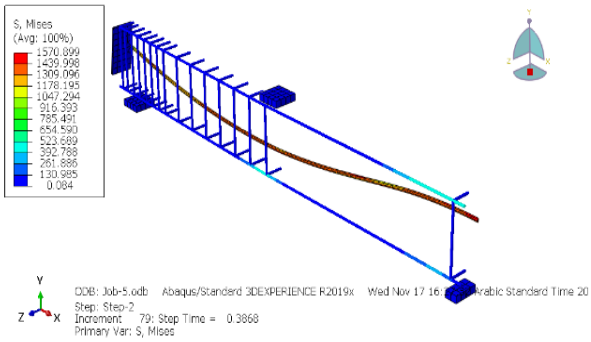

SB8

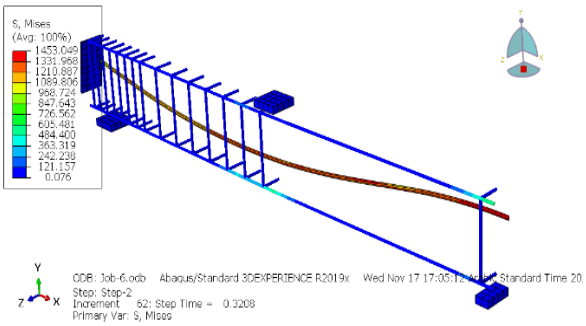

SB9

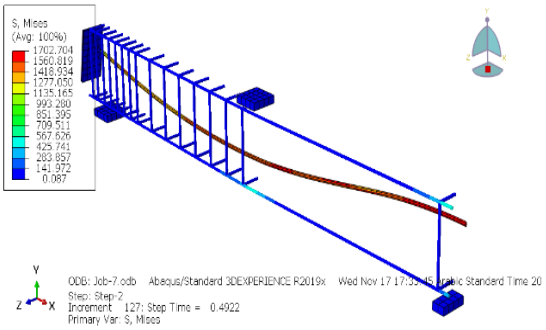

SB10

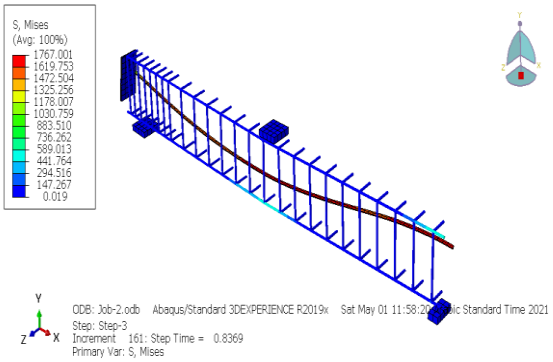

FB2

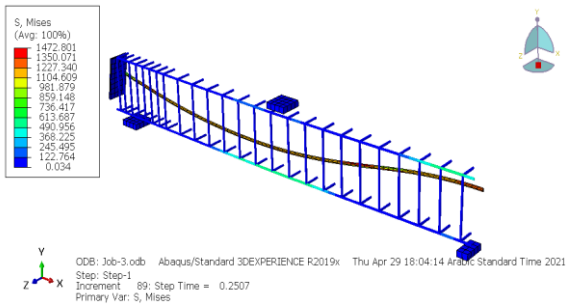

FB4

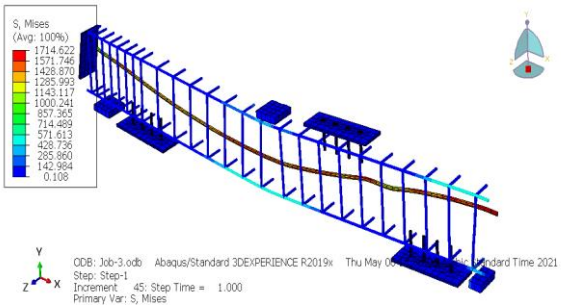

FB6

Continued Figure (5-5) The strand and reinforcement bars stresses

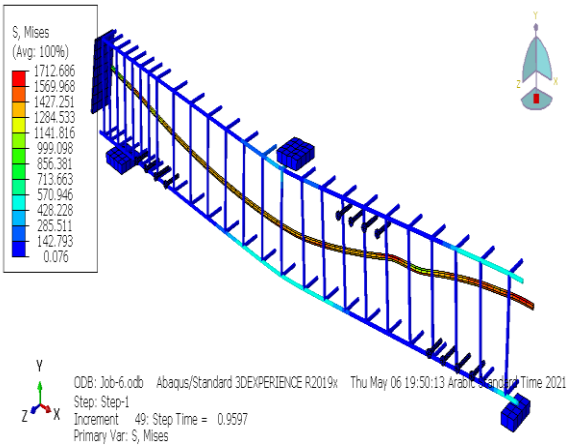

FB8

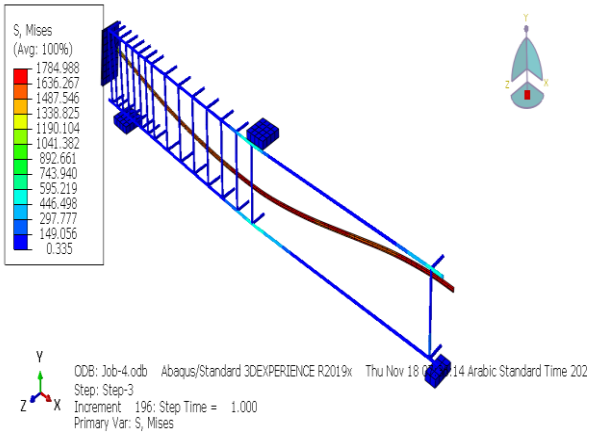

SB2

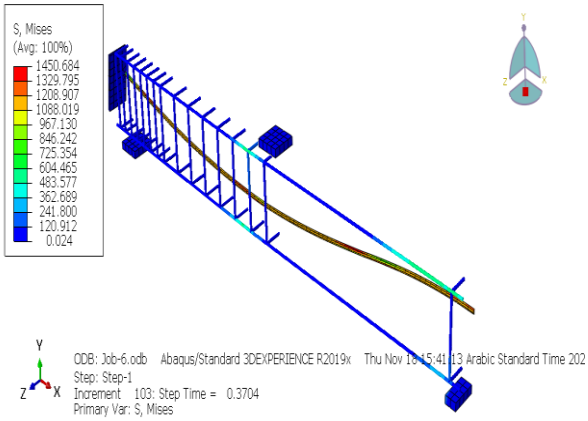

SB4

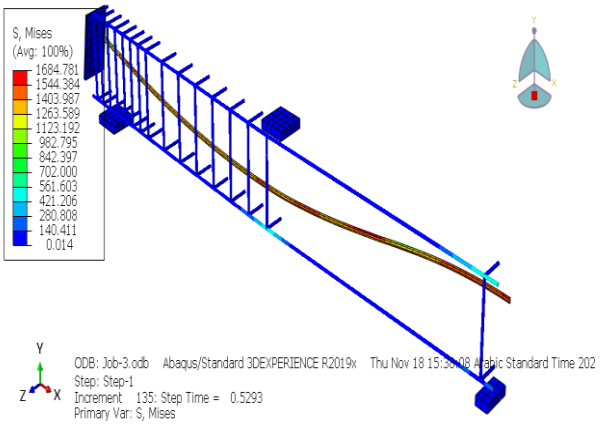

SB6

Continued Figure (5-5) The strand and reinforcement bars stresses

5.3.3 Crack Patterns

The crack patterns of the tested beams obtained by ABAQUS models can be shown in Figure (5-6) at failure stages. By comparing them with crack patterns found in the experimental work, it can be seen the clear match between the practical and theoretical results. So, depending on the above results it can say that the present analysis with the ABAQUS program agreed well with the practical results. This indicates that the ABAQUS model, which was used for the analysis of the continuous beams in the present study, can capture the structural behavior of all tested beams: unstrengthened and strengthened beams.

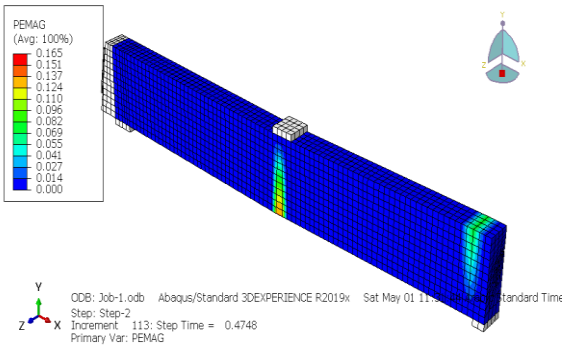

FB1

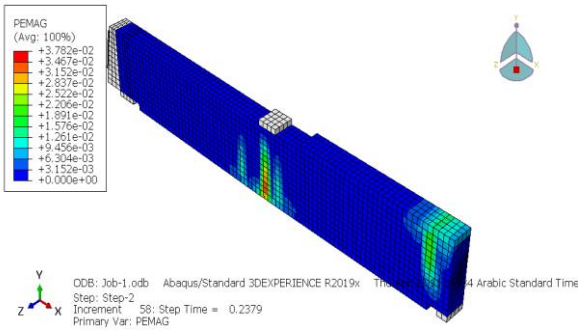

FB3

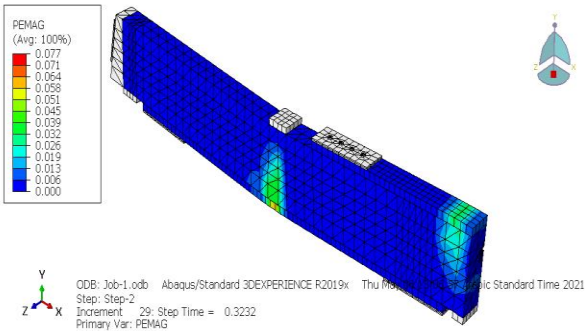

FB5

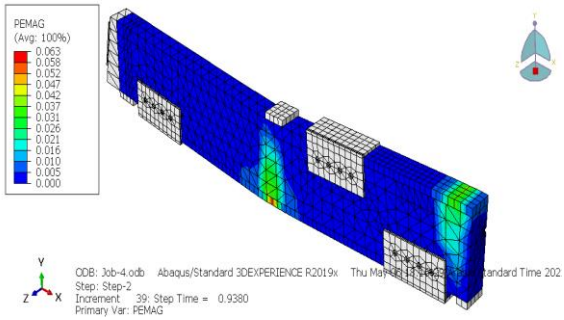

FB7

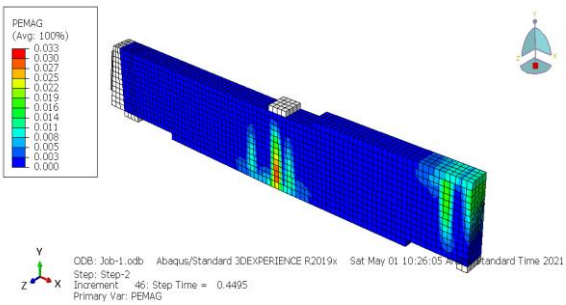

FB9

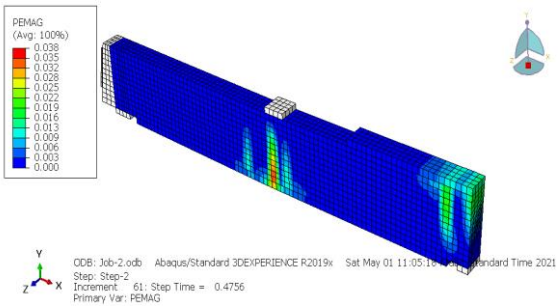

FB10

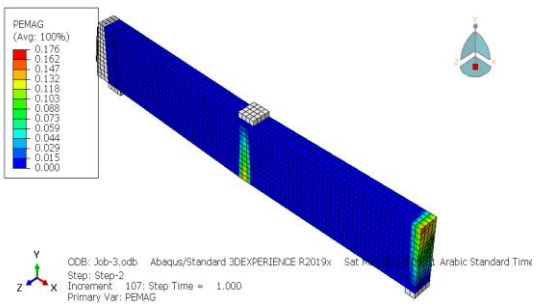

SB1

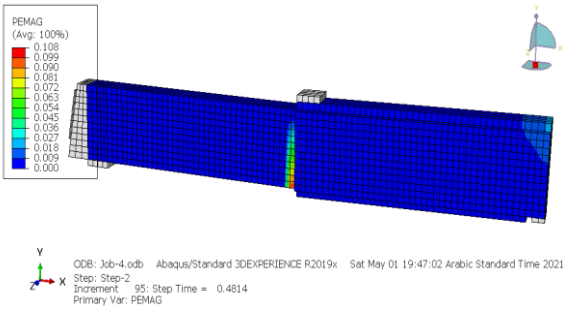

SB3

Figure (5-6) ABAQUS failure shape of all tested beams

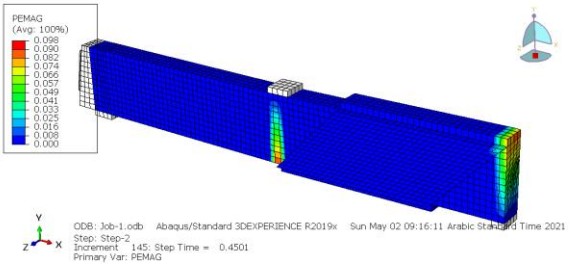

SB5

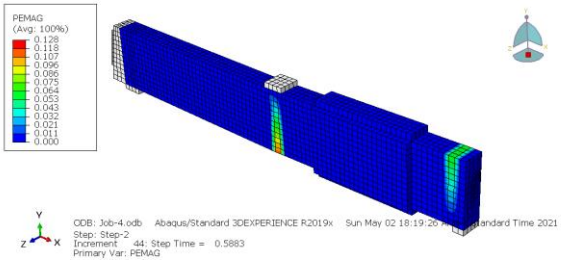

SB7

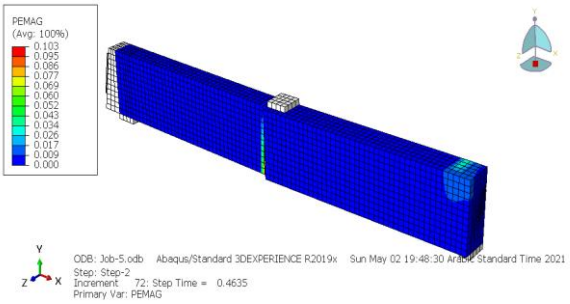

SB8

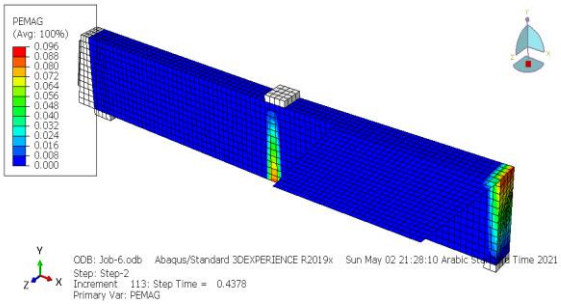

SB9

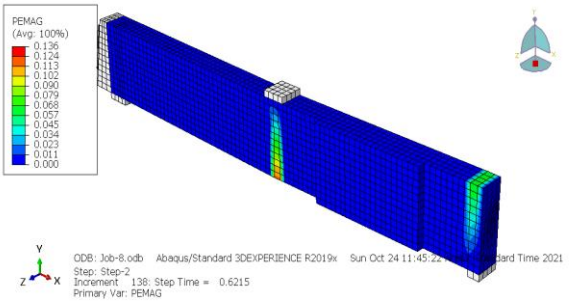

SB10

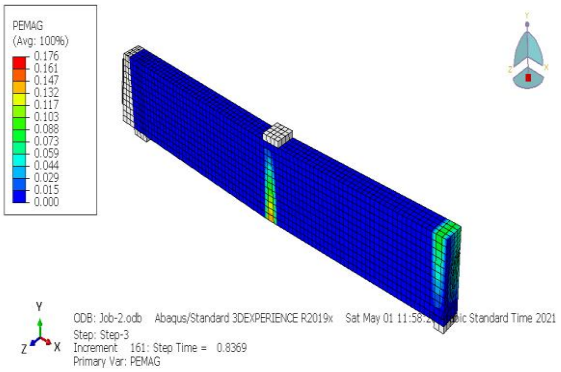

FB2

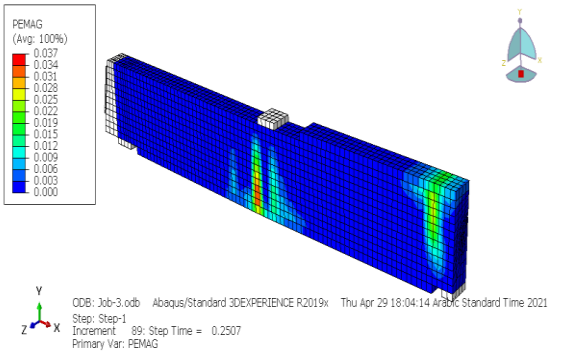

FB4

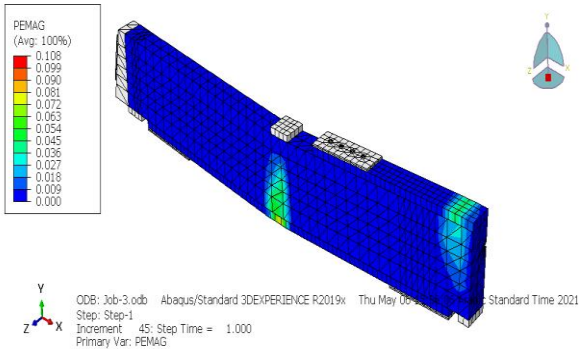

FB6

Continued Figure (5-6) ABAQUS failure shape of all tested beams

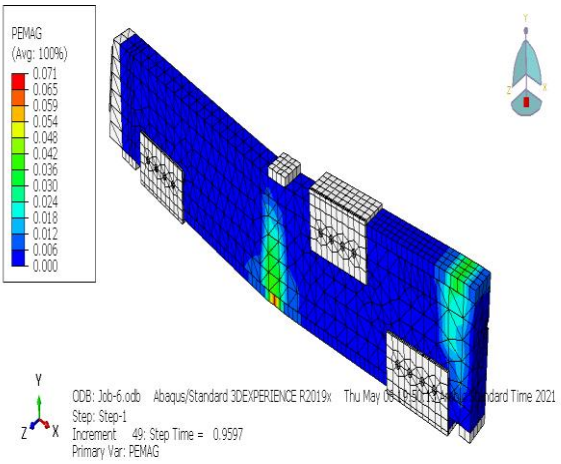

FB8

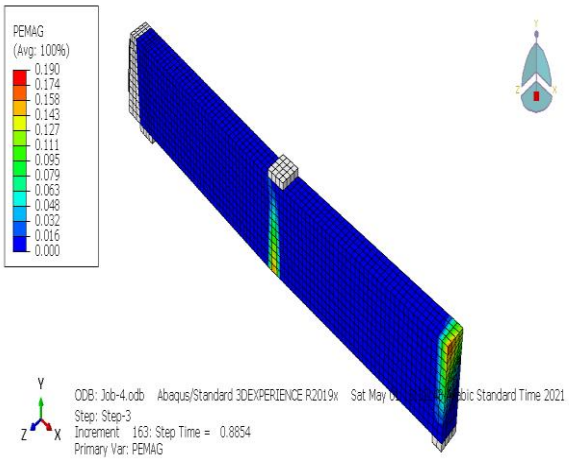

SB2

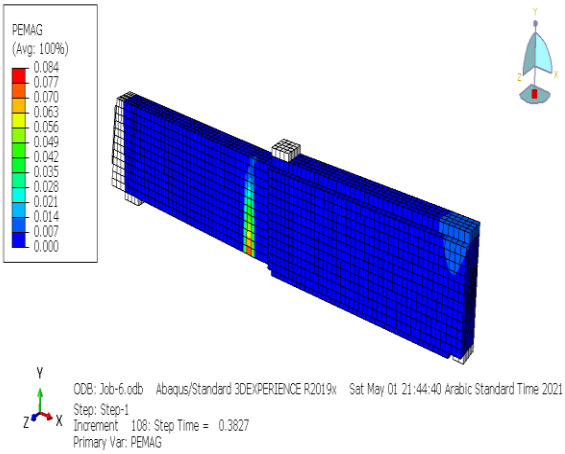

SB4

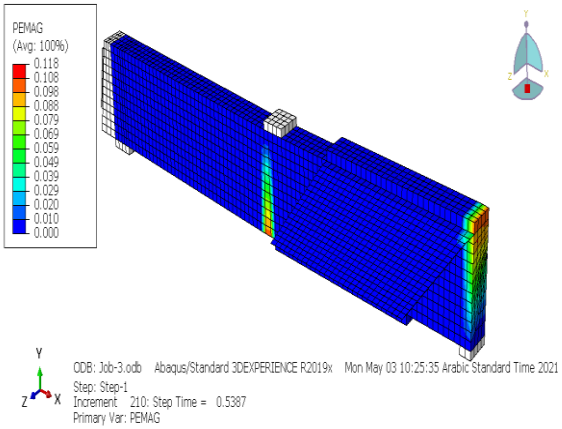

SB6

Continued Figure (5-6) ABAQUS failure shape of all tested beams

5.3.4 Stresses Distribution in Concrete

The nonlinear finite-element analysis explained locations of stress concentrations in continuous prestressed concrete beams in Figures (5-7) as follows: The overall stress paths become widest, and the values of these stresses increase with the more ultimate load capacity increase. This is evident in, loading point region, and the central support region.

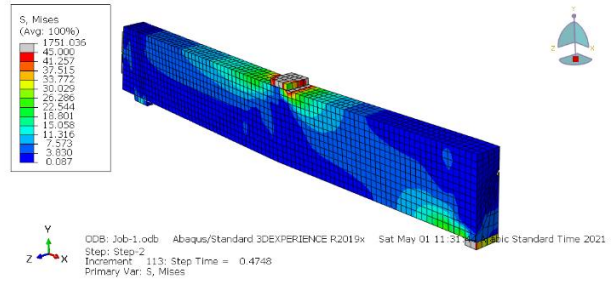

FB1

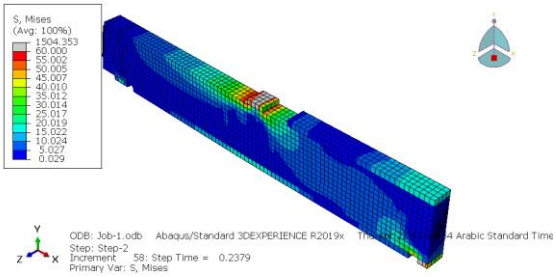

FB3

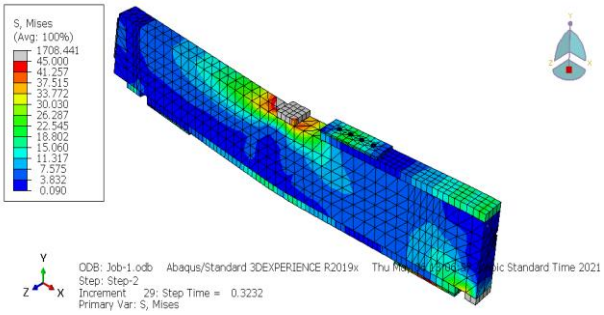

FB5

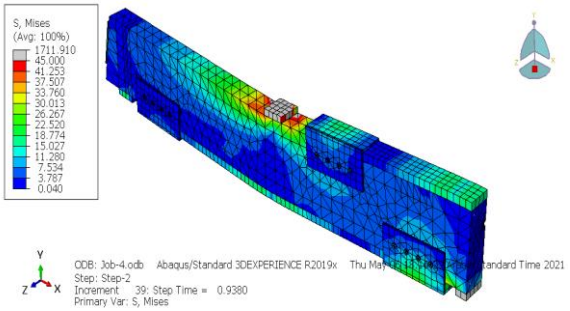

FB7

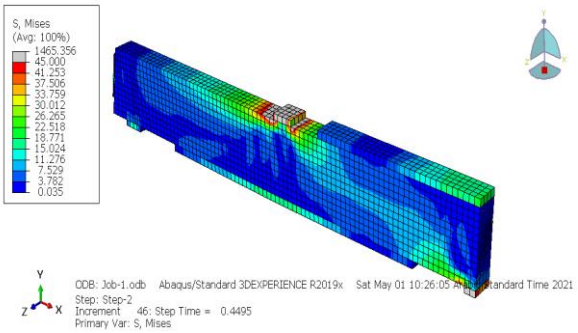

FB9

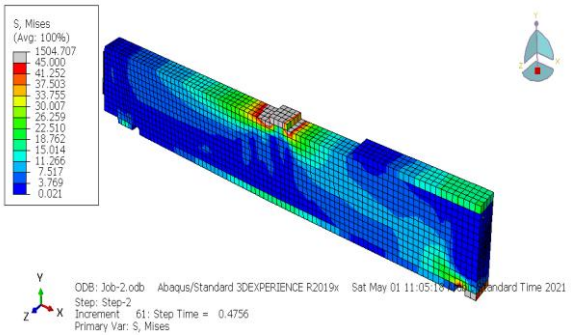

FB10

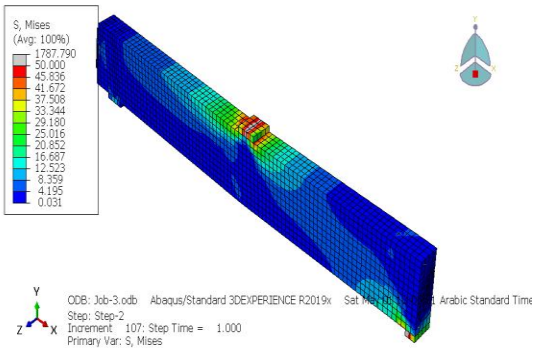

SB1

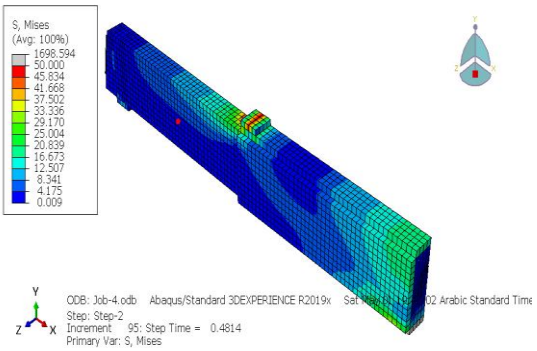

SB3

Figure (5-7) Numerical stresses distribution in concrete for all tested beams

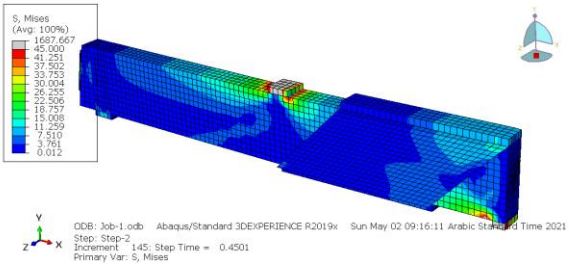

SB5

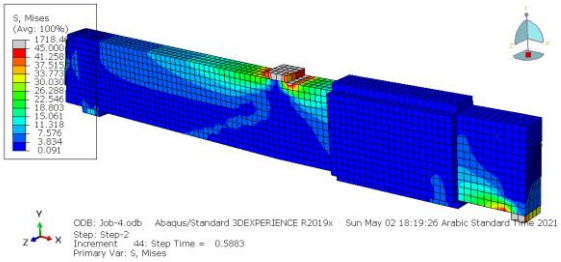

SB7

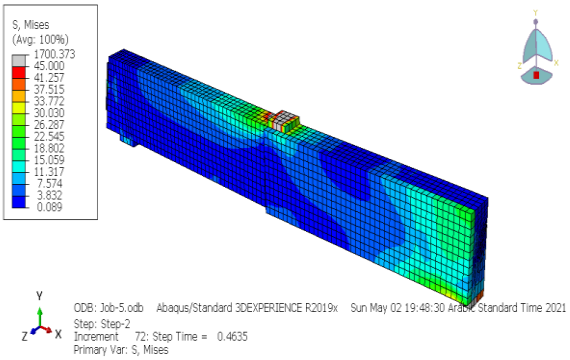

SB8

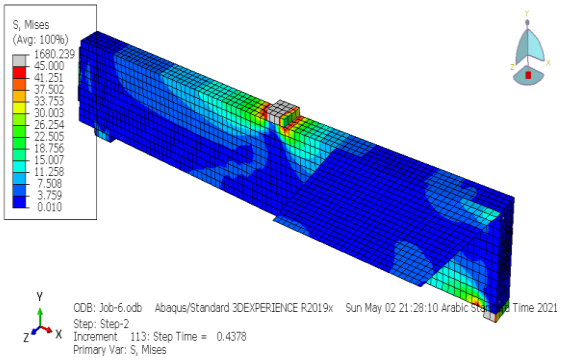

SB9

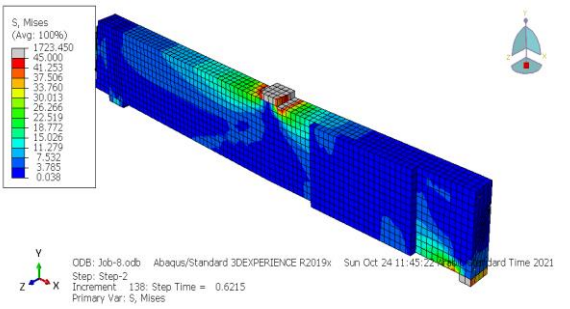

SB10

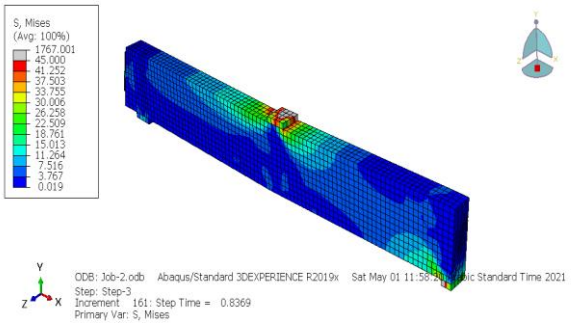

FB2

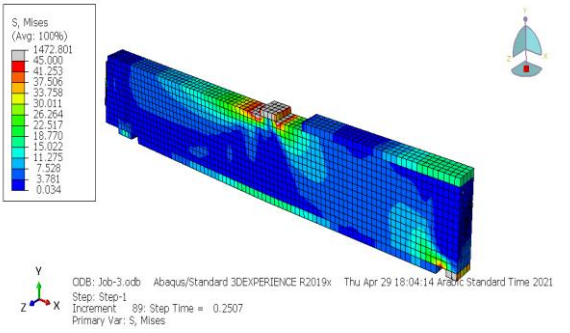

FB4

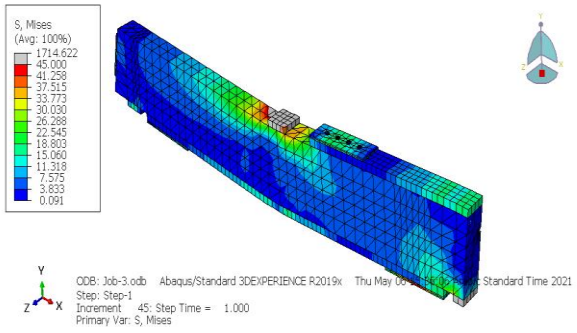

FB6

Continued Figure (5-7) Numerical stresses distribution in concrete

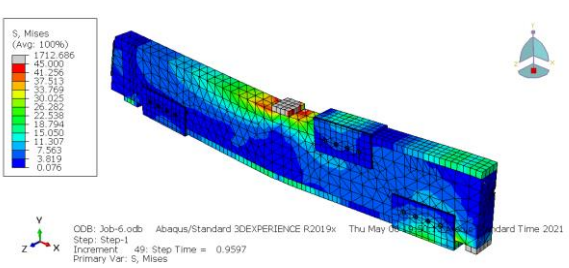

FB8

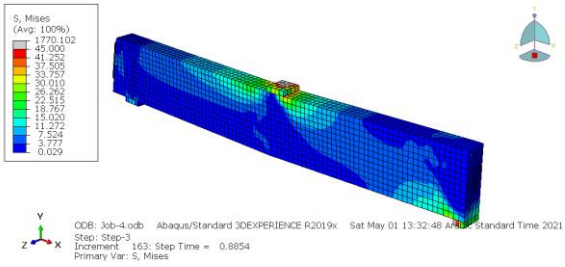

SB2

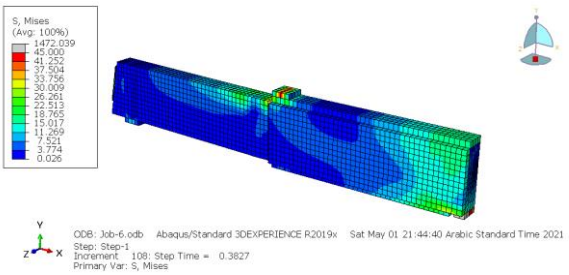

SB4

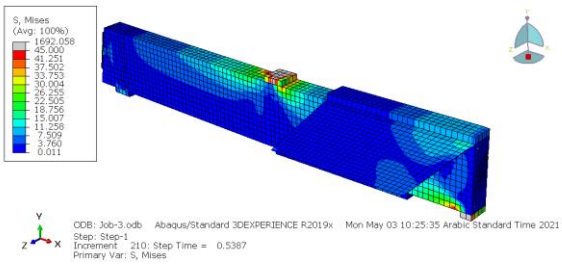

SB6

Continued Figure (5-7) Numerical stresses distribution in concrete

5.4 Parametric Study

Some important factors have been examined in the present study, using ABAQUS numerical model to examine their effect on the flexural and shear behavior of continuous prestressed concrete beams. Parameters considered are:

Loading type, using higher strength of concrete, and different levels of repeated load.

5.5 The Influence of Loading Type on Continuous Prestressed Concrete Beams

Since the goal of using strengthening by precast SIFCON laminate was to obtain high absorption of energy for continuous beams and to ensure redistribution of moments, another type of static loading was tested, which is then distributed loads along the beam. Considering that the redistributing of the moment is greater and clearer to the case of the distributed loads compared with

the concentrated loads at the middle of spans, as shown in Figures (5-8) and (5-9).

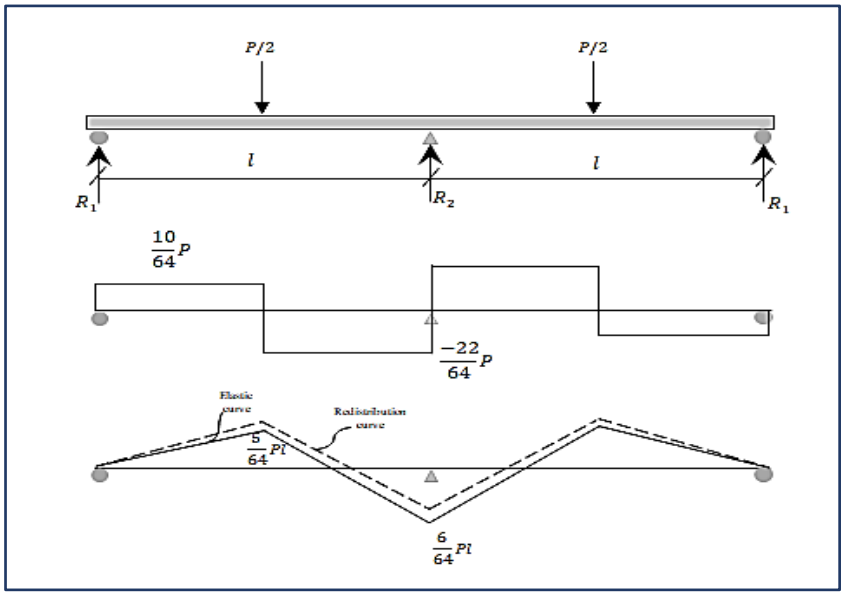

Figure (5-8) Elastic shear and bending moment diagrams of 2-point load[40]

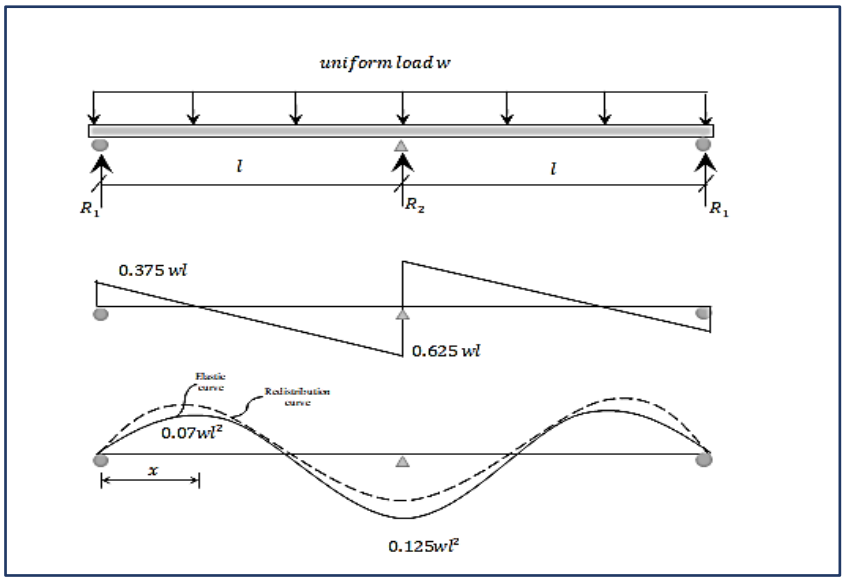

Figure (5-9) Elastic shear and bending moment diagrams of distributed loads[40]

5.5.1 Load-Deflection Response

Through using the model that was simulated in the ABAQUS program, the effect of changing load types is demonstrated. Figures (5-10) display the comparison of the load-deflection response between the two loading types.

According to elastic analysis, the continuous beam capacity will increase when the applied load is distributed uniformly on the beam compared with the case of two-point concentrated loading. This increased reach (120.2%), (97.9%), (105.6%), (93.9%), (113.4%), (97.9%), (111.7%) and (116.4%) moreover increased in ultimate deflection reach (59%), (255.2%), (186%), (182.2%), (42.3%), (133.5%), (66.4%) and (66.3%) for beams FB1, FB3, FB5, FB7, SB1, SB3, SB5 and SB7 respectively. These results indicated that the improvement of ultimate load capacity for all strengthened prestressed concrete beams is higher than for the control beam. It's clear that the higher increase in the capacity was for the prestressed beams strengthening with precast SIFCON laminates.

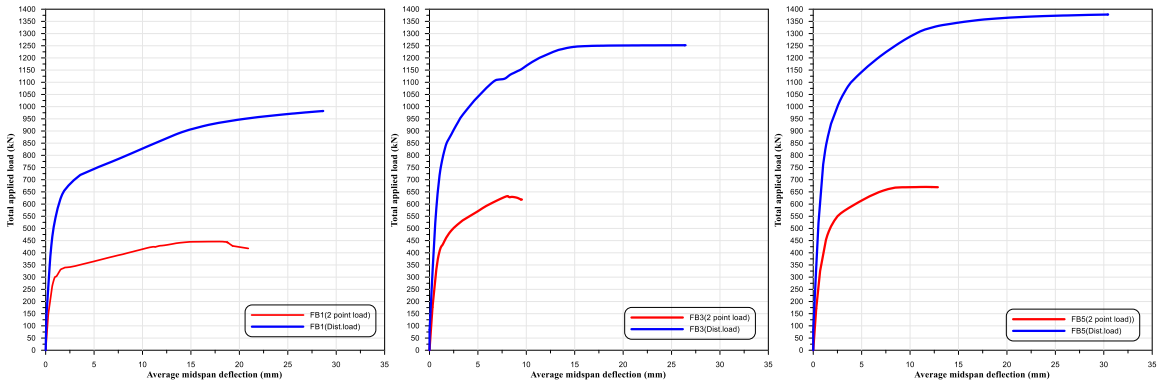

FB1 FB3 FB5

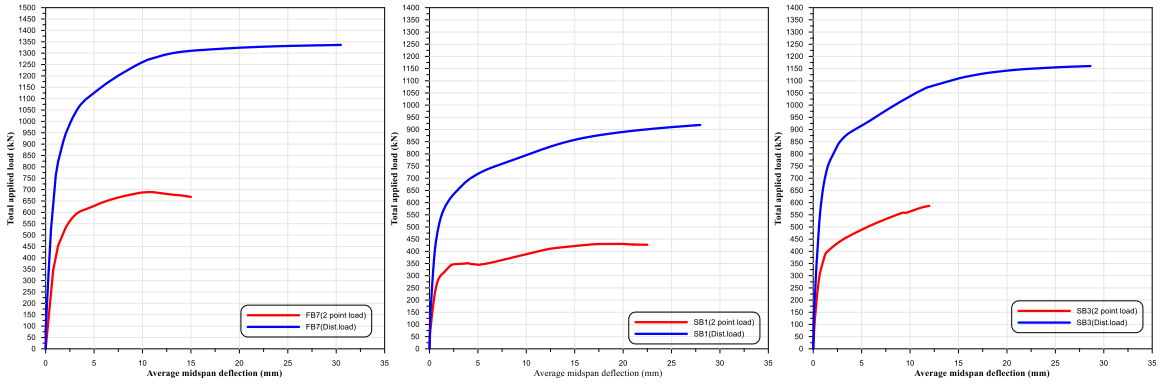

FB7 SB1 SB3

Figure (5-10) Comparison between the responses of beams under concentrated two-point loads and the distributed loads

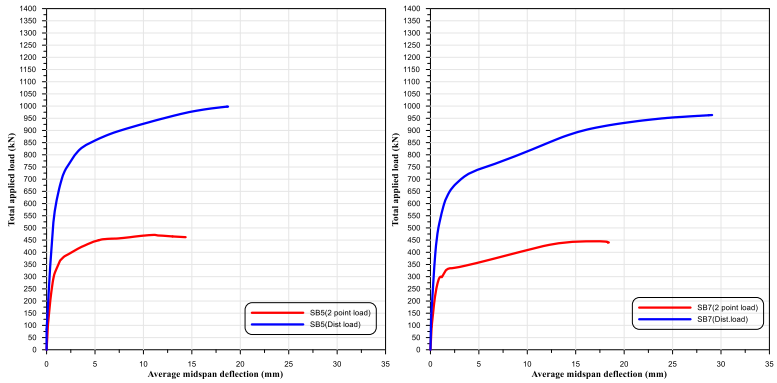

SB5 SB7

Continued Figure (5-10) Comparison between the responses of beams under concentrated two-point loads and the distributed loads

5.5.2 Moment Redistribution

Table (5-2) shows the numerical results of the moment capacity and moment redistribution ratio of the prestressed concrete continuous beams for different strengthening configurations under static uniformly distributed loads. The strengthened beams show large effects on the model response in respect of central support moment redistribution.

Table (5-2) Moment redistribution for all beams that tested numerically under uniformly distributed loads

Beam	P_u **(KN)**	**R (kN)**	**At central support(M-) (kN.m)**			**At mid span(M+) (kN.m)**		
			M_n	M_e	β	M_n	M_e	β
FB1	982.1	647.8	156.79	184.14	14.85	167.12	153.45	-8.91
FB3	1252.1	818.7	192.65	234.76	17.94	216.70	195.64	-10.76
FB5	1378.2	900.1	211.00	258.41	18.34	239.05	215.34	-11.01
FB7	1336.2	873.3	205.21	250.53	18.09	231.44	208.78	-10.85
M_e: Failure moment (elastic analysis) , M_n: Numerical failure moment R: Ultimate reaction of central support								

5.5.3 Toughness

Toughness values that are calculated depending on the area under load-deflection for the eight beams analyzed by ABAQUS under static uniform distributed loading system are explained in the Table (5-3). It is clear from the numerical results that toughness for beams under distributed loads improved by using precast SIFCON laminate in flexural strengthening prestressed beams and most cases of shear strengthening because the ductility of members increased.

Table (5-3) Toughness for beams that tested numerically under static uniformly distributed loads

Beam	Toughness (N.m)	%Increase over control beam
FB1	24392.294	-
FB3	29964.087	22.842
FB5	38373.258	57.317
FB7	37465.814	53.596
SB1	22456.618	-
SB3	29505.436	31.388
SB5	16362.285	-27.13
SB7	24427.049	8.774

5.6 The Influence of Using Higher Concrete Strength

In all previous studies, precast SIFCON laminates were used to strengthen beams made from the normal strength concrete, and in our present experimental work, we used high-strength concrete of more than (60Mpa) strength.The analysis with the ABAQUS tested the using a higher concrete strength of 80 Mpa to see the feasibility of strengthening methods to the higher concrete strength.

5.6.1 Load-Deflection Response

Through using the model that was simulated in the ABAQUS program, the effect of changing the used strength of concrete. Figures (5-11) display the comparison of the load-deflection response between the two used concrete types. According to FE analysis, the prestressed beam capacity will increase in most strengthened beams especially beams strengthening in the maximum shear region with the use of concrete strength (80Mpa) concrete. This increased reach (8.4%), (2.1%), (-0.9%), (-2.9%), (2.8%), (13.9%), (9.8%) and (9.9%) further increased in ultimate deflection reach (-18.6%), (-11.5%), (22.5%), (-4.1%), (1.4%), (55.3%), (29.7%) and (1.2%) for beams FB1, FB3, FB5, FB7, SB1, SB3, SB5 and SB7 respectively compared to the concrete strength used in experimental program. These results indicated that the used precast SIFCON laminates for strengthening the higher concrete strength for prestressed concrete beams are useful.

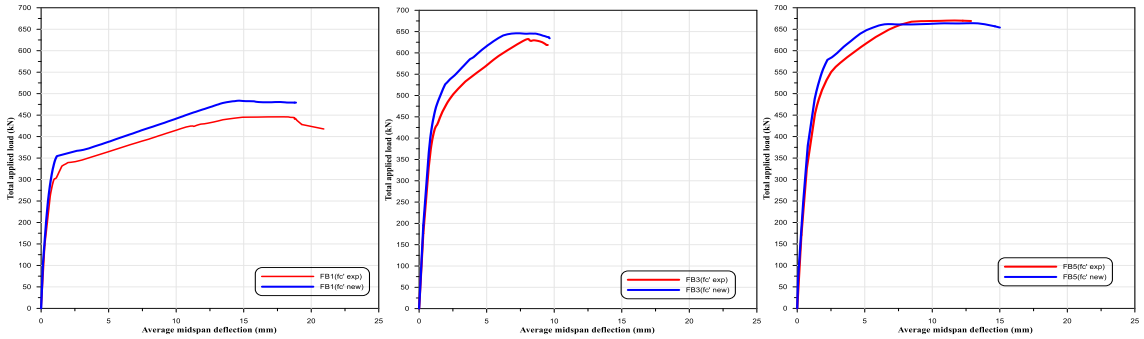

FB1 FB3 FB5

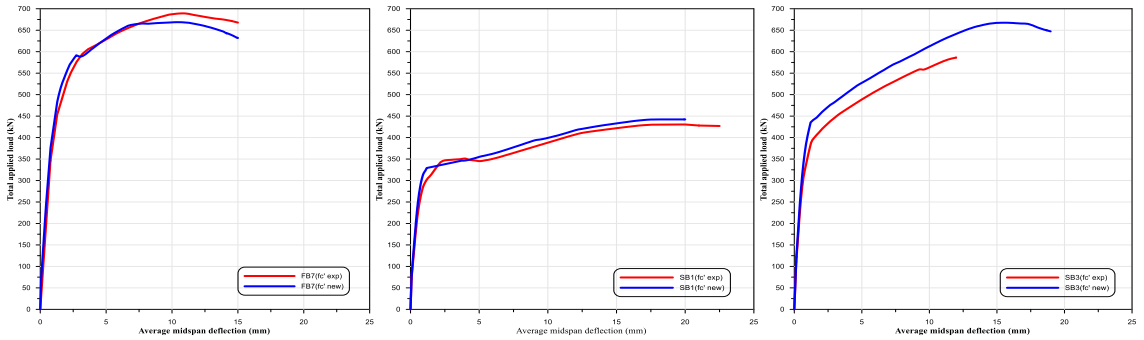

FB7 SB1 SB3

Figure (5-11) Effect of the concrete strength

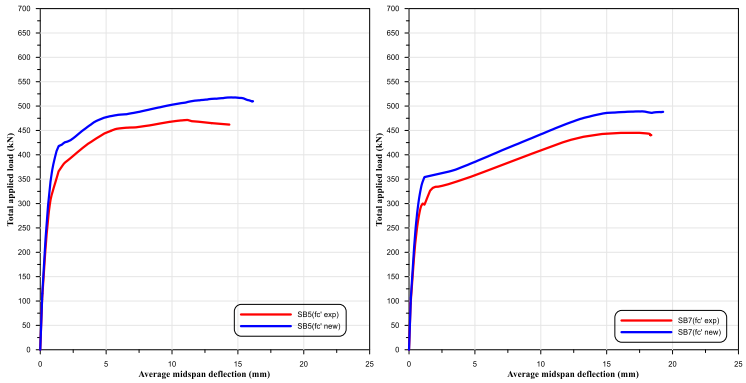

SB5 SB7

Continued Figure (5-11) Effect of the concrete strength

5.6.2 Moment redistribution

Table (5-4) shows the numerical results of the moment capacity and moment redistribution ratio of the prestressed concrete continuous beams using (80Mpa) concrete strength. The strengthened beams show effects on the model response in respect of central support moment redistribution.

Table (5-4) Moment redistribution for all beams

Beam	P_u **(KN)**	**R (kN)**	**At central support(M-) (kN.m)**			**At mid span(M+) (kN.m)**		
			M_n	M_e	β	M_n	M_e	β
FB1	483.6	328.1	86.26	90.69	4.88	77.79	75.57	-2.92
FB3	646.0	433.0	110.00	121.12	9.18	106.50	100.94	-5.51
FB5	664.0	444.8	112.81	124.51	9.39	109.61	103.76	-5.63
FB7	668.7	447.6	113.28	125.38	9.65	110.53	104.48	-5.79

M_e: Failure moment (elastic analysis)

M_n: Numerical failure moment

R: Ultimate reaction of central support

5.6.3 Toughness

It is clear from the numerical results that toughness for prestressed concrete beams using high strength concrete ($f_c' = 80\ Mpa$) improved by using anchorage end steel plate with precast SIFCON laminate in flexural strengthening prestressed beams and some cases of shear strengthening because the ductility of members increased.

Table (5-5) Toughness for beams use higher strength concrete

Beam	Toughness (N.m)	%Increase over control beam	Beam	Toughness (N.m)	%Increase over control beam
FB1	7968.871	-	SB1	7758.489	-2.640
FB3	5454.496	-31.552	SB3	10891.887	36.680
FB5	9201.185	15.464	SB5	7577.577	-4.910
FB7	9130.521	14.577	SB7	8188.414	2.755

5.7 The Effect of Different Level of Repeated Load

Through using the model that was simulated in the ABAQUS program, the effect of applied (0.75 P_u) of repeated loads for each beam at up to failure loading stage (after 20 cycles of loading and unloading).

Figures (5-12) display the comparison of the load-deflection response between the two used concrete types. The load decreased reach (10.5%), (4.1%), (5%), (5.4%), (8.1%), (4.2%), (3.9%) and (5.9 %) further increased in ultimate deflection reach (-15.9%), (44.5%), (29.2%), (2.5%), (-19.6%), (-0.6%), (23.7%) and (6.3 %) for beams FB1, FB3, FB5, FB7, SB1, SB3, SB5 and SB7 respectively.

From the results, it is clear that the ultimate flexural and shear strength is decreased by raising the level of repeated loads. The results also show the clear positive effect of using the precast SIFCON laminates in strengthening prestressed concrete beams by reducing the value of the deterioration in the

resistance of these beams when increasing the repeated loading rate compared to the reference beam.

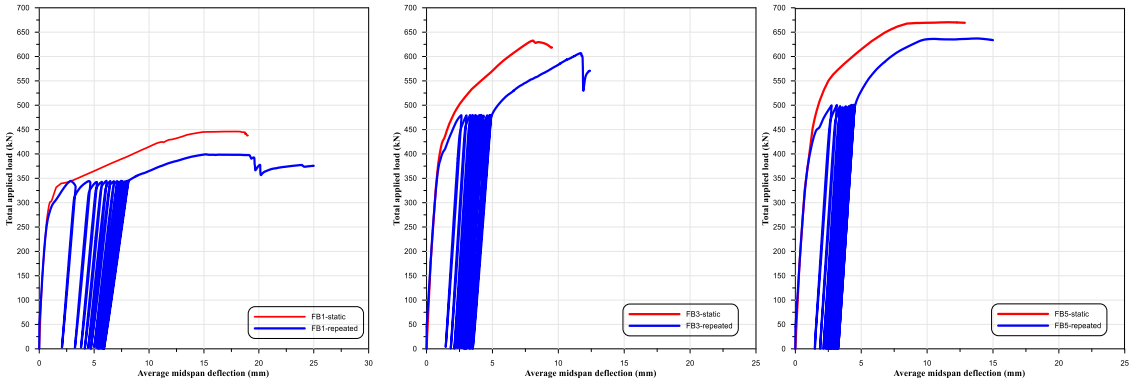

FB1 FB3 FB5

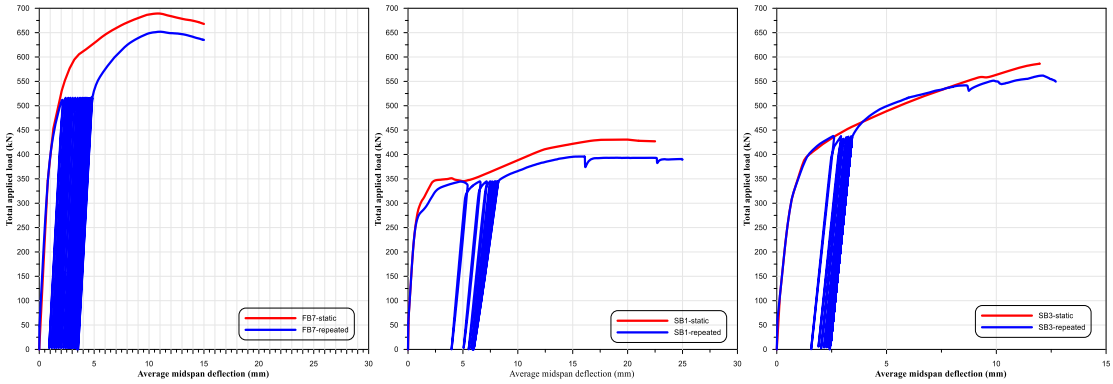

FB7 SB1 SB3

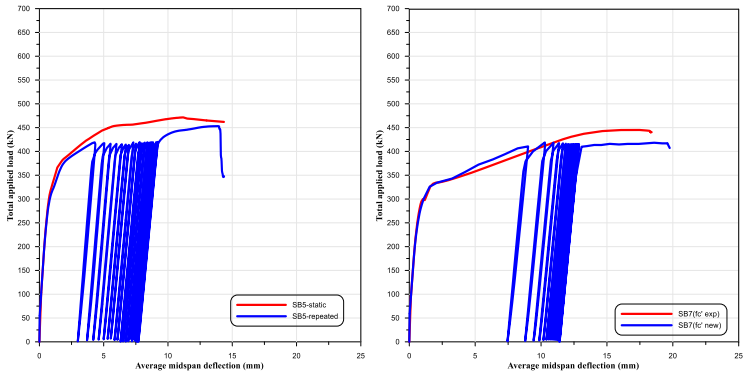

SB5 SB7

Figure (5-12) Comparison between the responses of beams with use different repeated loads level

CHAPTER SIX

CONCLUSIONS AND RECOMMENDATIONS

CHAPTER SIX

CONCLUSIONS AND RECOMMENDATIONS

6.1 General

In this chapter, the conclusions based on the experimental and numerical results of flexural and shear behavior of prestressed concrete continuous beam specimens strengthened with precast SIFCON laminates under the effect of monotonic static and repeated loading are presented. Recommendations for future works are also offered in this chapter.

6.2 Conclusions

In general, the following four sections the conclusions can be stated:

6.2.1 The Flexural Strengthening

The conclusions related to this group of beams can be summarized as follows:

- The results of the experimental study indicate that externally bonded precast SIFCON laminates bonding using epoxy resin can be used effectively to strengthen the prestressed concrete continuous beams. Where all laminate lengths glued by epoxy resin improved the flexure behavior of the tested beams. It is increasing the ultimate flexural load capacity of the test beams (36.9%-43.6%), Increasing the time for the first crack to appear and increasing the first cracking load between (56.1%-60%).
- The strengthening with precast SIFCON laminates bonded by using the epoxy resin method solved the sudden failure problem but resulted in independent failures in epoxy resin that was used to bind the laminates led to laminates end debonding.

- Regarding the effect of the length of laminates, an increase in flexural strength is achieved with the increase of the length of laminates in both the hogging and sagging regions comparison with the beams that strengthened with less length laminate as well as end debonding occurred with the laminates that have less length.
- It is advantageous to use the new proposed end anchorage systems: rectangular and U shape end-anchored steel plates especially U shape in order to prevent the end-debonding failure in the specimens strengthened by precast SIFCON laminates glued by epoxy resin had a major contribution in increasing the flexural capacity in the strengthened beam using the presented system.
- The two types of end-anchored steel plates can be used effectively to strengthen the continuous prestressed concrete beams. It positively affects by delayed the first crack appearance time, increasing the first cracking load between (97.8%-102.2%) and the ultimate load capacity of the tested continuous beams (52.4%- 57%) and prevent any separation at the ends of the SIFCON laminates from the surface of the beam, as well as increased toughness (33-38.5) %.
- The width of the cracks in both mid-span and central support regions for the strengthened beams is generally less than unstrengthened beams this indicates an improvement in crack behavior.
- Experimental results explained that the ultimate flexural load capacity for beams that are tested under repeated loads is a little reduced (0.86%-5.87%) compared with the strength of the same beams under monotonic static loading and increasing the maximum

deflection after ten cycles of repeated loading, increased about (8.4%-25.3%).

- It is clear that there is an improvement in moment redistribution with an increase in the laminate length and using the anchored steel plate. The strengthened beams with static loading conditions show significant growth in moment redistribution (9.1-10.6) % at the central support and (5.5-6.4) % at mid-span, respectively. The ratio for moment redistribution for the negative moments of the strengthened beams tested under repeated load increased by about (5-9.03%) compared with similar beams under static loading conditions.

6.2.2 The Shear Strengthening

The conclusions related to this group of beams can be summarized as follows:

- The results of the experimental study indicate that the use of precast SIFCON laminates as external reinforcement for prestressed concrete beams is a highly effective technique in increasing the beam shear capacity. It has also achieved a decrease in shear cracks during the loading process the cracks were wider and deeper.
- Strengthening the maximum shear regions with precast SIFCON laminates glued by epoxy resin led to improve the shear behavior the delay in first crack appearance time, increasing the first cracking load between (23.7% -105.7%), increased the ultimate shear load capacity of the tested beams about (10.3%-46.5%).

- An increase in shear strength is achieved with a full wrapping of laminates by comparison same strengthening pattern but has partial wrapping.
- Experimental results explained that the ultimate shear load capacity for beams that are tested under repeated loads is a little reduced (2.2%-3.8%), comparing with the strength of the same beams under monotonic static loading.
- The strengthening gives a good reduction in crack width especially strengthening full wrapping.

6.2.3 Common Conclusions of The Two Groups Tested Beams

- The manufacture of different shapes and the immense sizes of precast SIFCON laminates is not a complicated process. With prefabrication, the most crucial benefit comes from being able to customize its dimensions and thickness. Consequently, the criteria of excellence that guide behavior will be of the highest possible level. Compared to other techniques of strengthening, the cost is predicted to be lower with this option.
- Decrease in the value of strain capacity in concrete at central support and mid-span region in flexural and shear strengthened beams where the strengthened beams exhibited more rapid strain than the unstrengthened beams beam.
- The current study also showed the possibility of transforming a brittle failure mode to relatively ductile failure by changing precast SIFCON laminates arrangements and eventually failed after warning signs such as snapping sounds and peeling of the SIFCON with ample warnings before failure.

6.2.4 Numerical Analysis of Prestressed Concrete Beams

The following conclusions can be drawn from the results of this thesis' finite element analysis:

- The three-dimensional finite element model utilized in this research is able to simulate the prestressed concrete continuous beams strengthened with precast SIFCON laminates under monotonic static loading and repeated loading, the cracking loads, crack patterns, and ultimate loads predicted are close to those measured during the experimental testing.
- The moment redistribution for the reference beam and the strengthened beams by application distributed loads is more crucial than that obtained from the moment redistribution values when applied two-point loading.
- The precast SIFCON laminates can use with efficiency to strengthen the prestressed concrete beams that have a higher strength of concrete.
- The results show that the effect of increasing the repeated loading rate (20 cycles of 75% from the ultimate capacity and then loaded up to failure) led to decreasing the ultimate load capacity and increasing the deflection remarkably of most beams compared with the range used in experimental work.

6.3 Recommendations for Future Work

The following suggestions can be recommended for future works:

- Investigate the use of different sizes with different thicknesses of precast SIFCON laminates for strengthening prestressed concrete beams.

- Investigate the strengthening prestressed concrete beams under repeated loading of high load range such as between (40%) to (80%) of ultimate monotonic static loading.
- Studying the same types of tested specimens under reversal repeated loading (Load is exposed from up and from below) with different loading ranges.
- Strengthening different beam sections such as T, I, and box beam sections should be investigated under repeated loading.
- Additional tests series under realistic loading conditions should be performed the same as tested beams under distributed loads.
- Using precast SIFCON laminates to strengthening prestressed slabs at different locations.

CHAPTER SEVEN

REFERENCES

CHAPTER SEVEN

REFERENCES

[1] Afefy, Hamdy M., Khaled Sennah, and Antonio Cofini. "Retrofitting actual-size precracked precast prestressed concrete double-Tee girders using externally bonded CFRP sheets." Journal of Performance of Constructed Facilities 30.2 (2016): 04015020.

[2] Hussien, O. F., et al. "Behavior of bonded and unbonded prestressed normal and high strength concrete beams." HBRC journal 8.3 (2012): 239-251.

[3] Hameed, Dalya H., Shakir A. Salih, and Galib M. Habeeb. "Strengthening of concrete by using hybrid SIFCON sections." CEMENT WAPNO BETON 25.2 (2020): 115-126.

[4] Gilbert, Raymond Ian, and Neil C. Mickleborough. Design of prestressed concrete. CRC Press, 1990.

[5] Mahamid, Mustafa, et al. Structural engineering handbook. McGraw-Hill Education, 2020.

[6] Libby, James R. Modern prestressed concrete: design principles and construction methods. Springer Science & Business Media, 2012.

[7] Benaim, Robert. The design of prestressed concrete bridges: concepts and principles. CRC Press, 2007.

[8] Hassoun, M. N., and A. Al-Manaseer. "Structural Concrete theory and design, Jhon Wiley & Sons." (2008).

[9] Darwin, David, Charles William Dolan, and Arthur H. Nilson. Design of concrete structures. Vol. 2. New York, NY, USA:: McGraw-Hill Education, 2016.

[10] Varghese, P. C. Building materials. PHI Learning Pvt. Ltd., 2015.

[11] ACI Committee 363. Report on High-Strength Concrete (ACI 363R-10). ACI, 2010.

[12] Https://www.pondio.com/en/proyecto/4th-bridge-over-panama-canal, “4th bridge over Panama Canal - Pondio Ingenieros.” .

[13] Oukaili, Nazar K., and Mohammed M. Khattab. "Serviceability and ductility of partially prestressed concrete beams under limited cycles of repeated loading." GEOMATE Journal 17.60 (2019): 9-15.

[14] Khamees, Shahad S., Mohammed M. Kadhum, and Nameer A. Alwash. "Experimental and numerical investigation on the axial behavior of solid and hollow SIFCON columns." SN Applied Sciences 2.6 (2020): 1-15.

[15] Sampath, P., and P. Asha. "Forcasting on Mechanical Characteristics of Slurry Infiltrated Fibrous Concrete (SIFCON) using Math Cad." Journal of Critical Reviews 7.4 (2020): 1205-1213.

[16] Yazıcı, Halit, et al. "Improvement on SIFCON performance by fiber orientation and high-volume mineral admixtures." Journal of materials in civil engineering 22.11 (2010): 1093-1101.

[17] Šušteršič, J., and A. Zajc. "SIFCON with Latex Modified Cement Slurry Used for a Thin Overlay of a Bridge Deck." Restoration of Buildings and Monuments 18.3-4 (2012): 195-202.

[18] Kalfat, Robin, et al. "Post-tensioned concrete beams strengthened in shear using fiber-reinforced polymer laminates and patch anchors." Journal of Composites for Construction 24.2 (2020): 04019065.

[19] Reed, Calvin E., and Robert J. Peterman. "Evaluation of prestressed concrete girders strengthened with carbon fiber reinforced polymer sheets." Journal of Bridge Engineering 9.2 (2004): 185-192.

[20] Larson, Kyle H., Robert J. Peterman, and Hayder A. Rasheed. "Strength-fatigue behavior of fiber reinforced polymer strengthened prestressed concrete T-beams." Journal of Composites for Construction 9.4 (2005): 313-326.

[21] Kang, Thomas H-K., and Moustapha Ibrahim Ary. "Shear-strengthening of reinforced & prestressed concrete beams using FRP: Part II—Experimental investigation." International Journal of Concrete Structures and Materials 6.1 (2012): 49-57.

[22] Truong, Q. P. T., et al. "Flexural behavior of unbonded post-tensioned concrete T-beams externally bonded with CFRP sheets under static loading." International Conference on Advances in Computational Mechanics. Springer, Singapore, (2017).

[23] Mohamed Reda, Ramy Mostafa. "A State-of-the-Art Review: Side Near Surface Mounted (SNSM) Technique for Strengthening of RC Beams." The Egyptian International Journal of Engineering Sciences and Technology 31.Civil and Architectural Engineering (2020): 19-34.

[24] Ghasemi, Saeed, et al. "Sagging and hogging strengthening of continuous unbonded posttensioned HSC beams by NSM and EBR." Journal of Composites for Construction 20.2 (2016): 04015056.

[25] Kuntal, Vikas Singh, Maheswaran Chellapandian, and Shanmugam Suriya Prakash. "Efficient near surface mounted CFRP shear strengthening of high strength prestressed concrete beams–An experimental study." Composite Structures 180 (2017): 16-28.

[26] Obaydullah, M., et al. "Prestressing of NSM steel strands to enhance the structural performance of prestressed concrete beams." Construction and Building Materials 129 (2016): 289-301.

[27] Kwon, Seung-Jun, Keun-Hyeok Yang, and Ju-Hyun Mun. "Flexural tests on externally post-tensioned lightweight concrete beams." Engineering Structures 164 (2018): 128-140.

[28] Reza Aram, Mohammad, Christoph Czaderski, and Masoud Motavalli. "Effects of gradually anchored prestressed CFRP strips bonded on prestressed concrete beams." Journal of Composites for Construction 12.1 (2008): 25-34.

[29] A. A. Allawi, "Behavior of Strengthened Composite Prestressed Concrete Girders under Static and Repeated Loading," adv. Civ. Eng., vol. 2017, (2017).

[30] P. J. Hegger, "Shear Strengthening of Prestressed Concrete Beams Under Cyclic Loading With Textile Reinforced Concrete," no. July :1–8, (2013).

[31] V. Pino, A. Nanni, D. Arboleda, C. Roberts-Wollmann, and T. Cousins, "Repair of Damaged Prestressed Concrete Girders with FRP and FRCM Composites," *J. Compos. Constr.*, vol. 21, no. 3,: 04016111, (2017).

[32] Chang, Hong, and Wei Zhou. "Flexural behaviour of unbonded posttensioned concrete beam strengthened with aluminium alloy plates." Mathematical Problems in Engineering 2020 (2020).

[33] Kar, David R. Lan. "Properties, applications: Slurry infiltrated fiber concrete (SIFCON)." Concrete International 6.12 (1984): 44-47.

[34] Salih, Shakir, Qais Frayyeh, and Manolia Ali. "Fresh and some mechanical properties of sifcon containing silica fume." MATEC Web of Conferences. Vol. 162. EDP Sciences, (2018).

[35] Flaga, K. "Advances in materials applied in civil engineering." Journal of Materials Processing Technology 106.1-3 (2000): 173-183.

[36] Sonebi, Mohammed, Lucie Svermova, and Peter JM Bartos. "Factorial design of cement slurries containing limestone powder for self-consolidating slurry-infiltrated fiber concrete." Materials Journal 101.2 (2004): 136-145.

[37] Khamees, Shahad S., Mohammed M. Kadhum, and A. Alwash Nameer. "Effects of steel fibers geometry on the mechanical properties of SIFCON concrete." Civil Engineering Journal 6.1 (2020): 21-33.

[38] Tuyan, Murat, and Halit Yazıcı. "Pull-out behavior of single steel fiber from SIFCON matrix." Construction and Building Materials 35 (2012): 571-577.

[39] Manolia, A. A., A. S. Shakir, and J. F. Qais. "The effect of fiber and mortar type on the freezing and thawing resistance of Slurry Infiltrated Fiber Concrete (SIFCON)." IOP Conference Series: Materials Science and Engineering. Vol. 454. No. 1. IOP Publishing, 2018.

[40] A. Saeed and M Dawood , "Flexural Behavior of Reinforced Concrete Composite Continuous T-Beam with Hybrid Reinforcement under Repeated Load," Ph. D Thesis, civil engineering dep., university of babylon , Iraq 2019.

[41] Chun, Pang-jo, et al. "Experimental study on blast resistance of SIFCON." Journal of Advanced Concrete Technology 11.4 (2013): 144-150.

[42] Shannag, M. J., S. Barakat, and F. Jaber. "Structural repair of shear-deficient reinforced concrete beams using SIFCON." Magazine of Concrete Research 53.6 (2001): 391-403.

[43] Balamuralikrishnan, R. "Cyclic behavior of reinforced concrete beams retrofitted with externally bonded SIFCON laminates." Asian Journal of Civil Engineering 16 (2015): 1063-1075.

[44] Dhamak, Yogesh N., and Madhukar R. Wakchaure. "Use of precast SIFCON laminates for strengthening of RC beams." International Journal of Engineering and Computer Science 4.9 (2015): 14261-14266.

[45] Sandanshiv, Jitendra Nana, S. K. Dubey, and S. S. Bachhav. "Experimental Study on Retrofitted RC Beams with Externally Bonded SIFCON Laminates." International Journals on Advanced Research in Science Management and Technology 2.5 (2016): 1-10.

[46] Kumar and J. S. M. Sarathkumar, "Strengthening of RC Beam with Sifcon Laminates" IJSRD - International Journal for Scientific Research & Development 5.06, (2017) :389–395.

[47] Venkatesh, A., and K. Kannan. "Experimental Study of Glass Fiber Reinforced Concrete With Precast SIFCON Laminate." Int. J. Sci. Res. Civ. Eng 2.2 (2018): 16-19.

[48] Sisupalan, Aswathi, and Mathews M. Paul. "Strengthening of Rc And Frc Beams With Precast Sifcon Laminates-An Experimental Study." (2019): 4336–4342.

[49] Hameed, Dalya H., Shakir A. Salih, and Ghalib M. Habeeb. "Precast epoxy fasten SIFCON layers as a retorting material for defected concrete." AIP Conference Proceedings. Vol. 2213. No. 1. AIP Publishing LLC, 2020.

[50] S. A. S. Dalya Hekmat Hameed, "assessment the behaviour of hybrid secti ons of normal concrete and sifcon products," Ph. D Thesis, civil engineering dep., UOT, Iraq 2020.

[51] ACI 318, "318M–19: Building Code Requirements for Reinforced Concrete and Commentary", 2019.

[52] Wilden, H., and PCI Design Handbook. "Precast and Prestressed Concrete." PCI Design Handbook 7th ed., Prestressed Concrete Institute (2014).

[53] Iraqi Standard No. 5, “Iraqi Specification Standards IQS No.5, ‘Portland Cement,’ Central Agency for Standardization and Quality Control, Planning Council, Baghdad, IRAQ,(1984) :1–8.

[54] Ali, M. A. "Properties of slurry infiltrated fiber concrete (SIFCON), Ph. D Thesis, civil engineering dep., UOT, Iraq (2018).

[55] ASTM “Standard Test Method for Sieve Analysis of Fine and Coarse Aggregates,” (2014).

[56] “Iraqi Specification Standards IQS No.45, "Aggregate from Natural Sources for Concrete and Construction, Baghdad, IRAQ, (1984).

[57] ASTM C 1240/C 1240M - 05, “Standard Specification for Silica Fume Used in Cementitious Mixtures,” 2005.

[58] ASTM, “Standard Specification for Coal Fly Ash and Raw or Calcined Natural Pozzolan for Use,” (2010).

[59] ASTM, “A820 Standard Specification for Steel Fibers for Fiber-Reinforced Concrete,”, vol. 98, October 2011.

[60] S. Specification, “Standard Specification for Steel Strand , Uncoated Seven-Wire for Prestressed,” (2012)

[61] S. Specification, “Standard Specification for Steel Welded Wire Reinforcement , Plain , for Concrete 1,” February (2002).

[62] American Concrete Institute, 355.2-07 Qualification of Post-Installed Mechanical Anchors in Concrete & Commentary (2007).

[63] ACI Committee 211, “ACI 211.4R-08: Guide for Selecting Proportions for High-strength Concrete Using Portland Cement and Other Cementitious Materials,” (2008).

[64] ASTM,, “Standard Test Method for Slump of Sealants 1, (2014).

[65] ASTM, “C1437 - Standard test method for flow of hydraulic cement mortar,” *ASTM Int.*(2013).

[66] A. Koksal, “Bs 1881-116:1983,” *Constr. Stand.*,(2010).

[67] ASTM “Standard Test Method For Splitting Tensile Strength Of Cylindrical Concrete Specimens,” (2012).

[68] ASTM, “Standard Test Method for Flexural Strength of Concrete (Using Simple Beam with Third-Point Loading),” *Hand*, vol. C78-02, (2010).

[69] Manolia Ali, Shakir Salihو Properties of Slurry Infiltrated Fiber Concrete (SIFCON), ” Ph. D Thesis, civil engineering dep., UOT, Iraq 2018.

[70] Maghsoudi, A. A., and H. Akbarzadeh Bengar. "Moment redistribution and ductility of RHSC continuous beams strengthened with CFRP." Turkish Journal of Engineering and Environmental Sciences 33.1 (2009): 45-59.

[71]ABAQUS, “Abaqus 6.14,” *Abaqus 6.14 Anal. User’s Guid.*, 2014.

[72] Shahrokh Esfahani, Marjan, and Rasoul Nilforoush Hamedani. "Numerical Evaluation of Structural Behavior of the Simply Supported FRP-RC Beams." (2012).

[73] Ahmed, Ali. "Modeling of a reinforced concrete beam subjected to impact vibration using ABAQUS." International Journal of Civil & Structural Engineering 4.3 (2014): 227-236.

[74] Eriksson, D., and T. Gasch. "FEM-modeling of reinforced concrete and verification of the concrete material models available in ABAQUS." Royal Institute of Technology, Department of Mechanics: Stockholm, Sweden (2010).

[75] Lee, Seong-Cheol, Joung-Hwan Oh, and Jae-Yeol Cho. "Compressive behavior of fiber-reinforced concrete with end-hooked steel fibers." Materials 8.4 (2015): 1442-1458.

[76] Hillerborg, Arne. "The theoretical basis of a method to determine the fracture energyG F of concrete." Materials and structures 18.4 (1985): 291-296.

[77] Iyengar, KT Sundara Raja. "Two-dimensional theories of anchorage zone stresses in post-tensioned prestressed beams." Journal Proceedings. Vol. 59. No. 10. 1962.

[78] M. H. N. Al-Mamoori and N. A. Alwash, "Structural Behavior of Highly Strength Reinforced Concrete Beams with Elliptical Arched Bottom,"Ph. D Thesis, civil engineering dep., babylon university, Iraq 2020.

[79] Malm, Richard. Shear cracks in concrete structures subjected to in-plane stresses. Diss. KTH, 2006.

[80] Obaidat, YASMEEN TALEB. "Structural retrofitting of concrete beams using FRP." Department of Construction Sciences, Structural Mechanics, Lund University, Lund, Sweden (2011).

[81] B. S. Anthony J. Wolanski, "Finite Element Analysis of Reinforced Concrete and Steel Fiber," May, 2018.

[82] A. J. Wolanski, "Flexural Behavior Of Reinforced And Prestressed Concrete Beams Using Finite Element Analysis," *Ph.D. Thesis, Marquette Univ.*, (2004) :352

APPENDIX (A)

Appendix (A)

Design of Continuous Unbonded Post-Tensioned Prestressed Concrete Beam

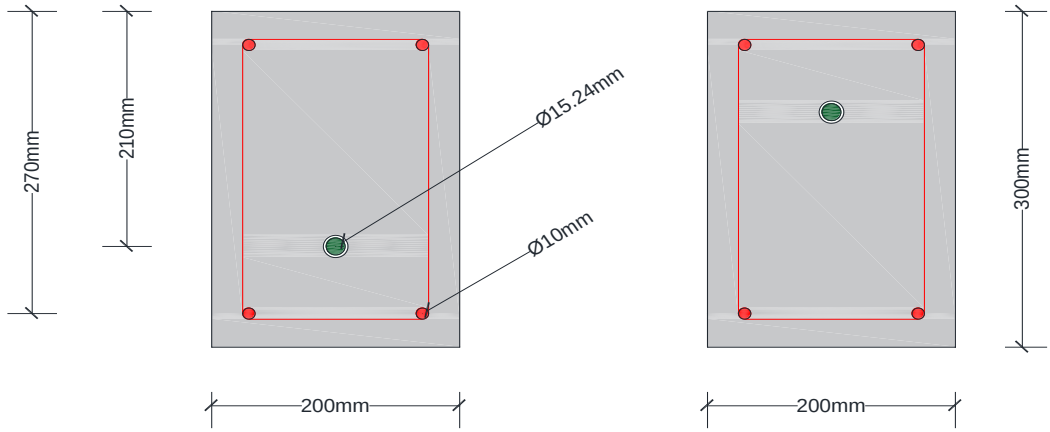

a- Beam section of sagging region b - Beam section of hogging region

Figure (A.1) Specimen Dimensions Rectangular Cross-Section

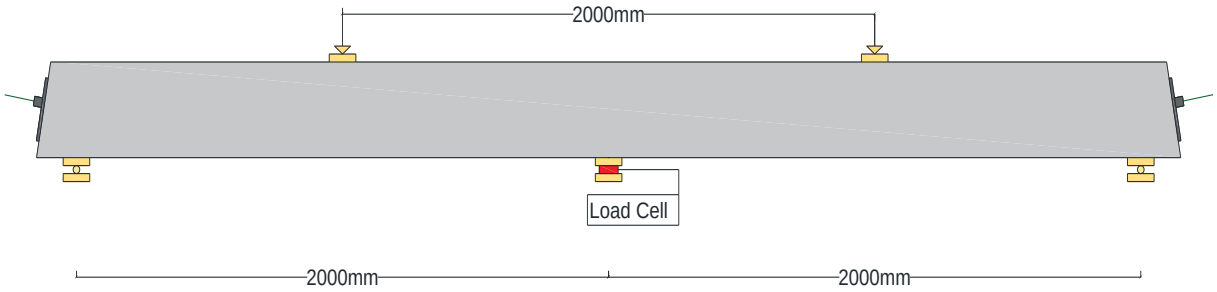

Figure (A-2) Geometry of Test Beam Test Setup, Supports and Load Application

Dimensions

L(length)=4300 mm, b=200 mm (width), h=300 mm (hight), $C_1 = C_2 = 150\ mm$,$A_g = bh = 60 \times 10^3 mm^2$, $I_g = {bh^3}/{12} = 4.5 \times 10^8 mm^4$

,$r^2 = {I_g}/{A_g} = 7500\ mm^2$, S=I/C=32× $10^5 mm^3$

$W_g = \gamma bh = 1.44\, {kN}/{m}$, $M_g = {wl^2}/{8}$=0.72 kN.m

$d'_s = 40\ mm$, $d_s = 260\ mm$, $d_p = 210\ mm$, $e_{max} = 60\ mm$

Ordinary Steel Reinforcement

2Φ10 mm @top and bottom

$A_s = A'_s = 157\ mm^2$, $f_{y=}$570 Mpa, E_s =2× $10^5\ Mpa$

Concrete Properties

$use\ f'_c = 0.8\ f_{cu} = 60\ MPa$, E_c=3320$\sqrt{f'_c}$+6900=32616.6 ${N}/{mm^2}$

$n_p = {E_p}/{E_c}$=6.06 , $n_s = {E_s}/{E_c} = 6.13$

Restressing Steel

Low relaxation seven wire 270 ksi, Diameter=15.24 mm, plastic duct dim 20mm

$f_{pu} = 1895\ Mpa$, $f_{py} = 1737\ Mpa$, $E_p = 197900 Mpa$, $A_{ps} = 141.31\ mm^2$

Check duct hole effectivity in beam section

$A_g = 200 * 300 = 60000\ mm^2$

$A_{hole} = 314.159\ mm^2$

${A_{hole}}/{A_g}$ =× 100% → 0.8% < 5%

$\therefore\ duct\ hole\ is\ not\ effective$

Prestressing Force

Prestressing Level 0.55 f_{pu}

$f_{pj} = 0.55 \times 1895 = 1042.25\ Mpa$

, Jacking force p_j=147.28 KN

At transfer assume 10% losses

$f_{pi} = 0.9 \times 0.55 \times 1895 = 938\ Mpa$

p_i=132.6 KN

At service assume 20 % losses

$f_{se} = 0.8 \times 0.55 \times 1895 = 833.8\ Mpa$

$p_e = 117.8\ kN$

The ram area of single -pull juck=42 cm

Jack pressure =$\frac{prestressing\ \ force}{ram\ area} = \frac{147.28 \times 100 kgf}{42\ cm}$=350.6 bar

Design of flexural reinforcement

$f_{se} = 833.8\ Mpa < 0.5\ f_{pu} = 947.5$ Mpa

Determine $f_{ps}\ by\ strain\ compatibility$

Step 1 calculate the initial prestressing strain $\varepsilon_{pe} = \varepsilon_1$

$\varepsilon_{pe} = \frac{f_{se}}{E_p} = \frac{833.8}{197900}$ =0.004213

Step 2 calculate the decompression strain $\varepsilon_{ce} = \varepsilon_2$

$$\varepsilon_{ce} = \frac{p_e}{A \times E_c}\left[1 + \frac{e^2}{r^2}\right]$$

$\varepsilon_{ce} = 0.000087$

Assume f_{ps}=1447.95 Mpa

ε_{ps}=*0.00736*

$a = \frac{A_{ps}f_{ps}+A_s f_y}{0.85\, f_c' b}$ =27.454

$\beta_1 = 0.728$ $ACI318-19$

C=42.238

ε_3 =$\varepsilon_c(\frac{d-c}{c})$=0.0119>0.005

The total strain =0.0161>0.00736

For the 2nd trial

$a = 30.3$,C=46.6,ε_3 =0.0105

ε_{ps}=$0.0147 > 0.0105$

3rd trail

ε_{ps}=0.009,a=31.29,C=48.1, ε_3 =0.01

ε_{ps}=0.01$\cong 0.009\ ok$

since C<3d ignore compression reinforcement in calculation of moment capacity

According to ACI 318-19 the member in tension controlled ε_t>0.005

Mn=$A_{ps}f_{ps}\left(d_p + \frac{a}{2}\right) + A_s f_y\left(d + \frac{a}{2}\right)$

Mn=65.76 KN.m

Moment due to self-weight =0.72 KN.m

Mn=65.76-0.72=65.04 KN.m

Mn=$\frac{3PL}{16}$ → P=173.4KN

Total applied load= 346.8 KN

$V_n = \frac{11P}{16} + \frac{5wl}{8}$=121.01KN

Design of shear reinforcement

V_u =0.75V_n=90.7 KN

$M_u = 0.9Mn$=58.5 KN

$\lambda = 1(\ for\ normal\ weight\ concrete)$

$f_{pe} > 0.4f_{pu}$

$\therefore\ use\ ACI\ alternative\ design\ method$

$V_c = bd_b\left[0.6\lambda\sqrt{f_c'} + 700\frac{V_u d_p}{M_u}\right]$=102.28KN

$\frac{V_u d_p}{M_u} < 1$ → 0.373 < 1 OK

$V_c \geq 2\ \lambda\sqrt{f_c'}bd_p$ → 102.28 > 53.4685 OK

$V_c \leq 5\ \lambda\sqrt{f_c'}bd_p$ → 102.28 < 133.67 OK

$V_u/_{\emptyset} \leq {}^{V_c}/_2 \rightarrow 121.01 > 51.14$ *hence steel is needed*

$V_u/_{\emptyset} \leq V_c \rightarrow 121.01 > 102.28$

$V_s = \frac{V_u}{\emptyset}$ -V_c=18.73 KN

$V_s > 8\ \lambda\sqrt{f_c'}bd_p$ →18.73< 213.87 ∴ *minimum web steel*

Min $\frac{A_v}{s} = \frac{A_{ps}f_{pu}}{80f_y d_p}\sqrt{\frac{d_p}{b}}$

Min $\frac{A_v}{s} = 0.001249$ *Smaller control*

And Min $\frac{A_v}{s} = \frac{50b}{f_y}$=.005714

or Min $\frac{A_v}{s} = 0.75\sqrt{f_c'}\frac{b}{f_y}$=0.006925

$\frac{A_v}{s} = \frac{V_u/_{\emptyset} - V_c}{f_y d_p} \geq \text{Min}\frac{A_v}{s} \rightarrow 0.0054 > \text{Min}\frac{A_v}{s}$ ok

Then the minimum required web shear steel

Min $\frac{A_v}{s} \rightarrow 0.0054$

Use stirrups $\emptyset$ 10 mm

$A_v = 2 * 78.5 = 157.01$ mm^2

S$\leq 0.75h(225) \leq 600 \geq min\ s\ req$

Use stirrups $\emptyset$ 10 mm@200 mm c/c for ensure flexure failure increase spacing to 100mm

Design of Anchorage zone

d_{burst}=0.5(h-e_{anc})=0.5(300-2*0) =150 mm

$P_{pu} = 1.2(0.55f_{pu})A_{ps}$=176.7KN

$$T_{burst} = 0.25P_{pu}\left(1 - \frac{h_{anc}}{h}\right) = 0.25 * 176.7\left(1 - \frac{30}{300}\right) = 39.8\ KN$$

The area of steel needed to resistance T_{burst} is:

$min\ A_s = \frac{T_{burst}}{\emptyset f_y}$=95.41 mm^2

∴Use ∅10 closed stirrups for the end zone

Bearing plate at end block

$$f_{br} = \frac{P_j}{A_{br}}$$

Assume area of bearing plate to be (200*200) mm thickness 10 mm

$A_{br} = 200 * 200 = 40000$ mm^2

$f_{br} = \frac{147.28*10^3}{40000}$=3.68 Mpa

$A_g = 200 * 300 = 60000$ mm^2

$f_{br)all} = 0.48 f_{ci}\sqrt{\frac{A_g}{A_{br}}} \leq 0.8 f_{ci}$

$f_{br)all}$ =35.27Mpa <48 Mpa

$f_{br} < f_{br)all}$

Ok we can use this plate

Transformed section

$A_t = (n_s - 1)A_s + (n_{ps} - 1)A_{ps} + A_c$=62659.5 mm^2

$y_t = \frac{(n_s-1)A_s d_s+(n_{ps}-1)A_{ps} d_p+(n'_s-1)A'_s d'_s+bh*0.5h}{(n_s-1)A_s+(n_{ps}-1)A_{ps}+(n'_s-1)A'_s+bh}$ =150.8 mm

$$I_t = \frac{by^3}{3} + \frac{b(h-y)^3}{3} + (n_s - 1)A_s(d_s - y)^2 + (n_{ps} - 1)A_{ps}(d - y)^2 + (n'_s - 1)A'_s(y - d'_s)^2$$

$I_t = 5.08 * 10^8\ mm^4$

e =59.2 mm

$C_t = 150.8\ mm$,$C_b = 149.2\ mm$

Find C-line by Superposition Method

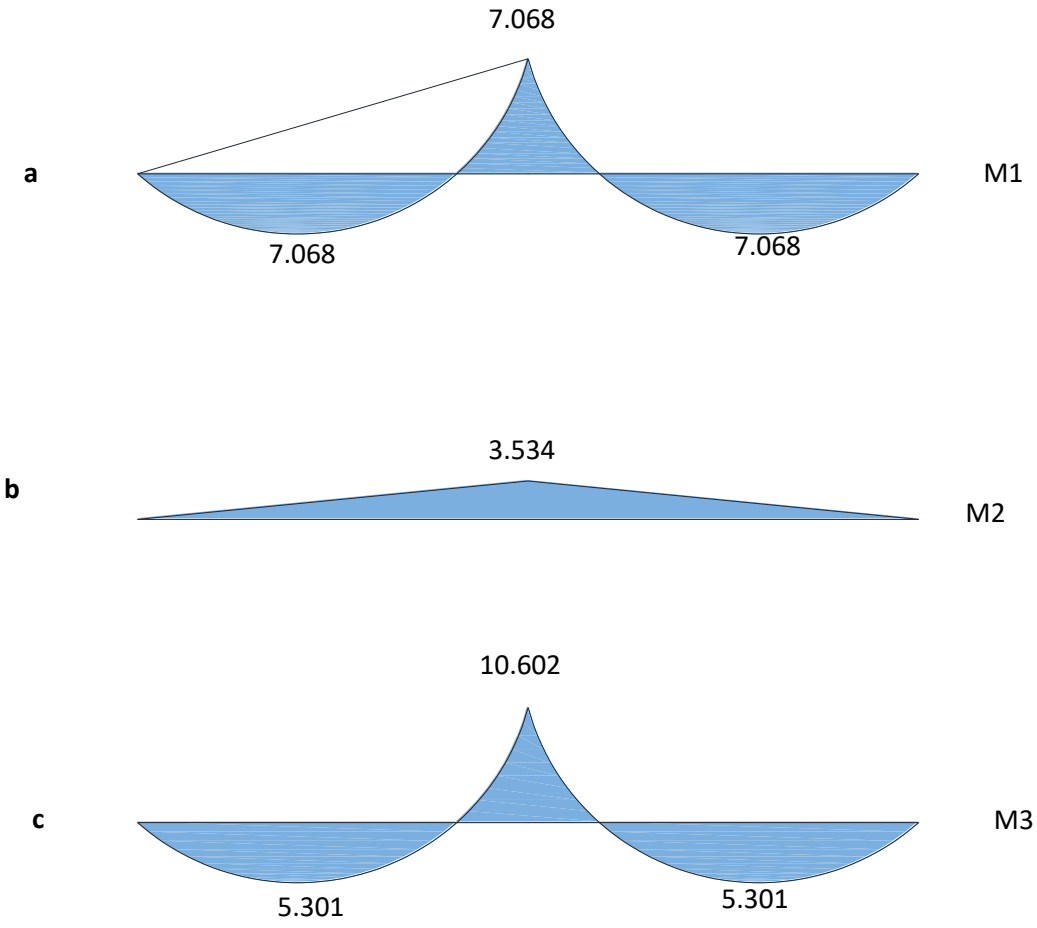

Figure (A-1) a-primary moments M1, b-secondary moments M2, c-total moments M3=M1+M2

At mid span

$M_1 = P_e * e$ =7.068 KN.m

At central support

M_1=7.068 KN.m

$$d_p = \frac{1}{EI}\left[\left(\frac{2}{3}\times 2\times 10.602\times\frac{1}{2}\times 2\right)-\left(\frac{1}{2}\times 2\times 7.068\times\frac{2}{3}\times 2\right)\right]$$

$\frac{1}{EI}(4.712)$up ward

$d_p = \frac{1}{EI}\left[\left(\frac{1}{2}\times 2\times R_b\times\frac{2}{3}\times 2\right)\right]=\frac{1}{EI}(1.333R_b)$

$R_b = 3.534KN$

$$e^* = \frac{M_T}{P_e}$$

@Mid span

$$e^* = \frac{5.301}{117.8} = 45\ mm$$

@ Central support

$$e^* = \frac{10.602}{117.8} = 90mm$$

Top and bottom concrete fiber stresses at transfer

At initial stage

$P_i = 0.9 * 0.55 * 1895 * 141.31 * 10^{-3} = 132.5\ KN$

$f_{top} = -\frac{P_i}{A_t}\left(1-\frac{e^* c_t}{r^2}\right)$= - 6.183 Mpa

At support<0.7f_{ci}=-42 Mpa ok

All location<0.6f_{ci}=-36 Mpa ok

$f_{bot} = -\frac{P_i}{A_t}\left(1+\frac{e^* c_b}{r^2}\right)$=1.766Mpa

<0.25$\sqrt{f_c'}$=1.936 Mpa ok

<0. 5$\sqrt{f_c'}$=3.873 Mpa ok

After all losses

$P_e = 0.8 * 0.55 * 1895 * 141.31 * 10^{-3} = 117.8\ KN$

$f_{top} = -\frac{P_e}{A_t}\left(1 - \frac{e^* c_t}{r^2}\right)$=-5.497 Mpa

<0.6f_c'=-36 Mpa ok

$f_{bot} = -\frac{P_e}{A_t}\left(1 + \frac{e^* c_b}{r^2}\right)$=1.57Mpa

<0.62$\sqrt{f_c'}$=4.8 Mpa ok

Check with self-weight @initial

$f_{top} = -\frac{P_i}{A_t}\left(1 + \frac{e^* c_t}{r^2}\right) - \frac{M_g}{S_t}$=-6.408Mpa

<0.6f_{ci}=-36 Mpa ok

$f_{bot} = -\frac{P_i}{A_t}\left(1 + \frac{e^* c_b}{r^2}\right) + \frac{M_g}{S_b}$=1.900Mpa

<0.25$\sqrt{f_c'}$=1.936 Mpa ok

Check with self-weight after losses

$f_{top} = -\frac{P_e}{A_t}\left(1 + \frac{e^* c_t}{r^2}\right) - \frac{M_g}{S_t}$=-5.722Mpa

<0.6f_{ci}=-36 Mpa ok

$f_{bot} = -\frac{P_e}{A_t}\left(1 + \frac{e^* c_b}{r^2}\right) + \frac{M_g}{S_b}$=1.795 Mpa

<0.25$\sqrt{f_c'}$=1.936 Mpa ok

LOSSES OF PRESTRESS

Immediate Losses

a-anchorage slip

b-wobble and curvature friction

c-elastic shortening

Time Dependent Losses

a-creep

b-shrinkage

c-relaxation

For Post Tension Member

$\Delta f_{P\,T} = \Delta f_{P\,A} + \Delta f_{P\,es} + \Delta f_{P\,f} + \Delta f_{P\,sh} + \Delta f_{P\,cr} + \Delta f_{P\,R}$

$\Delta f_{P\,T}$ total losses

$\Delta f_{P\,A}$ anchorage slip losses

$\Delta f_{P\,es}$ elastic shortening losses

$\Delta f_{P\,f}$ wobble and curvature friction losses

$\Delta f_{P\,sh}$ shrinkage losses

$\Delta f_{P\,cr}$ creep losses

$\Delta f_{P\,R}$ steek relaxation losses

Anchorage Slip Losses

$\Delta f_{P\,A} = 0$

Due the wobble and curvature are small the slip effect is confined to the region close to the jacking anchorage.

It will be assumed the slip effect doesn't propagate.

Wobble And Curvature Friction

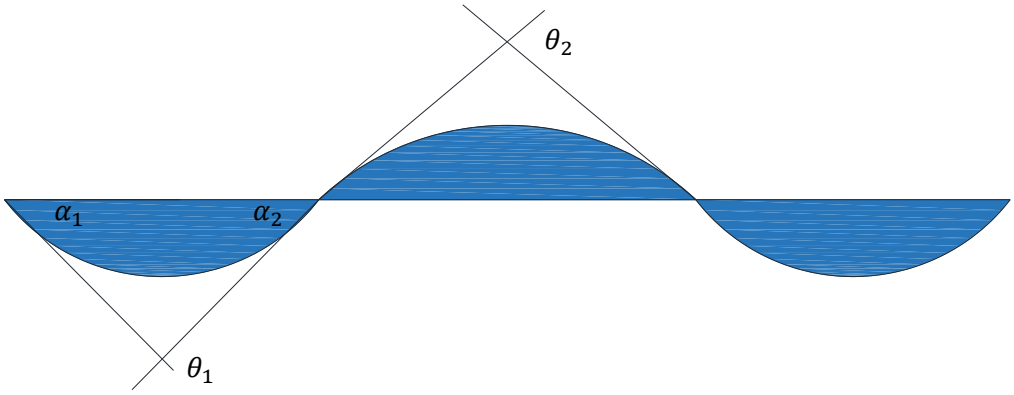

$m \cong 1.5\, y$

$\alpha_1 = 0.09\, rad$

$\alpha_2 = 0.19\, rad$

$\theta_1 = 0.28\, rad$

$m \cong 2\, y$

$\theta_2 = 0.22\, rad$

Wobble coefficient (k) parameter

K=0.0016

Curvature coefficient (μ)=0.15

(kl+$\mu\alpha$)1,3 =0.0016*1.455+0.15*0.28

$= 0.044 < 0.3\ ok$

(kl+$\mu\alpha$)2 =0.0016*1.455+0.15*0.22

$= 0.034 < 0.3\ ok$

f_{pj}=1024.25 Mpa

Δf_{p1}=1024.25*0.0044=45.067 Mpa

f_{p1}=1024.25-45.067=979.183 Mpa

Δf_{p2}=979.183 *0.034=33.292 Mpa

f_{p2}=979.183 -33.292=945.891 Mpa

Δf_{p3}=945.891 *0.044=41.619 Mpa

f_{p3}=945.891-41.619=904.272 Mpa

To next step f_{pi}=904.272Mpa

Elastic Shortening

Here only one tendon there is no loss

$\Delta f_{P\ es} = 0$

Creep losses

Pi=f_{pi} ∗Aps=904.272*141.31/1000

=127.782 KN

$f_{cs} = -\frac{P_i}{A}\left(1 + \frac{e^2}{r^2}\right) + \frac{M_g}{I} * e$=-3.056

$\Delta f_{P\ cr} = fcs * np * kcr$

Kcr=1.6 for post tensioned member

Np= modular ratio=6.784

$\Delta f_{P\ r} = 33.171\ Mpa$

Shrinkage losses

$\Delta f_{P\,sh} = \varepsilon_{sh} * E_p$=200*$10^{-6} * 1979$

$\Delta f_{P\,sh} = 39.58\ Mpa$

Steel relaxation losses

$$\Delta f_{P\,R} = f_{pi}\frac{\log t}{k}\left(\frac{fpi}{fpy} - 0.55\right) = 1.178\ Mpa$$

Summary of stresses

Type	Stress
Anchorage slip	0
Friction	119.978
Elastic shortening	0
Shrinkage	39.58
Creep	33.171
relaxtion	1.178
Total of Immediate Losses	119.978
Total of Time Dependent Losses	74.038
Total losses	194.016
Stress before losses	1024
Stress after losses	829.984
% Losses	18.946%

Where:

p_j $Jacking\ prestressing\ force$

p_i $Initial\ prestressing\ force$

f_{pu} $Ultimate\ stress\ of\ strand$

A_{ps} $Prestressing\ steel\ area$

r $Raduis\ of\ gyration$

f_{se} $Effective\ prestressing\ stress$

f_{pi} $Initial\ prestressing\ stress$

APPENDIX (B)

Appendix (B)

Summary of Material

B-1 Cement Properties

Table (B-1) Chemical Physical Properties of the Cement

Chemical Requirements		Testing method	Limitation	Test result
Sulfate content SO_3	%	IQ 472/1993 BS EN 196-2/2013	2.5 if $C_3A \leq 3.5$ 2.8 if $C_3A \geq 3.5$	2.38
Magnesium oxide MgO	%		≤ 5.0	1.77
Chloride content	%		≤ 0.1	0.02
Physical and mechanical Requirements			Limitation	Test result
Finesse	m^2/kg	IQ 198/1990 BS EN 196-3/2016	Not specified	395
Initial setting time	min		≥ 45	150
Final setting time	hr.		≤ 10	3.27
Soundness Le chatlie	2d		≤ 10	0.68
Compressive strength is not less than (N/mm^2)	28 d	BS EN 196-1/2016	≥ 20	25.3
			≥ 42.5	53.9

B-2Fine Aggregates Properties

Table (B-2) Sieve Analysis of Fine Aggregates

Sieve Size (mm)	% Passing by Weight	Limits of the Iraqi Specification No.45/1984 (zone 2)
9.5	100	100
4.75	99	90-100
2.36	83	75-100
1.18	70	55-90
0.60	58	35-59
0.30	26	8-30
0.15	5	0-10

Table (B-3) Physical and Chemical Properties of the Fine Aggregates

Physical Properties	Test Results	Limits of the Iraqi Specification No.45/1984
Specific gravity	2.1	≤5
Sulfate content	0.1 %	≤ 0.50 %
Absorption	0.75 %	-

B-3 Coarse Aggregates Properties

Table (B-4) Sieve Analysis of Coarse Aggregates

Sieve Size(mm)	Passing%	Limits of Iraqi Specification No.45/1984
37.5	100	100
19	88	95-100
9.5	21	30-60
4.75	1	0-10

Table (B-5) Physical Properties and Sulfate Content of Course Aggregates

Physical Properties	Test Results	Limits of the Iraqi SpecificationNo.45/1984
Specific gravity	0.16	-
Sulfate content	0.022	≤ 0.1 %

B-4 The Manufacture Company Catalogue of Silica Fume

Construction Chemicals

MegaAdd MS(D)

Densified Microsilica

DESCRIPTION

MegaAdd MS(D) is a very fine pozzolanic, ready to use high performance mineral additive for use in concrete. It acts physically to optimize particle packing of the concrete or mortar mixture and chemically as a highly reactive pozzolan.

MegaAdd MS(D) in contact with water, goes into solution within an hour. The silica in solution forms an amorphous silica rich, calcium poor gel on the surface of the silica fume particles and agglomerates. After time the silica rich calcium poor coating dissolves and the agglomerates of silica fume react with free lime ($CaOH_2$) to form calcium silicate hydrates (CSH). This is the pozzolanic reaction in cementitious system.

STANDARDS

ASTM C1240

USES

MegaAdd MS(D) can be used in a variety of applications such as concrete, grouts, mortars, fibre cement products, refractory, oil/gas well cements, ceramics, elastomer, polymer applications and all cement related products.

ADVANTAGES

- High to ultra high strength
- High resistance to chlorides and sulfates
- Protection against corrosion
- Increased durability, longer service life for structures
- Enhanced rheology, control of mixture segregation and bleed
- Greater resistance to chemicals

TYPICAL PROPERTIES at 25°C

PROPERTY	TEST METHOD	VALUE
State	Amorphous	Sub-micron powder
Colour	-	Grey to medium grey powder
Specific Gravity	-	2.10 to 2.40
Bulk Density	-	500 to 700 kg/m^3
Chemical Requirements		
Silicon Dioxide (SiO_2)	-	Minimum 85%
Moisture Content (H_2O)	-	Maximum 3%
Loss on Ignition (LOI)	-	Maximum 6%
Physical Requirements		
Specifi Surface Area	-	Minimum 15 m^2/g
Pozzolanic Activity Index, 7 days	-	Maximum 105% of control
Over size particles retained on 45 micron sieve	-	Maximum 10%

COMPATIBILITY

MegaAdd MS(D) is suitable for use with all types of cement and cementitious materials.

With Admixtures :

MegaAdd MS(D) is compatible to use with all types of water reducing plasticisers / superplasticisers and poly carboxylate based superplasticiser.

DOSAGE

The normal dosage of **MegaAdd MS(D)** is 5 - 8% by weight of cement, but it can be used up to 10%. Site trials should be carried out to establish the optimum dosage for the mix to be used as the dosage varies depending on application.

CC/MAPDS08/Ver1/11/15 1/2 Technical Datasheet

Construction Chemicals

MegaAdd MS(D)

BATCHING	Batch **MegaAdd MS(D)** into the concrete mixer and mix thoroughly with the other mixture ingredients, adopting a procedure that ensures full dispersion of the product.	
PACK SIZE	600 Kgs and 1200 Kgs Jumbo bags	
GENERAL INFORMATION	**Shelf Life**	12 months from date of manufacture when stored under warehouse conditions in original unopened packing. Extreme temperature / humidity may reduce shelf life.
	Cleaning	Clean all equipments and tools with water immediately after use.
HEALTH and SAFETY	**PPE's**	Gloves, goggles and suitable mask must be worn.
	Precautions	Contact with skin, eyes, etc. must be avoided.
	Hazard	Regarded as non-hazardous for transportation.
	Disposal	Do not reuse bags. To be disposed off as per local rules and regulations.
	Additional Information	Refer MSDS. (Available on request.)
TECHNICAL SERVICE	**CONMIX Technical Services** are available on request for onsite support to assist in the correct use of its products.	

MSASA
Construction Solutions for Africa

CAPE TOWN
Tel: +27 (0)87 231 0253
Unit 5 | M5 Freeway Park
Upper Camp Rd | Maitland | 7405
Cape Town | South Africa

JOHANNESBURG
Tel: +27 (0)82 785 8529
64 Maple Street | Pomona
Kempton Park | Johannesburg | 1619
South Africa

Email: info@msasa.co.za | www.msasa.co.za

Manufacturer:
CONMIX LTD.
P.O. Box 5936, Sharjah
United Arab Emirates
Tel: +971 6 5314155
Fax: +971 6 5314332
Email: conmix@conmix.com

Sales Office:
Tel: +971 6 5682422
Fax: +971 6 5681442
www.conmix.com

ISO9001 CERTIFIED VINÇOTTE

B-5 The Manufacture Company Catalogue of fly ash

Product Data Sheet
Edition 03, 2008
Version no. 03.08

Construction

Sika Fly Ash®

Concrete Additive

Product Description	Sika Fly Ash® is a concrete additive of a new generation in fine powder form and spherical particles which reduces the water requirements and creates a lubricating effect that causes concrete to flow and pump better. In addition the concrete is more cohesive and is less prone to segregation
Uses	Sika Fly Ash® is used in structural concrete, precast concrete and other fields of concrete constructions where high demands are imposed on the quality of fresh and hardened concrete such as : 1- High- rise structures. 2- Dams and roads. 3- Power stations. 4- Bridges and tunnels.
Advantages	Sika Fly Ash® contains extremely fine latently reactive silica presence of this substance imparts greatly improved internal cohesion and water retention. When additionally using Sikament® super plasticizer, the concrete will show the following properties: ■ Excellent workability ■ Increased durability ■ High early strengths ■ Increased ultimate strengths ■ Increased resistance to abrasion ■ Highly increased water tightness ■ Highly reduced chloride diffusion ■ Easy to work and economic benefits ■ Chloride free - does not attack any reinforcement
Technical Data	
Composition	Alumina silicate pozzolan
Appearance / Colour	Grey- fine powder / odourless
Specific Gravity	Typically 2.2
Packaging	25 kg bags Special packs and bulk silo deliveries also available on request.
Storage	Sika Fly Ash® is not affected by frost. It must be stored in dry conditions.
Shelf life	12 months from date of production if stored properly in original unopened packing.
Application	
Dosage	25 - 35 % by weight of cement. For optimum results in concrete, always use in conjunction with Sikament® super plasticizer.
Mixing	Sika Fly Ash® is added with the cement to the concrete at the batching plant before the gauging water. Optimum mixing time 90-seconds. The quantity of water should be adjusted to suit the dosage of Sika Fly Ash®, Sikament® and the final consistency required.
Important Note	Sika Fly Ash® concrete should be handled and placed in the same way as conventional mixes. Standard good concrete practice should be observed throughout, and proper curing procedures should be initiated immediately after placement.

Construction

Safety Instructions

Safety Precautions	Wear a face mask against dust if there is heavy dust development. Accidental splashes to the skin must be washed off with water and soap. Accidental splashes to the eyes or mucous membrane must be rinsed with clean warm water. Seek medical attention without delay.
Ecology	Residues of material must be removed according to local regulations. Fully cured material can be disposed of as household waste under agreement with the responsible local authorities.
Transport	Non-hazardous
Toxicity	Non-Toxic under relevant health and safety codes.

Legal notes

Sika Egypt for Construction Chemicals
El Abour City
1st industrial zone (A)
Section # 10 Block 13035,
Egypt

Tel :+202-4 6100714/15/16/17/18
Fax :+202- 46100759
Mob :+2012- 3908822/55
www.sika.com.eg

B-6 Chemical Admixtures (Sika ViscoCrete® 5930-L)

Construction

Product Data Sheet
Edition 02, 2015
Version no. 12.2014

Sika ViscoCrete® -5930

High Performance Superplasticiser Concrete Admixture

Product Description

Sika ViscoCrete® -5930 is a third generation super plasticizer for concrete and mortar. It meets the requirements for super plasticizer according to ASTM-C- 494 Types G and F and BS EN 934 part 2: 2001.

Uses

Sika ViscoCrete® -5930 is suitable for the production of concrete.

Sika ViscoCrete® -5930 facilitates extreme water reduction, excellent flowability at the same time optimal cohesion and highest self compacting behaviour.

Sika ViscoCrete® -5930 is used for the following types of concrete:

- Precast concrete.
- Ready Mix Concretes.
- Concrete with highest water reduction (up to 30%).
- High strength concrete.
- Hot weather Concrete.
- Self compacting concretes.

High water reduction, excellent flowability, coupled with high early strengths, have a positive influence on the above mentioned applications.

Advantages

Sika ViscoCrete® -5930 acts by different mechanisms. Through surfaces adsorption and sterical separation effect on the cement particles, In parallel to the hydration process, the following properties are obtained:

- Strong self compacting behaviour. Therefore suitable for the production of self compacting concrete.
- Extremely high water reduction (resulting in high density and strengths).
- Excellent flowability (resulting in highly reduced placing - and compacting efforts)
- Increase high early strengths development.
- Improved shrinkage- and creep behaviour.
- Reduced rate of carbonation of the concrete.
- Improved Water Impermeability.

Sika ViscoCrete® -5930 does not contain chloride or other, steel corrosion promoting ingredients, It may therefore be used without any restrictions for reinforced and prestressed concrete construction.

Technical Data

Basis	Aqueous solution of modified Polycarboxylate
Appearance	Turbid liquid
Density	1.095 kg/lt. (ASTM C494)
Packaging	5 Kg, 20 Kg pails 200 kg drums Bulk Tanks are available upon request.
Storage/ Shelf Life	In unopened, undamaged original container, protected from direct sunlight and frost at temperatures between + 5 °C and + 35°C. Shelf life at least 12 months from date of production.

Sika ViscoCrete® -5930 1/2

Construction

Application

Dosage	Recommended dosage: ■ For soft plastic concrete: 0.2 - 0.8 % litre by weight of cement ■ For flowing and self compacting concrete (S.C.C.) 0.8 - 2 % litre by weight of cement
Addition	Sika ViscoCrete® -5930 is added to the gauging water or simultaneously with it poured into the concrete mixer. For optimum utilisation of the high water reduction we recommend through mixing at a minimal wet mixing time of 60 seconds. The addition of the remaining gauging water - to fine tune concrete consistency - may only be started after 2/3 of wet mixing time, to avoid surplus water in the concrete.
Concrete Placing	With the use of Sika ViscoCrete® -5930 concrete of highest quality is being produced. The standard rules of good concreting practice (production as well as placing) must also be observed with Sika ViscoCrete® -5930 concrete. Fresh concrete must be cured properly.
Frozen Sika ViscoCrete® -5930	Frozen Sika ViscoCrete® -5930 may be used after It has been slowly thawed at room temperature and intensively mixed.
Combinations	Sika ViscoCrete® -5930 may be combined with the following Sika products: ■ Sika Pump®. ■ Sika Rapid®. ■ Sika Ferrogard®-901. ■ Sikafume®. ■ Sika Fro®-V5A ■ Sika Retarder® Pre-trials are recommended if combinations with the above products are being made. Please consult our technical service.
Important Flowing Concrete S.C.C	Sika ViscoCrete® -5930 is also used to produce flowing and self compacting concrete (S.C.C.) For these, special mix designs are required, contact our Technical Service division.

Safety Instructions

Ecology	Do not dispose of into water or soil, but according to local regulations.
Transport	Non-hazardous.
Safety Precautions	In contact with skin, wash off with soap & water. In contact with eyes or mucous membrane, rinse immediately with clean warm water and seek medical attention without delay.
Toxicity	Non-Toxic under relevant health and safety codes.

Legal notes

The information and in particular the recommendations relating to the application and end-use of Sika products, are given in good faith based on Sika's current knowledge and experience of products when properly stored, handled and applied under normal conditions. In practice, the differences in materials, substrates and actual site conditions are such that no warranty in respect of merchantability or of fitness for a particular purpose, nor any liability arising out of any legal relationship whatsoever, can be inferred either from this information, or from any written recommendations, or from any other advice offered. The proprietary rights of third parties must be observed. All orders are accepted subject to our current terms of sale and delivery. Users should always refer to the most recent issue of the technical data sheet for the product concerned, copies of which will be supplied on request.

For further technical information, please consult our technical service department.

Sika Egypt for Construction Chemicals
El Abour City
1st industrial zone (A)
Section # 5930 Block 13035,
Egypt

Tel :+202- 4481 0580
Fax :+202- 4481 0459
Mob :+2012- 2390 8822/55
www.sika.com.eg

B-7 Steel Fiber

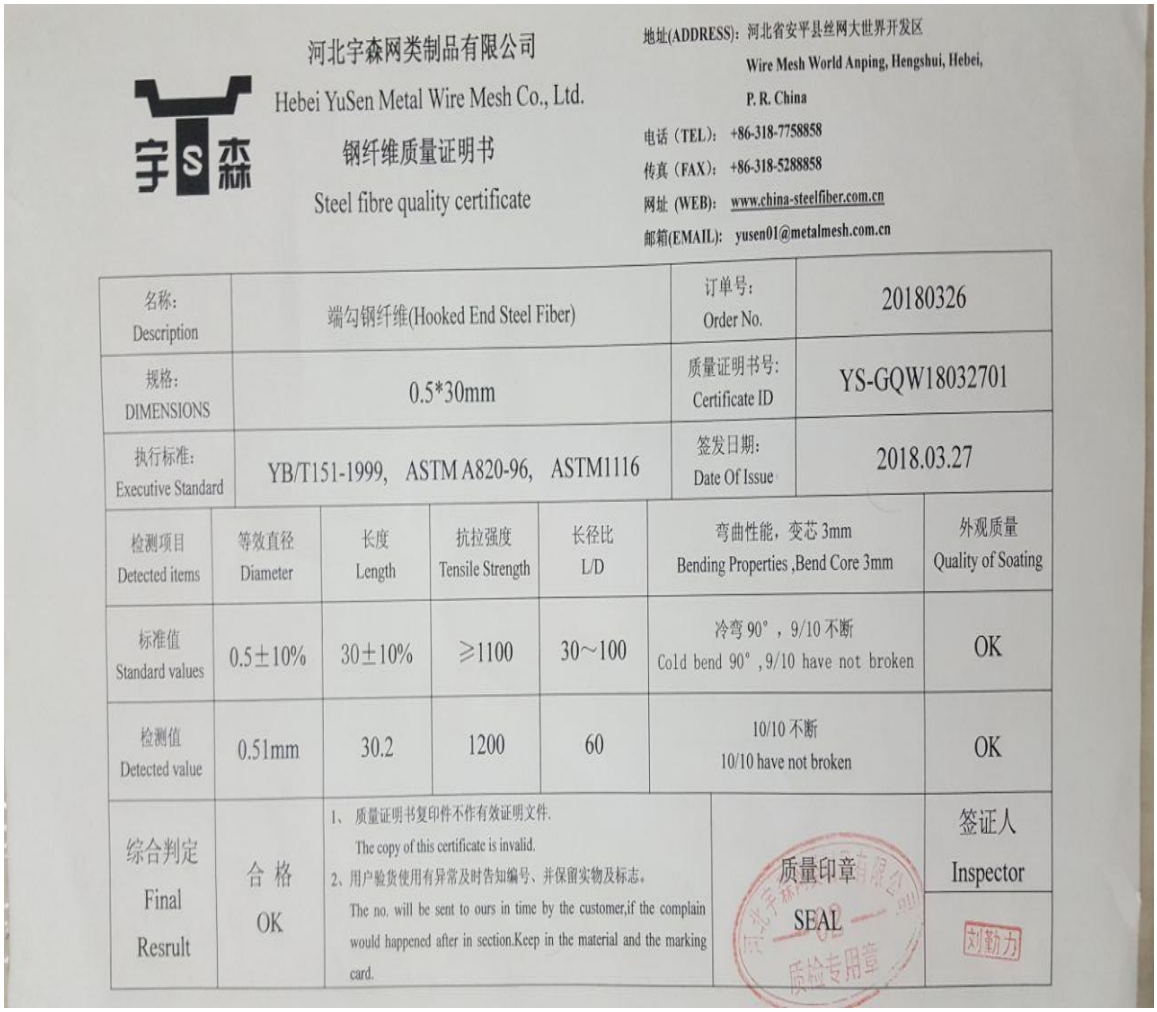

河北宇森网类制品有限公司
Hebei YuSen Metal Wire Mesh Co., Ltd.
钢纤维质量证明书
Steel fibre quality certificate

地址(ADDRESS)：河北省安平县丝网大世界开发区
Wire Mesh World Anping, Hengshui, Hebei, P. R. China
电话（TEL）：+86-318-7758858
传真（FAX）：+86-318-5288858
网址 (WEB)：www.china-steelfiber.com.cn
邮箱(EMAIL)：yusen01@metalmesh.com.cn

名称：Description	端勾钢纤维(Hooked End Steel Fiber)	订单号：Order No.	20180326
规格：DIMENSIONS	0.5*30mm	质量证明书号：Certificate ID	YS-GQW18032701
执行标准：Executive Standard	YB/T151-1999, ASTM A820-96, ASTM1116	签发日期：Date Of Issue	2018.03.27

检测项目 Detected items	等效直径 Diameter	长度 Length	抗拉强度 Tensile Strength	长径比 L/D	弯曲性能，变芯 3mm Bending Properties ,Bend Core 3mm	外观质量 Quality of Soating
标准值 Standard values	0.5±10%	30±10%	≥1100	30～100	冷弯 90°，9/10 不断 Cold bend 90°,9/10 have not broken	OK
检测值 Detected value	0.51mm	30.2	1200	60	10/10 不断 10/10 have not broken	OK
综合判定 Final Resrult	合 格 OK	1、质量证明书复印件不作有效证明文件。The copy of this certificate is invalid. 2、用户验货使用有异常及时告知编号、并保留实物及标志。The no. will be sent to ours in time by the customer,if the complain would happened after in section.Keep in the material and the marking card.			质量印章 SEAL	签证人 Inspector 刘勤力

B-8 Strand

Table (B-6) Properties of Strand

Grade	Elongation%	Breaking stress (Mpa)	Yield strength (Mpa)	Steel area of strand(mm)	Kg/1000m
270	12	1895	1737	141.31	1108

B-9 Deformed Steel Bars

Table (B-7) Properties of Deformed Steel Bars

Nominal Bar Size, (mm)	Area A_b, (mm^2)	Yield Strength f_y, (MPa)	Ultimate Strength, (MPa)	Weight per 1 Meter Length, (g /m)	Elong.
10-Deformed	75.2	570	648	602	12%

B-10 Epoxy type (Sikadur-331)

Construction

Product Data Sheet
Edition 16 December 2014

Sikadur® -31

Thixotropic epoxy resin adhesive mortar

Description	Sikadur-31 is a thixotropic adhesive mortar based on a 2-component solvent free epoxy resin containing fillers. Sikadur-31 will bond and fill a wide variety of building and construction materials and may be used in both dry and damp conditions thereby providing an adhesive mortar ideally suited to site application. It is available in three grades: rapid, normal and long potlife for low, medium and high ambient temperatures respectively.
Uses	Sikadur-31 may be used as a thin layer levelling mortar, repair mortar or adhesive for most building materials (concrete, brick, stone, ceramics, cement mortar, GRC, fibrous cement, iron and steel and epoxy mortar). Sikadur-31 may also be used to anchor holding down bolts, starter bars etc. as a bonding bridge between old concrete and Sikadur-41 mortar. The material is also ideally suited for bonding of external reinforcement and as a general structural adhesive. Special higher strength grades of the material are available for segmental bridge and other construction.
Advantages	▪ Chemical resistant ▪ Insensitive to moisture during application, cure or whilst in service ▪ Applicable at low temperatures ▪ Excellent adhesion to most building materials even when damp ▪ High abrasion resistance ▪ Approved for use in contact with potable water ▪ High early strength ▪ High tensile and flexural strength ▪ Supplied in factory proportioned units ▪ Easily applied – thixotropic, non-sag ▪ Proven in service ▪ Shrink free ▪ Two components of different colours enabling visual control of degree of mixing.
Storage and Shelf Life	Minimum shelf life is approximately 3 years. Store under controlled conditions in original containers (minimum 5°C, maximum 35°C temperature range).
Instructions for Use	
Surface Preparation	All surfaces must be clean, sound and free from dust, ice, oils, grease, or other surface contaminants such as form release residues and curing membranes. Concrete, Mortar, Stone: Mechanically abrade the surface with a needle gun, mechanical wire brush, grit blast or grind. All surface laitance must be removed. Cement and concrete should be at least 3-4 weeks old. Metals: Remove any paints, oils, grease, rust and oxide films by grit blasting. Apply Sikadur-31 without delay. Plastics: (epoxy, polyester) abrade and rinse with Sika Colma Cleaner.
Mixing	Sikadur-31 is supplied in factory proportioned units comprising the correct quantities of Part A (Resin) and Part B (Hardener). Thoroughly stir both components separately using a slow running drill/stirrer with a helical paste mixer (max. speed 600 rpm). Decant all Part B into Part A and mix thoroughly together until a uniform mix is achieved (typically 3 mins). A streaky colouration is indicative of inadequate or incomplete mixing. Apply immediately. Small units may be hand mixed provided an even colour is achieved.

Sika®

Product Data Sheet
Edition 16 December 2014

Application	Apply Sikadur-31 to the prepared substrate by trowel, brush or gloved hand. Ensure the material is worked well (scrubbed) into the surface, this is particularly important on damp surfaces. There should be no standing water on concrete surfaces. When at least 2 mm thick, apply the fresh Sikadur-41 mortar immediately. If using Sikadur-31 as an adhesive, coat both adherends and press into place (on vertical and overhead situations temporary support must be provided). The adhesive layer should not be less than 2 mm and not more than 30 mm thick for Normal and Long Potlife; 20 mm for Rapid.
Cleaning	Uncured material may be cleaned from application tools, etc. by using Sika Colma Cleaner (flammable solvent). Cured material can only be removed mechanically.

Technical and Physical Data

Form	Thixotropic paste		
Density	1.90 kg / litre approx.		
Volume solids	100% (solvent free)		
Secant Flexural Modulus of Elasticity (BS 6319) @ 7 days	Rapid @ 20°C 5.2 GPa approx.	Normal @ 20°C 5.8 Gpa approx.	Long Potlife @ 35°C 4.2 Gpa approx.
Compressive strength @ 7 days (AS 1478.2) @ 24 hours	Rapid @ 20°C 40 MPa approx. 25 MPa approx.	Normal @ 20°C 55 MPa approx. 35 MPa approx.	Long Potlife @ 35°C 60 MPa approx. 40 MPa approx.
Flexural strength @ 7 days (BS 6319)	Rapid @ 20°C 24 MPa approx.	Normal @ 20°C 22 MPa approx.	Long Potlife @ 35°C 22 MPa approx.
Tensile strength @ 7 days (BS 6319)	Rapid @ 20°C 12 MPa approx.	Normal @ 20°C 6 MPa approx.	Long Potlife @ 35°C 9 MPa approx.
Adhesion to concrete (EN 1542)	3.5 MPa approx. (concrete failure all grades)		
Adhesion to steel (EN 1542)	20 MPa approx. (Normal/Rapid) 15 MPa approx. (Long Potlife)		
Application Temperature (min.-max.)	5°C – 20°C (Rapid) 10°C-30°C (Normal) 20°C - 45°C (Long Potlife) (substrate and ambient temperatures)		
Approvals/Standards	Testing according to ASTM C881M-02 Type 1, Grade 3 and Class B+C Testing according to EN 1504-4		
Cure time	Initial cure 24 hours. Full cure 3-7 days (Subject to ambient temperature)		
Consumption/Coverage	1.9 kg/m² approx. per mm thickness (dependent on surface profile, texture, temperature and wastage)		
Colour	Part A – White Part B – Dark Grey Mixed product uniform grey colouration		
Packaging	6 kg pre-batched unit Mixing Ratio (A:B = 2:1)		

Potlife

Temperature	Rapid	Normal	Long Potlife
5°C	34 mins	*	*
20°C	15 mins	50 mins	125 mins
35°C	*	20 mins	55 mins

*not recommended for use at these temperatures

(The temperature at which the Sikadur-31 is stored during the 24 hours before it is mixed will govern it's potlife when mixed).

B-11 Epoxy type (Sika Anchor Fix)

Construction

Product Data Sheet
Edition 16 December 2014

Sikadur® -31

Thixotropic epoxy resin adhesive mortar

Description	Sikadur-31 is a thixotropic adhesive mortar based on a 2-component solvent free epoxy resin containing fillers. Sikadur-31 will bond and fill a wide variety of building and construction materials and may be used in both dry and damp conditions thereby providing an adhesive mortar ideally suited to site application. It is available in three grades: rapid, normal and long potlife for low, medium and high ambient temperatures respectively.
Uses	Sikadur-31 may be used as a thin layer levelling mortar, repair mortar or adhesive for most building materials (concrete, brick, stone, ceramics, cement mortar, GRC, fibrous cement, iron and steel and epoxy mortar). Sikadur-31 may also be used to anchor holding down bolts, starter bars etc. as a bonding bridge between old concrete and Sikadur-41 mortar. The material is also ideally suited for bonding of external reinforcement and as a general structural adhesive. Special higher strength grades of the material are available for segmental bridge and other construction.
Advantages	• Chemical resistant • Insensitive to moisture during application, cure or whilst in service • Applicable at low temperatures • Excellent adhesion to most building materials even when damp • High abrasion resistance • Approved for use in contact with potable water • High early strength • High tensile and flexural strength • Supplied in factory proportioned units • Easily applied – thixotropic, non-sag • Proven in service • Shrink free • Two components of different colours enabling visual control of degree of mixing.
Storage and Shelf Life	Minimum shelf life is approximately 3 years. Store under controlled conditions in original containers (minimum 5°C, maximum 35°C temperature range).
Instructions for Use	
Surface Preparation	All surfaces must be clean, sound and free from dust, ice, oils, grease, or other surface contaminants such as form release residues and curing membranes. Concrete, Mortar, Stone: Mechanically abrade the surface with a needle gun, mechanical wire brush, grit blast or grind. All surface laitance must be removed. Cement and concrete should be at least 3-4 weeks old. Metals: Remove any paints, oils, grease, rust and oxide films by grit blasting. Apply Sikadur-31 without delay. Plastics: (epoxy, polyester) abrade and rinse with Sika Colma Cleaner.
Mixing	Sikadur-31 is supplied in factory proportioned units comprising the correct quantities of Part A (Resin) and Part B (Hardener). Thoroughly stir both components separately using a slow running drill/stirrer with a helical paste mixer (max. speed 600 rpm). Decant all Part B into Part A and mix thoroughly together until a uniform mix is achieved (typically 3 mins). A streaky colouration is indicative of inadequate or incomplete mixing. Apply immediately. Small units may be hand mixed provided an even colour is achieved.

Sika®

Sikadur®-31 1/4

APPENDIX (C)

APPENDIX (C)

FINITE ELEMENT MODELING STEPS

C.1 General

At the first step, the full beam was modeled in the ABAQUS program but needed a very long run time, therefore, modeling a quarter of beam to useful from the benefit of symmetry in x and z-axis. It led to the achievement of the purpose of modeling. This consists of the following steps:

C.2 Creating the Prestressed Concrete Beam and Strengthening Parts

Create individual parts by drawing imported they are geometry for each component of the model. Generally, many parts were involved in modeling the beam modes. Those parts were concrete beam, 7-wire prestressed strand, non-prestressed stirrups, steel reinforcement at the top and the bottom fiber, end anchorage steel plates, bearing plates, steel plates for the loading and supporting condition, anchorage bolt, rectangle steel plate, U shape steel plate and different size and shapes of SIFCON laminate. Each of those parts at first draw then the different parts were assembled and merged to produce the modeling beams specimens as shown in Figure (C1-C7).

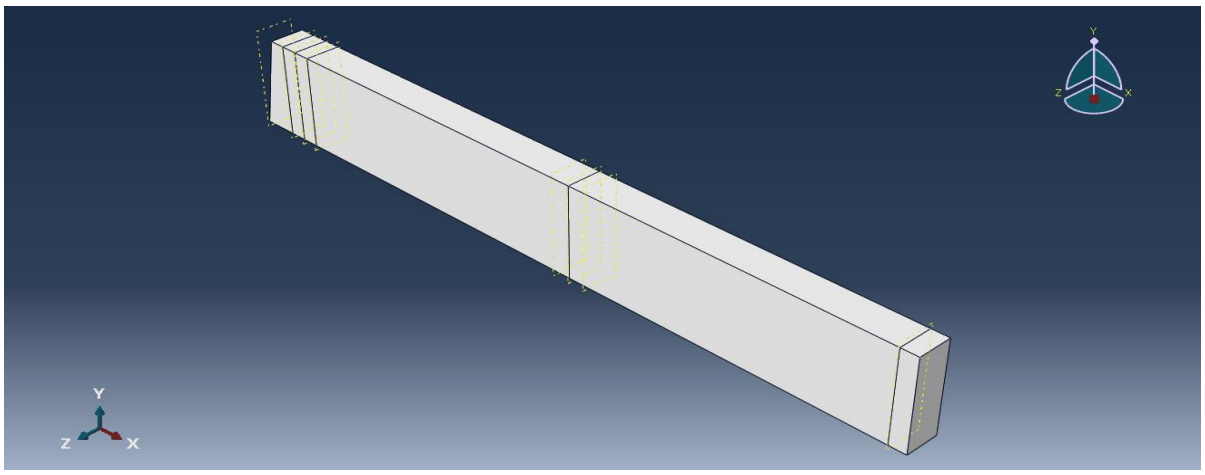

Figure(C-1) Concrete beam

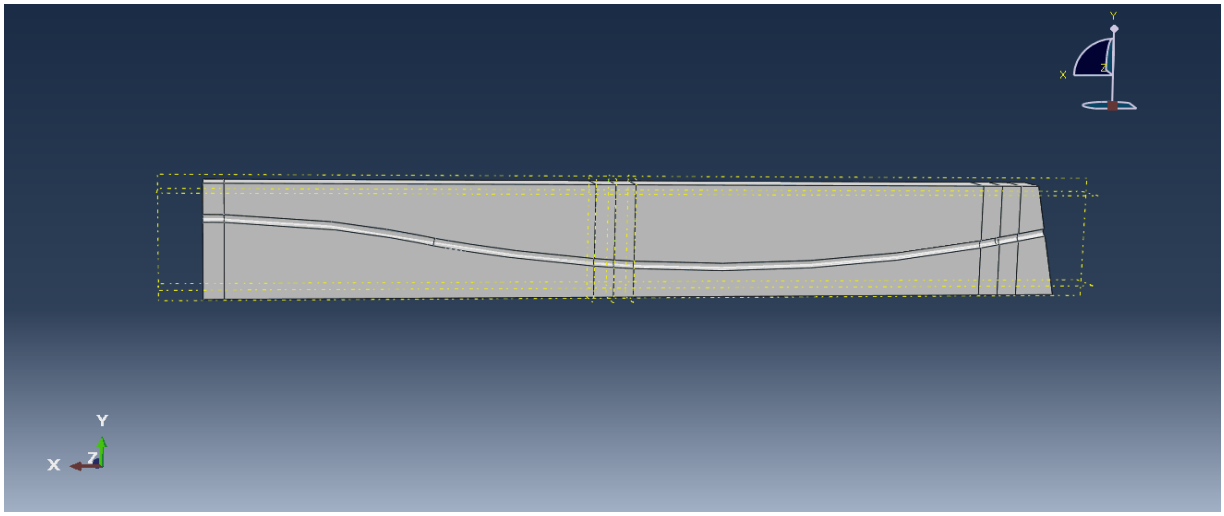

Figure(C-2) Concrete beam with hole

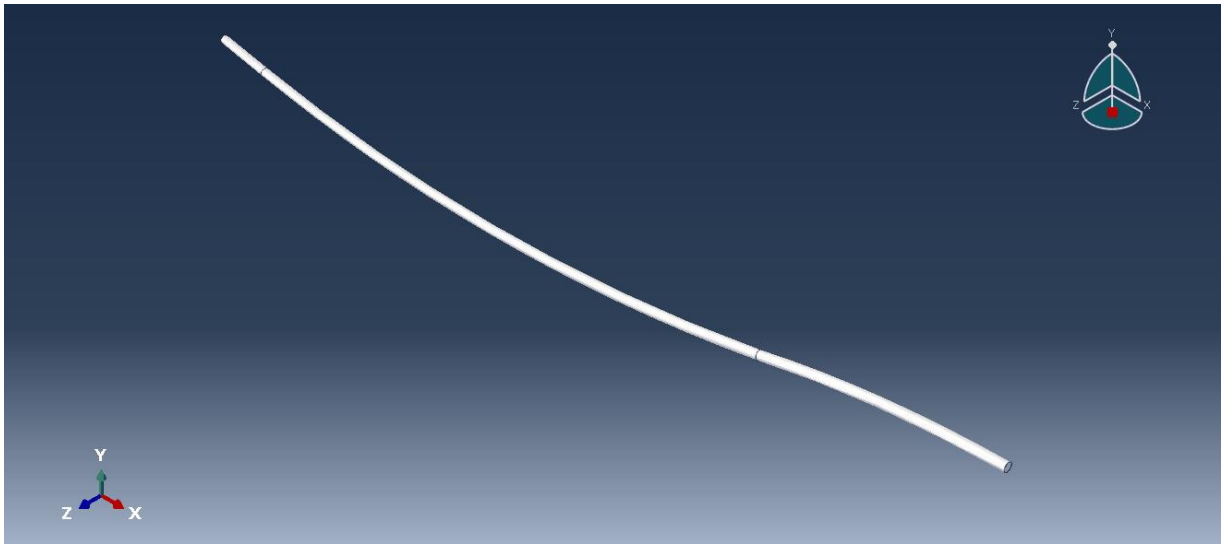

Figure(C-3) Strand

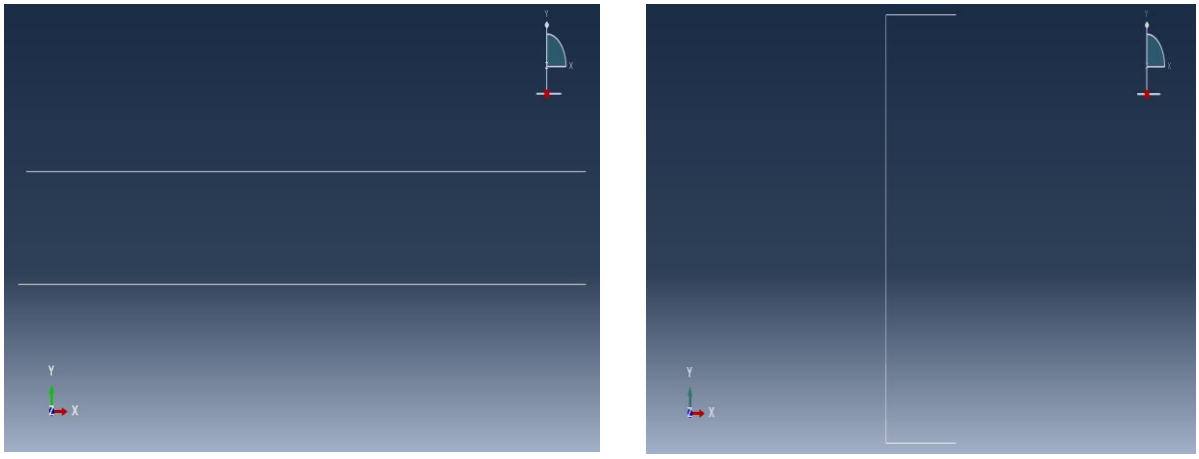

Figure (C-4) Reinforcement bars and stirrups

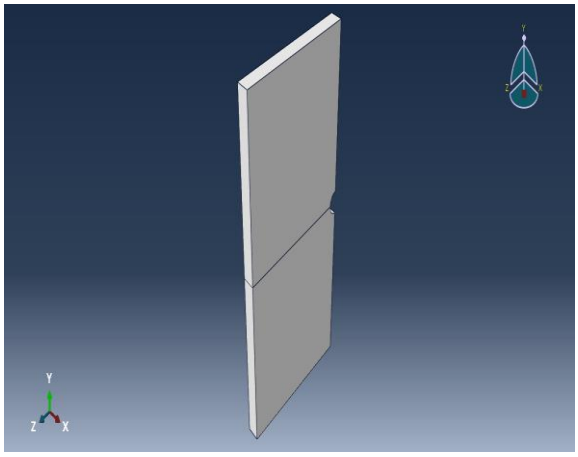

Figure(C-5) End steel plate

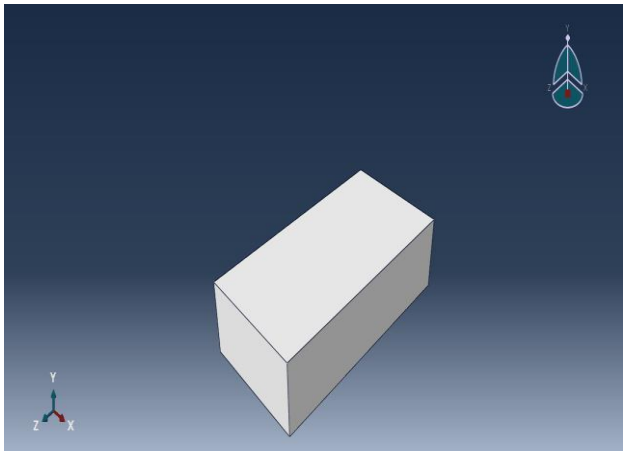

Figure(C-6) Steel plate

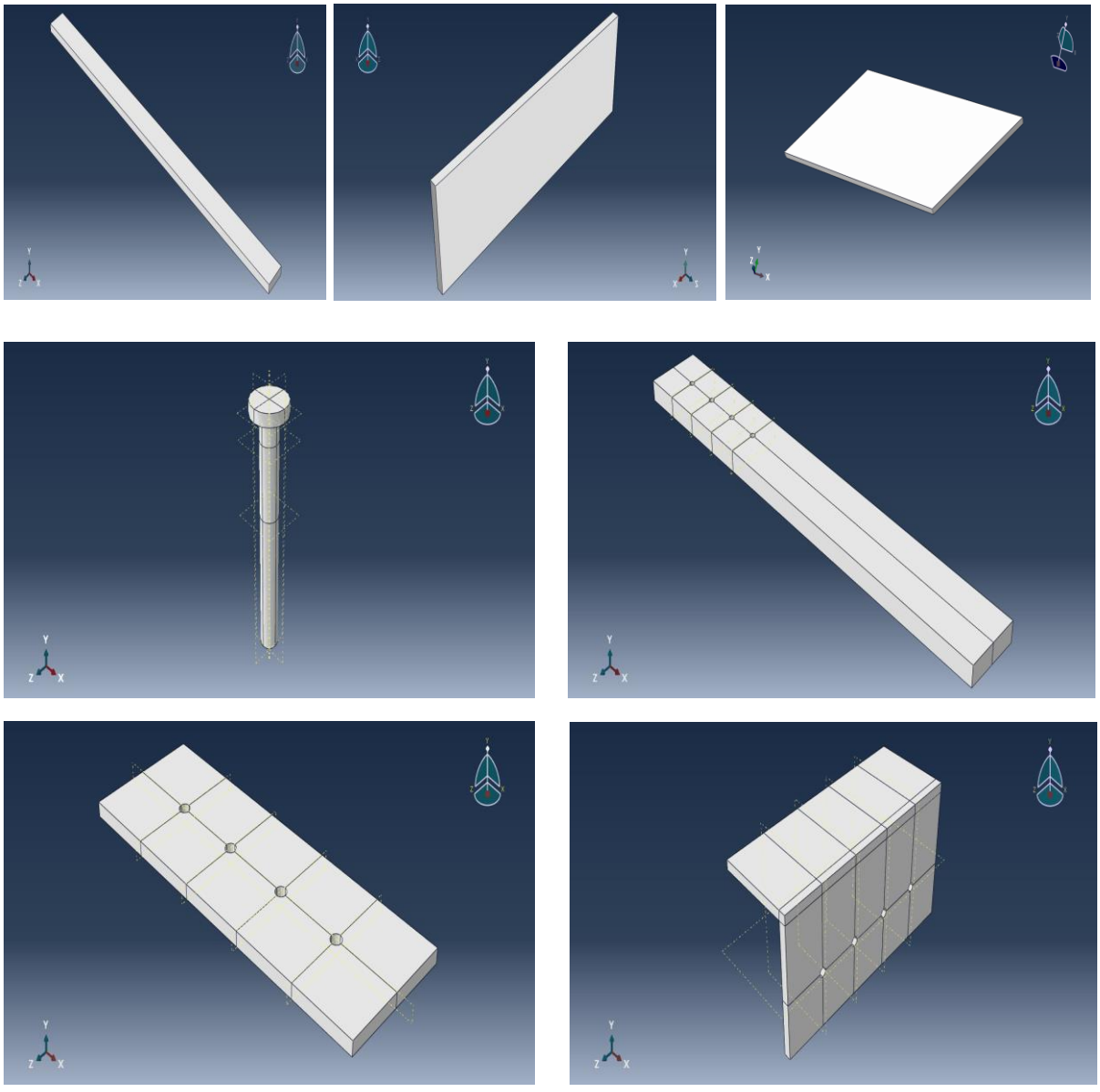

Figure(C-7) Strengthening parts

C.3 Concrete Properties Modelling

Mainly, there are three material models for analyzing concrete at low confining pressures in ABAQUS; Concrete smeared cracking model in ABAQUS/Standard, Concrete damaged plasticity model (CDP) in both ABAQUS/Standard, and ABAQUS/Explicit and brittle cracking model in ABAQUS/Explicit. In present study, concrete damage plasticity model was used to model the concrete.

C.3.1 Concrete Damaged Compressive Behavior

Compressive behavior of the HSC is assumed that the high strength concrete material has a linear elastic behavior up to 40% of its compressive strength and then its non-linear behavior initiates due to the appearance of the bond cracks. Other points up to f_c should be calculated according to the Eq. (C-1) and the number of defined points is arbitrary and describes the accuracy of compressive behavior of concrete material model [72].

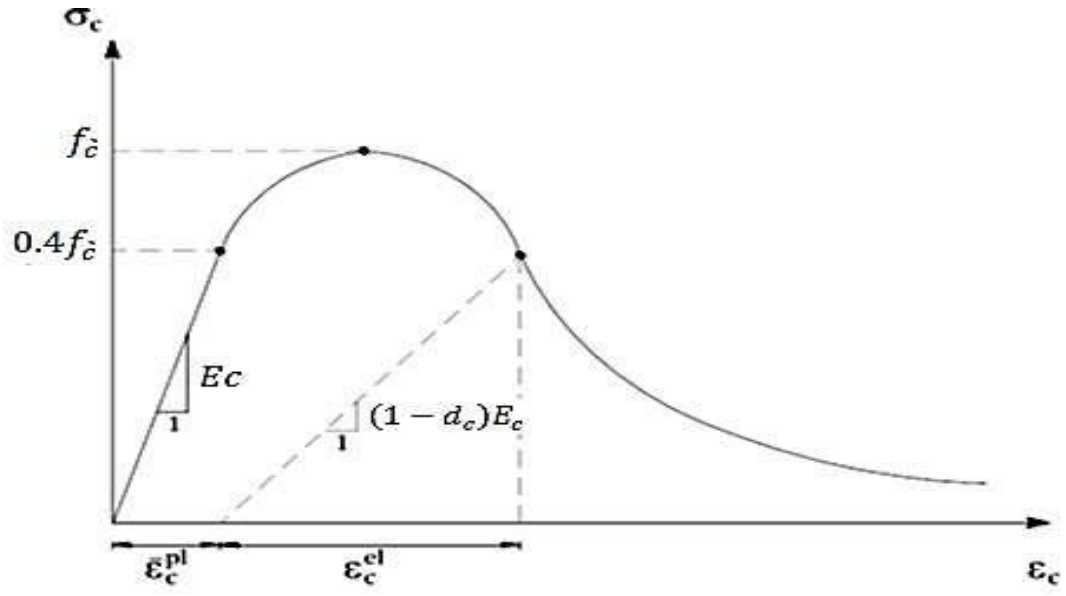

Figure (C-8) Uniaxial Compressive Behavior of High Strength Concrete [73]

$$\sigma_c = f_c[2x - x^2] \quad \text{..... (C-1)}$$

Where:

σ_c: the compressive stress of concrete

f_c: the compressive cylinder strength of concrete

$x = \frac{\varepsilon_c}{\varepsilon_{co}}$: the normalized strain, ε_c is the strain at any point, $\varepsilon_{co} = 2f_c/E_c$ is the strain at peak stress.

$$\therefore \sigma_c = f_c \left[2\left(\frac{\varepsilon_c}{\varepsilon_{co}}\right) - \left(\frac{\varepsilon_c}{\varepsilon_{co}}\right)^2\right]$$

Plastic strain εpl at each point can be calculated according to Eq. (C-2),

$$\varepsilon_{pl} = \varepsilon_c - \frac{\sigma_c}{E_c} \quad \text{..... (C-2)}$$

Where:

E_c is young's modulus of concrete [72].

The compressive behavior of concrete after reaching the ultimate strength can be considered linear until zero stress [74].

For SFRC the relation of stress-strain in compression is obtained from Lee, et al. [75] equation (C-3) relationships which is described below:

$$f_c = f_c' \left[\frac{\left(\frac{\varepsilon_c}{\varepsilon_0}\right)}{A-1+\left(\frac{\varepsilon_c}{\varepsilon_o}\right)^B}\right] \text{..... (C-3)}$$

For pre peak=A=B=$\frac{1}{1-\left(\frac{f_c'}{\varepsilon_o E_c}\right)}$ for$\frac{\varepsilon_c}{\varepsilon_0} \leq 1.0$

For post peak: B=$\left(\frac{f_c'}{50}\right)^{0.064}\left[1 + 0.882\left(V_f \frac{l_f}{d_f} - 0.882\right)\right] \geq A$

A=$1 + 0.723\left(V_f \frac{l_f}{d_f}\right) - 0.957\ for\ \frac{\varepsilon_c}{\varepsilon_0} > 1.0$

$$\varepsilon_0 = \left(0.0003V_f \frac{l_f}{d_f} + 0.0018\right) f_c^{0.12}$$

where:

f_c' = peak stress obtained from a cylinder test (MPa).

ε_0 = strain when fc reaches fc'.

V_f = fiber volumetric ratio.

$\frac{l_f}{d_f}$ = fiber aspect ratio.

C.3.2 Concrete Damaged Tensile Behavior

For defining tensile behavior of concrete, under uniaxial tension, as can be seen in Figure (C-9), the stress increases with a linear elastic relationship with strain up to the ultimate tensile strength, and then micro-cracks form microscopically with a tension softening response. There are three different methods to define tension softening response in ABAQUS; stress-strain, stress-displacement or by use of fracture energy, *Gf* [71].

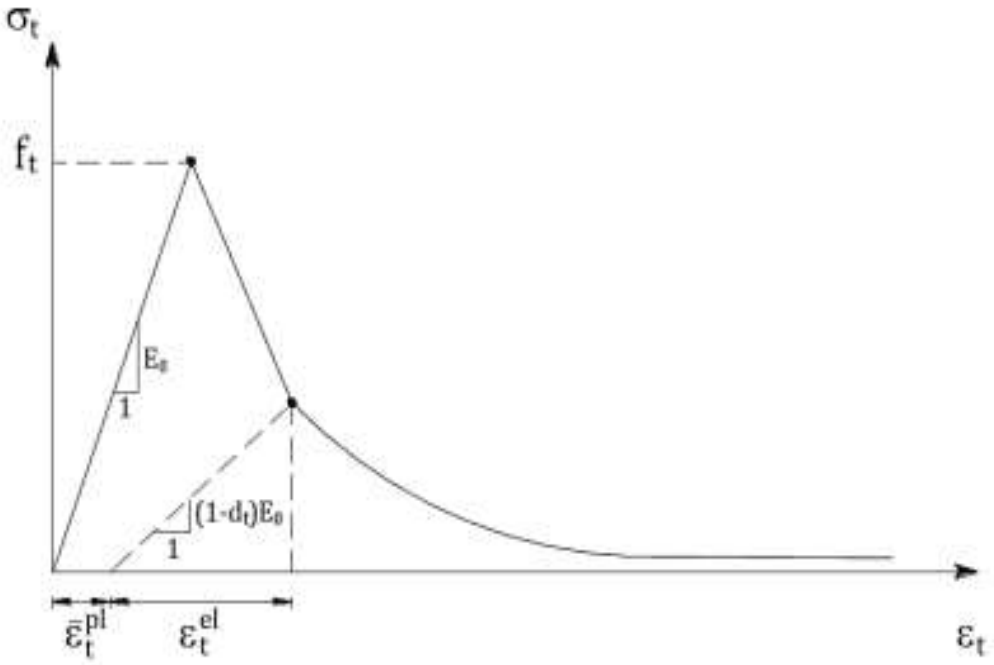

Figure (C-9) Uniaxial tensile stress-strain relationship for concrete [72]

According to Hibbit et al. it is recommended to use a stress-displacement approach. In the stress-displacement alternative, a linear tension stiffening function can be used. Therefore, only one displacement point needs to be defined, as can be seen in Figure (C-10) (a).

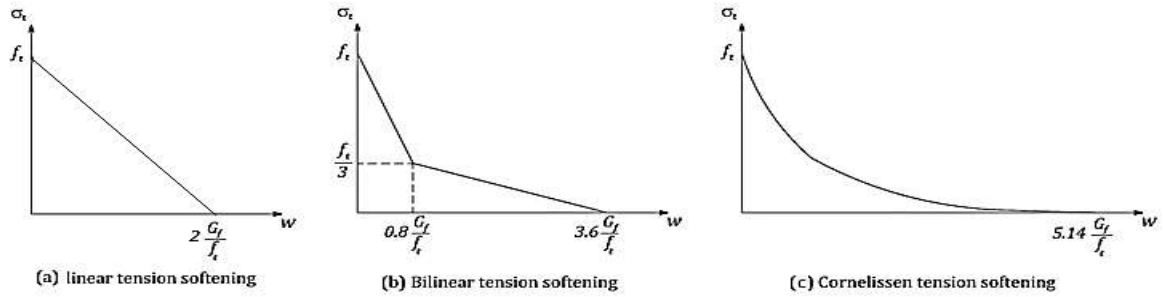

Figure (C-10) Different tension softening functions, reproduction by [71],[76],[77]

In this regard, w_c is the point at which stress no longer can be transferred. A linear stiffening function can be calculated according to Eq. (C-3) [72]:

$$w_c = 2\frac{G_f}{f_t} \quad \text{(C-3)}$$

f_t: is the maximum tensile strength; In the present study, the flexural tensile strength (f_r) is adopted which obtained from the experimental result in ch4.

Gf: is the fracture energy of concrete.

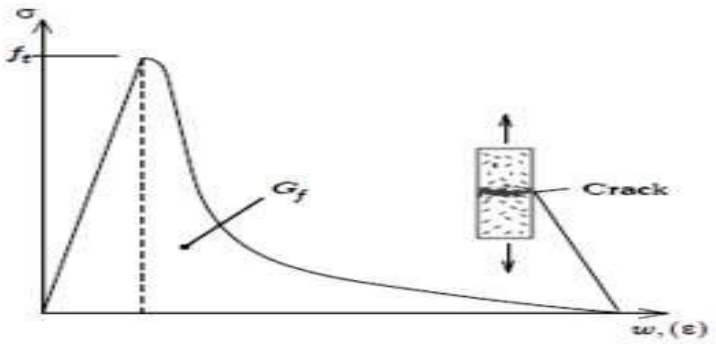

Figure (C-11) Crack opening with fracture energy[78]

Fracture energy is energy required to open a unit area of a stress-free crack, which is defined by Hillerborg with using brittle fracture concept. This energy is equal to the area under the tension-softening curve and according to Hilleborg bilinear tension stiffening curve, as can be seen in Figure (C-10) (b), would be implemented to model the tension softening behavior of concrete [79].

Furthermore, according to Karihaloo (2003) the by far best and most accurate model is the exponential function experimentally derived by Cornelissen et al. (1986) and is presented in Figure (C-10) (c) [72].

The following exponential model was proposed by Cornelissen et al. [72]:

$$\sigma_t = f_t\left[f(w) - \frac{w}{w_c} f(w_c)\right] \quad \text{.....(C-4)}$$

where *f(w)* is a displacement function given by:

$$f(w) = \left[1 + \left(\frac{c_1 w}{w_c}\right)^3\right] exp\left(-\left(\frac{c_2 w}{w_c}\right)\right) \quad \text{..... (C-5)}$$

where,

w: is the crack opening displacement at any point.

w_c: is the crack opening displacement at which stress can no longer be transferred.

where w_c for concrete equal:

$$w_c = 5.14 \frac{G_f}{f_t}$$

c_1 is a material constant and $c_1 = 3.0$ for normal density concrete.

c_2 is a material constant and $c_2 = 6.93$ for normal density concrete [72]

G_f, is the area under the softening curve and is according to Beton (1993) estimated as [80]:

$$G_f = G_{fo}\left(\frac{f'_c}{10}\right)^{0.7} \quad \text{..... (C-6)}$$

Where the fracture energy G_{fo} is a constant value depends on the concrete grade and aggregate size $D_{max.}$ can be obtained from Table (C-2).

Table (C-2) Fracture Energy for Different Concrete Grade and Aggregate Sizes [79]

	G_{fo}(N/m)							
$D_{max}(mm)$	C12	C20	C30	C40	C50	C60	C70	C80
8	40	50	65	70	85	95	105	115
16	50	60	75	90	105	115	125	135
32	60	80	95	115	130	145	160	175

Fracture of concrete reinforced with a single type of fiber (SFRC) is also approximated by a bi-linear law, the first branch is steeper and simulates the bridging of the early micro-cracks. The second branch simulates the aggregate interlocking in plain concrete or the fiber links in fiber reinforced concrete. When more than one type of fiber is adopted, it may be necessary to use a polylinear law with more branches since different fibers activate at different cracks. In this thesis one type of fiber is applied, so a bi-linear law is sufficient. [81]

C.3.3 Plasticity Parameters

1-Dilation angle (ψ), is a material parameter determined at a high confining pressure in confining pressure (p) and von Mises stress (q) plane and indicates the inclination of an incremental plastic strain. ψ has a maximum value of 56.3° and a minimum value is approximately0°. Upper values are more ductile behavior, whereas lower values are more brittle. According to Malm [79]better

agreement was reached with the experimental findings for dilation angles between 30° to 40° and for normal concrete ψ equal 30° considers suitable.

2– Eccentricity (Є): defines the change rate of plastic flow potential function. In ABAQUS 0.1 can be considered as the eccentricity default value, where the dilation angle has no change for a wide range of confining pressure. For low confining pressure a higher eccentricity value than 0.1 induces a rapid increase in the dilation angle. Although a lower value than 0.1 will cause a problem of convergence when the material is submitting to the low values of confining pressure.

3– σ_{bo}/σ_{co} refers to the ratio of initial equibiaxial compressive yield stress to initial uniaxial compressive yield stress. In the present study the value 1.16 was used which is ABAQUS default amount.

4– Kc: is the rate of the second stress invariant in the tensile meridian to compressive meridian for any known value of the pressure invariant at initial yield. The value of Kc is in range (0.5-1) and its default value that used in ABAQUS is 0.667.

5– μ : represents the viscosity parameter which is used in ABAQUS to improve the convergence. Its default value is zero.

C.4 Steel Properties Modelling

The steel reinforcement and stirrups are modeled analytically as elastic-perfectly plastic depending on the von mises failure which considers the material elastic behavior until the yield stresses and beyond this point became perfectly plastic as shown in Figure (C-12) [71]. For linear isotropic part is defined by modulus of elasticity of reinforced and the Poisson's ratio, which are taken as 200×10^3 MPa and 0.3, respectively. For bilinear isotropic part is defined by yield stress as presented in Table (4-8) and Table (4-9). The steel bearing plates and

support plates are modelled as a linear isotropic material. For linear isotropic part is defined by modulus of elasticity of steel plates and the Poisson's ratio which are taken for each plate as 200×10^3 MPa and 0.3, respectively

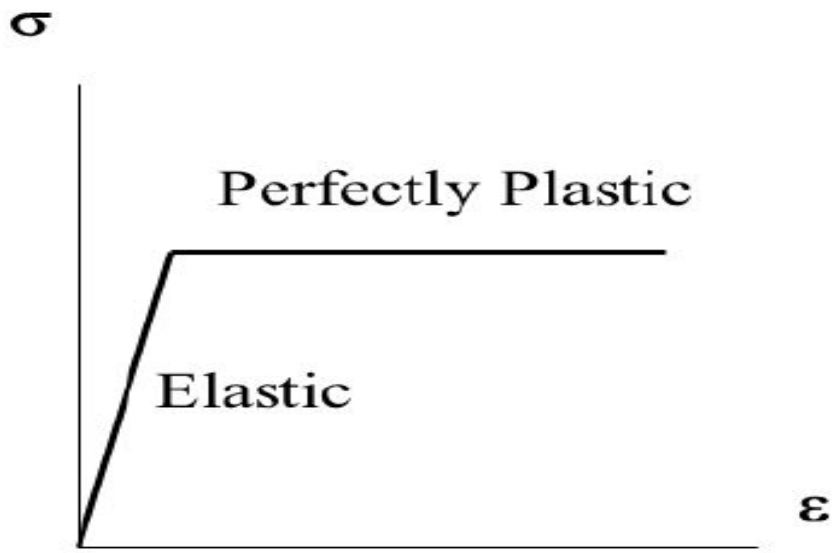

Figure (C-12) Bilinear stress-strain curve for the reinforcing steel[71]

The prestressing steel was modeled as multilinear isotropic material. Multilinear stress-strain curve developed by using the following equations [82]:

$\varepsilon_{ps}\leq 0.008; f_{ps}=28000\times\varepsilon_{ps}(ksi)$

$\varepsilon_{ps}>0.008; f_{ps}=268-\frac{0.075}{\varepsilon_{ps}-0.0065}<0.98\times f_{pu}(ksi)$

$\varepsilon_{ps}^{pl}=\varepsilon_{ps}-\varepsilon_{ps}^{el}$

Where:

ε_{ps}: Prestressing steel strain.

f_{ps}: Stress in prestressing steel MPa.

f_{pu} :is the ultimate strength of the prestressing strands, taken as 1848 MPa or 268 4ksi.

εps: Total strain in prestressing strand

ε_{ps}^{pl}: Plastic strain in prestressing strand

ε_{ps}^{el}:elastic strain in prestressing strand

C-5 Assembly the Model Parts

When generating a part, it is located in its coordinate system, independent of the other parts of the model. Therefore, ABAQUS uses the assembly module to create instances of parts and to place related instances in a global coordinate system (assemble parts to create the entire structure). Thus, the ABAQUS model includes only one assembly selection. Assembly of volume parts and wire parts are exhibited in Figures (C-13) to (C-17).

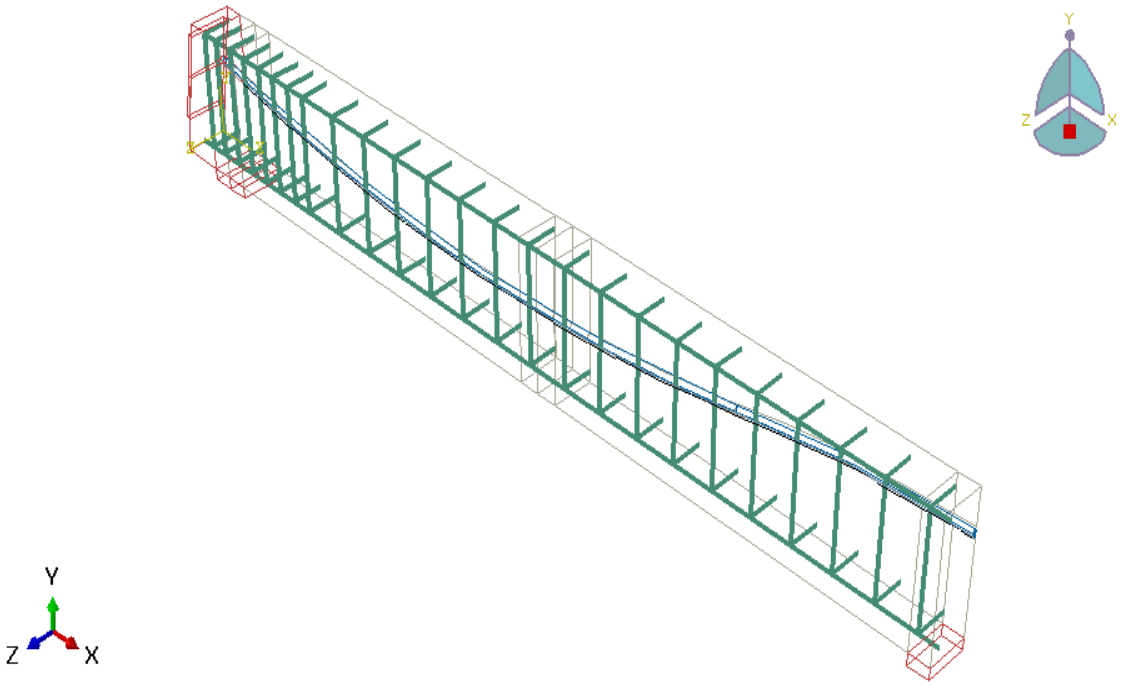

Figure (C-13) Assembly of steel parts

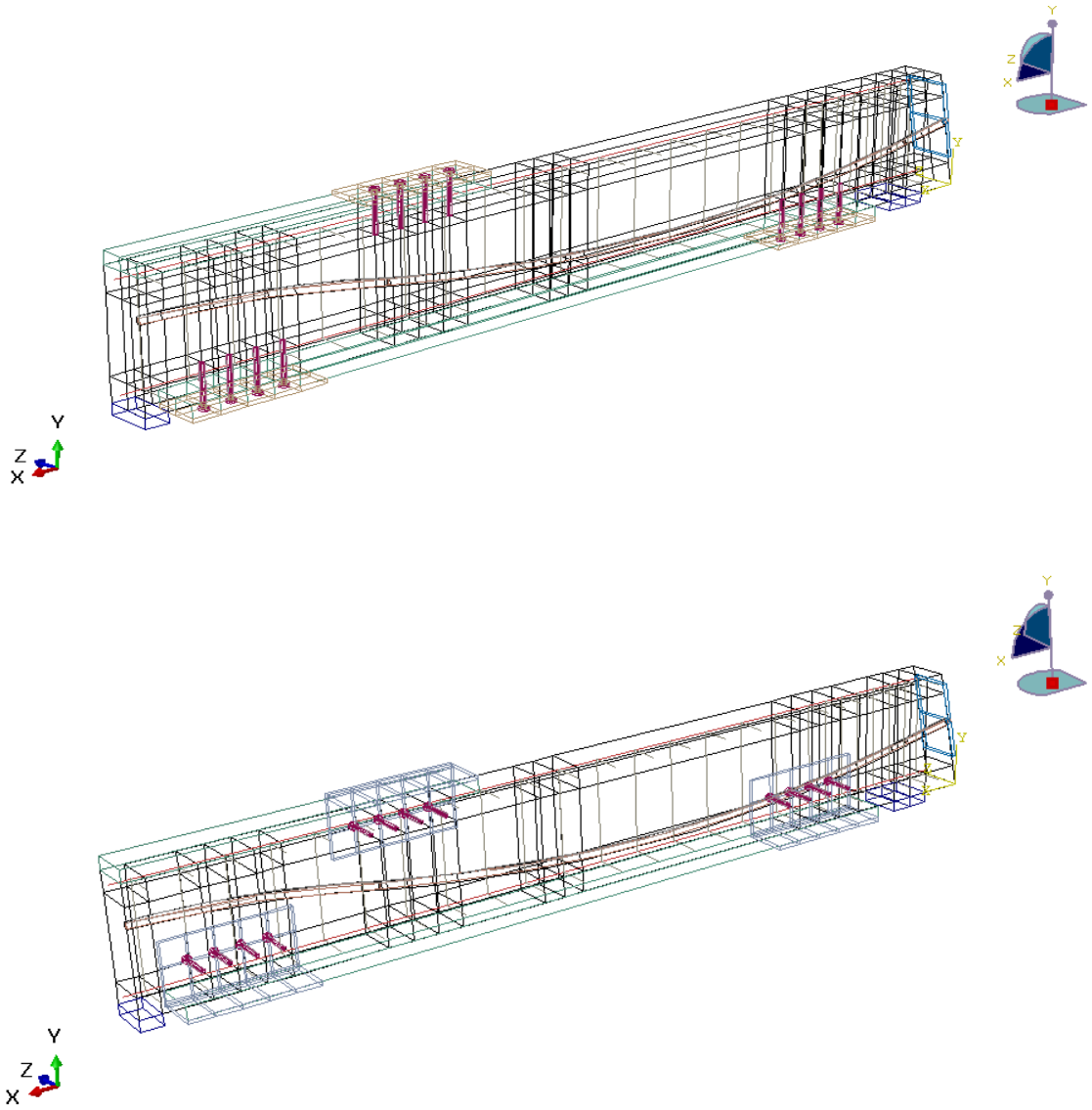

Figure (C-13) Assembly of steel parts -continued

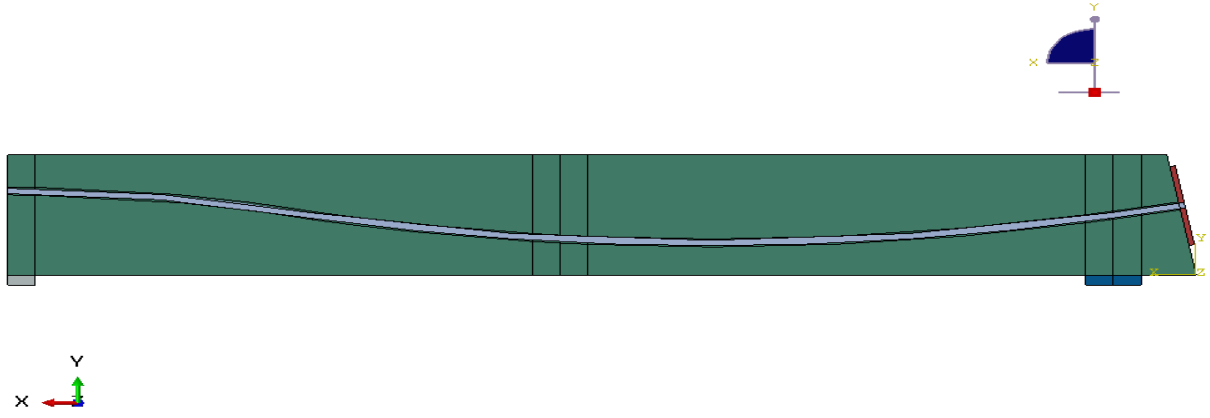

Figure (C-14) Assembly of all beam

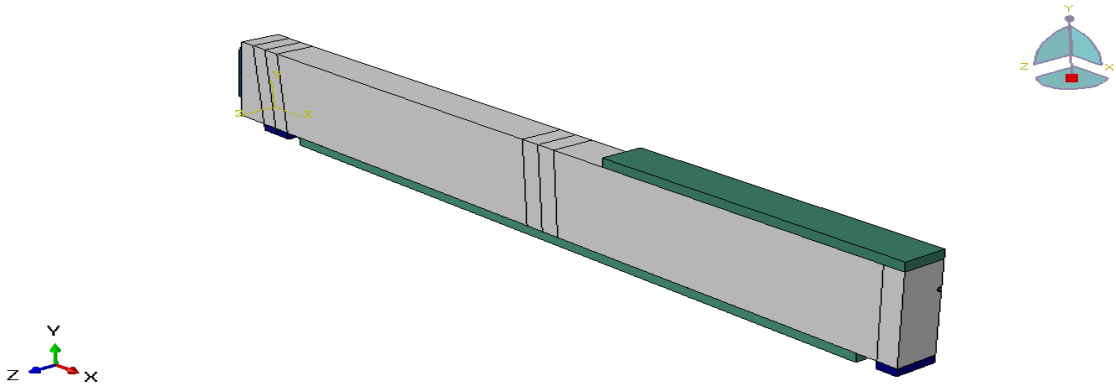

Figure(C-15) Assembly of SIFCON laminates with beam

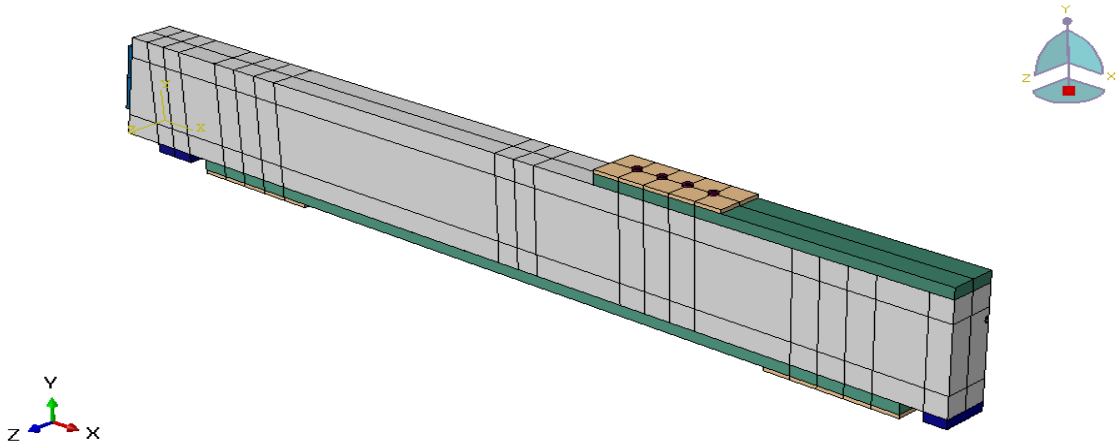

Figure(C-16) Assembly of rectangle anchorage end steel plate

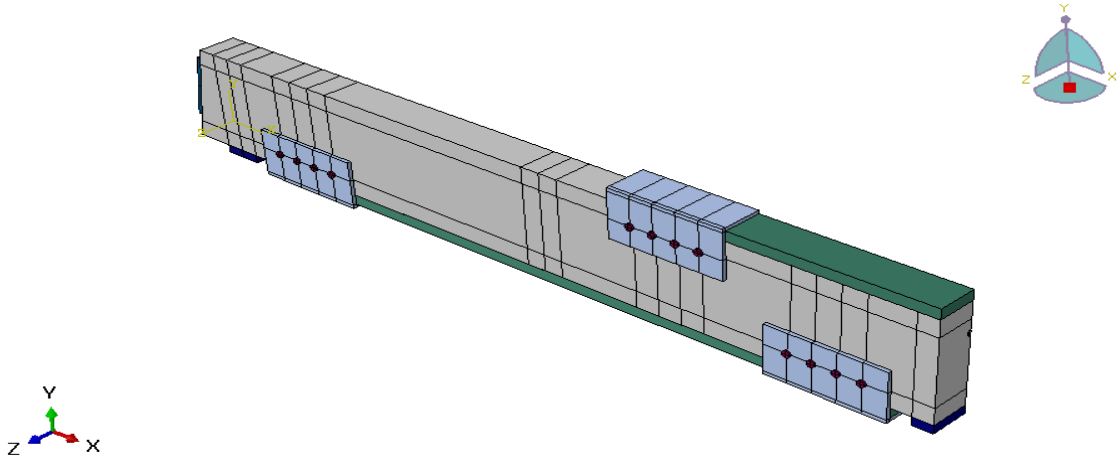

Figure(C-17) Assembly of U anchorage end steel plate

C-6 Contact Interaction between the Model Parts

The interaction module allows the setting up of interactions between parts. In ABAQUS, several contact interactions models. Each contact interaction can refer to a contact property that provides a model for interaction between the contact surfaces. The concrete beam is used as a host element.

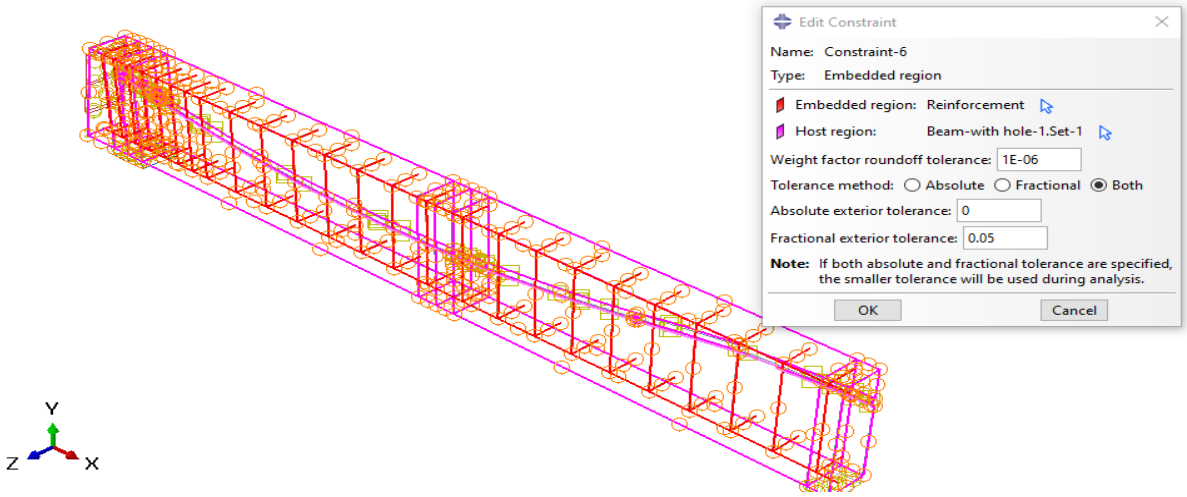

Figure(C-18) Interaction between steel bars and concrete

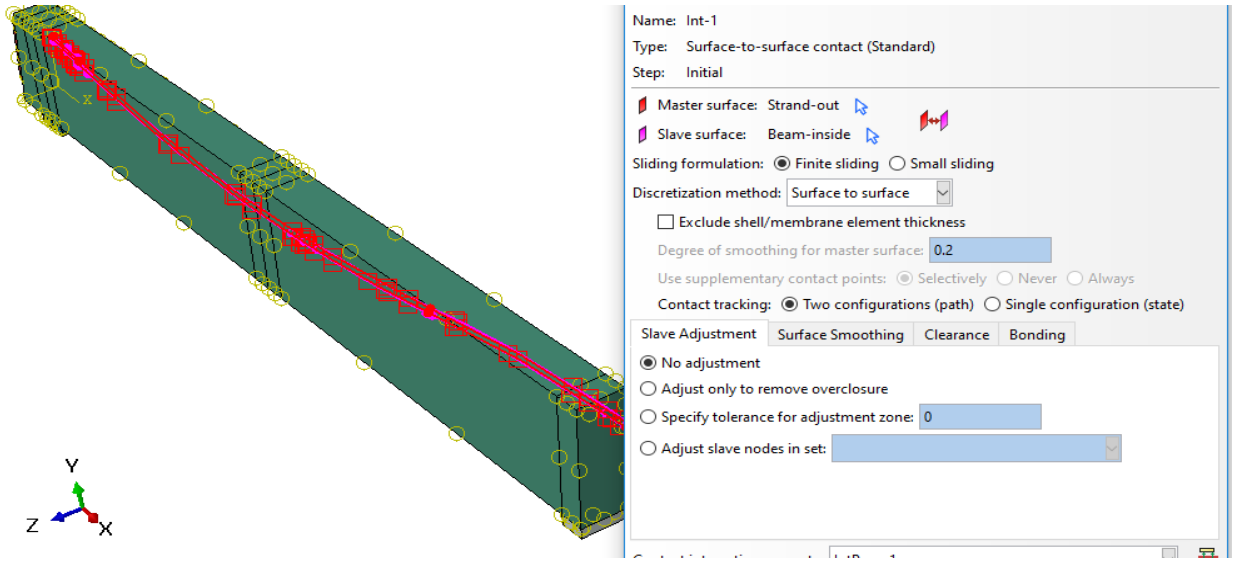

Figure(C-19) Contact interaction, (Surface to surface method), for prestressing strand with concrete beam.

C-7 Applying Load and Boundary Conditions

Load cases are groups of loads and boundary conditions used to determine a particular load state. The boundary conditions used for the beam are demonstrated in Figure (C-20) a continuously supported boundary conditions were assigned to the beam-ends.

Stress in (directions x) as initial condition in prestressing strand was applied for beam subjected to external prestressing. In the second step of modeling, the addition of pressure load was applied uniformly steel load plate.

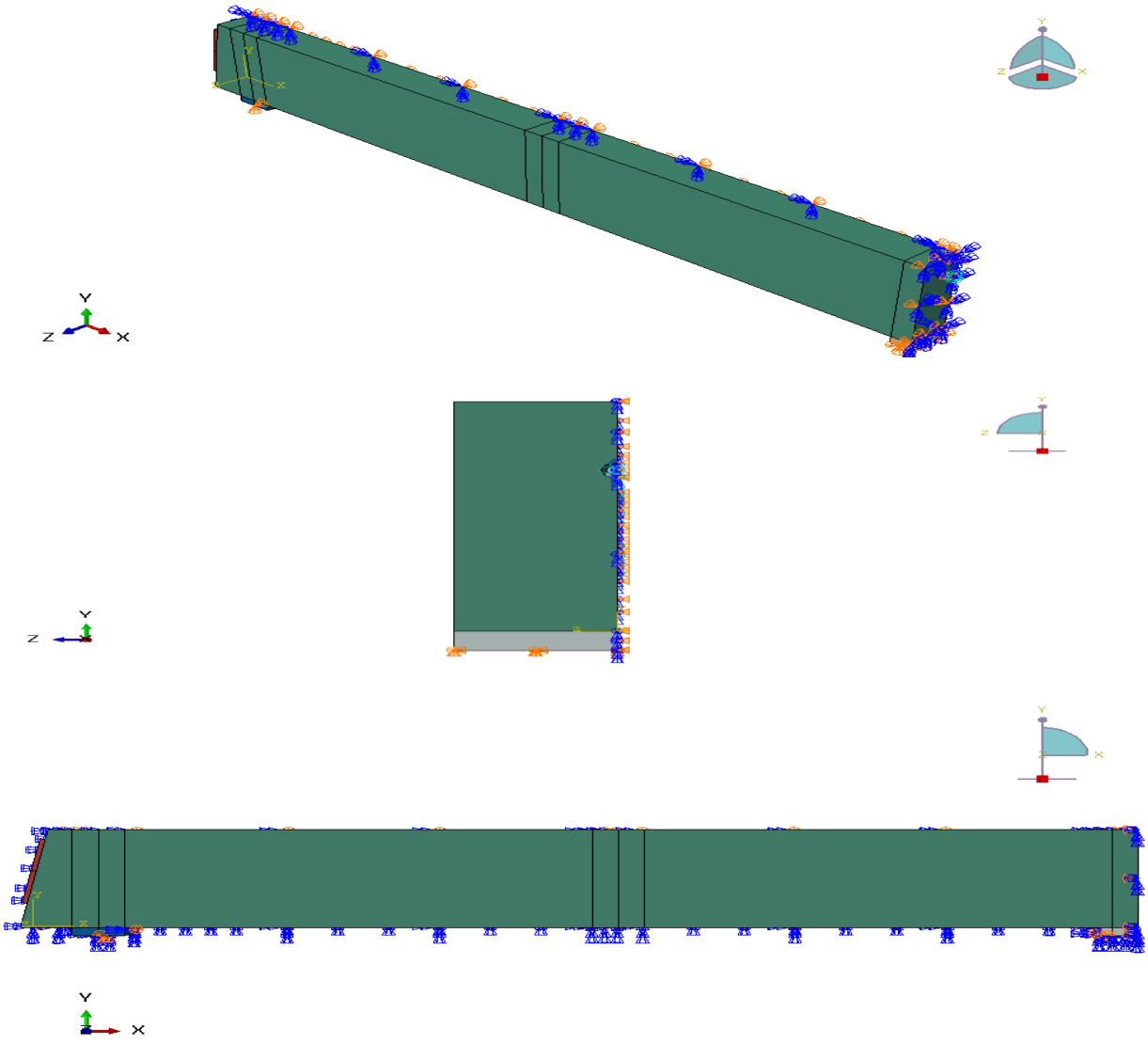

Figure (C-20) BC

C-8 Meshing of the Model

An important step in finite element modeling is the selection of the mesh density. A convergence of results is obtained when an adequate number of elements is used in a structure. This is practically achieved when an increase in the mesh density has a negligible effect on the results. Therefore, in this finite element modeling, a convergence study was carried out to determine an appropriate mesh density. The convergence study was made by increasing the number of elements (mesh) in each direction z, y, and x.

The prestressed concrete CONTINUOUS beams are modeled here in 3D stress element for all components except steel reinforcements is modeled utilize standard 2D elements.

These elements are providing with suitable integration rules based on the experimental response to the specimen. The reinforcement steel can be modeled by solid, beam, or truss elements. The use of solid elements is computationally expensive and therefore not chosen. Since reinforcement bars do not supply very high bending stiffness, the truss elements are used and modeled as an embedded element, and their bond to concrete is to be completely bonded.

Linear brick hexahedral C3D8R elements are continuum element (C) having 3D eight nodes (8) with reduced integration (R) were selected for the finite element models for concrete beam, support plates, end bearing plates, and strand volumes, while T3D2 elements are element (T) having 2D two nodes (2) were selected for the finite element models steel bars.

Different mesh size has been checked for the simulated model of the beam specimen to select the suitable model meshing which can satisfy both minimum finite element numbers and good convergence. Mesh size (25) mm gave the best result.

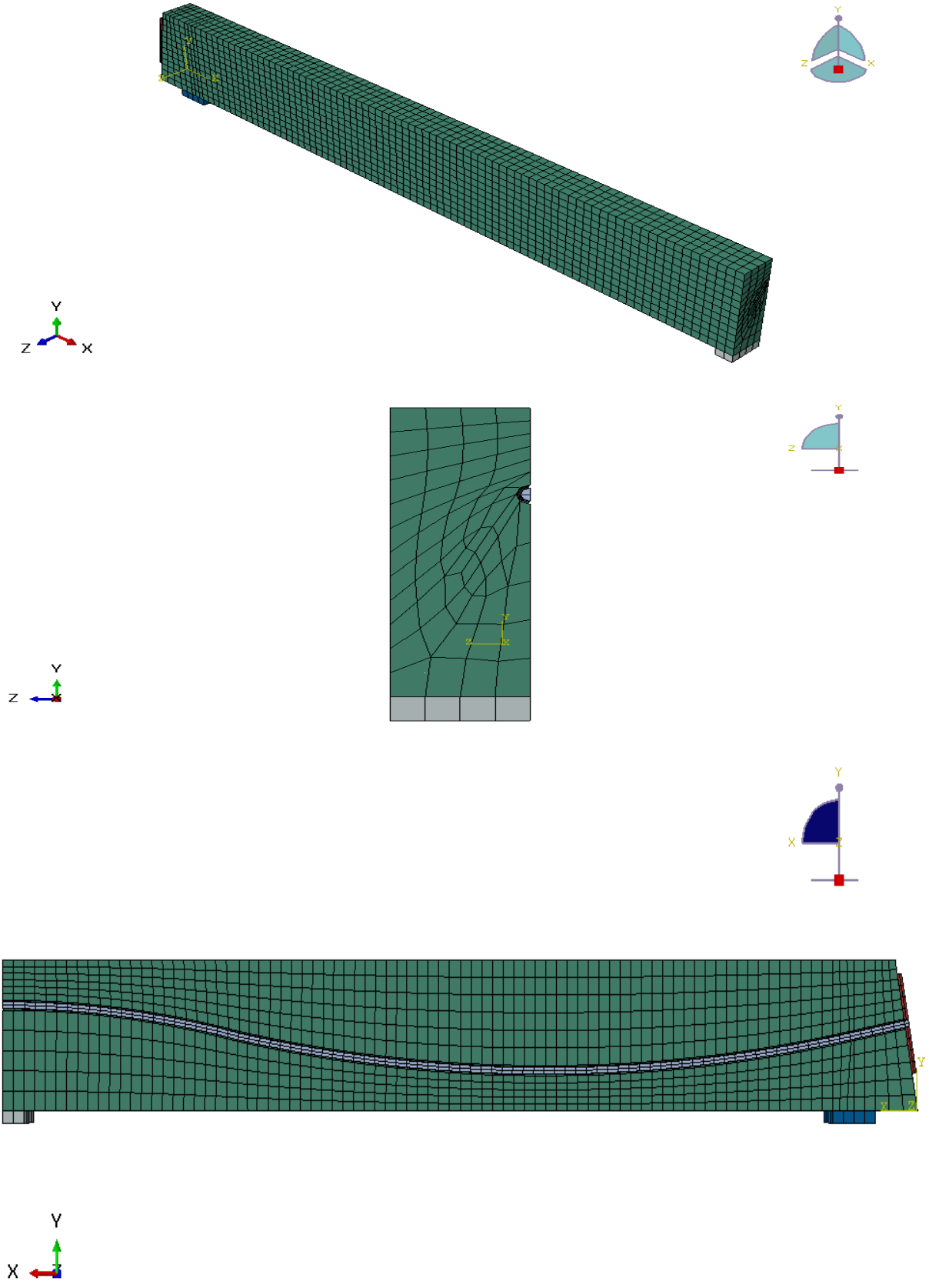

Figure (C-21) Model meshing for combined brick elements modelling

C-9 Evaluation the Job

This module allows submitting the model for analysis.

C-10 Visualizing the Results and Sketch

This order allows looking at the model after deformation and can also plot values of stress, displacement..

الخلاصه

غالبًا ما يتكرر التحميل على الجسور والموانئ ومرائب السيارات متعددة الطوابق ومرافق المطارات والعديد من الهياكل الأخرى التي يتم بناؤها عادةً باستخدام العتبات الخرسانية مسبقة الإجهاد. يمكن أن تكون هذه العتبات معيبه بسبب الأضرار التي تحدث في الموقع وتتسبب في حدوث تشققات نتيجة النقل غير السليم والمناولة لذلك من المهم جدًا تطوير تقنية تقوية فعاله لاستعادة القدره المفقوده أو حتى التفوق عليها. يُقترح هنا حل موثوق وأقل تكلفة لتعديل العتبات في موقع البناء بدلاً من إعادتها إلى المصنع.

تقدم هذه الدراسة استقصاءً تجريبياً وعددياً لسلوك الانثناء والقص للعتبات الخرسانية سابقة الإجهاد المحدده المقواة بشرائح (الملاط الخرساني المتخلل للألياف) مسبقة الصب تحت التحميل الساكن والمتكرر لدورات محدوده. تم إجراء البرنامج التجريبي على عشرين عينة من العتبات الخرسانة عالية المقاومة سابقة الإجهاد غير المربوطة ذات مقطع عرضي مستطيل (٢٠٠ × ٣٠٠) مم بطول (٤٣٠٠ مم) تم اختبارها على أنها مدعومه بشكل مستمر تخضع تحت نقطتي تحميل مركزه في منتصف كل فترة وتستخدم لتقوية هذه العتبات ستة وستون شريحه مسبقة الصب من (الملاط الخرساني المتخلل للألياف). تم تقسيم النماذج إلى فئتين متطابقتين، كل واحدة تتكون من عشر عينات. درست الفئة الأولى سلوك الانثناء؛ الفئة الثانية درست سلوك القص. تتكون كل فئة من مجموعتين على النحو التالي: المجموعة الأولى تتكون من عتبات تم اختبارها تحت تحميل ساكن، وتتكون المجموعة الثانية من عتبات تم اختبارها تحت التحميل المتكرر تتراوح بين ٠,٤ إلى ٠,٦ من الأحمال النهائية الناتجة عن الاختبار الساكن. تمت دراسة متغيرات مختلفة في البرنامج التجريبي منها طول الشرائح في منطقة التقعر والتحدب، وثلاث طرق ربط مختلفة اثنتان منها مبتكره، التغليف الكامل والجزئي، وأنماط مختلفة من تقوية القص. تم قياس الهطول في منتصف كل فضاء، ووضع الفشل، والصلابة، وتوزيع العزوم، وعرض الشقوق، والانفعالات في الخرسانة.

تشير النتائج التجريبية إلى أن تقوية الانحناء للعتبات الخرسانيه سابقة الإجهاد أدت إلى تأثر إيجابي بتأخير وقت ظهور الشق الأول وزاد حمل الشق الاول للعتبات المختبرة بين (٥٦,٢٪ -١٠٢,٢٪)، وزيادة قدرة الانثناء القصوى لعتبات الاختبار (٣٦,٩٪ -٥٧٪). كما أثبتت أنظمة تثبيت النهايات المبتكرة الجديدة فعاليتها في منع فشل إزالة الترابط لشرائح (الملاط الخرساني المتخلل للألياف) كما كان لها مساهمة كبيرة في تحسين السلوك ككل.

عندما يتم اختبار العتبات تحت الأحمال المتكررة تقل الاحمال بصوره قليله، تقل قوة الانثناء القصوى لعتبات الاختبار (٠,٨٦٪ -٥,٨٧٪) مقارنة مع قوة نفس العتبات تحت تحميل ساكن. تظهر العتبات

المعززه بظروف تحميل ساكنه نموًا ملحوظا في إعادة توزيع العزوم (٩,١-١٠,٦) ٪ عند المسند المركزي و (٥,٥-٦,٤) ٪ في منتصف المدى، على التوالي وتزيد نسبة إعادة توزيع العزوم للعزوم السالبة للعتبات المختبرة تحت الحمل المتكرر بحوالي (٥٪ -٩,٠٣٪) مقارنة بالعتبات المماثلة تحت ظروف التحميل الساكن. تشير النتائج أيضًا إلى أن استخدام شرائح (الملاط الخرساني المتخلل للألياف) سابقة الصب كتقويه خارجيه لمنطقة القص للعتبات الخرسانية سابقة الإجهاد هي تقنية فعالة في زيادة قدرة قص للعتبات حيث ادت إلى تأخير وقت ظهور الشق الأول وزاد حمل الشق الاول للعتبات التي تم اختبارها بين (٢٣,٧٪ -١٠٥,٧٪)، زيادة قدرة القص النهائية للحزم المختبرة (١٠,٣٪ -٤٦,٥٪)، وكذلك العتبات التي تم اختبارها تحت الأحمال المتكررة، تقل قليلاً في قدرة القص النهائية (٢,٢٪ -٣,٨٪)، مقارنة بقوة نفس العتبات تحت التحميل الساكن. كما أظهرت الدراسة الحالية أيضًا إمكانية تحويل الفشل من وضع الفشل الهش إلى فشل مطيل نسبيًا في النهاية بعد ظهور علامات التحذير مثل أصوات الانفصال وتقشير شرائح (الملاط الخرساني المتخلل للألياف) مع تحذيرات وافره قبل الفشل.

في الجزء العددي من هذه الدراسة تم استخدام برنامج الأباكوس لتحليل جميع العينات المختبره ومقارنة النتائج مع نتائج العمل التجريبي ودراسة متغيرات أخرى جديده. تم الحصول على توافق جيد بين النتائج التحليليه والتجريبيه.

الاستنتاجات الرئيسية التي يمكن استخلاصها هي: أن هذه التحقيقات أعطت مؤشرًا جيدًا حول استخدام شرائح (الملاط الخرساني المتخلل للألياف) مسبقة الصب في تحسين قوة الانحناء والقص للعتبات مسبقة الاجهاد عاليه المقاومه المستمره كانت طرق الربط المبتكرة في هذه الدراسة فعالة للغاية، وكان تأثير دورات التحميل المتكرره المحدوده على العينات المختبره ضئيلا.

جمهورية العراق
وزارة التعليم العالي والبحث العلمي
جامعة بابل
كلية الهندسة
قسم الهندسه المدنية

سلوك الانحناء والقص للعتبات الخرسانية مسبقة الإجهاد المقواة بصفائح (الملاط الخرساني المتخلل للألياف) مسبقة الصب تحت الأحمال التكرارية

أطروحة
مقدمة الى كلية الهندسة في جامعة بابل
كجزء من متطلبات نيل درجة دكتوراه فلسفة في الهندسة/الهندسة المدنية / إنشاءات

من قبل
حوراء محمد علي محمد طاهر جمال
(بكالوريوس هندسة مدنية -٢٠٠٢)
(ماجستير هندسة مدنية (أنشاءات) - ٢٠١٦)

أشراف
أ.د. مصطفى بلاسم داود

شُـباط **٢٠٢٢**